Virtual Display of Tactile Graphics and Braille by Lateral Skin Deformation

Vincent Lévesque

Department of Electrical & Computer Engineering
McGill University
Montreal, Canada

August 2009

A thesis submitted to McGill University in partial fulfillment of the requirements for the degree of Doctor of Philosophy.

Abstract

Graphical content is increasingly pervasive in digital interfaces and documents yet it remains accessible to visually impaired persons almost exclusively on media with limited flexibility such as embossed paper. Textual content is more accessible but nevertheless limited by the cost and functionality of refreshable Braille displays and voice synthesis. This thesis explores the use of a novel tactile stimulation approach that relies on lateral skin deformation for the computerized display of virtual Braille and tactile graphics.

Tactile synthesis by lateral skin deformation is initially explored in the context of Braille. The feasibility of producing virtual Braille by laterotactile stimulation is first demonstrated by creating the illusion of brushing against a line of Braille dots through the synchronization of a travelling wave of skin deformation with the displacement of a tactile array of eight actuators. This principle is then extended to complete 6-dot Braille cells by distributing lines of virtual dots onto the rows of actuators of a general-purpose STReSS^2 tactile array. Reading the resulting virtual Braille is shown to generally be feasible but demanding, suggesting that a specialized laterotactile Braille display should be devised or that dots be rendered for contrast rather than realism.

Tactile rendering by lateral skin deformation is then further explored with the gradual development of a virtual tactile graphics framework that emulates conventional features such as raised lines and areal textures through a coherent set of patterns that includes grating textures, stroked and dotted shapes, bitmap-based masks, and composite patterns. Dynamic rendering is also exploited to produce novel effects such as tactile flow, reactive textures dependent on the exploration behaviour, and interactive content with alternate views. The usability of the framework is informally evaluated with visually impaired volunteers and early tactile patterns studied through formal experiments. The tactile patterns are presented on the Tactograph, a haptic interface redesigned specifically for the display of tactile graphics that combines a STReSS^2 display with an instrumented planar carrier.

This thesis demonstrates the potential of lateral skin deformation for the display of Braille and tactile graphics, and explores in the process the ways in which this novel approach to tactile stimulation can be applied to produce meaningful tactile sensations.

Sommaire

Le graphisme gagne en présence dans les interfaces et documents numériques mais est accessible aux personnes non-voyantes quasi-exclusivement sur media à flexibilité limitée tel que le papier embossé. Le texte est plus accessible mais néanmoins limité par le coût et les fonctionnalités des afficheurs Braille et de la synthèse vocale. Cette thèse explore l'utilisation d'une nouvelle approche pour la stimulation tactile opérant par déformation latérale de la peau pour l'affichage informatisé de Braille et de graphiques tactiles virtuels.

La synthèse tactile par déformation latérale de la peau est initialement explorée dans le contexte du Braille. La faisabilité de produire du Braille virtuel par stimulation latérotactile est d'abord démontrée en créant une illusion de frottement contre une ligne de points par la synchronisation d'une onde progressive de déformation de la peau avec le déplacement d'une plage tactile à 8 actionneurs. Ce principe est ensuite étendu au Braille à 6 points par la distribution de lignes de points virtuels sur les rangées d'actionneurs d'un afficheur tactile STReSS^2. La lecture de ce Braille virtuel est généralement faisable mais exigeante, suggérant qu'un afficheur Braille latérotactile soit conçu ou que le rendu des points vise le contraste plutôt que le réalisme.

Le rendu tactile par déformation latérale de la peau est ensuite exploré plus à fond avec le développement graduel d'un système de graphique tactile virtuel qui émule des éléments conventionnels tels que les traits surélevés et les surfaces texturées à travers un ensemble cohérent de motifs incluant des textures à rayure, des formes tracées ou pointillées, des masques par image, et des motifs composites. Le rendu dynamique est ensuite exploité pour produire de nouveaux effets tel que le flot tactile, les textures réactives répondant au comportement d'exploration, et le contenu interactif avec vues alternatives. L'ergonomie du système est évaluée informellement avec des volontaires non-voyants et les premiers motifs tactiles étudiés à travers des expériences formelles. Les motifs tactiles sont présentés sur le Tactograph, une interface haptique reconçue spécifiquement pour l'affichage de graphiques tactiles qui combine un afficheur STReSS^2 à un charriot planaire instrumenté.

Cette thèse démontre le potentiel de la déformation latérale de la peau pour l'affichage de Braille et de graphiques tactiles, et explore ainsi comment cette approche à la stimulation tactile peut être appliquée à la production de sensations tactiles signifiantes.

Acknowledgments

Foremost, I would like to thank my supervisor, Prof. Vincent Hayward, without whom this work would not have been possible. His support, encouragement and creativity have made this challenging experience both pleasant and rewarding.

This thesis also rests on an innovative technology that was developed under his supervision by Christine Desmarais, Juan Manuel Cruz-Hernandez, Jérôme Pasquero, and Qi Wang. I am indebted to them all for their dedication and hard work, and wish to particularly thank Qi Wang for his help and support with the latest prototype.

I have had the chance to work alongside many inspiring and helpful colleagues during my years in the Haptics Laboratory. Jérôme Pasquero has been a valuable collaborator and friend, and has influenced this work through innumerable discussions. Andrew Gosline patiently shared his mechanical engineering skills and helped me with the design of the Tactograph. Mounia Ziat's expertise was invaluable for the supplementary statistical analysis presented in Chapters 4 and 6. I would also like to thank other past and present members of the Haptics Lab and Center for Intelligent Machines for their support and friendship (in alphabetical order): Omar Ayoub, Gianni Campion, Hanifa Dostmohamed, Diana Garroway, Prasun Lala, Akihiro Sato, Qi Wang, and Hsin-Yun Yao. I'm especially grateful to Sandra Skaff with whom I've shared much of this experience and who has proved a supportive and valuable friend.

I would also like to thank Jean-Samuel Chenard for sharing his electronics expertise and saving in extremis a demonstration of the tactile graphics system, and Don Pavlasek of the Mechanical Workshop (ECE dept.) for his advice and meticulous work. This work also benefited from a collaboration with Gregory Petit (UdeM), Prof. Aude Dufresne (UdeM), Nicole Trudeau and Pierre Ferland (INLB), with whom I've had numerous interesting discussions about tactile graphics. I would also like to thank Maryse Legault (HumanWare), Chantal Nicole (INLB) and Marie-Chantal Wanet-Defalque (INLB) for their assistance. VisuAide, now HumanWare Canada, also provided the initial impetus for this research and donated experimental hardware used for the early work on Braille.

Last but not least, I wish to thank my parents, Suzanne and Viateur Lévesque, my sister, Danny Lévesque, as well as my family and friends for their support and encouragement throughout these years.

Contents

List of Figures

List of Tables

List of Acronyms

CPR	Counts per Revolution
CRIR	Centre de Recherche Interdisciplinaire en Réadaptation du Montréal Métropolitain
DOF	Degrees of Freedom
FPGA	Field-Programmable Gate Array
GPS	Global Positioning System
INLB	Institut Nazareth et Louis-Braille
PC	Pacinian Corpuscle
PNG	Portable Network Graphics
PWM	Pulse Width Modulation
RA	Rapidly Adapting
RFID	Radio Frequency Identification
STReSS	Stimulator of Tactile Receptors by Skin Stretch
STReSS^2	Second Generation STReSS Display
SA	Slowly Adapting
THMB	Tactile Handheld Miniature Bimodal Device
TVSS	Tactile-Video Substitution System
USB	Universal Serial Bus
VBD	Virtual Braille Display
WPM	Words per Minute
XML	Extensible Markup Language

Chapter 1

Introduction

A visual impairment forces a person to develop a strong ability to make functional use of other often-neglected senses. The sense of touch can, as a result, be developed to interpret sophisticated tactile patterns such as Braille and gather a surprising amount of information through subtle tactile cues such as the friction of a white cane against the ground. This attention and appreciation for the sense of touch makes visually impaired persons natural users of haptic technologies and invaluable allies in the development of experimental interfaces that aim to communicate information through this underused sense. In this thesis, tactile sensations synthesized using programmable tangential strain patterns are developed in the context of Braille and tactile graphics in an effort to improve both the accessibility of textual and graphical content for visually impaired persons, and the understanding of this approach to computerized tactile stimulation.

Accessibility

Braille has played a significant role in the empowerment of visually impaired persons by defining a tactile code that can not only be read but also written, and hence enabling literacy. Refreshable Braille displays, and more recently voice synthesis hardware and software, have for many years maintained the accessibility of written information as it migrated gradually to digital media. These solutions nevertheless present drawbacks. Refreshable Braille displays are limited to a single line by space and cost constraints yet generally more expensive that the personal computer they are used with. Voice synthesis, on the other hand, reduces control over the reading rate and provides an al-

together different communication medium that hides individual characters and hence a crucial aspect of the written language. There is therefore much room for improvement and innovation in the delivery of textual information to visually impaired readers.

The use of these technologies with screen readers has nevertheless provided an acceptable solution for access to computer interfaces and digital media until recently. The increasingly pervasive use of visual content, however, threatens to severely limit the usability of digital interfaces and hence exclude the visually impaired community from some of the most exciting innovations. Graphical information is no longer restricted to isolated pictures and diagrams, and instead often provides the bulk of the content in applications such interactive mapping systems or a coherent structure for textual content in documents such as web pages. Providing access to this graphical information is complicated by technological as well as physiological issues. Although the means of production have improved in recent years, tactile graphics are still created through a cumbersome process that results in static, physical media and are hence much less flexible and immediately accessible than their visual counterparts. The conversion of visual graphics into a tactile form furthermore requires a simplification of the content and reduction of the information density to accommodate the lower acuity of the sense of touch, often resulting in a set of complementary tactile graphics for a single visual equivalent. These issues could be alleviated by providing interactive access to dynamic graphical content through refreshable tactile graphics interfaces. The development of such interfaces, however, remains an open research topic.

Haptic Interfaces

The design of haptic interfaces has been an active research topic in recent years, with much effort focusing on the display of virtual or refreshable tactile patterns with direct or indirect applications for visually impaired persons. Alternative technologies for the display of Braille have been investigated but none has been able to dislodge the expensive but effective piezoelectric refreshable Braille cell. Technologies for the refreshable display of tactile graphics have on the other hand remained, with few exceptions, experimental and have yet to be used widely by the visually impaired community. Force-feedback interfaces with a single point of contact have notably been used to display virtual surfaces and hence show maps, diagrams and other tactile graphics.

A wide variety of skin stimulation methods have similarly been used to create tactile transducers that produce a programmable distributed stimuli on the skin. A typical approach consists of approximating the local height of a 3D surface with a programmable matrix of actuated pins. Despite much progress, a variety of technical and practical issues have prevented these novel tactile interfaces from gaining wide acceptance in the visually impaired community as viable alternatives to more established methods such as embossed paper and thermoformed plastic.

This thesis focuses on a novel approach to skin stimulation that synthesizes artificial tactile sensations by creating tangential strain patterns on the fingerpad skin. Referred to as laterotactile stimulation, this approach triggers the impression of brushing against tactile features through the controlled activation of a dense array of laterally-actuated contactors held against the fingerpad skin. This concept of tactile rendering by lateral skin deformation is explored and elaborated in the context of Braille and tactile graphics by giving rise to virtual tactile patterns as fingerpad-sized laterotactile arrays are physically displaced over a line or plane.

Problem Statement

The programmable display of dynamic tactile patterns by lateral skin deformation presents an opportunity to improve the accessibility of textual and graphical content for visually impaired persons. This approach to tactile stimulation, however, presents significant challenges due to the limited knowledge of the relation between lateral skin deformation and tactile perception. A laterotactile array does not artificially reproduce the physical properties of a tactile object, but rather creates the illusion of brushing against it through a perceptual and physiological process that has yet to be fully understood. The production of meaningful and useful tactile sensations through the controlled activation of a laterotactile display's actuators, a process referred to as tactile rendering, is therefore an open research problem and the primary topic addressed in this thesis.

The research presented in this thesis aims to demonstrate the feasibility of producing by lateral skin deformation virtual tactile patterns that are suitable for use in the context of two applications for persons with visual impairments — Braille and tactile graphics — and in the process gain a better understanding of this novel tactile

stimulation method. This entails the empirical development and evaluation of rendering algorithms producing sensations that either resemble those experienced with conventional tactile media, or allow the communication of equivalent information. The content of a Braille character can, for example, be presented either realistically or through higher-contrast, abstract patterns that reproduce the cell's spatial layout. Efforts are also made to identify optimal rendering parameters and to exploit novel affordances introduced by the dynamic properties of laterotactile Braille and graphics. A re-evaluation and adaptation of conventions designed for other media having different strengths and weaknesses is also required.

These objectives are addressed through the iterative development, evaluation, and refinement of laterotactile rendering algorithms. The relevant application domains are first studied to determine best practices and identify potential improvements in the user experience. Rendering algorithms are then empirically developed based on experience and intuition, and a wide range of parameters made available for fast alteration. The resulting rendered patterns are then informally evaluated with a small number of reference users, and the feedback provided used to perform an initial tuning of the rendering algorithms and narrow down the parameter space for further investigation. The resulting tactile rendering algorithms are finally formally evaluated based on performance at a critical task, such as the identification of Braille characters, and the effect of a small number of parameters of particular interest estimated. This process is repeated to iteratively refine the tactile rendering algorithms and gain a better understanding of their practical usability.

Thesis Overview

This thesis investigates the synthesis of tactile sensations by lateral skin deformation and its applications for the accessibility of textual and graphical content by visually impaired persons. The core of the thesis can be divided in two main parts. Chapters 3 and 4 first describe the design, refinement and evaluation of novel techniques for the display of virtual Braille by laterotactile stimulation. This work is then extended in Chapters 5 to 9 to the display of virtual tactile graphics, introducing a dedicated haptic interface and a flexible framework for the rendering of static and dynamic tactile patterns. Chapters 3 to 6 reproduce the content of published manuscripts documenting the

progression of the concept of laterotactile rendering in these two domains. The next three chapters present unpublished work describing the latest developments and accumulated knowledge on laterotactile rendering and its applications for virtual tactile graphics. Each chapter is described in more details below.

Chapter 2 provides an extensive review of the literature on visual impairment and assistive technologies for visually impaired persons, with special emphasis on the applications of haptic and tactile feedback. The chapter includes in-depth coverage of conventional and experimental approaches to Braille and tactile graphics.

Chapter 3 reports on the design and evaluation of tactile rendering algorithms for the display of lines of virtual Braille dots by lateral skin deformation. This work was realized using a specially-designed electromechanical tactile display prototype with fewer but stronger actuators than its predecessors, allowing the feasibility of producing Braille-like sensations by tangential deformation to be demonstrated for the first time. Travelling waves of local skin strain were tuned to approximate the sensation of brushing against lines of Braille dots and reading shown to be possible but demanding.

Chapter 4 reports on the design and evaluation of extended rendering algorithms for the display of complete 6-dot Braille. This work was realized with the STReSS^2, a newly available general-purpose tactile display with a 10×6 array of laterally-moving skin contactors [289]. Rendering 6-dot Braille cells was accomplished by distributing lines of virtual dots onto the rows of the tactile array and optionally increasing contrast with a textured pattern in place of dots. Reading was shown to be possible in most cases but difficult and slow, suggesting that a specialized Braille display be devised or realism be abandoned in favour of high-contrast symbolic patterns.

Chapter 5 shifts focus to the display of virtual tactile graphics through a haptic memory game that requires tactile rather than visual patterns to be matched. Performed with an interface named Tactograph that combines a STReSS^2 tactile array with an instrumented planar carrier, this early work re-purposes rendering approaches designed for Braille and introduces concepts such as grating textures, dot patterns and vibration rendering that form the basis of a virtual tactile graphics framework refined and evaluated in later chapters.

Chapter 6 presents a more detailed description and evaluation of an improved virtual tactile graphics framework that supports arbitrarily-oriented grating textures, radially-rendered dots, vibrating patterns and bitmap-based masks. The results of ex-

periments performed with both sighted and visually impaired subjects demonstrate the feasibility of displaying identifiable shapes and textures by tangential skin deformation, and provide insight into practical considerations such as the minimal spatial wavelength difference necessary to distinguish adjacent grating textures.

Chapter 7 reports on the design and implementation of an improved haptic interface designed specifically for the display of virtual tactile graphics that addresses many limitations of its predecessor. This redesigned Tactograph includes improvements such as a larger virtual canvas and additional sensors for the measurement of the orientation of the tactile array and the pressure applied with the reading finger.

Chapter 8 presents a comprehensive framework for the rendering of virtual tactile graphics by lateral skin deformation that extends previously-described rendering approaches, introduces novel ones, and re-frames the whole as a coherent set of tactile patterns. The concept of a grating texture is, for example, extended to include axial and radial gratings, and gaps optionally inserted between grating ridges for better definition. Major additions to the framework include a set of compositing operators allowing complex tactile patterns and textures to be created, as well as vector graphics drawing capabilities introduced through the concept of a tactile stroke.

Chapter 9 finally describes extensions to the virtual tactile graphics framework that take advantage of the opportunities afforded by dynamic tactile rendering. Tactile flow is first introduced in the rendering of textures, stroked shapes and dotted shapes through the motion of tactile features. Reactive rendering is then investigated through the alteration of textures in response to changes in exploration behaviour. Interactive graphics are finally briefly explored in the form of alternative views of a canvas' content.

Chapter 10 concludes the thesis with a summary of the main findings and discussion of future directions in which this research could be taken.

Summary of Contributions

This thesis makes the following contributions:

1. The design, implementation, and experimental evaluation of laterotactile rendering patterns simulating the sensation of brushing against lines of Braille dots and complete 6-dot Braille cells through travelling waves of lateral skin deformations.

2. The design and implementation of a haptic interface designed specifically for the display of virtual tactile graphics by lateral skin deformation that combines a STReSS^2 tactile display with a specially-designed instrumented planar carrier.

3. The design, implementation, and experimental evaluation of a comprehensive framework for the rendering of virtual tactile graphics by lateral skin deformation that emulates tactile features found in conventional tactile graphics and provides basic vector drawing capabilities through a set of tactile features comprising:

   - textures rendered with vibrations, gratings, or tiled patterns;
   - raster images used as masks;
   - textured strokes and stroked shapes;
   - raised dots and dotted shapes;
   - composite patterns formed by superposition of simpler textures or patterns.

4. The design, implementation, and preliminary evaluation of dynamic effects in the rendering of virtual tactile graphics by lateral skin deformation, such as:

   - the rendering of tactile flow along textures, stroked shapes, and dotted shapes;
   - the reactive rendering of textures as a function of the exploration behaviour;
   - the interactive selection of alternate tactile graphics views.

Chapter 2

Assistive Technologies for Visually Impaired Persons

2.1 Introduction

Blind and visually impaired persons have long been believed to be well positioned to reap the benefits of haptics research. While sighted persons are often not keenly aware of the importance of their non-visual senses, blind persons depend on them and are thus in a unique position to appreciate and make functional use of haptic interfaces. The efforts necessary to design aids that meet the needs and requirements of persons with visual impairments, however, should not be underestimated. This chapter therefore aims to provide background information pertinent to the development and the design of assistive devices for visually impaired users that leverage haptic technologies.

The chapter begins with a brief introduction to human haptics and haptic technologies, followed by an overview of the literature on blindness intended to help designers better understand the needs of the blind community. The literature on assistive technologies for visually impaired persons is then surveyed, covering a wide range of topics including graphics, Braille and mobility aids, with special emphasis on the use of haptic interfaces. The chapter finally closes with general recommendations for the design of assistive devices and a speculative discussion about the future of technological aids and applications of haptics for visually impaired persons.

2.2 Haptics

The term *haptics* is generally used to refer both to the study of the human somatosensory system, and to the development of technologies that artificially stimulate it. The somatosensory system comprises the senses of discriminative touch, pain and temperature, as well as proprioception, the sense of the position and movement of the limbs and body [242]. The perception of limb movement is also often referred to as kinaesthesia.

The sense of touch is mediated by four types of mechanoreceptors embedded in the glabrous skin. Four types of mechanoreceptive afferents have similarly been identified by microneurography and tentatively matched to mechanoreceptors [81]. The afferents vary based on their rate of adaptation to stimuli, either slowly adapting (SA) or rapidly adapting (RA), as well as the size of their receptive field, small (I) or large (II). The slowly adapting receptors, Merkel receptors (SA I) and Ruffini cylinders (SA II), are respectively most sensitive to pressure (0.3-3 Hz) and stretching of the skin (15-400 Hz) [81]. The rapidly adapting receptors, Meissner corpuscles (RA I) and Pacinian corpuscles (PC or RA II), are on the other hand most responsive to taps on the skin (3-40 Hz) and vibrations (10-500 Hz) [81]. The neurophysiology of touch is however much less developed than that of vision or audition, with recent studies, for example, shedding doubt on the very existence of Ruffini cylinders in the human glabrous skin [200].

Haptic technologies generally fall within the broad categories of force-feedback interfaces, which stimulate primarily kinaesthesia, and tactile interfaces, which stimulate the cutaneous senses. Force-feedback interfaces typically monitor the position of a manipulandom, often a pen or thimble, and produce forces that simulate the interaction between a tool and physical objects. The most common interface of this type is the PHANTOM (SensAble Technologies Inc., Massachusetts), which applies forces with 3 or 6 degrees of freedom (DOF) through an actuated arm. Many other force-feedback interfaces, both experimental and commercial, have also been proposed, including actuated gloves such as the CyberGrasp (Immersion Corp., California) and haptic mice such as the WingMan force-feedback mouse (Logitech International S.A., Switzerland). The most common tactile interfaces are simple vibrotactile stimulators, as used in mobile phones and computer mice such as the Logitech iFeel mouse. Another type

of tactile interface, less common but of relevance to this thesis, is a device called a tactile display that applies distributed tactile stimuli to the skin, most often at the fingertip. Tactile displays often consist of large arrays of raised pins such as the Dot View DV-2 (KGS Corp., Japan), or smaller movable arrays such as the VTPlayer (VirTouch, Israel), a mouse with two 4×4 matrices of actuated pins. The work presented in this thesis relies on tactile displays of the latter category but operating by lateral skin deformation, a novel approach to skin stimulation that shows promise for the display of virtual tactile patterns.

2.3 Blindness and Visual Impairment

2.3.1 Definition, Prevalence and Causes

Vision loss affects a wide variety of persons and takes diverse forms depending on the cause of the impairment and its impact on the visual acuity and visual field [294, 100]. The degree of impairment can range from a slight blurring of the vision to a complete loss of light perception, with every gradation in between. The field of view may similarly be narrowed or limited by "blind spots." The age of onset of blindness also varies and may be significant since it can affect a person's perception, representation of space and attitude towards blindness.

The relevant terminology differs depending on countries and contexts. The term *vision loss* generally refers to any difficulty in seeing that cannot be addressed with corrective lenses [11]. More restrictive terms such as *low vision* and *blindness* (or *legal blindness*) are defined in the United States as a visual acuity worse than 6/12 or 6/60 respectively [167]. A visual acuity of 6/60, for example, indicates that letters read only at 6 m could be read at 60 m by a person with perfect sight [11]. A visual field of 20° or less is also considered sufficient for blindness. The term *visually impaired* is often used to collectively refer to persons with either low vision or blindness. Similar terminology is used with different definitions by the World Health Organization, complicating the compilation of statistics [167]. The terms *congenital* and *adventitious*, or *early* and *late*, are also occasionally used to describe whether a vision loss has occurred at birth or later in life. Although defined strictly for legal and statistical purposes, many of these terms are also often used more loosely in the literature and in everyday parlance.

The prevalence of blindness and low vision in Canada has been estimated at 0.24%

and 0.71% respectively (or approximately 78 000 and 234 000 persons) [167]. The American Foundation for the Blind (AFB) reports that the number of Americans with significant vision loss reaches more than 20 million [11]. Of these, 1.3 million were reported to be legally blind in a 1994 survey, 80% of them having some residual vision [11, 154]. A more recent report indicates that there are approximately 57,696 legally blind children in the U.S. [11]. Another study estimates that 937,000 Americans older than 40 years are blind, and an additional 2.3 million have low vision [272]. The prevalence of visual impairment significantly increases with age [272, 11, 191, 154]. Vision loss among seniors and persons aged from 45 to 64 years reaches approximately 6.2 and 9.0 millions respectively in the U.S. [11]. The prevalence of visual impairments is therefore expected to increase with the aging of the population in developed countries [272, 11, 154, 100]. Worldwide, an estimated 37 million persons are believed to be blind and 124 million more to have low vision, 90% of them in developing countries and 75% due to causes that are preventable or curable [269].

Only a minority of visual impairments appear at birth [90] and a significant proportion of persons with vision loss also have other impairments [191]. The leading causes of visual impairment in Canada are estimated to be cataracts, age-related macular degeneration and visual pathway and other retinal diseases [167]. Cataracts, glaucoma and macular degeneration are similarly identified as leading causes worldwide [225]. Of particular interest is diabetic retinopathy which not only impairs vision but also touch, and may therefore affect the usability of haptic interfaces. According to the American Diabetes Association, “diabetes is responsible for 8% of legal blindness, making it the leading cause of new cases of blindness in adults 20-74 years of age” [10].

2.3.2 Neurology and Psychology

Deprivation of visual input to the brain during a critical period of development is known to cause permanent damage to the visual cortex [100]. Experiments have, for example, shown that animals deprived of vision during this developmental period do not respond to visual stimuli once their sight is restored. Similar clinical observations have been made when restoring sight to congenitally blind persons, for example, by removal of cataracts.

Brain imaging techniques have been used to study in more details the functional re-

organization occurring in the brain as an adaptation to blindness. Studies with Braille readers have, for example, shown that the cortical representation of the dominant reading finger is disproportionately large [60, 80]. Similarly, studies have shown that the visual areas of the brain can be activated by tactile or auditive stimulation in blind persons [76, 74, 80]. The significance of these results is the subject of debate. It is not clear, for example, that an increase in cortical representation of a finger translates into an increase in tactile acuity. Studies have shown however that deactivation of the primary visual cortex (V1) causes a drop in Braille reading performance for early blind persons [74], and interferes with verbal processing in blind persons [9].

This debate finds echoes at the perceptual level with the theory of sensory compensation, according to which a blind person's unimpaired senses are heightened to compensate for the loss of sight. While many textbooks on blindness take a conservative stance against the theory [294, 100], there is mounting evidence from recent studies for limited sensory compensation [19]. It has, for example, been suggested that blindness, particularly when occurring early, enhances auditory perceptual and cognitive functions [262]. The tactile acuity of an average blind person has also been shown to be the same as that of a sighted person of the same gender but 23 years younger [80]. Other studies, however, report mixed evidence concerning tactile perception of pattern and form [294] and that some sound localization skills may be impaired by early blindness [311].

Despite the controversy, it is generally agreed that visually impaired persons are more proficient at attending to non-visual stimulus and make better functional use of non-visual senses [294, 100]. It seems, for example, that "the blind have, through need, learned to attend better to auditory stimuli and therefore can make more use of the available auditory information than sighted people" [294, p. 67]. A good example is the *obstacle sense* that allows blind persons to feel the presence of obstacles. Researchers have shown that the obstacle sense is mediated by audition and can be learned by blindfolded sighted subjects. The use of efficient strategies and exploratory techniques has similarly been shown to be responsible for the better performance of visually impaired persons at judging the curvature of a long object such as a ruler [100].

The mental images of visually impaired persons have also raised much interest. Defined as a "mental experience which occurs in the absence of stimulation, but which resembles the experience that occurs when a stimulus is actually present" [100, p. 83],

a mental image tends to be strongly visual for a sighted person, even when arising from touching an object [100]. Mental images are also experienced by early blind persons but seem to be of a different nature, allowing, for example, the perception of "both the front and back of a palpated object at the same time" [100, p. 86]. The extent to which vision is necessary to mediate the perception of space is also the subject of much debate [273, 125].

2.4 Technological Aids

Visually impaired persons have at their disposal a variety of simple yet effective specialty items that facilitate the performance of tasks of daily living. This includes special watches and alarm clocks, magnetic Braille labels, tactile tags for clothing colors, and even adapted mobile phones. Other aids such the long cane and the guide dog are also widely used to improve the mobility and independence of visually impaired persons. This section surveys a wide range of assistive technologies, many of which have not reached the prominence of these simple aids but have nevertheless proved quite useful. Assistive devices aimed at mobility and orientation are first described. The accessibility of text and graphics, the main topic of this thesis, are then covered in details, followed by non-visual human-computer interaction. Vision substitution systems and advances in sight recovery are finally discussed. Special attention is given to applications of haptic technologies throughout the survey.

2.4.1 Orientation and Mobility

The ability to navigate safely and efficiently in an unknown environment is essential for the independence, well-being and participation in society of visually impaired individuals. The skills required for independent travel are classified as orientation and mobility, with the former term referring to the ability to situate oneself in an environment and find a route to a destination, and the latter referring to the ability to negotiate obstacles and find a clear path. Despite much effort to develop more sophisticated aids, orientation and mobility needs remain most commonly addressed with the long cane or guide dog.

Invented in the 1940s, the long cane is the most widely used mobility aid with a recent estimate of 109,000 American users [11, 100]. The cane allows the detec-

tion of obstacles and drop-offs but does not warn of overhanging objects such as tree branches. Its short range of approximately one meter forces users to be prepared to stop or correct course quickly and therefore limits walking speed [100]. The cane is also easily identified, warning bystanders to clear the way but also marginalizing its users [33]. Despite these shortcomings, the long cane is an invaluable instrument that provides rich information through both audio and tactile feedback. Used by making arcs, the cane taps against the ground and informs its user not only of obstacles but also of the texture, material and slope of the ground. The sound emitted by the contact also serves for obstacle detection by echolocation [33, 100]. A wide variety of long canes is available, including telescopic or folding canes that can conveniently be hidden away when not in use [8].

The guide dog is also a popular mobility aid with approximately 7,000 American users [11]. Guide dogs have been shown to improve a visually impaired person's mobility and to bring benefits such as independence, confidence, companionship and socialization [298]. Guide dogs, however, must be cared for by their owners and trained by professionals at significant expense, reducing their availability.

Much effort has gone into the development of sophisticated electronic travel aids that leverage technology to address the limitations of the long cane and guide dog. Most wisely aim to supplement rather than replace these effective aids [28], and none has yet to gain widespread acceptance in the blindness community despite many commercialization attempts [231]. The remainder of this section provides a brief overview of aids addressing mobility and orientation needs. Readers are referred to [109, 231, 33, 47, 191, 100, 90, 12] for more extensive surveys.

Mobility

Typically used in conjunction with a long cane or guide dog, mobility aids assist visually impaired travelers in finding a safe, clear path by providing advance warning of obstacles that may otherwise go undetected. Most mobility aids aim to extend the range of detection and protect against over-hanging obstacles.

Vision substitution systems, covered in more details in Section 2.4.5, provide visual information through sophisticated audio or tactile feedback and can therefore serve as mobility aids. The SonicGuide, for example, converts readings from ultrasound sensors embedded in a pair of glasses into a stereo audio signal encoding the dis-

tance, size, texture and direction of obstacles through variations in pitch, amplitude, timbre and stereo delay [3, 124]. Although the richness of the information provided can be extremely useful, its interpretation requires much effort and is possible only after extensive training [56]. Most mobility aids therefore choose to process the environmental data gathered with their sensors and present simplified information to the user [231, 109]. This approach has the benefits of requiring less training, reducing the cognitive load of device operation and lowering costs.

(a) (b)

Fig. 2.1 Examples of electronic mobility aids: (a) the MiniGuide and (b) the UltraCane. (Pictures used with permission from GDP Research and Brian Hoyle respectively.)

A recent survey has identified and classified 146 electronic travel aids and found twelve of them to be available commercially as obstacle detectors [231]. These aids rely on infrared, ultrasonic or laser technologies to sense the environment. Although most support audio feedback, many also provide tactile feedback as a primary or secondary output. The MiniGuide (Figure 2.1a), for example, is held like a flashlight and indicates the distance of objects detected by an ultrasound beam with a vibrotactile or audio signal of variable frequency [97]. The UltraCane (Figure 2.1b), on the other hand, has the appearance of a normal long cane but indicates the presence and distance of obstacles through two vibrating buttons on its handle [209]. Other aids are carried around the neck, head mounted or attached to a white cane [231].

Many more experimental mobility aids have been proposed in the literature. The Teletact2, for example, conveys the distance to obstacles through vibrators located under four fingers [109]. Many have similarly attempted to convey obstacle directions or guidance cues through arrays of vibrotactile stimulators disposed on the torso or around the waist [253, 38]. Others have opted instead for the use of mobile robots as replacements for guide dogs. The GuideCane, for example, is a small robot that

determines a safe path by ultrasound and guides the user pushing it by simple rotation of its wheels [253]. A similar approach has also been used with additional guidance information and obstacle warnings provided by an electrotactile display [264].

Orientation

Although obstacle detection and avoidance are important, commonly-used travel aids such as the long cane and the guide dog perform those tasks satisfactorily for many blind individuals. Orientation in an unknown environment and navigation towards a destination, on the other hand, are problematic issues that are not properly addressed by these aids [47].

The orientation needs of visually impaired persons can be handled by disposing accessible navigation signs in the environment. Although fairly simple technically, this solution generally requires retrofitting buildings and street signs to incorporate active or passive beacons. The Talking Signs system (Tactile Signs, Inc, Louisiana), for example, relies on infrared transmitters that broadcast verbal messages to handheld receptors (Figure 2.2a). Although installed in some cities, these systems have yet to become widespread and are unlikely to become so unless co-opted by society at large for other purposes [18].

(a) (b)

Fig. 2.2 Examples of orientation aids: (a) Talking Signs receiver, and (b) Humanware Trekker with GPS receiver. (Pictures used with permission from Talking Signs, Inc. and HumanWare respectively.)

A more promising approach is to rely on advances in location-aware computing, which are now becoming commonplace in cars, mobile phones and even cameras. A recent survey has, for example, identified eight commercially-available electronic mobility aids that provide navigation assistance to visually impaired travelers using position information obtained from Global Positioning System (GPS) receivers (Fig-

ure 2.2b) [231]. These aids provide information about a person's location, nearby points of interest, and routes to destinations through speech and non-speech audio as well as, in some cases, refreshable Braille. More experimental aids have also attempted to provide navigational cues through vibrators disposed on belts or vests [233, 63, 96]. These aids greatly benefit from their reliance on sophisticated but affordable technologies developed for larger markets.

Unfortunately, GPS receivers are known to be unreliable in dense urban areas with high-rise buildings and generally unusable indoors [109]. These issues could potentially be partially addressed using other triangulation sources, such as wireless networks or mobile phone towers, as well as dead-reckoning with inertial sensors. Computer vision could also be relied upon to identify known environmental markers. The detection of crosswalks was, for example, shown to be possible using nothing more than a mobile phone equipped with a camera [246]. An orientation aid should ultimately be capable of providing rich semantic information about a person's environment including not only street names but also door labels and more subtle cues such as the presence of light in a room [109].

2.4.2 Reading and Writing

Invented in 1829, Braille is a tactile code that replaces printed characters with simplified patterns of raised dots adapted to the tactile sensitivity of the fingertip [65]. Each Braille cell is formed of a 2×3 matrix of dots that encodes a character or group of characters. The success of Braille over competing tactile codes owes not only to the efficiency with which it is read, but also to the possibility of writing it with simple tools, a necessity for the development of literacy [261]. Braille proficiency has notably been associated with higher employment rates and educational levels, self-sufficiently, independence, self-esteem and feelings of competence [236, 241]. Contrary to general belief however, Braille literacy is low and declining [154, 100, 236, 241, 261]. This may be explained by the effort necessary to learn Braille and the stigma associated with this symbol of blindness [241], and more recently by the availability of alternative media. An estimated 5,626 legally blind children nevertheless use Braille as their primary reading medium in the United States [11].

Although considerable variations can be observed between individuals, Braille is generally read slower than print [65]. A recent study, for example, reports average

reading rates of 124 words per minute (wpm) for Braille and 251 wpm for print, noting however that the fastest Braille readers can match or even exceed the speed of sighted readers [151]. Although all fingers often contribute, Braille is generally read mainly with one or both index fingers [65]. Both hands are nevertheless often used. The slower readers use their second hand for nonreading functions such as finding the next line whereas the fastest readers use both index fingers cooperatively to avoid regressions and reduce wasted intervals while switching lines. Braille is moreover read by brushing against it rather than by resting on it [254, 52].

Braille is generally produced on paper with specialized printers, resulting in highly-readable but bulky documents that deteriorate with use (Figure 2.3a). Digitized content can alternatively be read on refreshable Braille displays which typically present a line of forty or eighty electromechanical Braille cells (Figure 2.3b). Each Braille cell consists of a 2×4 matrix of dots actuated by cantilevered piezoelectric bending motors [274]. Commercially available for many decades, refreshable Braille displays have proved effective but expensive due to the large number of actuators required to activate every dot. Although desirable, full-page Braille displays are economically unviable with this actuation technology.

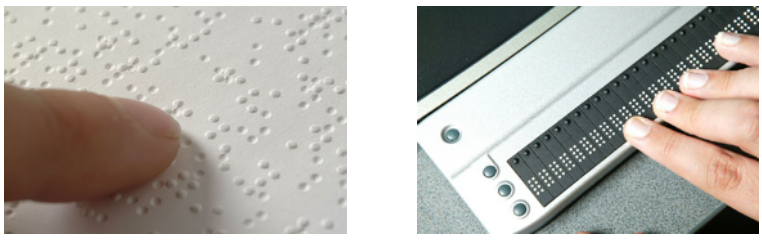

(a) (b)

Fig. 2.3 (a) Paper Braille and (b) refreshable Braille display. (Pictures used with permission from Mario Sánchez Bueno and Pulse Data International Ltd. respectively)

Numerous efforts have therefore been made to improve upon the piezoelectric Braille display. A majority of these attempted to actuate dots or dimples using alternative technologies such as solenoids [51], piezoelectric linear motors [40, 281], relays [259], bimetallic strips [46], flappers [302], shape memory alloys [87], ultrasonic motors [142] and electrorheological fluids [2]. The batch fabrication and miniaturization of Braille cells has also been investigated with microelectromechanical systems

such as microheating elements [150, 138], microvalves [300, 303], and polymeric actuators [122]. While promising, these technologies have yet to prove sufficiently practical and economical to replace the piezoelectric Braille cell.

The display of moving Braille to passive fingers has also attracted attention for its potential to significantly reduce the complexity of displays [198, 85, 29]. Braille pins moving at the edge or rim of a rotating wheel can, for example, be set in the correct state by a small number of actuators as they enter a reading window [192, 228]. Conversely, attempts have been made to create the illusion of a large Braille line using small moving tactile arrays [68, 66, 221]. Ramstein, for example, mounted a pair of Braille cells on a planar carrier and displayed a sequence of characters as they were displaced along a virtual line, resulting in less realistic but readable Braille [221]. Braille-like patterns have also been produced using electrotactile [218], thermal [29] and vibrotactile [41] stimulation. Although they present advantages, the acceptability of these approaches to visually impaired readers has yet to be demonstrated.

Written information can also be accessed by pre-recorded or synthesized speech. Digital talking books and the Digital Accessible Information SYstem standard (DAISY), for example, allow efficient navigation through indexed audio content. Much cheaper than refreshable Braille displays and requiring no knowledge of Braille, voice synthesis is also popular for access to digital media and more generally to computer interfaces. Although normal speech can be fairly slow, it can be compressed to reach rates up to 275 wpm without affecting comprehension or retention significantly [294].

Numerous efforts have also been made to provide equal access to the vast quantities of material available only in print. The Kurzweil Reading Machine was the first to combine an optical scanner, optical character recognition software, and a speech synthesizer [100]. These components are now widely available commercially and allow blind readers some access to printed material. Such a system, however, is not portable and may not be capable of recognizing degraded text or handwriting. Using a different approach, the Optacon directly maps images from a camera to a vibrotactile equivalent (Figure 2.4a). Tactile sensations are experienced through a miniature tactile display consisting of an array of 24×6 vibrating pins [31]. As the camera slides over a printed character, a corresponding tactile sensation moves across the fingertip. With considerable training, a typical reading speed of 30 to 60 wpm can be achieved [79]. The device can also be used, to a lesser extent, to explore printed graphics. A similar

device, the Top-Braille (Vision SAS, France), has recently been marketed for a similar purpose using a single Braille cell or synthesized speech as a communication medium (Figure 2.4b).

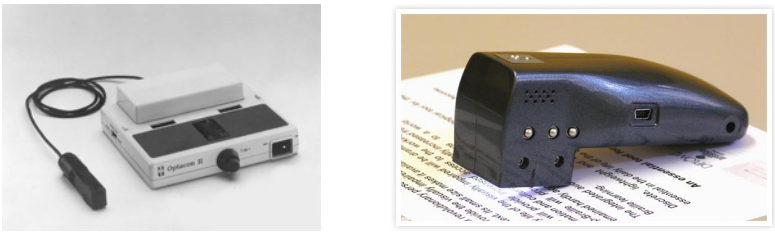

(a) (b)

Fig. 2.4 Example of print reading aids: (a) Optacon II, and (b) Top-Braille (used with permission from Vision SAS).

2.4.3 Graphics

Conventional Tactile Graphics

Visual representations of information are used extensively by the sighted but are much less accessible than textual content for visually impaired persons. Graphical content can nevertheless be adapted for tactile consumption and produced on static media such as embossed paper, thermoformed plastic or a collage of mixed materials [59, 235]. Tactile graphics are used in a variety of contexts but are most critical in the classroom where scientific and technical topics are often taught using graphs, bar charts (Figure 2.5a), geographical maps (Figure 2.5b) and other visual representations [59, 36, 99, 98, 6, 247]. Tactile maps can also provide sufficient information for visually impaired persons to orient themselves and navigate autonomously in an unknown environment [59, 91].

Producing effective tactile graphics, however, presents significant challenges. Visual material must be simplified to take into account the lower resolution of the sense of touch [100, 91] and carefully adapted to avoid visual conventions such as perspective which may be understood only with extensive training [100]. The density of information found in tactile graphics such as maps is generally much lower than for their visual counterparts, forcing producers to eliminate details or spread them across multiple sheets [201, 110, 59]. Tactile graphics are generally produced by

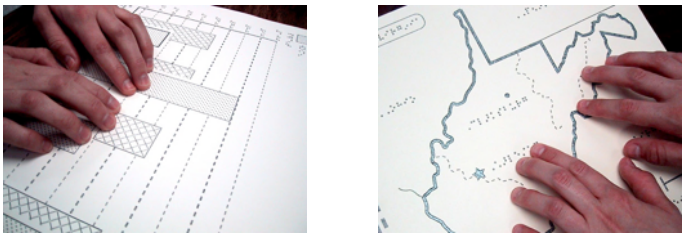

(a) (b)

Fig. 2.5 Examples of tactile graphics: (a) bar chart and (b) map. (Pictures used with permission from GH, LLC, www.gh-accessibility.com.)

trained experts through a time-consuming process. Promising attempts have nevertheless been made to partially or fully automate this process using image processing techniques [144, 296].

Detailed guidelines for the design of effective tactile graphics have been proposed by numerous practitioners [59, 34]. It is generally recommended, for example, to leave a clear separation between tactile elements and to use contrasting tactile textures. Maps are built with point symbols representing items of interest such as cities, line symbols delimiting contours and defining paths, and areal symbols replacing colors with tactile textures [59, 34, 268, 278, 111]. Tactile patterns evoking recurring elements such as water or mountains are often sought although no fixed convention exists.

Graphics can also be drawn by visually impaired persons by, for example, raising lines on microcapsule paper using a heat pen. Erasing, however, is not allowed by most drawing media and feeling graphics as they are being drawn is generally difficult [91]. Many researchers have nevertheless observed the way in which blind persons draw in order to gain insight on their representation of space. Although some features appear to be universal, the drawings of a blind person are in many ways different from those of a sighted person [91]. It has, for example, been noted that many visual conventions such as perspective are not respected, and that objects are sometimes folded out or flattened and their hidden parts represented [137]. These observations may be relevant to the production of adapted tactile graphics.

Refreshable Tactile Graphics

Numerous attempts have been made to address the limitations of conventional tactile graphics using technological solutions. Tactile content can, for example, be produced

with high-density dot embossers [288] or 3D printers [174]. Tactile graphics can also be augmented with location-based speech or non-speech audio when combined with a tablet or other pointing device, thereby reducing the need for Braille labels and therefore clutter [297, 13, 108, 212, 165, 181, 202]. Much research has also considered the display of virtual or refreshable graphical content using haptic interfaces such as force-feedback devices and tactile displays (Figure 2.6).

(a) (b)

Fig. 2.6 Examples of haptic interfaces: (a) Phantom Omni and (b) VT-Player (used with permission from Christophe Jacquet).

Force-feedback interfaces such as the PHANTOM simulate interaction forces between a probe and a 3D environment and can therefore be used to display virtual scenes to visually impaired persons [207, 89, 48, 170, 245, 276, 103, 168]. Objects of significant complexity have been found to be identifiable [169]. This approach has notably been used for the design of haptic games and interaction techniques that facilitate the non-visual exploration of a virtual environment [255]. Detailed 3D maps have also been displayed by force-feedback using information captured by cameras [186]. Virtual environments can alternatively produce 3D surfaces similar to conventional tactile graphics using either sophisticated interfaces or consumer-grade ones such as haptic mice. This approach has notably been used to produce maps [240, 201, 145, 82, 186], 3D data set visualizations [69], and electric circuits [216]. The display of multimodal graphics such as bar charts has also been extensively studied using line drawings produced as virtual grooves [307]. A sophisticated system allowing graphics to be drawn by blind users using positive or negative relief has similarly been designed [128, 224]. The display of audio-tactile maps with consumer-grade devices has also been explored with bumps and vibrations representing elements such as political boundaries and cities [201]. Graphs have similarly been presented using vibrotactile stimulus provided by a modified pen tablet [64]. A mixture of 3D objects and 2D surfaces with

grooves and textures is often used in practice, and has notably been applied to the development of haptic games and educational applications [207, 237, 267].

Attempts have also been made to display tactile graphics using tactile displays that produce distributed tactile stimuli on the skin. Although a wide variety of skin stimulation methods and actuation technologies have been experimented with [287, 282], many arrays employ a technology similar to that used for the refreshable display of Braille. Large pin arrays have therefore been used for drawing as well as displaying animations, complex patterns, games, mathematical graphics, and web pages [249, 131, 130, 295, 4, 234]. Experimental displays with controllable elevation have similarly been used to display Chinese ideograms, familiar objects, maps and scientific illustrations [252, 123]. Other displays have often been evaluated based on their ability to convey simple geometric patterns or letters [265, 23, 171, 250] and may have potential for the display of more complex graphics.

Virtual graphics can also be produced with fingerpad-sized arrays by altering the tactile stimuli as the device or a separate pointing device is displaced. The VTPlayer, a mouse-like interface with two 4×4 pin arrays, has, for example, been used to display virtual patterns either directly [115] or by combination with a PHANTOM's probe [287, 286]. Many small arrays have similarly been evaluated based on their performance for the display of virtual shapes, letters or textures [172, 173, 195, 309, 141]. Although mainly used as a reading aid in practice, the Optacon has also been evaluated for the exploration of large tactile patterns [31, 95, 135]. Most small tactile arrays, however, have been mainly evaluated for the passive display of tactile patterns. Many displays have been used to display simple geometric patterns [139, 143, 140, 14, 117, 116, 279] as well as bars or gratings [187, 120]. The VTPlayer has also been used to display static and dynamic directional icons which were used as guidance cues for the exploration of shapes and electric circuits [215, 193]. Many of these tactile displays nevertheless present potential for the display of more complex virtual tactile graphics.

2.4.4 Human-Computer Interaction

While early computer interfaces such as command-line prompts could easily be communicated sequentially through voice synthesis or Braille, the visual content of graphical user interfaces and relative pointing devices such as the mouse are largely inaccessible to visually impaired computer users. Computers are nevertheless accessible

through screen reader software that transparently reinterprets graphical user interfaces and communicates their content by refreshable Braille or voice synthesis. The user experience is however much less satisfying than for the sighted due to the sequential nature of the presentation and loss of spatial information.

Attempts have been made to address these issues using audio and haptic feedback. O'Modhrain and her colleagues, for example, designed a planar haptic device to reintroduce tactile and kinaesthetic interaction in the sound studio, a traditionally accessible environment from which blind sound engineers found themselves excluded with the introduction of computers [78]. Visual widgets were mapped to tactile sensations so as to provide non-visual access to the Microsoft Windows desktop [197]. The edge of a window was, for example, represented as a groove and a check box as an attracting spring or repelling block. Gravity was introduced in direct manipulations so that the weight of objects could be felt. The PC-Access project similarly improved the accessibility of the desktop using spatial information provided by haptic stimuli, including boxes for the size of objects and gutters for boundaries [222]. Distance information was provided by dynamic forces, such as rubber bands, when moving icons or resizing windows.

Researchers have also attempted to provide specialized computer interfaces better adapted to the needs of blind users. A chat room client was, for example, designed to provide control over the reading of incoming communications, a simple improvement that can have a significant impact on usability [88]. A touch tablet covered with a tactile overlay was similarly designed to provide a user interface for navigating through hypermedia applications [212]. An accessible text editor was also designed using voice recognition, speech synthesis and a Braille terminal [20]. Sjöström has experimented with haptic computer interfaces and designed a number of tools, such as radial menus, that facilitate interactions [255]. He has also designed haptic games involving the exploration of virtual environments with a PHANTOM such as the Memory House, in which pairs of buttons must be matched, and Submarines, a boardgame in which the state of squares is represented by intuitive tactile sensations such as waves. Although custom interfaces and applications are likely to be more usable than the reinterpretation of a GUI, they are less flexible, require more work for their implementation and may not be accepted by the users who often wish not only access to the computer, but also access to the interface of the sighted.

The accessibility of the Internet finally deserves special attention since this resource offers a wealth of previously inaccessible information. Despite the publication of web accessibility guidelines, many web sites are difficult, frustrating and inefficient to browse with a screen reader [75, 299]. Irritants include the lack of alternate text for images, the repetition of headers on every page, as well as the difficulty of obtaining an overall view of a page and extracting relevant information. The use of contextual voices and keyword extraction have been proposed as partial solutions for these problems [308]. The virtual or refreshable display of graphical content on haptic devices such as tactile displays could also improve the accessibility of webpages [234].

2.4.5 Vision Substitution

Vision substitution systems convert information acquired from cameras or other spatial sensors to rich audio or tactile signals with the intent of developing in blind persons perceptual abilities similar to those allowed by vision.

One of the most extensive studies on vision substitution, the Tactile-Video Substitution System (TVSS), has experimented since 1963 with the conversion of video images into electrotactile or vibrotactile patterns applied to the abdomen, back or thigh with arrays of 100 to 1,032 points, and more recently with electrical stimulation of the tongue [15]. Although extensive training was required, it was shown that subjects could "learn to make perceptual judgments using visual means of analysis, such as perspective, parallax, looming and zooming, and depth judgments" [15, p. 287]. Moreover, sensations were eventually exteriorized and no longer felt as being applied to the skin [153]. Subjects would even duck as if to avoid an incoming object when the tactile image was suddenly magnified [47]. Despite these results, the concept was found to be of limited practical value since complex, outdoor scenes were impossible to interpret [47]. The necessary concentration was moreover too great for prolonged use or to concurrently perform other tasks [47].

The question of user expectations is also interesting. Despite the name, a vision substitution system does not allow a blind person to experience or recover sight, often leading to disappointment [153]. The new perceptions also do not carry subjective or emotional value. Similar observations have been made about the recovery of sight by congenitally blind persons (see Section 2.4.6). Bach-y-Rita, Tyler and Kaczmarek [15, p. 293] nevertheless note that "a blind infant using a vision substitution system smiles

when he recognizes a toy and reaches for it."

Many other vision substitution systems have been designed, including the SonicGuide, introduced in Section 2.4.1 as a travel aid, and a similar device called the vOICe which creates a 3D audio signal as a video image is swept [180]. Another example attempts to create a bas-relief representation of a stereo image using a wire-based haptic interface [53]. Haptic feedback has also been used to design sensory substitution systems for deaf persons, for example, to communicate the emotional content of a film's soundtrack [121].

2.4.6 Sight Recovery

Medical interventions are sometimes able to restore sight to a blind person. As briefly mentioned in Section 2.3.2, the results are highly dependent on the age of onset of blindness. For example, while the functional sight of late blind persons can be restored almost completely when removing cataracts, early blind persons show "some improvement of their vision with the passage of time, and the gaining of visual experience, but in most cases they never [develop] anything approaching normal vision" [100, p. 40]. Despite having apparently good vision, patients are incapable of recognizing shapes or faces, or making much functional use of their vision. About a third even revert to blindness, preferring dark rooms and walking with their eyes shut [1].

Much research has also gone into creating electronic devices that can be implanted in the brain or on the retina of blind patients to trigger visual sensations from external stimulus, such as images recorded from a camera embedded in a glass eye. Electrical stimulation of the visual cortex has been shown to produce the perception of light spots or phosphenes [54, 100] and low-resolution implants have been successfully tested. Given greater resolution, these implants may eventually provide sufficient usable vision to travel independently or to recognize faces and objects. Like cataract surgery, visual prostheses may not restore functional sight to all blind patients, and particularly to those who lost their sight early. See [35] for more information on this topic.

2.5 Discussion

2.5.1 Assistive Technologies Market

Developers of assistive technologies should not be unduly encouraged by the statistics of Section 2.3.1. The potential market for assistive devices is far from reaching the 37 million blind people in the world, most of which live in the third world and cannot afford them. The remaining blind community varies in buying capability (depending on the level of governmental or insurance support) and in receptiveness to new technologies. The American Foundation for the Blind estimates, for example, that approximately 5.7 million Americans with vision loss have an annual family income of less than $20,000 and reports that as little as 19% of legally blind adult Americans may be employed [11]. There are also significant differences in ability to use assistive devices [56]. It was noted, for example, that the one third of visually impaired persons less than 65 years old accounts for two thirds of long cane usage [231]. The situation may be worse for complex devices such as electronic travel aids [109]. Users who succeed at learning and making effective use of complex aids may well be the exception rather than the norm.

Although technology is pervasive in the life of many blind people, most of the more advanced aids have met with limited commercial success. Despite much research on the topic [28], it was estimated, for example, that only 3,000 to 3,500 electronic travel aids had been sold by 1985 [191]. This may be due to the satisfactory mobility afforded by simpler aids such as the long cane and guide dog [191]. It is also conceivable that many prefer caregiver assistance when available [232]. While there is clearly a demand, the blind population is not desperate for assistive devices and will not embrace them at all costs. The design of assistive technologies must therefore be approached with the same attention to detail as any other consumer product and the needs of users considered at every step of their development.

Considering the efforts required to learn the use of some assistive devices, it is also important to consider whether the blind community trusts the claims made by researchers and manufacturers of assistive devices. The marketing of devices often exaggerates their benefits, raising expectations and leading ultimately to disappointment. The mainstream media is also quick to accept and disseminate these optimistic claims. In such a context, it is easy to understand why the blind community is wary of

embracing new technologies, and is sometimes even cynical. Baldwin [17] writes, for example, that "[t]here is great scepticism in the blind community, and well meaning inventors have not always been welcomed with open arms." Similarly, Lauer [147] writes: "High hopes and exaggerated claims in the 1970s had left a backlash of people who were disappointed at the long training needed to use the Optacon, the difficulty of learning to use it, and the price. The blind public grew disillusioned and all but forgot how useful the instrument had become to several thousand of them."

A related issue is the instability of manufacturers and product lines [56]. Many devices have been discontinued by their manufacturers because they were not commercially viable. This causes significant problems for those who have invested time, money and efforts into mastering these aids, sometimes becoming dependent on them. When the Optacon was pulled from the market in 1996, many of its devoted users were, for example, extremely disappointed and now fear being deprived of their aid if it breaks down [260]. Considering the history of assistive device commercialization, it is hard to convince a potential buyer that the latest device will be supported and serviced years from now.

Although the market for assistive devices is not as forgiving as some might hope, there remain many areas where current aids are inadequate and technological solutions are much needed. This is particularly the case for employment and education where visually impaired persons must have efficient access to computers and graphics in order to compete with their sighted colleagues. There may therefore be a significant market for devices such as tactile arrays that allow the display of virtual or refreshable tactile graphics and enable immediate access and interaction with graphical content. Many other areas are well supported by existing aids but nevertheless leave much room for improvement. The accessibility of Braille could, for example, be greatly improved with a reduction of the cost of refreshable Braille technologies.

2.5.2 Recommendations

Many recommendations and guidelines have been put forward to help designers better meet the requirements of the blind community. This is particularly true of portable devices, such as electronic travel aids. A portable device "must be comfortable, ergonomically sound and convenient to use and to 'park' when not in use" [56]. It must similarly be autonomous, light, robust, visible but discrete, inexpensive, and remov-

able [152]. A travel aid should ideally not interfere with the normal use of the senses, such as require the user to wear gloves or earphones, although some users contend that this may be acceptable if the aid provides more appropriate information [56]. These requirements may not have the same importance for non-portable assistive devices but are nevertheless often desirable.

Designers must also appreciate the importance of social factors. As with any other consumer product, there is an emotional component attached to the purchase and use of an assistive device. The goal of greater mobility, for example, may conflict with that of integration into society if an aesthetically unpleasant aid must be worn. Most blind persons will not accept to use devices that marginalize them, even if they prove very useful. This is understandable considering that sighted persons often involuntarily change their attitude when interacting with blind persons [100].

Finally, collaboration between the blindness, rehabilitation and research communities is crucial for assistive devices of practical use. Designers of innovative devices must be ready, however, to face a natural opposition to changes that go against conventional wisdom. Even Braille, a now well-established aid, was not readily accepted when first introduced [65]. Moreover, it must be remembered that no blind person can speak for the entire community as opinions and needs vary between individuals. One also should not assume that a blind person, like any other consumer, is aware precisely and completely of all his needs and of the best way to meet them. Soliciting feedback from a representative sample of the blind community is nevertheless essential to ensure that a novel aid meets their needs.

2.5.3 Trends and Future Developments

The current trends in technology allow us to speculate on the future of technological aids for visually impaired persons [16, 77, 18]. Long the holy grail in rehabilitation research, neural and retinal implants could soon provide much higher resolution and therefore a limited degree of functional vision. It must be remembered however that these medical procedures may not restore vision for some people, particularly if the loss of sight has occurred early, due the brain's adaptation to blindness (Section 2.3.2).

Advances in pervasive and ubiquitous computing will also likely benefit the blind community. Smart homes could facilitate the control of appliances and provide information in an intuitive manner, possibly through natural language. Similarly, Radio

Frequency Identification (RFID) tagging could allow items to be identified and located by their radio signature. Computers are also becoming increasingly portable, now being even embedded in clothing. This computational power can be harnessed for many purposes such as navigational assistance. Systems using GPS and other positioning methods are therefore likely to proliferate and grow in usefulness as geo-tagged information becomes increasingly available. These advances in assistive aids will greatly benefit from their reliance on generic technologies.

While the trends described so far benefit the blind community, others could leave them behind. The most serious issue is the increasing use of graphical user interfaces and visual metaphors in computing. This is particularly problematic since many traditionally accessible appliances and commodity items are now switching to programmable, visual interfaces such as touchscreens. Promising efforts are currently under way to address these issues. The Alternative Interface Access Protocol, for example, could allow users to interact with any compliant system using a universal remote console of their choosing [310]. An adapted remote console would discover the system's functionalities and provide a non-visual user interface. The introduction of haptic feedback in touchscreens, discussed next, could also restore a certain degree of accessibility to such interfaces.

2.5.4 Applications of Haptics

As discussed in Section 2.4, many assistive devices rely on the haptic sense to provide information to the user. Haptic interfaces notably take the form of simple vibrotactile stimulators (MiniGuide), multiple vibrating buttons (UltraCane) and complex two-dimensional arrays of tactile stimulators (e.g., TVSS, Optacon). Many research projects also used force-feedback devices such as the PHANTOM or less expensive consumer-grade mice, joysticks and trackballs. The use of haptics seems to have been well received by the blind community even though few of the aids mentioned have been widely adopted. In this context, it is interesting to look at the opportunities still available for haptic research with a potential benefit for visually impaired persons.

Practical aids for visually impaired persons must often be portable. This imposes strict design constraints such as limitations on power consumption and size. Meeting these requirements with haptic interfaces is a significant challenge that has until recently limited commercial offerings of portable devices to simple vibratory tactile

feedback. There is however a growing interest in the use of more sophisticated haptic feedback in portable devices such as mobile phones. Higher-performance actuators have, for example, been used to provide rich vibrotactile feedback both in experimental devices [196] and commercial ones, such as TouchSense-enabled phones (Immersion Corp., California). Actuators have notably been used to provide tactile feedback while using touchscreens, reintroducing much-needed physical interaction in this otherwise purely visual medium [217, 178]. Such innovations may have a significant impact on the usability of consumer devices for visually impaired persons, and on the availability of haptic technologies suitable for assistive devices. An actuated touchscreen was, for example, recently used to communicate a Braille character as a series of pulses produced either as a spatial or temporal representation of a cell's dots [223]. Such creative ways to provide feedback to visually impaired persons are likely to gain in importance as haptic feedback becomes ubiquitous in consumer products [219].

Haptic interfaces also present many advantages over more common audio interfaces. The sense of touch is, for example, largely unused while traveling and can be tapped without interfering with normal activities and environmental cues. Haptic stimuli can also be delivered privately to a user without disturbing other people. More importantly, haptic feedback is generally more appropriate for the communication of complex spatial information. Screen readers, for example, are unable to efficiently present the spatial organization of a webpage or computer desktop using voice synthesis or other sequential information presentations such as refreshable Braille. The display of this information using a combination of virtual or refreshable tactile graphics and speech and non-speech audio feedback could therefore greatly improve the accessibility of computer interfaces and digital documents. A virtual tactile graphics interface would moreover have a significant impact on the education and employability of visually impaired persons by offering them a tactile interface with a flexibility approaching that of visual displays. As shown in Section 2.4.3 however, graphics interfaces based on force-feedback or tactile display technologies have shown promise but have yet to produce a sufficiently practical solution.

More generally, most advances in haptic interfaces have potential applications for the design of assistive devices. The recent interest in low-cost, low-power haptic mechanisms could, for example, allow the interface of existing aids such as digital book readers to be augmented with haptic feedback. Haptic knobs are now available com-

mercially at moderate cost [83] and could be used to improve the control of media playback [257]. Some practical considerations must nevertheless go in the design of the finished haptic interface intended for visually impaired users. One must, for example, be aware that haptic sensations can be altered by the removal of supporting visuals from multimodal interfaces [112]. A blind user must also be able to easily find the manipulandum of a device. It has also been noted that usability evaluation methods may need to be adapted for use with visually impaired persons, particularly when audio feedback [39] or children [220] are involved. With these considerations in mind, much haptic research can be applied to the design of aids for visually impaired users.

2.6 Conclusion

The design of aids for visually impaired persons is in many ways similar to any other user-centered design effort. Getting feedback from members of the target user group at different stages of the design process is essential. This is particularly critical for sighted designers who may be unaware of subtle differences between visually impaired and sighted users. Blind persons, for example, are better at attending to non-visual stimulus and at making functional use of their unimpaired senses. Moreover, blindness may alter a person's perception of space and mental representation of objects. Blind persons also form a heterogeneous community with needs and abilities that depend, in part, on the degree of visual impairment and the age of onset of blindness. A significant proportion of blind persons are also elderly or suffer from other impairments. This may affect their receptiveness to new technologies and their ability to make use of complex aids. These facts should be taken into account when evaluating potential applications for novel technologies or making design decisions.

A wide range of technological aids have been designed over the years, many leveraging haptic technologies. The limited commercial success of most advanced aids may be due to the satisfying lifestyle already afforded by the long cane, the guide dog, Braille and simple aids such as talking clocks. While no aid is desperately needed, there is nevertheless room for improvements in many areas. The long cane, for example, does not warn of overhanging objects and is of little use for orientation. Interacting with computers is also critical but remains ineffective and frustrating. The growing use of graphical user interfaces, particularly in traditionally accessible domains, is also

problematic. Graphical content is more generally important for education and employment but is greatly limited by its production on static tactile media. Haptic interfaces for the display of virtual or refreshable tactile graphics are needed but unfortunately not yet sufficiently mature or practical to gain wide acceptance. Many of these challenges underscore the need for more effective non-visual interfaces.

This context offers interesting opportunities for applications of haptics research. Many problems encountered when using haptics with blind persons are not fundamentally different from those encountered with other user groups. This allows many advances in haptics to be readily applied to interfaces for blind persons. Adoption of haptics, however, is currently hampered by the limited performance of technologies suitable for mobile use, a common requirement for practical assistive devices. Haptics also has yet to reach the level of practicality of many audio or visual technologies that it aims to provide an alternative for, such as speakers and touchpads. Further research will finally be necessary to design more sophisticated interfaces such as tactile arrays suitable for the display of tactile graphics or other complex haptic patterns.

Work remains to be done to fulfill the promises of haptics for blind users. This includes not only designing novel haptic interfaces, but also finding more effective ways to use existing technologies. Current trends, however, suggest that advances in haptics will have a role to play in the improvement of the quality of life of persons with a visual impairment.

Chapter 3

Display of Virtual Braille Dots by Lateral Skin Deformation: Feasibility Study

Preface to Chapter 3

This chapter appeared in:

[161] Vincent Lévesque, Jérôme Pasquero, Vincent Hayward, and Maryse Legault. Display Of Virtual Braille Dots By Lateral Skin Deformation: Feasibility Study. *ACM Transactions on Applied Perception.* 2(2):132–149, 2005.

This chapter introduces the concept of tactile rendering by lateral skin deformation through the display of virtual Braille dots, and hence presents the first application-oriented research on laterotactile stimulation. A linear tactile array with 12 laterally-moving contactors, less sophisticated but stronger than its predecessors [92, 205], was designed specifically to investigate the feasibility of simulating the sensation of brushing against a line of Braille dots by lateral skin deformation. Tactile stimulation in the form of travelling waves was empirically designed to approximate the sensation, marking the beginning of laterotactile rendering and informing the design of subsequent tactile patterns both for Braille (Chapter 4) and tactile graphics (Chapters 5, 6, 8 and 9). The results of an experiment with Braille readers were sufficiently promising to warrant the extension of this work to the rendering of 6-dot Braille, presented in the next chapter.

Contributions of Authors

This chapter is the result of a close collaboration between Vincent Lévesque and Jérôme Pasquero, with both authors contributing equally to the work. The chapter was written by these authors and edited by Vincent Hayward. The work presented herein was similarly performed by V. Lévesque and J. Pasquero under the supervision of V. Hayward. While both first authors participated in all aspects of the work, the design and implementation of the tactile rendering algorithms can be attributed mainly to V. Lévesque, and that of the tactile display hardware to J. Pasquero. Maryse Legault contributed her expertise on Braille and design for the visually impaired, and served as a reference user for the design of the tactile rendering algorithms.

Display of Virtual Braille Dots by Lateral Skin Deformation: Feasibility Study

Abstract

When a progressive wave of localized deformations occurs tangentially on the fingerpad skin, one typically experiences the illusion of a small object sliding on it. This effect was investigated because of its potential application to the display of Braille. A device was constructed that could produce such deformation patterns along a line. Blind subjects' ability to read truncated Braille characters ('○○', '○●', '●○', and '●●') using the device was experimentally tested and compared to their performance with a conventional Braille medium. While subjects could identify two-character strings with a high rate of success, several factors need to be addressed before a display based on this principle can become practical.

3.1 Introduction

3.1.1 Braille Displays

Louis Braille's reading and writing system has given the blind access to the written word since the early 19th century. Braille characters replace the sighted's written letters with tactile equivalents. In the Braille alphabet, each character consists of an array of two columns and three rows of raised, or absent dots. Traditionally embossed on paper, Braille has more recently also been provided by refreshable Braille displays that generally add a fourth row of dots. Refreshable Braille displays were initially the only type of computer interface available for the blind. Despite the growing popularity of more affordable speech synthesis hardware and software, refreshable Braille remains a primary or secondary access medium for many blind computer users.

Commercially available refreshable Braille displays have changed little in the past 25 years. Today's displays do not differ substantially from what is described by [274]. Typical systems use cantilevered bimorph piezoactuators (reeds) supporting vertical pins at their free end. Upon activation, a reed bends, lifting the pin upward. Braille characters are displayed by assembling six or eight of these mechanisms inside a package called a cell (see Figure 3.1(a)). A basic system includes 40 or 80 cells to display a line of text (Figure 3.1(b)), plus switches to navigate in a page (Figure 3.1(c)) [263].

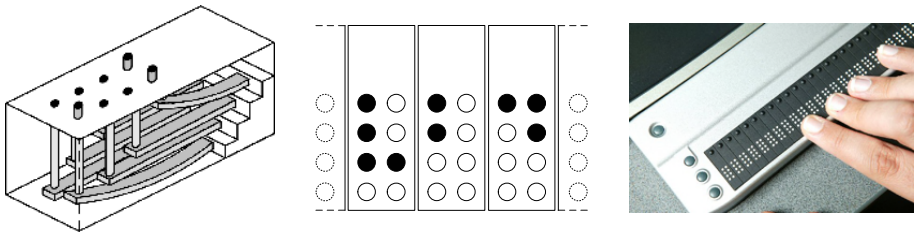

(a) (b) (c)

Fig. 3.1 Conventional Braille display: (a) cell actuation mechanism, (b) array of cells, and (c) picture of a commercially available Braille display (used with permission from Pulse Data International Ltd).

While the elements of these cells are simple and inexpensive, the cost is driven by the necessity to replicate the cell 40 or 80 times, or more if one contemplates the display of a full page. Typical Braille displays cost much more than a personal computer.

3.1.2 Alternative Technologies

In recent years many alternative designs have been proposed, all sharing the principle of raising individual pins, or dome shapes, out of a surface [29, 227, 303]. In 2004 alone, no less than six U.S. patents related to Braille cells have been granted, and many others are pending (e.g., [210, 301, 25]). While most of the research focuses on reducing the cost of actuation, very little work is concerned with new approaches to the display of Braille.

Of note is a system proposed by Tang and Beebe [265] who sandwiched discrete electrodes in a dielectric. The application of high voltage to these electrodes causes the skin to adhere locally to a glassy surface, thereby creating small tactile objects. Patterns resembling Braille characters could presumably be displayed with this method, however it appears to suffer from sensitivity to environmental factors such as humidity or skin condition.

Several investigators proposed the idea of a single display moving with the scanning finger rather than the finger scanning over an array of cells. Fricke [66] mounted a single Braille cell on a rail and activated its pins with waveforms resembling "pink noise" in an attempt to imitate the effect of friction of the skin with a pin. Ramstein [221] designed an experiment with a Braille cell used in conjunction with a planar "Pantograph" haptic device in an attempt to dissociate character localization from character recognition. The haptic device was programmed to indicate the location of the characters in a page, while the cell was used to read individual characters. Comparative tests were performed in different conditions with one or two hands. Again, the goal was to create an "array of Braille characters" with a single cell and reasonable reading performance could be achieved.

3.1.3 Overview

This paper reports on a feasibility study conducted to evaluate the potential of a new approach to the refreshable display of Braille. When the skin of the fingertip is locally deformed in the manner of a progressive wave, one typically experiences the illusion of objects sliding on the skin, even if the deformation contains no normal deflection [92]. An electromechanical transducer was designed to create such skin deformation patterns with a view to investigate the feasibility of displaying Braille dots. The novelty

of this approach lies in that it creates a progressive wave of lateral skin deformation, instead of a wave of normal indentation (e.g., [277]) or localized vibration (e.g., [31]). Our approach also relies on scanning motion, which is often mentioned as necessary to "refresh" the skin receptors and combat adaptation [66].

The transducer that we constructed was similar in principle to the 'STRESS' display [205], but had only one line of actuated contactors. This configuration allowed us to significantly increase the forces and displacements produced by the contactors. The Braille dots created by this device were "virtual" in that we attempted to recreate only the essential aspects of the skin deformation occurring when brushing against raised dots without actual physical dots.

The resulting system and the particular strain pattern — collectively termed "VBD" for virtual braille display — were empirically designed with the assistance of the fourth author, a blind accessibility specialist, who also participated in the study in the capacity of "reference subject."

An experiment was conducted to tune the pattern's parameters to create a sensation as similar as possible to that experienced when brushing against physical Braille dots. The legibility of strings of truncated Braille characters — those comprising a single row of dots — was evaluated with five Braille readers on the VBD, and on a conventional Braille medium (embossed vinyl). The subjects' success rate and reading patterns were recorded and analyzed.

The study shows that reading with the VBD is possible with a high legibility rate given some personalization of the strain pattern. Reading is, however, more demanding and error-prone than on conventional media. More importantly, the study helped identify the strengths and weaknesses of the current prototype, and indicates how the device could be improved to yield a workable system.

3.2 Virtual Braille Display

3.2.1 Device

The VBD device consisted of a tactile display mounted on a laterally-moving frictionless slider (see Figure 3.2) and interfacing control electronics.

Reading virtual Braille was done by applying the tip of the index finger against the tactile display and sliding it laterally, as shown in Figure 3.3. When activated,

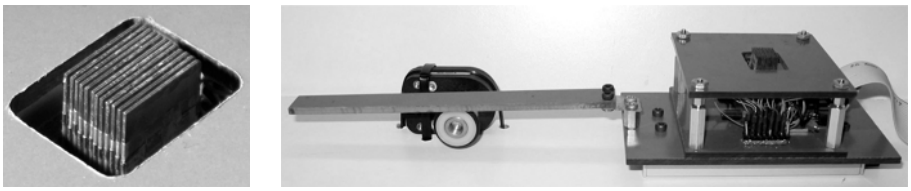

(a) (b)

Fig. 3.2 VBD device: (a) STREss-type tactile display, and (b) display mounted on a slider with rotary encoder.

the tactile display caused lateral deformation to the fingertip skin that could be varied in response to slider movement. The finger remained in contact with the display and dragged it along the reading surface. Although this principle could allow reading with multiple fingers, the width of the display limited the reader to the use of a single finger.

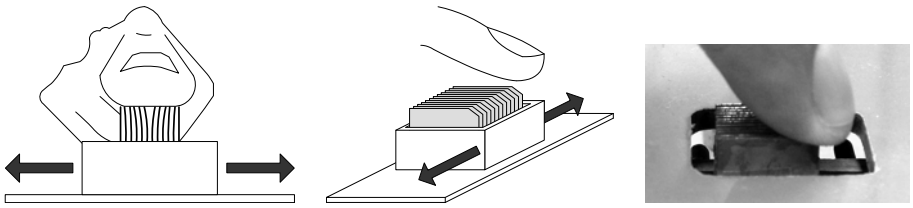

(a) (b) (c)

Fig. 3.3 Interaction with the VBD: (a) strain applied during exploration, (b) illustration and (c) picture of finger contact with the VBD.

Tactile Display

The tactile display was made of a stack of twelve 0.38-mm-thick piezoelectric bender plates[1], sandwiched at their base between neoprene spacers and clamped between two rigid endplates using four locating pins and four screws (see Figures 3.4(a) and (b)). The spacers were cut in a 12-mm-high T-shape so that they rested on the locating pins and allowed room for electrical connections (see Figure 3.4(b)). Once tightly secured, the spatial period ϵ, or contactor pitch, was approximately 0.7 mm. This assembly method was selected for the convenience of allowing the design parameters such as thickness, length, shape and material of the actuators, and spacers to be changed. In the present study, however, only one configuration was used.

[1] Y-poled, 31.8 mm x 12.7 mm, high performance bending motors from Piezo Systems Inc., part number T215-H4CL-303Y.

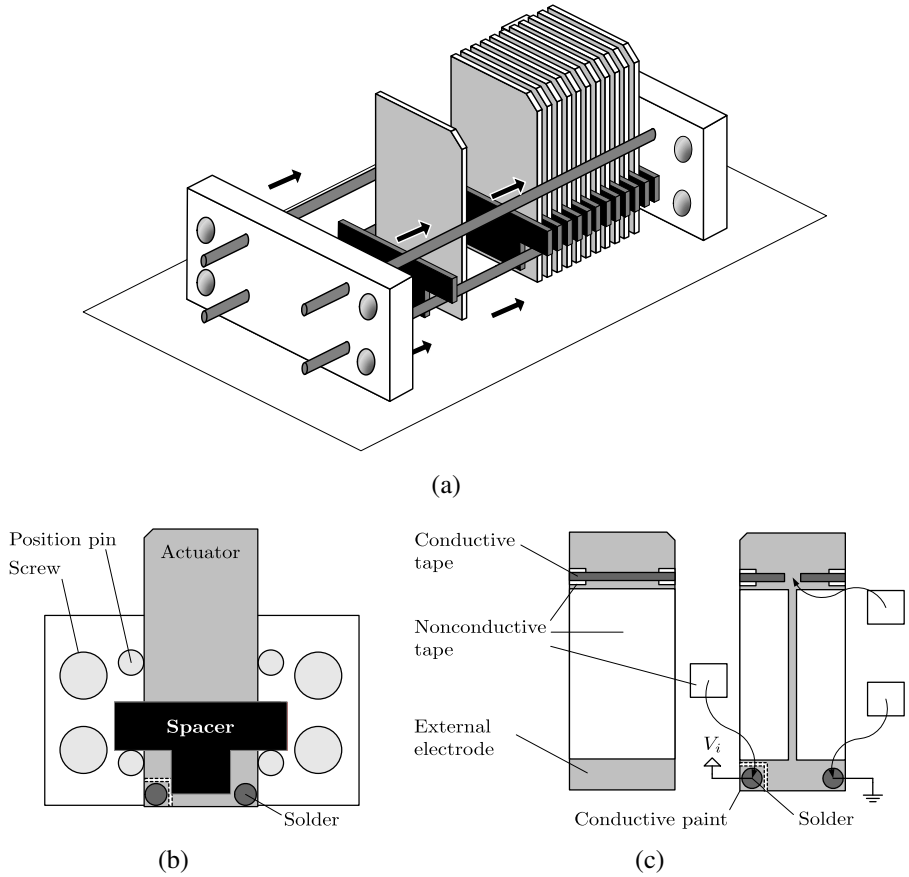

Fig. 3.4 Assembly of the VBD's tactile display: (a) perspective and (b) frontal views of stacked assembly, and (c) actuator fabrication process.

The actuators were driven by a bipolar voltage applied between their central electrode and their two electrically-connected external electrodes. Because of the small space between adjacent plates, the electrodes could not be connected using the methods recommended by the motor supplier. Therefore, the actuators were prepared as shown in Figure 3.4(c). The external electrodes were joined with adhesive electrically conductive tape[2] running over nonconductive tape on the sides to prevent shorting with the central electrode. One corner of an external electrode was soldered to a ground wire. The other corner was turned into a small electrode pad (isolated from the rest by grinding off the conductive layer) and connected to the central electrode with conductive paint. A wire used for the control voltage was then soldered to this pad. To prevent

[2] 3M Corporation, EMI copper foil shielding tape 1181.

contact with the adjacent actuator, the solders were kept significantly thinner than the spacers (0.5 mm) and were protected with nonconductive tape. Traces of conductive paint were applied along the length of the electrodes to improve their reliability (not shown). The actuators were then isolated from the metallic locating pins using nonconductive tape. As illustrated in Figure 3.3(b), the top corners on one side of the blades were beveled to create a narrow linear array of skin contactors (around 0.2 mm^2 in area each). Finally, the tips of the actuators were coated with varnish to isolate them from the skin.

The display could be used by applying the finger either on the large horizontal contact surface or against the surface formed of the beveled corners of the contactors. The latter surface, as shown in Figure 3.3, provided a narrower contact area more appropriate for the display of dots and was the only one used in this study.

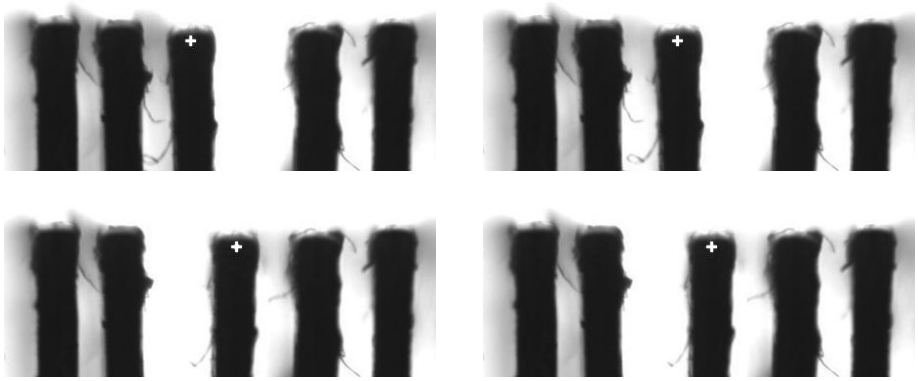

(a) (b)

Fig. 3.5 Visual estimation of unloaded actuator deflection for (a) full range and (b) restricted range. Adjacent actuators were held deflected away from the actuator under study.

The deflection of the actuator tips was estimated with the help of a camera. Two sample measurements are shown in Figure 3.5. When not loaded by the finger, the deflection range was estimated to be 0.4 mm. As explained in the next section, the motion was limited in practice to a restricted range of approximately 0.3 mm. The deflection when loaded with the fingerpad could not be quantified but appears to be significantly lower than when unloaded.

Control System

The position of the linear slider on which the tactile display was mounted was measured by an optical encoder with a nominal resolution of 17 µm. Interfacing electronics was constructed to permit the refresh of the actuators at 500 Hz according to patterns programmed on a personal computer. This enabled us to program the deflection of each actuator with arbitrary functions of space (see Section 3.2.2).

The interfacing electronics, adapted from a previous project, made use of a field-programmable gate array (FPGA) development board[3] with a universal serial bus (USB) 1.1 interface. It was programmed to convert control frames coming from the computer, or "tactile images", into 12 bender voltages by means of 156-kHz pulse-width modulation (PWM). The same, however, could be accomplished by adopting a variety of other approaches, including the use of microcontrollers or dedicated logic, interfaced to the computer via parallel I/O or high-speed serial I/O.

The computer generated a set of 8-bit actuator control values based on the encoder readout every 2 ms on average. These tactile images were sent to the FPGA by packets of 5 through the USB channel where a FIFO buffer regulated the flow of tactile images to ensure a constant output rate. The logic-level signals were then amplified to a ± 40 V range and low-passed by the circuit shown in Figure 3.6. In order to avoid nonlinearities in the signal amplification at extreme PWM duty cycles, the control values were restricted to the range 10 (0x0A) to 250 (0xFA).

3.2.2 Skin Deformation Patterns

Trial and error led us to select a pattern solely on the basis of the resemblance of the sensation it provided compared to that of actual Braille, as felt by the reference subject. We are however unable to offer a principled explanation as to why this particular pattern creates sensations that resemble Braille dots more than others. The determination of the actual parameters is described in Section 3.3.

The deflection δ_i of each actuator i was a function of the slider position x_s obtained from the encoder. The actuators followed the same deflection function $\delta(x)$, where x was the actuator position along the reading surface, as illustrated in Figure 3.7. The physical configuration of actuators introduced a spatial phase difference of ϵ. The first

[3] Constellation-10KE™ from Nova Engineering Inc. operating an Altera FLEX 10KE™ chip.

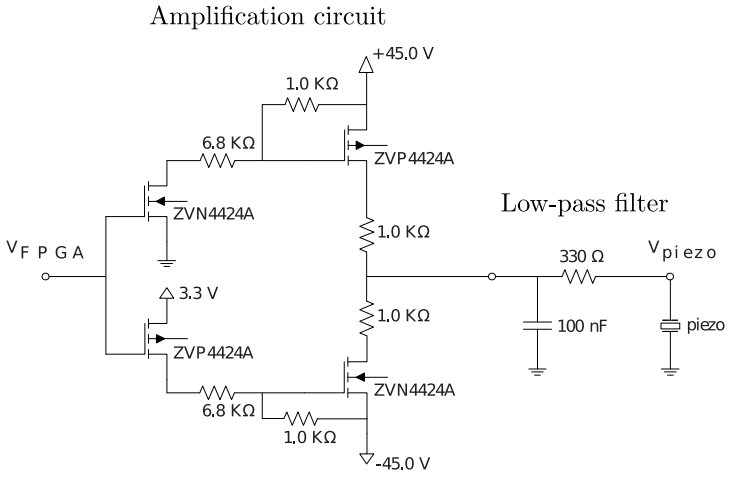

Fig. 3.6 Electronic circuits: amplification circuit (left) and low-pass filter (right).

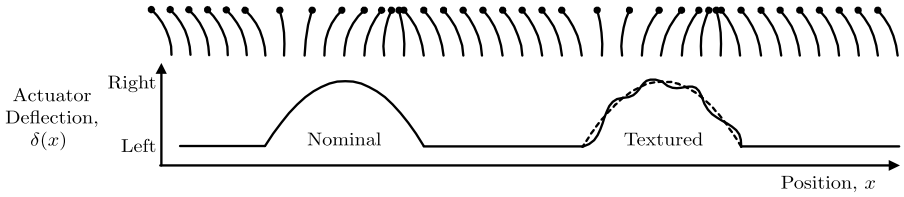

Fig. 3.7 Actuator deflection as a function of position. The curve shows the actuator deflection function with respect to actuator position for a nominal dot (left) and a textured dot (right). The deflection of actuators is illustrated at discrete points along the virtual reading surface. Texture was always applied either to all dots or none.

actuator was given a position corresponding to the slider position.

$$\delta_i(x_s) = \delta(x_s + i\epsilon), i = 0, \ldots, 11 \tag{3.1}$$

What we selected was a pattern[4] such that the deflection of each actuator swept the first half-cycle of a sinusoid, starting from the left position, as it scanned a virtual dot, as shown in Figure 3.7. A small-amplitude, high-frequency sinusoid could also be added to the nominal waveform to enhance contrast. These representations were termed nominal and textured.

These patterns were found to better approximate the sensation of scanning over

[4]Movies of the VBD in action can be found online on the Haptic Laboratory's VBD web page, http://www.cim.mcgill.ca/∼haptic/vbd.html.

Braille dots than others that were experimented with, such as triangular or square waves, full-cycle sinusoids, or textured blanks.

The spatial phase difference between actuators resulted in the representation of dots as a traveling wave. Figure 3.8 and 3.9 illustrate the movement of actuators as a virtual dot traverses the length of the display. Moving the slider in one direction across a region containing a dot resulted in a wave of actuator deflections traveling at the same speed in the opposite direction on the tactile display, causing the illusion that the reading finger was scanning over stationary Braille dots. Since the deflection function was independent of direction, it caused actuator deflections in the direction of finger movement when reading from left to right, but opposing movement when reading from right to left. The resulting sensations, however, seemed to be similar.

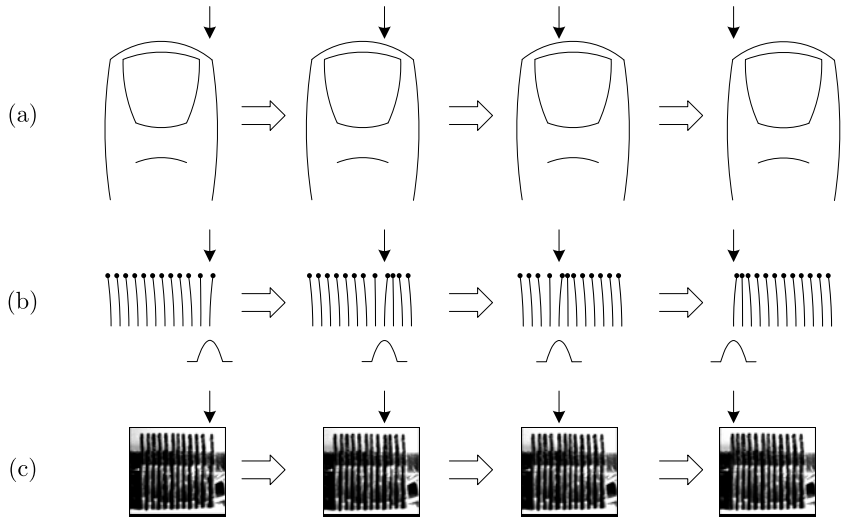

Fig. 3.8 Traveling wave representation of a Braille dot at four points in time: (a) finger-dot interaction, (b) depiction of the actuator deflection and corresponding deflection function, and (c) picture of the actuator deflection. The dot center is indicated by arrows.

This pattern had two distinct effects on the skin deformation. The first was to cause a net displacement of a skin region around each contactor. The second was a pattern of compression and expansion of each small region of skin located between two contactors. Patterns of expansion and compression can actually be observed when a finger scans over small shapes [157]. The strain variations Δ_i caused by a pair of actuators is represented in Figure 3.10. The width ω of a virtual dot is shown relative to the spatial period ϵ. If $\omega < \epsilon$, then there was no overlap between the deflections

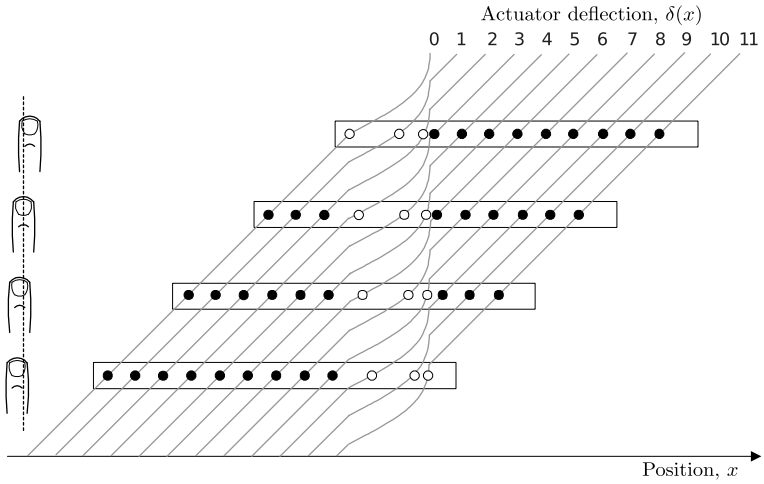

Fig. 3.9 Traveling wave corresponding to a single dot as the slider passes over it. Top-view of actuator deflections and corresponding finger-dot interactions are shown at four locations. Each of the twelve curves indicates the deflection pattern followed by an actuator as the slider moves from left to right.

of adjacent actuators. If $\omega > \epsilon$, then an overlap existed and there was a continuous transition from expansion to compression. If $\omega > 2\epsilon$ expansion and compression never reached their maximum values. It is not known whether local displacement or local variations in strain, or both forms of stimulation, caused the illusion of the dot moving under the finger.

The tactile display could only display a single row of Braille dots. From the Braille character set, the three characters that have dots in row 1 only, or a total absence of dots, could be displayed: ‘a’, ‘c’, and ‘ ’, see Figure 3.11. The fourth possible combination, unused in Braille, was called ‘dot #4’.

3.3 Parameter Tuning

Braille is normally produced according to strict geometrical specifications, but the manner in which these specifications translated into the VBD’s parameters was not straightforward. For this reason, a first experiment was carried out to find the parameters that produced virtual Braille of appropriate dimensions. For the purposes of the feasibility study, only the width and the separation of dots were adjusted. The amplitude of the virtual dot sinusoid was set to the maximum that the system could provide.

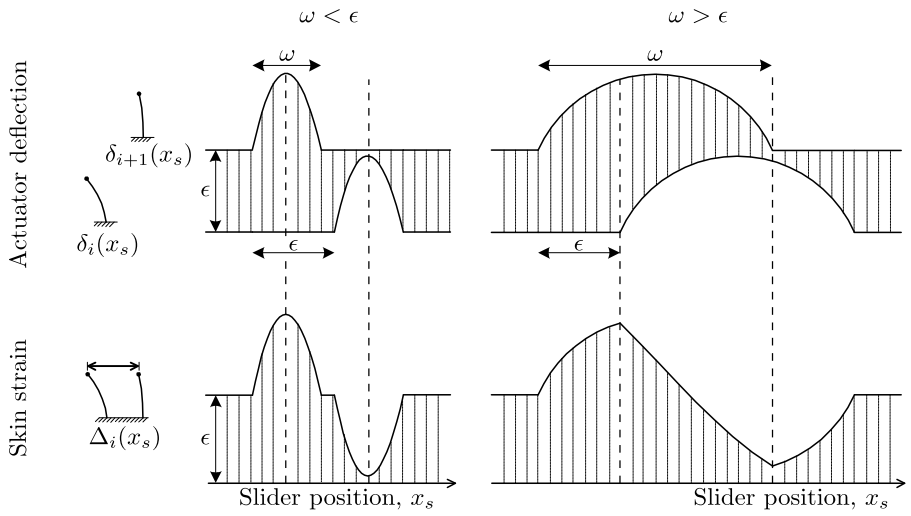

Fig. 3.10 Displacement of two consecutive actuators and corresponding skin strain patterns as functions of slider position, for width ω of virtual Braille dots smaller or greater than spatial period ϵ.

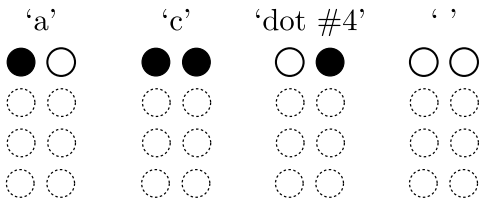

Fig. 3.11 Braille characters displayed by the VBD.

The amplitude and the wavelength of the texture were set empirically to values equal to 1/8th those of the virtual dot sinusoid.

3.3.1 Method

With the help of the reference subject, the width of a virtual dot was first adjusted to match the sensation caused by a single physical Braille dot. Then, the distance between dots within a virtual character was adjusted. The intercharacter spacing value was inferred from the value found for intracharacter dot spacing.

The tuning experiment was conducted following a two-alternative forced choice protocol, using the two-hand method in order to speed up the process and facilitate comparisons. The subject was asked to touch a reference stimulus produced by a conventional refreshable Braille display with her left index. She then immediately

explored two stimuli on the VBD with her right index and selected the one that best matched the reference stimulus. Dots were always displayed with texture. After a short experimentation used to determine an appropriate range, the virtual dot width was varied among six equally spaced values from 0.5 mm to 3.0 mm. The intracharacter dot spacing of the character '⁘' (●●) was similarly varied from 1.0 mm to 2.5 mm. The dot width found in the first step was used in the second.

3.3.2 Procedure

Both tuning experiments proceeded in the same manner. The reference subject moved the VBD toward the left, waited for an audible signal, explored the two different Braille dots or pairs of Braille dots, and verbally reported the stimulus that best matched the reference stimulus. Answers were logged by the experimenter. Each of the 30 possible ordered pairs of nonidentical stimulus was presented to the subject three times, for a total of 90 trials. The different pairs of stimuli were presented in randomized order.

3.3.3 Results

Figure 3.12 shows the results of the two tuning experiments. The preferred virtual dot width was found to be 2.0 mm, the most frequently selected parameter during the first step. The virtual intracharacter separation was also found to be 2.0 mm, between the two most frequently selected values during the second step.

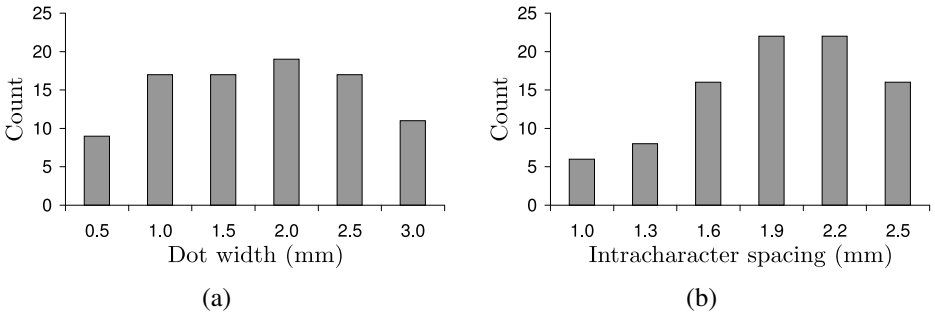

Fig. 3.12 Results of tuning steps: frequency distribution of (a) dot widths, and (b) intra-character dot spacings.

These parameters corresponded to an intracharacter dot spacing of 4 mm, compared to 2.29 mm for standard English Braille. The standard horizontal character-to-

character distance of 6 mm was scaled accordingly to a virtual distance of 10.48 mm as illustrated by Figure 3.13.

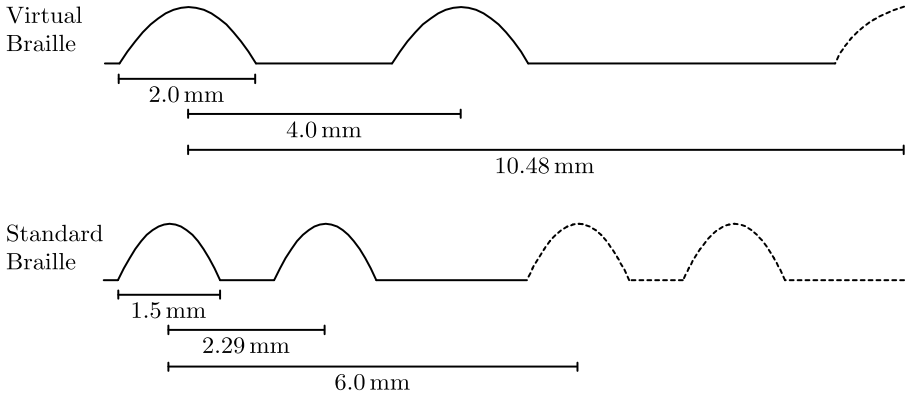

Fig. 3.13 Dimensions of virtual and standard English Braille.

3.3.4 Discussion

The preferred virtual dot width of 2.0 mm turned out to be greater than the spatial period ϵ of 0.7 mm, leading to a strain pattern similar to that shown on the right-hand side of Figure 3.10. Moreover, since the dot width was more than twice the spatial period, the peak strain was lower than the maximum achievable. Assuming that loaded actuator deflections are half those measured without load (Section 3.2.1), this pattern resulted in strains in the order of $\pm 20\%$.

Although the tuning experiments allowed us to find reasonable parameters, the tuning should ideally have been done either with a representative population of Braille readers or individually for each subject. Moreover, the use of texture on the dot may have contributed to an overestimation of the virtual dimensions. The two-hand comparison method may also have introduced errors, but constantly switching from a conventional Braille display to the VBD was impractical. Finally, the intercharacter distance should have been tuned too. These coarse results were found to be sufficient given the scope and the aim of this study.

3.4 Virtual Braille Legibility

The next step needed to evaluate the feasibility of the tangential skin deformation approach for reading Braille was to determine whether blind subjects could read the subset of characters that could be displayed by the VBD. Here, we hoped to also begin identifying the strengths and weaknesses of the concept.

3.4.1 Method

Participants

Two females and three males, experienced Braille readers, volunteered for the study. All subjects were blind from birth. Their ages varied between 22 and 55. The subjects' primary reading finger was the right-hand index. All subjects except the reference subject had never experienced the VBD or heard about our efforts.

Task

The reading task was designed to evaluate the legibility of sequences of first-row characters displayed on the VBD. Subjects were asked to read individual four-character strings using their dominant reading finger. The first and last characters of each string was always '⠉' (●●). The two middle characters could be any of the 16 combinations of the characters '⠁' (●○), '⠉' (●●), 'dot #4' (○●), and ' ' (○○): "●● ●○ ○● ●●", or "●● ○○ ●● ●●", for example. The character '⠉' (●●) was chosen as the string delimiter to avoid confusion.

Procedure

The subjects were given written Braille instructions and had supervised practice trials until they felt comfortable with the task. They were presented with strings to read in block trials. They placed the slider to the left, waited for an audible signal, read the string, and reported verbally the two middle characters. There was no time limit but they were strongly encouraged to answer quickly. In case of doubt, they were asked to give their best guess. Subjects could stop at any time if they no longer felt comfortable (e.g., loss of tactile sensation, fatigue). They were given the choice of doing the trials with texture, without texture, or in both conditions. Some subjects were tested in

both conditions, while others decided to experiment with only one type. A trial block comprised 80 strings with each of the 16 possible combinations appearing five times in randomized order.

Data Collection

The experimenter logged the subject's answer for each trial. The slider trajectory was automatically recorded by the system. It was analyzed offline to compute the duration of trials. A trial was considered to begin when the rightmost actuator first arrived at the leftmost virtual dot, and to end when it crossed this dot again for the last time in the opposite direction. In other words, the leading and trailing parts of the slider trajectory for which no actuator was affected by the Braille string were discarded.

3.4.2 Results and Discussion

The main results of this legibility experiment as well as those of a control experiment with conventional Braille (Section 3.5) are summarized in Table 3.1.

Legibility

Legibility was defined by the proportion of correct identifications of two-character strings. Results suggest that the effect of adding texture was idiosyncratic (see Table 3.1). A dramatic improvement in performance was seen in one subject, while a

	Number of Trials			Legibility (%)			Average Trial Duration (s)		
Subject	Nominal	Textured	Control	Nominal	Textured	Control	Nominal	Textured	Control
CN	80	160	80	97.5	88.1	100.0	4.8±2.7	4.6±2.2	3.4±0.7
RB	0	80	80		95.0	100.0		10.8±7.0	7.4±1.4
ML	80	0	80	98.8		100.0	4.6±3.2		2.3±0.6
AB	40	80	80	45.0	86.3	100.0	18.6±12.2	10.5±6.3	2.4±0.7
MS	80	80	80	71.3	66.3	100.0	8.0±2.7	9.1±3.0	5.8±1.7
Average	56	80	80	78.1	83.9	100.0	9.0	8.8	4.3

Table 3.1 Summary of results from legibility experiments. Results from the first experiment (VBD, Section 3.4) are presented in columns "nominal" and "textured." Results from the second experiment (conventional Braille, Section 3.5) are presented in the column "control." Trial durations are shown with their standard deviation.

loss was observed in two other subjects. Retaining the best conditions for each subject, the legibility rates were between 71.3% and 98.8%.

Legibility rates were also plotted over time to assess the effect of fatigue. Without texture, no significant change with time could be noticed. However, for some subjects, performance tended to decrease noticeably after about 50 trials when texture was used (see Figure 3.14 for one of the worst-case examples).

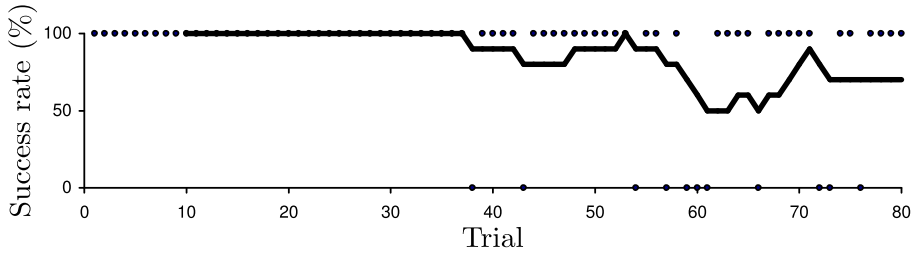

Fig. 3.14 Worst-case example of gradual decrease in performance over time (subject AB, with texture). Dots indicate individual trial results. The curve is a moving average over the past 10 trials.

Character Pairs Legibility

Regardless of the string, individual characters having one dot, '●○' or '○●', were harder to read than characters having no or two dots, '●●' or '○○' (see Table 3.2). The legibility also varied with the two-character string (see Table 3.3). Except for special cases such as the pair "○○ ○○" which was read perfectly, no insight could be gained regarding the cause of variations in reading difficulty. It is not clear, for example, why the string "●○ ○●" has much lower legibility than "○● ●○".

●○	○●	●●	○○
83.3	88.9	92.2	98.1

Table 3.2 Average character legibility (%). The average was computed across all subjects using individual subject means to compensate for the unequal number of trials under the different conditions.

Table 3.4 shows the confusion matrix for individual characters. No clear pattern emerged, except perhaps that '●●' and '○○' were rarely mistaken for one another. Similarly, Table 3.5 shows the confusion matrix for pairs of characters. Again there was

●○ ○●	●○ ○○	○● ●●	●○ ●●	●● ●○	○● ○●	●● ○●	●○ ●○
66.0	74.0	76.0	77.5	78.0	81.0	81.7	84.5
○○ ●○	○● ●○	●● ○○	○● ○○	○○ ●●	○○ ○●	●● ●●	○○ ○○
85.0	90.0	92.0	92.0	94.0	95.0	98.0	100.0

Table 3.3 Average two-character string legibility (%). The average was computed across all subjects using individual subject means to compensate for the unequal number of trials under the different conditions.

no clear pattern. However, it does seem that the most frequent errors ($n = 3, 4, 5$) generally corresponded to the insertion of a single extra dot or to the incorrect localization of a dot within a character.

		Answered			
		●○	●●	○○	○●
Presented	●○	284	17	23	20
	●●	11	315	0	13
	○○	7	1	327	0
	○●	22	9	13	298

Table 3.4 Confusion matrix for individual characters. Answers from all trials were pooled together.

Reading Patterns

Table 3.1 shows the average duration of trials. The reading speed was far from the expected Braille reading speed of 65 to 185 words per minute [151], but the conditions are so different that a direct comparison is not possible.

Correlations between reading speed and string legibility were also investigated but none could be found, even though there could be important duration variations between trials of a same subject. If it is assumed that the time taken to read a pair of characters is an indication of the confidence the subject has in her or his answer, the characters that the subjects thought were hard to read were not necessarily the ones they had difficulty reading.

The recorded trajectory of the slider was used to investigate the reading pattern used by the subjects. Three classes of patterns were identified (see Figure 3.15). Subjects often used one or two straight passes over the dots. On other occasions, they would explore the virtual Braille string with short back-and-forth motions. In all cases

Presented \ Answered	●○ ●○	●○ ●●	●○ ○○	●○ ○●	●● ●○	●● ●●	●● ○○	●● ○●	○○ ●○	○○ ●●	○○ ○○	○○ ○●	○● ●○	○● ●●	○● ○○	○● ○●
●○ ●○	37	·	·	·	·	1	1	·	2	·	·	·	·	·	3	·
●○ ●●	1	34	·	3	·	1	·	1	·	2	·	1	·	1	·	·
●○ ○○	·	·	29	·	1	·	5	·	·	·	1	·	·	·	5	·
●○ ○●	2	1	2	25	·	·	·	2	2	1	·	4	1	·	1	1
●● ●○	·	·	1	·	35	2	3	·	·	·	·	·	2	·	·	·
●● ●●	·	·	·	·	1	39	·	·	·	·	·	·	·	·	·	·
●● ○○	·	·	2	·	2	·	37	·	·	·	·	·	·	·	·	·
●● ○●	1	·	·	·	4	1	2	33	·	·	·	·	1	1	·	·
○○ ●○	·	·	·	1	·	·	·	·	37	1	·	5	·	·	·	·
○○ ●●	·	·	·	·	·	·	·	·	·	41	·	2	·	·	·	·
○○ ○○	·	·	·	·	·	·	·	·	·	·	42	·	·	·	·	·
○○ ○●	·	·	·	1	·	·	·	1	2	·	·	38	·	·	·	·
○● ●○	·	·	·	1	·	·	2	·	·	·	·	·	37	1	·	1
○● ●●	·	1	·	·	·	·	·	·	1	2	·	·	4	35	·	2
○● ○○	1	·	1	·	·	·	·	·	1	·	·	·	·	·	37	·
○● ○●	1	·	·	·	·	1	·	·	1	·	·	2	2	1	1	35

Table 3.5 Confusion matrix for pairs of characters. Answers from all trials were pooled together.

it appeared that subjects read from left to right since they moved slower in that direction.

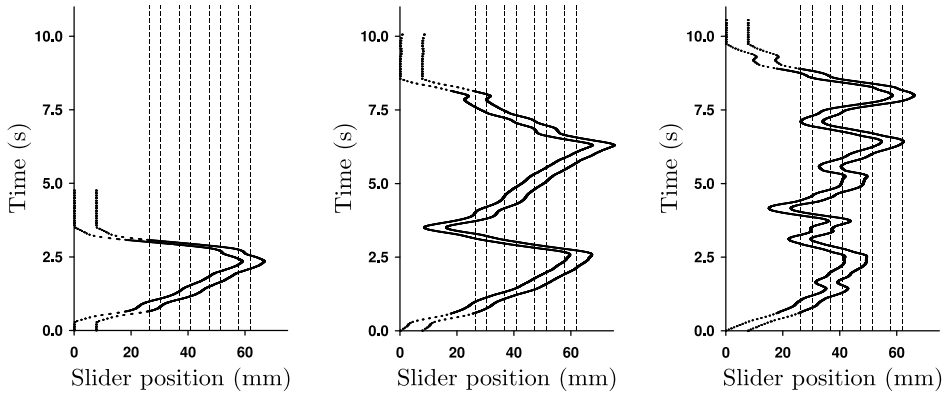

Fig. 3.15 Typical reading patterns: (a) one pass, (b) two passes, and (c) character re-scan. The band between the two curves indicates the span of the display. Dotted sections were not taken into account when computing trial durations. Vertical dashed lines indicate the location of the eight Braille dots.

Verbal Reports

All subjects reported that reading requires concentration, mostly because the dots were subtle (possibly due to the limited range of motion of actuators) and differed in perceived shape from physical Braille dots. Adding texture seemed to facilitate the perception of the dots for some subjects, while others found the sensation unpleasant. Some subjects also complained of loss of tactile sensation over time in both nominal and textured conditions. The occasionally observed decrease in performance over time seems to confirm that a loss of tactile sensation was occurring with the textured representation and was likely due to the adaptation of tactile receptors.

Subjects also reported difficulties with locating the stationary Braille dots on the virtual Braille line. Most subjects mentioned that the display of characters with more than one row of dots and having meaning would help reading.

Finally, contrary to our expectations, subjects reported that scanning constrained by a slider was beneficial because it guided their hand movement. They found it to be an advantage over paper Braille.

3.5 Control Experiment

The reading task performed in the legibility experiment was not representative of typical Braille reading. It was hypothesized that the reading difficulties experienced by some subjects were inherent to reading a single row of Braille dots. The dots found in the bottom rows of most Braille characters could facilitate the localization of the dots within the cell. Without this extra information, locating a dot completely depends on evaluating the length of the spaces between dots.

A follow-up experiment was designed to test the subjects' ability to read single-row Braille characters on a conventional Braille medium: Braille embossed on vinyl tape.

3.5.1 Method

Participants

The experiment was conducted with the same five participants, one year after the original experiment.

Materials and Tasks

The reading task was identical to that used in the original experiment. Subjects were asked to read sequences of four single-row Braille characters starting and ending with '●●'. The Braille strings were embossed on 1/2″ adhesive vinyl tape using a Braille labeler. The nonexistent 'dot #4' character was produced by sanding down the extra dot on character '.' of the embossing wheel.

The resulting Braille has smaller, sharper dots than paper Braille but is still easily readable and commonly used. Vinyl was preferred over paper because it afforded better control on the uniformity of the test plates.

Sixteen Braille labels (one per string) were produced. Each was affixed to a thin, right-angled metallic plate. The placement of the tape was carefully controlled to minimize differences between the plates and to allow sufficient space for the finger. During trials, the plates were held down by a switchable magnetic clamp that allowed us to change the strings quickly, see Figure 3.16(a). A single flattened dot was printed on the extreme-left of the tape to serve as a starting point for reading.

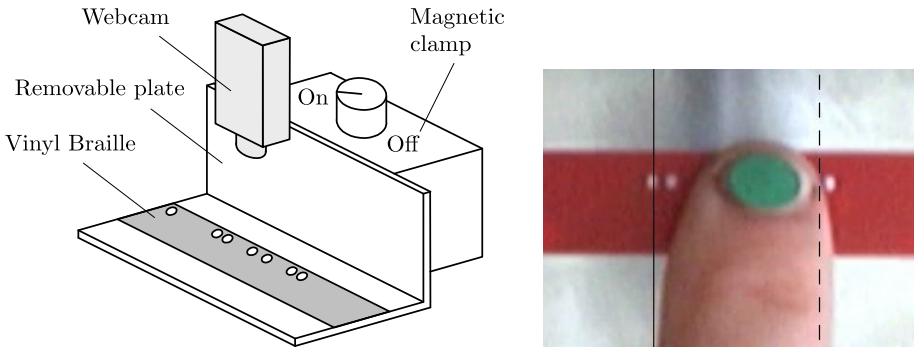

Fig. 3.16 Control experiment with conventional Braille: (a) apparatus, and (b) example of image processing. The location of the leftmost Braille dot is indicated by a solid line. The right edge of the finger is indicated by a dotted line. A green dot was affixed to the nail but not used for processing.

Procedure

The subjects were read written instructions and had supervised practice trials until they felt comfortable with the task. They were presented with strings to read in block

trials. They placed their finger to the left of the plate, waited for an audible signal, slid their finger over the flattened positioning dot, read the string, reported verbally the two middle characters, slid their finger back over the tape, and removed it from the plate. They were instructed to read only with their right-hand index finger and to keep their other fingers against their palm. There was no time limit but they were strongly encouraged to answer quickly. In case of doubt, they were asked to give their best guess. The experimenter logged the result of each trial. A trial block comprised 80 strings with each of the 16 possible combinations appearing five times in randomized order.

Data Collection

A camera was positioned above the reading surface and was used to record color movies of the finger movements at a rate of 30 frames per second. The movies were compressed and stored for later analysis. A single, uncompressed image of the plate was also taken. The reading patterns and trial durations were analyzed from the movies captured during the experiment. Simple image-processing operations were applied on the plate image to extract the position of the leftmost dot of the four-character string. The absolute difference between the saturation levels of each frame with the background frame was then used to locate the fingertip in the image sequence. In order to approximate the definition of trial duration used in the original experiment, the trial was considered to begin as the rightmost part of the index crosses over the leftmost dot, and to end when it crosses it again in the reverse direction for the last time. The automated measurements were inspected visually and corrected for 75 of the 400 trials. The precision was estimated to be within three frames (± 0.1 s).

3.5.2 Results and Discussion

Legibility

All five subjects read the 80 strings presented to them with 100% accuracy. It is thus clear that the reading difficulty experienced by the subjects with the VBD cannot be explained solely by the inherent difficulty of the task.

Reading Patterns

Table 3.1 shows the timing measurements. The subjects read faster on vinyl Braille than on the VBD, more than twice as fast on average. However, one of the slowest subjects on the VBD (AB) is also one of the fastest on vinyl Braille. The reading patterns were also inspected visually to assess their naturalness. Some subjects clearly slowed-down when sliding over dots and frequently returned to previous dots, or to the beginning of the string. This suggests that the reading strategies used by the subjects were different from those used in normal Braille reading [239, 24, 182, ch. 3].

Verbal Reports

Most of the subjects mentioned spontaneously that the reading task was easier on embossed plastic than it was on the VBD. Upon questioning, however, some acknowledged that the reading task was more difficult than typical Braille reading due to the lack of context (meaningless strings) and the absence of cues on the bottom rows. Subjects were also uncomfortable reading with a single finger, and particularly with keeping the other fingers in a fist.

3.6 Conclusion and Future Work

This study showed that experienced Braille readers could read sequences of first-row Braille characters using the VBD with a legibility ranging from passable to excellent. This is encouraging considering that most subjects had little prior training with the device and that the character strings were meaningless.

Reading with the VBD was nevertheless difficult. The control experiment showed that subjects could read faster and with perfect accuracy when the strings were presented on embossed vinyl tape. This observation is confirmed by the subjects' verbal comments during both experiments.

Adding texture to the dots was found to increase performance for some subjects but was rejected by others. Prolonged use also seemed to cause tactile fatigue (numbness in the reading finger) as reported by subjects for both nominal and textured stimulus. This phenomenon was sometimes confirmed by an increase in the number of reading errors over time in the case of textured stimulus.

While this study was conducted with too few subjects to make it possible to draw final conclusions, it suggests nevertheless that reading Braille characters with devices based on the principle of the VBD could be possible. The study also helped identify the strengths and weaknesses of the current prototype and, more importantly, provides indications as to how it could be improved.

The strength of the dot sensation must be increased to realistically convey the illusion of a Braille dot. This issue involves the improvement of the actuators used and of their configuration. Ongoing work concerned with the micromechanical properties of the skin and the means to deform it at a very small scale is expected to yield an improvement in the performance of piezoelectric benders for this application [292]. Further experimentation with deflection functions could also lead to better approximations of the sensation of scanning over Braille dots. Designing deflection functions for maximum strain variations at skin mechanoreceptors may, for example, increase the strength of the dot sensation. Indeed static mechanical models of the skin designed by Phillips and Johnson [213] and Van Doren [55] suggest that deformation of receptors, as opposed to their displacement, is likely to determine sensation. The strain experienced by slowly adapting (SA) receptors may be particularly important to resolve the spatial details of scanned Braille [214].

The cause of tactile fatigue must also be addressed. It is not clear what causes it and how it can be avoided. It is likely however that replacing the contact line by a more uniform contact surface could significantly delay the onset of tactile numbness.

Reading with the VBD requires a scanning movement. While this allowed the VBD to render adequately the dynamic sensation of sliding over dots, it prevented the user from stopping over a region as is sometimes done when reading physical Braille. Display without net movement could be possible if the magnitude of the strain produced by the device was made to depend on the force applied by the subject. This not only could make the sensation of sliding over a dot more realistic, but also allow the subject to stop and press against virtual dots.

The results of the tuning experiment and of the legibility experiment conspire to indicate that perhaps the greatest problem with the current display design is the difficulties experienced by subjects in evaluating the distance between dots. This is suggested by the distortions in perceived Braille dimensions introduced by the VBD when compared to standard English Braille. This is also consistent with observed reading

errors and verbal reports of the legibility experiment.

Finally, the VBD should be extended to display complete Braille characters. Packing four rows of actuators capable of displaying forces and displacements similar to those of the VBD within the height of a Braille cell will be a significant technical challenge.

Acknowledgements

The authors would like to thank the reviewers for their contribution to the clarity and completeness of this paper. This project was mostly done under contract with VisuAide inc (Longueuil, Canada). The authors wish to thank Pierre Hamel and Jean-Michel Gagnon of VisuAide Inc. for management and technical support respectively, and the subjects who participated in the study. Others aspects of this project are supported by the E. (Ben) & Mary Hochhausen Fund for Research in Adaptive Technology For Blind and Visually Impaired Persons. Other contributions from the Canadian National Institute for the Blind (CNIB), the Institut Nazareth et Louis-Braille (INLB), and the Centre de Recherche Interdisciplinaire en Réadaptation du Montréal métropolitain (CRIR) are gratefully acknowledged. Vincent Lévesque would like to thank the Natural Sciences and Engineering Council of Canada (NSERC) and the Fonds Québécois de la recherche sur la nature et les technologies (FQRNT) for postgraduate fellowships. Jérôme Pasquero would like to thank FQRNT for a postgraduate fellowship. Vincent Hayward would like to thank NSERC for an operating grant.

Chapter 4

Braille Display by Lateral Skin Deformation with the STReSS^2 Tactile Transducer

Preface to Chapter 4

This chapter appeared in

[160] Vincent Lévesque, Jérôme Pasquero, Vincent Hayward. Braille Display by Lateral Skin Deformation with the STReSS^2 Tactile Transducer. *Proc. World Haptics Conference 2007*, pp. 115–120, Tsukuba, Japan, March 22–24, 2007.

Minor modifications have been made to the content of the published manuscript. The chapter extends laterotactile rendering of Braille dots to the display of complete 6-dot Braille characters. Lateral skin deformations were produced with the STReSS^2, a newly available general-purpose tactile display with a 10×6 matrix of laterally-moving contactors [289]. The rendering algorithms presented in the previous chapter were adapted for 6-dot Braille by producing virtual dots along the rows of the tactile array, and a texture-only dot representation introduced to compensate for the weaker forces applied by the actuated contactors. Reading Braille was shown to be possible but slow and demanding, suggesting that either a specialized Braille display be devised, or realism be abandoned in favour of high-contrast symbolic patterns. This chapter marks the end of the effort to display Braille by lateral skin deformation with subsequent chapters focusing instead on refreshable tactile graphics, a related application where much of the insight gained about tactile rendering was readily transferred.

Contributions of Authors

This chapter was written by Vincent Lévesque and revised by Jérôme Pasquero and Vincent Hayward. The work described herein was primarily performed by V. Lévesque under the supervision of V. Hayward. J. Pasquero nevertheless made significant contributions to many aspects of the work including the adaptation of the Braille rendering algorithms and the design, completion and analysis of the user experiments. The supplementary statistical analysis appended to this chapter was realized with the help of Mounia Ziat.

Braille Display by Lateral Skin Deformation with the STReSS^2 Tactile Transducer

Abstract

Earlier work with a 1-D tactile transducer demonstrated that lateral skin deformation is sufficient to produce sensations similar to those felt when brushing a finger against a line of Braille dots. Here, we extend this work to the display of complete 6-dot Braille characters using a general purpose 2-D tactile transducer called STReSS^2. The legibility of the produced Braille was evaluated by asking seven expert Braille readers to identify meaningless 5-letter strings as well as familiar words. Results indicate that reading was difficult but possible for most individuals. The superposition of texture to the sensation of a dot improved performance. The results contain much information to guide the design of a specialized Braille display operating by lateral skin deformation. They also suggest that rendering for contrast rather than realism may facilitate Braille reading when using a weak tactile transducer.

4.1 Introduction

The technology used to display Braille to visually-impaired computer users has not changed significantly for decades. Following the approach described in early patents [274], today's commercial Braille displays still rely on arrays of electromechanical Braille cells that control the protrusion of vertical pins with cantilevered piezoelectric bending actuators. This method has proved to be robust and effective, but the need for one actuator per pin pushes the price of these devices beyond that of a personal computer and makes multi-line displays economically unviable.

Several attempts have been made to reduce Braille displays to a few cells moving with the scanning finger. Fricke mounted a single cell on a slider and generated waveforms in an effort to produce sensations of friction on the skin [66]. Ramstein similarly used Braille cells in conjunction with a force-feedback planar carrier [221]. The success of this approach has been limited due to the difficulty of producing the sensation of brushing against Braille dots by indentation of the skin. These and other recent efforts at improving the refreshable display of Braille [29, 192, 228, 303] have largely focused on reducing the cost of actuation without reconsidering the necessity of creating dot-like protrusions out of a surface. Other methods of skin stimulation can be found in the literature on tactile displays [203].

We recently investigated the possibility of displaying Braille by lateral deformation rather than indentation of the skin [161]. This principle, which we name laterotactile, assumes that critical aspects of skin deformation patterns occurring during tactile exploration can be reproduced with lateral stimulation alone. A single array of lateral stimulators in fixed contact with the fingerpad may thus produce the sensation of brushing against tactile features as it deforms the skin in response to exploratory movements.

The feasibility of this approach was evaluated using a laterotactile display (see Fig. 4.1a) mounted on an instrumented slider [161]. This Virtual Braille Display (VBD) prototype reproduced the sensation of brushing against a single line of Braille dots with an array of twelve piezoelectric bending motors that caused programmable, dynamic lateral skin deformation patterns along the axis of motion of the slider. When appropriately synchronized with the exploratory movements of the finger, waves traveling across the tactile display resulted in the perception of static features resembling Braille

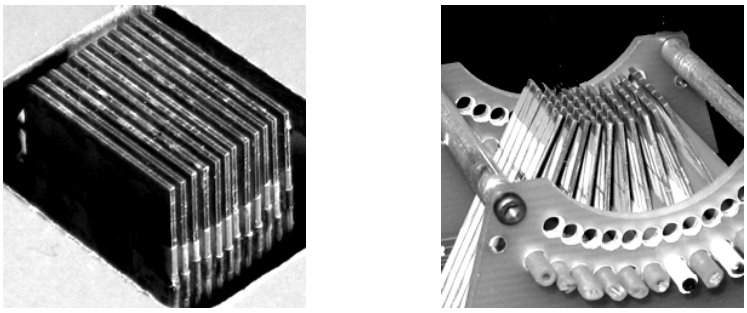

(a) (b)

Fig. 4.1 (a) 1-D tactile display used in [161] and (b) STReSS^2 general purpose 2-D display used in this work.

dots along the virtual surface. Braille readers who participated in the study were able to identify sequences of four Braille dots with an average rate of success of 90% after personalization of the sensation.

Efforts to design a general purpose 2-D laterotactile display have since resulted in the STReSS^2 [289], a third generation display with a 10-by-6 matrix of laterally-moving actuators (see Fig. 4.1b). The device shows promise for a number of application areas including the refreshable display of tactile graphics [293].

The work presented in this paper extends our earlier work to the display of complete 6-dot Braille characters using the STReSS^2. Although not designed with Braille in mind, the device's six rows of actuators make it possible to experiment with the display of multiple rows of Braille dots. The present study is a step toward the design of a laterotactile transducer optimized for the display of Braille.

4.2 Virtual Braille Rendering

The Braille rendering system comprised hardware and rendering algorithms which are described below.

4.2.1 Hardware

The STReSS^2 has an array of 10-by-6 independent skin contactors able to apply tangential forces to the skin [289]. It has an active area of 1.2 $\times$ 1.1 cm, a spatial resolution of 1.2 $\times$ 1.8 mm, and a contactor area of 0.5 $\times$ 1.6 mm. Its actuators are restricted

to lateral motion, deflecting towards the left or the right up to approximately 0.1 mm when unloaded. They exhibit a maximum force in the order of 0.15 N when prevented from moving. At the time of the present experiments, the leftmost column as well as two actuators near the center were defective. Only half of those were actually used for Braille rendering (see Section 4.2.2).

The STReSS^2 was mounted on a linear slider (see Fig. 4.2) that allowed users to explore a virtual surface as they moved the display laterally. The low-friction slider was connected to an optical encoder giving a spatial resolution of 17 µm. Actuator activation signals were produced with a resolution of 10 bits. The system was controlled by a personal computer running Linux and the Xenomai real-time framework (http://www.xenomai.org). The deflection of each actuator was updated at 750 Hz based on encoder readings.

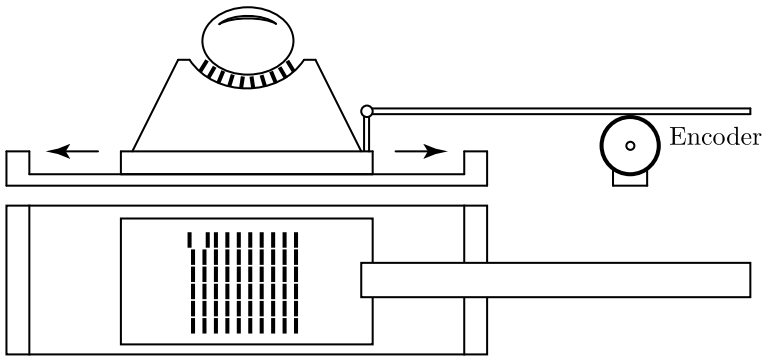

Fig. 4.2 Side view and top view of experimental apparatus comprised of a STReSS^2 tactile display mounted on an instrumented linear slider. Actuator deflection is illustrated in the upper-left corner of the display.

4.2.2 Skin Deformation Patterns

The realism and the effectiveness of the sensation crucially depend on the specification of actuator activation patterns in response to slider movements, a process that we term tactile rendering by analogy with graphics rendering. The Braille rendering algorithms described below were inspired by prior experience with the VBD [161] and tuned according to the feedback of an expert Braille reader received during an informal preliminary experimentation session. The deflection of unloaded actuators is used here as an approximation of the resulting skin deformation patterns. Actual deformation patterns differ due to the biomechanical properties of the skin [290].

Dot Rendering

The pattern that occurs for each virtual Braille dot was adapted from earlier work with the VBD [161]. Consider first a single row of actuators. The free deflection δ_i of each actuator i is a function of the position x_i of the actuator along the virtual surface. Given a pitch ϵ and slider position x_s, the actuator position is expressed as $x_i = x_s + i\epsilon$. All actuators thus follow the same deflection function along the virtual surface, but with a phase difference. This results in tactile features that appear to travel along the fingerpad as if fixed on the virtual surface.

The deflection profile for a single smooth dot swings the actuators back and forth as the dot is traversed. This gives a sensation comparable to that of brushing against a single bump. If the actuators swing back and forth many times, a sensation comparable to that of sliding over a rippled surface arises instead. The addition of such a texture to a smooth dot was earlier found to noticeably increase the stimulus strength and to facilitate reading [161]. Defining deflections of -1.0 and +1.0 as the rightmost and leftmost actuator positions, the deflection profile of a complete dot is expressed as a weighed sum of the following two profiles:

$$\delta_{\text{bump}}(p) = \begin{cases} \cos \pi p & \text{if } -1 \leq p \leq 1, \\ -1.0 & \text{otherwise;} \end{cases} \tag{4.1}$$

$$\delta_{\text{texture}}(p) = \begin{cases} \cos \pi k p & \text{if } -1 \leq p \leq 1, \\ -1.0 & \text{otherwise,} \end{cases} \tag{4.2}$$

where $p = (x_i - \text{center})/\text{radius}$ is the relative distance from the dot center and k is an odd number of cycles in the texture waveform. For a texture level T, the combined deflection profile is obtained by superposing the waveforms:

$$\delta(p) = (1 - T)\delta_{\text{bump}}(p) + T\delta_{\text{texture}}(p) \tag{4.3}$$

The preliminary experimentations indicated that texture level is an important factor for legibility. Dots without texture (T=0%), with low texture (T=25%) and with texture alone (T=100%) were thus selected for further experimentation. The preferred number of textural ripples k was 7. The resulting deflection profiles are illustrated in Fig. 4.3.

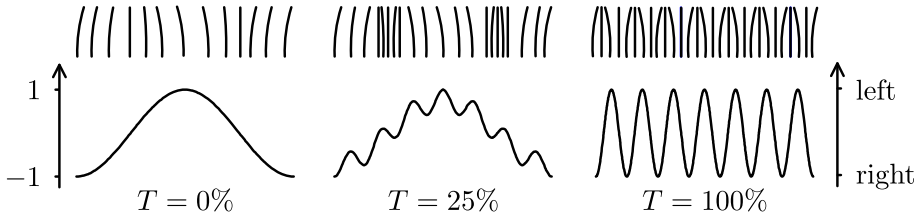

Fig. 4.3 Actuator deflection as a function of position for dots with different texture levels.

Cell Rendering

Lines of Braille dots were formed by combining dot patterns along the virtual surface. The preliminary tests showed that a strict adherence to standard Braille dimensions may not give sufficient separation between dots. Horizontal distances between dots of 3.7 mm within cells (1.6 × standard), and 7.4 mm between cells (2.0 × standard) were found to be reasonable. Dot deflection profiles were set to span 2.6 mm. The horizontal and vertical organizations of dots are illustrated in Fig. 4.4.

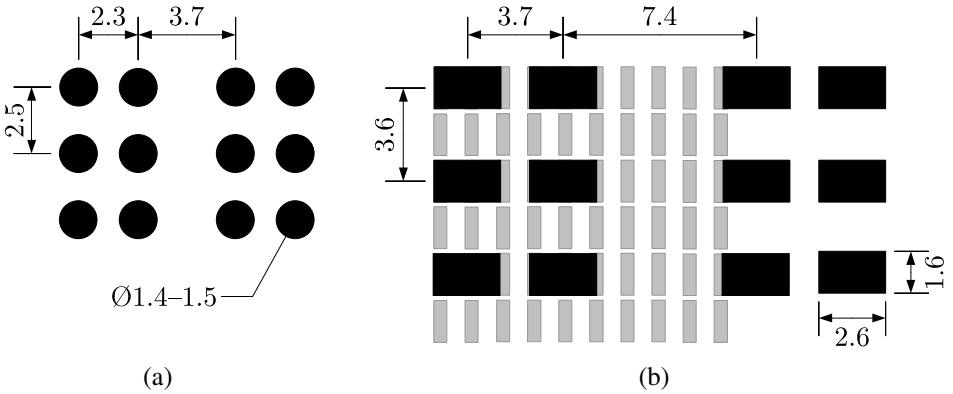

Fig. 4.4 Dimensions in mm of (a) standard Braille and (b) virtual Braille. The actuator array is illustrated in the background.

The rendering of Braille cells made use of the multiple rows of actuators available on the STReSS^2. Since the slider moves only horizontally, the three rows of dots of the 6-dot Braille cell had to be mapped to deflections along the six rows of actuators of the display. Four possibilities were implemented and evaluated.

The first method maximized the forces applied by mapping each row of dots to pairs of adjacent actuator rows (Fig. 4.5b). The second method inverted the phase of deflection profiles within a pair of actuator rows so as to maximize shearing of the

skin (Fig. 4.5c). The third method attempted to facilitate the perception of horizontal pairs of dots by showing the two column of dots of a Braille cell on different sets of actuators (Fig. 4.5d). The fourth and final method left odd rows inactive so as to increase separation between dot rows (Fig. 4.5e).

Although all methods were usable, the preliminary experimentations led to the selection of the fourth one. The first two methods were found to give slightly stronger sensations but the use of two rows per dot resulted in the perception of two dots, perhaps due to the large area of skin stimulated or the disjunction of actuators. The third method facilitated perception but felt like misaligned Braille. The selected method results in a vertical distance between dots of 3.6 mm (1.4 $\times$ standard), as illustrated in Fig. 4.4.

4.3 Virtual Braille Legibility

4.3.1 Method

The legibility of virtual Braille was evaluated by observing the performance of human subjects at reading tasks. Braille readers were asked to identify Braille strings composed of letters of the alphabet encoded according to the 6-dot Braille code (Fig. 4.6). The strings were either meaningless sequences of letters or familiar words. Following an experimental design similar to that used in [161], the level of texture applied to dots was varied to investigate its contribution to legibility. Dots were presented either without texture (T=0%), with low texture (T=25%) or with texture alone (T=100%). Other parameters were selected as described in the previous section.

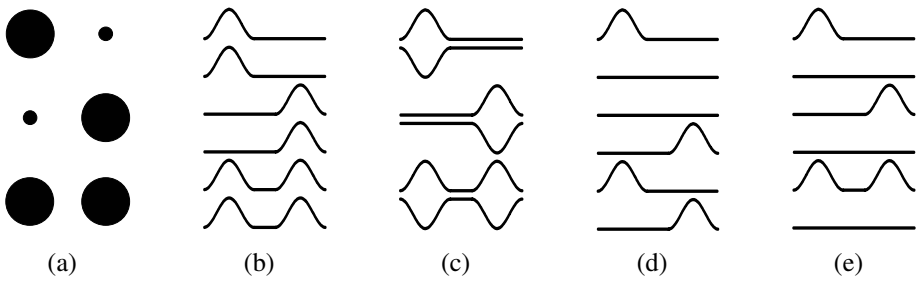

Fig. 4.5 Actuator deflection as a function of position for the six rows of the transducer. The rendering of (a) letter z is illustrated for four methods (b-e, see text). Method (e) was preferred.

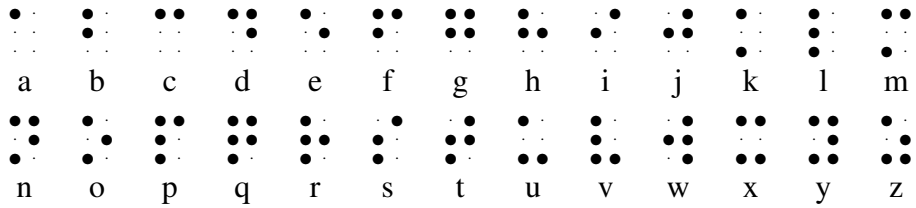

Fig. 4.6 Braille code for the alphabet.

Participants

Three female and four male experienced Braille readers volunteered for the study. Their age varied between 28 and 57, with a median of 52. Onset of blindness varied from birth to 19 years of age. The primary reading finger was the right-hand index for five subjects and the left-hand index for the other two. None of the subjects had tried the device prior to the experimental session.

Training

An experiment began with a short supervised training session during which Braille patterns of gradually increasing difficulty were displayed to the subjects. This allowed subjects to familiarize themselves with the device and the sensations it produced, thereby reducing training effects and providing time to adapt to the system's non-adherence to standard Braille dimensions.

Letter Identification

A first experiment was conducted to evaluate the legibility of meaningless strings of five letters. Subjects were asked to read using their dominant reading finger. They placed the slider to the left, waited for an audible signal, and proceeded to read the displayed string. They were instructed to verbally identify the string as soon as possible, with an audible warning after 30 seconds. Answers were logged by the experimenters. Supporting data such as the duration of trials were automatically recorded by the system.

An experimental session consisted of reading 26 five-letter strings for each of the 3 rendering modes, for a total of 390 letters. The order of presentation was randomized over two blocks of 39 readings with a short break in between. A similar difficulty level

was maintained across subjects and modes by using the same set of 26 strings in all cases. The strings were randomly assembled such that each letter appeared 5 times. Memorization effects were minimized by randomly reordering the letters of each trial's string. For example, the string *epkgn* was shown 21 times (7 subjects $\times$ 3 modes) but the order of the letters was varied randomly each time.

Word Identification

An additional experiment was conducted to evaluate legibility in a more natural context. Following a procedure similar to the first experiment, subjects were asked to identify 5-letter words in French, their native language. Forty familiar words were selected such that each letter of the alphabet was represented at least four times. Virtual Braille was rendered using the optimal texture level as obtained from the first experiment. Subjects were instructed to give their best guess or spell the letters they were reading in case of difficulty. The experiment was terminated when either all forty words were read or the hour alloted for the session was nearly over.

4.3.2 Results

Letter Identification

Performance at reading meaningless strings varied greatly between participants (Fig. 4.7). S1 had great difficulty reading and asked to halt the experiment after only a few trials. Other subjects correctly read 22% to 83% of the letters presented to them, for an average success rate of 57%. Reading appeared slow and laborious for most subjects, taking 12 seconds per string on average.

The texture level appeared to affect legibility. Average legibility increased from 50% to 56%, and then to 64% as the level of texture was increased. A series of paired t-tests confirmed that Braille with texture alone was better read than both with low texture (t=-3.246, $p<0.05$) and without texture (t=-4.456, $p<0.05$). The difference between low texture and no texture was not significant (t=-1.745, $p>0.05$). Reading speed similarly increased with the amount of texture but only the difference between Braille with texture alone and without texture was significant (t=2.688, $p<0.05$).

An inspection of reading errors shows that legibility decreased with the number of dots in a letter (Fig. 4.8). This is consistent with other reports about Braille read-

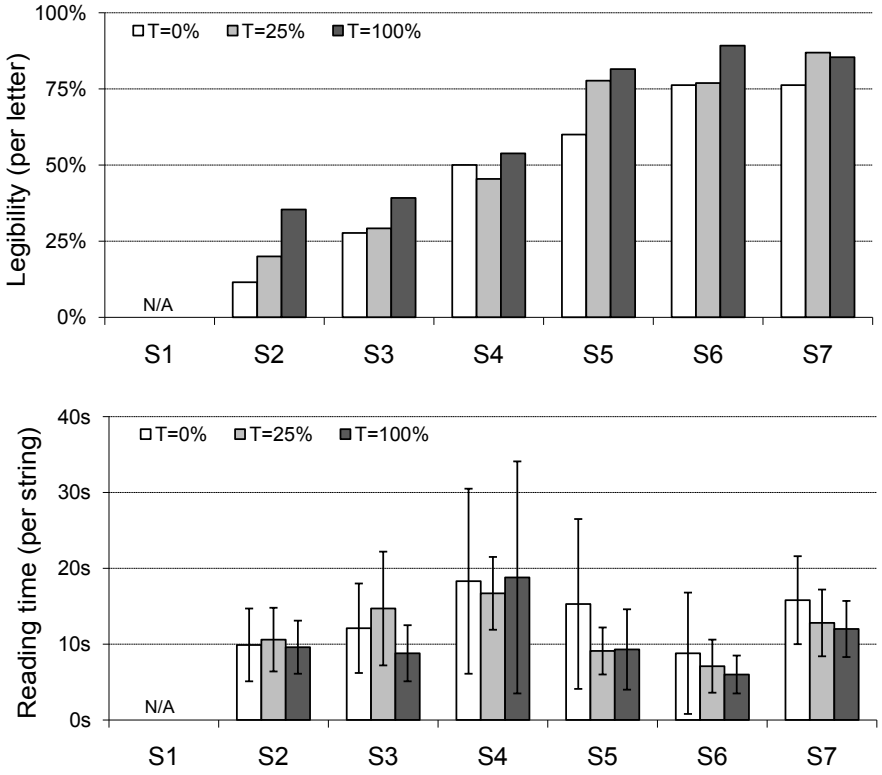

Fig. 4.7 Results of letter identification experiment.

ing [182]. Errors most frequently involved the addition or removal of a single dot (Fig. 4.8). The complete confusion matrix is shown in Table 4.1.

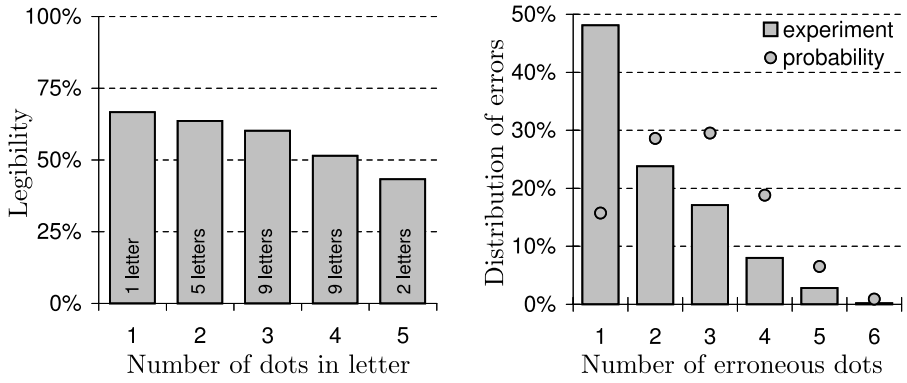

Fig. 4.8 Analysis of errors in letter identification experiment.

presented \ answered	a	b	c	d	e	f	g	h	i	j	k	l	m	n	o	p	q	r	s	t	u	v	w	x	y	z
a	**60**	1	22	2		1	1		1												1			1		
b	3	**46**		7	3	2	5	2	2	1	1	9							1	3		1	3		1	
c	17	1	**59**		1	1	4	1	1					1					2			1		1		
d	3	4	4	**54**	8	2	4	1		1		1	1			1	1		1			1	1	1	1	
e	3		1	3	**67**	1	1	3				1			3			2	1		1	1			1	1
f	3	8	1	2		**45**	5		2	1	2	2		1		11	1	1	2	3						
g	2	2	2	6	1	4	**44**	10	3	1				2			6	1				3	1	1		1
h	2			1	10	3	8	**45**		2						2		5		1	2	9				
i	6		5	2	1	6			**61**	2		1		2					1	2					1	
j		2	3	3	1	3	11	2	3	**47**			1	2	1	1			1	4			3	1		1
k	2	1		2	1				1	1	**53**	3	10	2	1			1	2		7	1		1		1
l		1	1	1		2		1				**66**				9	2			4		2			1	
m	3		8		4	1					9		**42**	11		4		1	1		1			4		1
n	2	1		1	1	1			1		2		9	**36**	13	2	2	2	3	2	2				6	4
o		1	1	1	4			2	4		2		1	2	**61**			1	3	1				1		5
p		1	1			2				1		17	1	1	2	**44**	5		3	9		1			1	1
q	3	1	2	1		2	3			1	2	6		1		9	**38**	10	1	2			1	2	3	2
r	1	1		2	1			2				9		1	2	2	2	**56**	2	1		4			2	2
s	2	3				1			1	1	1			4	1	5			**65**	4	1					1
t		3			2	1	2		1			2			1	3	5	1	12	**52**		1				4
u	4		1		2			2		1	2	1	1	2					2		**63**	2		3	2	2
v	1	2	1		1	1		1				7	2	1		1		4	1		1	**63**			1	2
w	2	3		4		1	1	1		4	1	8		2	2	2		3	2	7		1	**39**		6	1
x	3	1	4	1	2	2	2	1	1	1	3	1	6	3	1						16	1		**39**		2
y	1		1	1			2					4	1	12	3	1	9			3		5	1		**40**	6
z		1			2	1	1			1	2			6	12		1	5			6	3	1		4	**44**

Table 4.1 Confusion matrix with error counts above 4 and 9 shown with thin and thick boxes respectively.

Word Identification

Word reading experiments were performed with the level of texture most effective during the first experiment: low texture for S7 and texture alone for all others. Due to time constraints, S2 and S4 read 20 and 30 words respectively. The others read the complete set of 40 words. On average, subjects were more accurate and faster than

when reading meaningless strings (Fig. 4.9). They could read 69% of the words but only 57% of the letters in meaningless strings. The mean trial duration was 9 seconds for words and 12 seconds for meaningless strings. Individual performance at word identification was not strongly correlated with that of letter identification. S1, for instance, was unable to read meaningless strings even in a second attempt after reading words nearly flawlessly. S4 also performed much better at word reading, correctly reading 86% of the words but only 50% of the letters in meaningless strings. Overall, word reading rates were poor for two subjects (10%, 27.5%), reasonable for two others (70%, 87%), and excellent for the remaining three (95%, 97.5%, 97.5%).

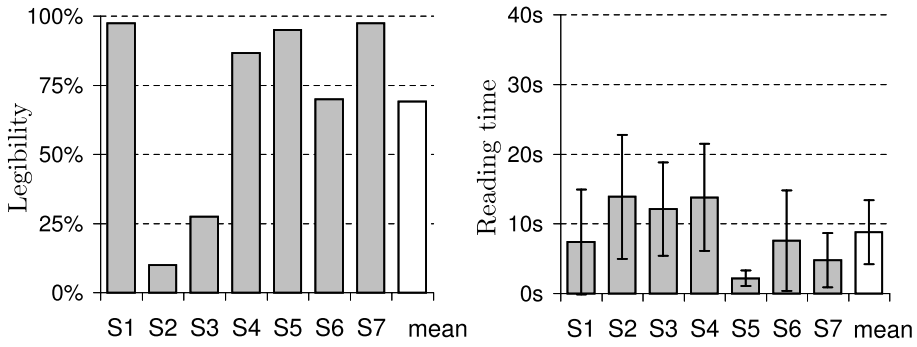

Fig. 4.9 Results of word identification experiment.

Verbal Reports

All participants felt that reading Braille rendered with the proposed system was difficult and demanded great concentration. Some compared the sensation to that of worn out or erased paper Braille. The participants expressed doubt about their skills and often reported feeling Braille characters other than the displayed letters such as punctuation. Many participants pointed out that reading was increasingly difficult over time, either due to tactile or mental fatigue. They were bothered by the large size of the virtual Braille cell and by the stimulation of parts of their fingertip generally unused for Braille reading.

The participants also confirmed that the use of texture facilitated reading by greatly increasing the strength and contrast of the dot sensation. Most participants slightly preferred the sensation of low texture although they often felt that texture alone had greater contrast. Some also suggested that the randomized presentation order of mean-

ingless strings caused masking effects when a non-textured string followed a textured one.

Despite having difficulty reading, most participants showed genuine interest in the concept and were enthusiastic about its potential for Braille and tactile graphics. Many participants compared the sensations produced by the STReSS^2 to those felt with the Optacon, a tactile transducer that enables the blind to read printed text by mapping images from a camera to vibratory patterns [163]. S1's reading difficulties were analogous to the subject's limited experience with the reading aid. S2, the only subject who still uses the Optacon regularly, felt that the STReSS^2 produced weaker sensations and had difficulty reading with it. S3 found the sensation of the STReSS^2 less irritating. Another subject who used the aid in the past had the reflex of looking for printed character patterns while reading with the STReSS^2.

4.4 Discussion

Prior work with the VBD was focused on achieving realistic sensations that approached those of physical Braille dots [161]. Our results indicated that this was possible for most subjects using the equivalent of the non-textured dot rendering used here. A small textural component, equivalent to the low texture used here, was shown to improve legibility for some users, but at the cost of some realism. The use of texture alone was never considered as it was deemed to unnecessarily stray away from standard Braille sensations.

The results obtained with the STReSS^2 point in a different direction. The ability of a laterotactile display to present realistic dot sensations appears to depend on the forces it is able to produce. Because its actuators are weaker than those of the VBD, the STReSS^2 produces subtler dot sensations that, taken together with the greater complexity of identifying Braille characters, prevent efficient reading. While texture only improved the contrast of the Braille dots on the VBD, it appears to be critical with the STReSS^2. A natural extension of this idea is to produce a purely symbolic representation of Braille patterns that leverages the Braille code without reproducing the sensation of Braille dots. As the experiment with texture alone demonstrates, knowledge of Braille appears to transfer well to this new medium.

This discussion leads to two possible approaches for the continuation of our work

on laterotactile display of Braille. A first approach is to remain within a symbolic framework and attempt to design optimal laterotactile symbols to replace Braille dots. The resulting Braille would work on most laterotactile displays but may encounter resistance from Braille readers. A second approach is to aim for realism and design a specialized laterotactile display. Large piezoelectric actuators could be cut so as to produce a dense array of three rows of skin contactors respecting Braille dimensions. The revised design may produce forces strong enough to render realistic Braille. The display could also be widened to accommodate reading with multiple fingers.

4.5 Conclusion

This paper presented the result of experiments evaluating the legibility of 6-dot Braille rendered by lateral skin deformation with a general purpose tactile transducer. Reading meaningless strings was difficult but possible for most subjects. Reading familiar words was generally faster and more accurate. The addition of a texture to the sensation of Braille dots improved legibility but reduced realism.

These results indicate that a symbolic representation of Braille dots in the form of texture may fare better than a more realistic rendition when a weak laterotactile display is used. Future work will therefore focus either on increasing the forces applied by the tactile transducer or on identifying optimal laterotactile symbols to replace Braille dots. Comments from subjects also suggest that respecting at least vertical dimensions of Braille cells is critical for comfortable reading. Rendering parameters that received attention only during the preliminary experimentation phase of this work, such as the vertical distribution of sensations along the transducer, will also be given a more rigorous treatment.

Acknowledgements

This study was approved by the Research Ethics Board of the Centre for Interdisciplinary Research in Rehabilitation of Greater Montreal. The authors thank Marie-Chantal Wanet-Defalque and Chantal Nicole of the Institut Nazareth et Louis-Braille, and Qi Wang of the Haptics Laboratory for their support.

Supplementary Statistical Analysis

Repeated measures one-way ANOVAs were conducted to evaluate the effect of the texture level (T=0%, T=25%, T=100%) on the legibility rate of characters and the reading speed of strings. The effect of texture level was found to be significant for the legibility rate [F(2,10)=10.849, p=0.003], but not for the reading speed [F(2,10)=2.841, p=0.105]. Post-hoc paired t-tests indicate a significant difference between the legibility rate of characters rendered with texture alone and either with low texture [t(5)=3.246, p=0.023] or without texture [t(5)=4.456, p=0.007], but not between those rendered without texture and with low texture [t(5)=-1.745, p=0.141].

This statistical analysis confirms the statistical difference between the legibility rate of characters rendered with texture alone and with either low texture or without texture. It does however invalidate the statistical difference reported in the reading time of strings rendered with texture alone and without texture.

Chapter 5

A Haptic Memory Game using the STReSS^2 Tactile Display

Preface to Chapter 5

This chapter appeared in

[293] Qi Wang, Vincent Lévesque, Jérôme Pasquero, and Vincent Hayward. A Haptic Memory Game using the STReSS^2 Tactile Display. *CHI '06 Extended Abstracts on Human Factors in Computing Systems*, ACM, Montréal, Québec, Canada, pp. 271–274, 2006.

This chapter presents early work on the rendering of virtual tactile graphics by lateral skin deformation that forms the basis of the framework developed in Chapters 6, 8 and 9. Written in support of a demonstration at the CHI'06 conference, it introduces a haptic memory game that demonstrates numerous graphics rendering concepts further developed and applied extensively in subsequent chapters, including the use of vibrations, grating textures, dot patterns and bitmap-based masks. Published prior to Chapter 4, this work leverages the insight gained while investigating Braille dot rendering (Chapter 3) in the related context of tactile graphics, the focus of the remainder of this thesis.

Contributions of Authors

This chapter was written by Vincent Lévesque in support of a demonstration of the STReSS^2 tactile display presented at the ACM CHI'06 conference and revised by his co-authors. The author list reflects the contributions of the authors to all aspects of the demonstration. Qi Wang designed and implemented the STReSS^2 transducer [289] and assembled the tactile graphics interface used in this chapter and the next, referred to as the Pantograph-based Tactograph in Chapter 7. He also contributed an early version of dot-based graphics and helped tune the rendering algorithms. V. Lévesque designed and implemented the tactile rendering algorithms and the memory card game based in part on earlier work and unpublished observations made while investigating Braille rendering in collaboration with Jérôme Pasquero (Chapter 3). J. Pasquero also contributed to the tuning of the rendering algorithms and to the selection of tactile memory cards. This work was supervised by Vincent Hayward.

A Haptic Memory Game using the STReSS^2 Tactile Display

Abstract

A computer implementation of a classic memory card game was adapted to rely on touch rather than vision. Instead of memorizing pictures on cards, players explore tactile graphics on a computer-generated virtual surface. Tactile sensations are created by controlling dynamic, distributed lateral strain patterns on a fingerpad in contact with a tactile display called STReSS^2. The tactile graphics are explored by moving the device within the workspace of a 2D planar carrier. Three tactile rendering methods were developed and used to create distinct tactile memory cards. The haptic memory game showcases the capabilities of this novel tactile display technology.

5.1 Introduction

The memory card game is played by randomly placing a set of cards face down on a table. Players turn over cards two at a time. If the pictures on the cards match, a point is scored and the pair is removed from the playing area. Pairs that do not match are turned back face down. To succeed, players must memorize the location of previously exposed cards. We revisited this classic game to explore the potential of a novel tactile display named STReSS^2 (pronounced "stress-square") [289]. We replaced the pictures with computer-generated virtual tactile graphics. Using carefully designed stimulation patterns, we produced 12 distinct tactile cards. Instead of seeing the pictures on the cards, players explore their tactile equivalent with a finger.

5.2 Technology

Tactile displays are computer-driven transducers able to create tactile sensations on the fingerpad [21]. The STReSS^2 is distinct from most other displays in that it takes advantage of the skin's sensitivity to distributed lateral deformation. The device has an active area of 12.0 $\times$ 10.8 mm, slightly larger than a fingerpad. It deforms the skin using a 10 $\times$ 6 array of piezoelectric bending motors (see Figure 5.1).

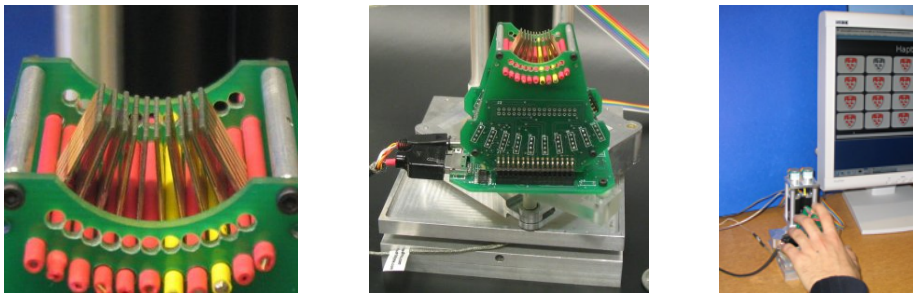

(a) (b) (c)

Fig. 5.1 STReSS^2 tactile display: (a) active area, (b) display on carrier that allows movement in the horizontal plane, and (c) player's left hand with index on the display.

The display is mounted on a Pantograph haptic device used as a passive 2D planar carrier [37]. Players explore a 11.3 $\times$ 6.0 cm virtual surface by moving the display within the carrier's workspace with a finger. The fingerpad remains fixed on

the display's active area. The skin deformation patterns are updated according to the exploratory movements, creating the sensation of sliding over embossed or textured virtual surfaces. Alternatively, the display can produce distributed vibratory patterns.

5.3 Tactile Rendering

The specification of programmed spatiotemporal actuator deflection patterns may be termed tactile rendering by analogy to graphics rendering. Three types of tactile rendering methods were developed.[1] They are illustrated in Figure 5.2. In each case, tactile patterns are specified as grayscale images (e.g. Figure 5.2a), making it possible to quickly draw complex tactile graphics using standard painting software.

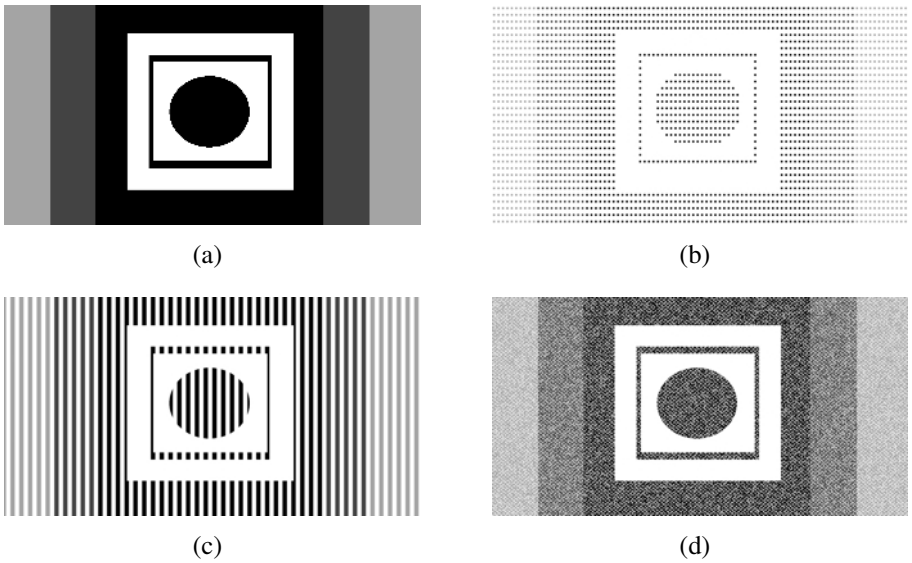

Fig. 5.2 (a) A pattern specified by a grayscale mask and a pictorial representation of its tactile rendering using (b) dots, (c) a grating texture or (d) vibration.

The first method divides the virtual surface into 94 $\times$ 33 cells, each containing a 1.2 $\times$ 1.8 mm tactile feature resembling an embossed dot (e.g. Figure 5.2b). The perceived height, or intensity, of each dot is controllable, giving rise to the tactile

[1]The statements found in this Chapter concerning the subjective experience of tactile renderings, their optimal use, and the selection of tactile cards are based on the impressions of the authors as well as feedback from a small group of volunteers who participated in informal evaluation sessions. A more rigorous evaluation of the tactile renderings is provided in the next Chapter.

equivalent of a coarse grayscale image. The deflection of each actuator is continuously updated based on its location within the surface. As an actuator traverses a dot, it smoothly sweeps its entire range of motion. The experience of a dot results from the local skin stretch and compression patterns occurring locally between adjacent actuators. A similar method was previously used to display virtual Braille dots [161]. This mode is particularly adequate for the display of contours, edges, and letters. It produces tactile graphics comparable to those obtained with Braille printers [190].

The second type of rendering fills areas with a spatial texture resembling an embossed horizontal grating (e.g. Figure 5.2c). The grating is produced from a traveling wave moving on the display in response to exploratory movements. As the wave travels in the direction opposite to the finger movement, one has the sensation of sliding over a rippled surface. The amplitude of the texture is modulated over the virtual surface to form simple shapes. Tactile maps for the blind commonly make a similar use of texture to mark regions such as bodies of water [59].

The third approach replaces the spatial texture with an amplitude-modulated vibrotactile stimulus (e.g. Figure 5.2d). The vibrotactile stimulus is produced by driving each actuator with a 50 Hz sinusoidal signal. The phase is inverted between adjacent actuators to maximize strain. Unlike the two previous methods, vibration provides strong stimulation even in the absence of exploratory movements. The resulting sensation, however, is difficult to relate to a natural tactile stimulus. Vibration was found to reliably convey thick line drawings and contours. This mode of stimulation is similar to the one used by the Optacon, a vibrotactile reading aid for the blind [163]. The STReSS^2, however, vibrates laterally instead of tapping against the skin, and allows more control over the stimulation frequency and amplitude. A similar use of image-based vibrotactile stimuli has also been made for the rendering of texture [104].

5.4 Haptic Memory Game

The game was implemented on a personal computer by replacing the pictures on the cards with tactile graphics. When the user clicks on a card using the mouse, the card becomes activated (highlighted) but its content is not revealed visually (see Figure 5.3). Instead, the player must explore an invisible tactile drawing.

The three modes of stimulation were used to design a set of 12 tactile memory

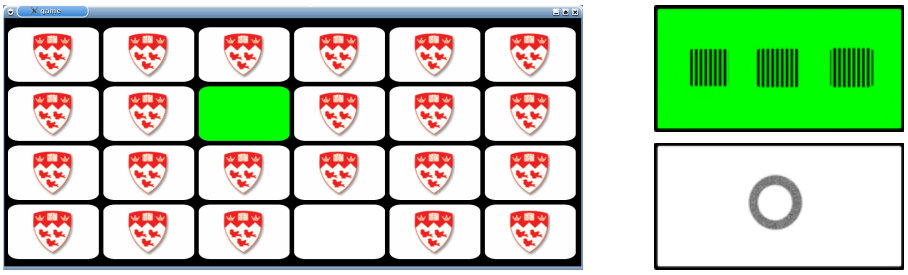

(a) (b)

Fig. 5.3 (a) Haptic memory game with currently selected card highlighted and (b) pictorial representation of exposed cards.

cards represented pictorially in Figure 5.4. After a short training period, the cards can be distinguished from one another using tactile stimuli alone.

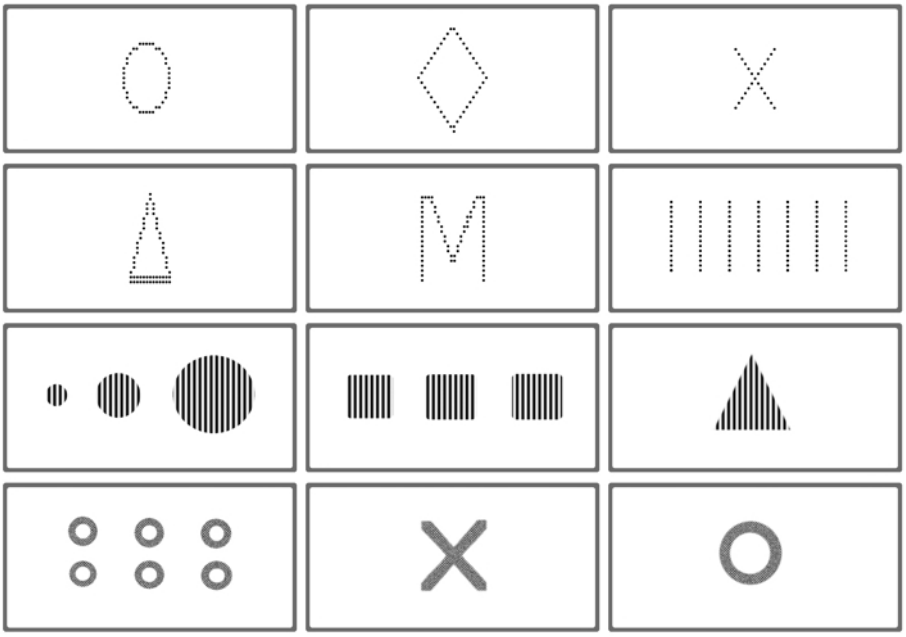

Fig. 5.4 Pictorial representation of 12 tactile cards selected for the memory game: dots, gratings, and vibration.

5.5 Conclusion

This paper introduced a new version of the memory card game that uses tactile feedback. The main purpose of the game is to exemplify the capabilities of the STReSS^2

tactile display. The game demonstrates that the display can be used to produce convincing tactile graphics. Although some visual feedback is currently required to select cards, this game could also easily be adapted for visually impaired players [255].

The three rendering methods introduce basic building blocks for simple shapes, and eventually for more complex drawings. One could consider, for example, drawing a bicycle using vibrating wheels, a dotted frame and grating-textured ground. The Pantograph could also be used to provide additional force feedback. We expect future work to yield a wider range of expressive capabilities as well as applications to other areas of human-computer interaction.

Acknowledgements

The authors would like to thank the members of McGill's Haptics Laboratory as well as Danny Lynch and Prasun Lala for their help and support. This research was supported by NSERC, the Natural Sciences and Engineering Research Council of Canada.

Chapter 6

Tactile Graphics Rendering Using Three Laterotactile Drawing Primitives

Preface to Chapter 6

This chapter appeared in

[159] Vincent Lévesque and Vincent Hayward. Tactile Graphics Rendering Using Three Laterotactile Drawing Primitives. *Proc. 16th Symposium on Haptic Interfaces For Virtual Environment And Teleoperator Systems*, IEEE, Reno, Nevada, pp. 429–436, 2008.

Additional information has been inserted in the published manuscript in the form of footnotes. The chapter presents a preliminary evaluation of an improved virtual tactile graphics framework that extends the laterotactile rendering approaches briefly described in the previous chapter. Major improvements include support for arbitrarily-oriented gratings and the elimination of restrictions on the placement and exploration direction of dots. The evaluation of the framework demonstrates that shapes and textures can be identified in a variety of conditions and provides insight into the optimization of rendering parameters for practical tactile graphics applications. The results of this work have informed further developments presented in Chapters 8 and 9, and prompted the design of an improved tactile graphics interface described in the next chapter that provides a larger canvas and measurement of the tactile array's orientation.

Contributions of Authors

This chapter was written by Vincent Lévesque and revised by Vincent Hayward. The work described herein was similarly performed by V. Lévesque under the supervision of V. Hayward. The supplementary statistical analysis appended to this chapter was realized with the help of Mounia Ziat.

Tactile Graphics Rendering Using Three Laterotactile Drawing Primitives

Abstract

This paper presents preliminary work towards the development and evaluation of a practical refreshable tactile graphics system for the display of tactile maps, diagrams and graphs for people with visual impairments. Refreshable tactile graphics were dynamically produced by laterally deforming the skin of a finger using the STReSS^2 tactile display. Tactile features were displayed over an 11×6 cm virtual surface by controlling the tactile sensations produced by the fingerpad-sized tactile display as it was moved on a planar carrier. Three tactile rendering methods were used to respectively produce virtual gratings, dots and vibrating patterns. These tactile features were used alone or in combination to display shapes and textures. The ability of the system to produce tactile graphics elements was evaluated in five experiments, each conducted with 10 sighted subjects. The first four evaluated the perception of simple shapes, grating orientations, and grating spatial frequencies. The fifth experiment combined these elements and showed that tactile icons composed of both vibrating contours and grated textures can be identified. The fifth experiment was repeated with 6 visually impaired subjects with results suggesting that similar performance should be expected from that user group.

6.1 Introduction

Refreshable braille displays and speech synthesizers have greatly improved access to textual information for visually impaired persons by giving them access to digitized content. Access to graphical information remains comparatively limited in part because visual graphics must be processed and simplified to be suitable for tactile use, but also because of the unavailability of reliable and affordable means to convey refreshable tactile graphics through a computer. Most tactile graphics are currently produced on physical media through a variety of methods including collage, embossed paper, thermoforming, printing on microcapsule paper and, more recently, high-density braille printing and 3D printing [59, 288, 175]. Tactile graphics produced with such methods have proved to be of great use for geographic and orientation maps, mathematical graphs and diagrams. These are particularly important in education where visually-impaired students must have access to the same information as their sighted peers [5, 146]. They can also provide information which would be difficult to grasp from direct experience of the environment or from verbal descriptions [27]. Tactile graphics produced on physical media, however, are typically bulky and often deteriorate with use. More importantly, physical media does not afford access to dynamic content such as interactive geographic information systems (GIS). The interactive control over features such as layer visibility and zoom level offered by these applications could be particularly valuable in the context of tactile graphics since information density must generally be reduced to cope with the skin's limited resolution. Refreshable tactile graphics could therefore improve the experience of interacting with graphical information for the visually impaired.

Various approaches have been explored to produce interactive tactile graphic displays. Pen-based 3D force-feedback devices can be used to simulate the exploration of raised-line drawings or other 3D patterns with a probe [186, 256, 305]. Patterns can similarly be produced with 2-DOF haptic devices such as consumer-grade haptic mice and joysticks [201, 305]. Although these approaches can be effective, interacting with a single-point of contact reduces realism and complicates exploration. An alternative consists of using a transducer known as a tactile display that produces programmable tactile sensations by deforming or otherwise stimulating the skin. Research on tactile displays has resulted in a wide array of prototypes using different skin stimulation

methods and actuation technologies [282]. The difficulty of designing tactile displays results largely from the high density of actuators needed to produce distributed sensations in the fingerpad. Although their use extends to other fields such as surgery simulation and gaming, many tactile displays have been evaluated on the basis of their ability to display shapes or other tactile patterns [265, 252, 139, 116, 23]. Readers are referred to [282] for a more complete survey of experimental tactile displays and their use as graphical displays for visually impaired persons.

Tactile displays can be divided in two classes depending on whether they provide a real or virtual surface for exploration. The first class of displays presents a large, programmable surface to be explored by the fingers or hands. The surface typically consists of an array of actuated pins that produce a discrete approximation of a 3D surface. Shimada et al., for example, designed a tactile graphics display system with a 32×48 array of braille pins manufactured by KGS Corp. (Japan) [248]. Although this approach closely approximates static tactile graphics, it also increases cost due to the large number of actuators needed. The large size of such tactile displays also hinders portability. The second approach consists of producing a large virtual surface out of a smaller tactile display. This is achieved by dynamically altering the sensation produced by a tactile display in fixed contact with the fingerpad in response to displacements. The most famous example is the Optacon, a reading aid commercialized in the 1970's that converted images of printed text captured from a mobile camera to tactile patterns on an array of 24×6 vibrating pins [163]. Reasonable reading rates were achieved after considerable training. Tactile displays of this class can also be used to explore virtual tactile graphics when connected to a personal computer. An example is the VTPlayer mouse with its two 4×4 braille pin arrays [115]. The main advantage of this approach is that fewer actuators are needed, reducing cost and size. Producing meaningful sensations without relative motion between the stimulator and fingerpad, however, is challenging.

The work presented in this paper aims to address this problem by producing controlled lateral skin deformation patterns rather than indenting the skin. This principle, which we name laterotactile stimulation, assumes that the critical deformation occurring at the level of the mechano-receptors can be approximated by laterally deforming the skin. A series of tactile displays have been designed to exploit this principle including 1D [161, 166] and 2D [289] arrays of laterally moving skin contactors. All

use a similar technology based on piezoelectric bending motors. Previous work has shown that when appropriately programmed, skin deformation patterns produced by these displays can evoke the sensation of brushing against localized features such as braille dots and gratings [161, 160, 166].

This paper presents our most recent work on the display of refreshable tactile graphics using the latest 2D laterotactile display, the STReSS^2 [289]. Three tactile rendering methods capable of producing the sensation of gratings, dots, and vibrating patterns are presented. An early version of these tactile rendering algorithms were previously used in a tactile memory game that demonstrated the capabilities of the STReSS^2 tactile display during the 2006 ACM Conference on Human Factors in Computing Systems [293].

This paper also reports on our efforts to evaluate the effectiveness of the system for the display of tactile graphics. A first experiment evaluated the identification of simple shapes using the three rendering methods. The next three experiments investigated the device's rendering of tactile gratings at various orientations and spatial frequencies. The final experiment combined shape and texture rendering to evaluate the system's ability to display tactile icons. The first four experiments were each conducted with 10 sighted subjects. The final experiment was conducted with 10 sighted and 6 visually impaired subjects to validate the results for the target user group. The elements of tactile graphics investigated here constitute a first step toward the design of tactile maps and diagrams adapted for display by laterotactile stimulation.

6.2 Tactile Display Prototype

The tactile rendering system used in this work is a prototype that combines a STReSS^2 tactile display with an instrumented 2D planar carrier (Fig. 6.1). The STReSS^2 revision used stimulates the skin by controlling the deflection of a matrix of 8×8 piezoelectric bending motors [289]. The actuators deflect toward the left or right by approximately 0.1 mm, and produce a blocked force in the order of 0.15 N. The center-to-center distance between adjacent actuators is 1.2×1.4 mm. The reading fingerpad therefore rests against an active contact area of 9×11 mm. Filters with a 200 Hz cut-off frequency enable more accurate signal reconstruction and attenuate most energy at the natural resonance frequency of the actuators, resulting in the elimination of most audi-

ble noise and in more natural tactile sensations.

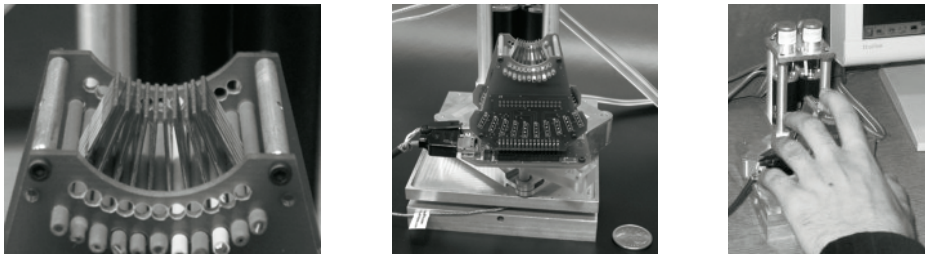

(a) (b) (c)

Fig. 6.1 (a) Active area of the STReSS^2 tactile display, (b) STReSS^2 mounted on a planar carrier, and (c) usage of the device.

The STReSS^2 was mounted on a planar carrier that allowed movement within a 11×6 cm virtual surface. The carrier was a 2 degree of freedom (2-DOF) haptic device with low friction and inertia called the Pantograph [37]. The device was used as a passive carrier and its motors were therefore inactive. The carrier measured position with a resolution better than 13 µm. The workspace of the Pantograph was slightly reduced to prevent collision with the tactile display, resulting in the above mentioned virtual surface dimensions. Rotation of the display was neither prevented nor measured and users were therefore required to maintain the orientation of the display. The tactile display's electronics were covered with a plastic protector and foam for safe and comfortable usage. More information about this apparatus can be found in [289].

The system's driving signals were produced at 1 kHz on a personal computer running Linux and the Xenomai real-time framework (http://www.xenomai.org). Actuator activation signals were produced with a resolution of 10 bits. Rendering algorithms and drivers were programmed in C++.

6.3 Tactile Rendering

The STReSS^2 display produces tactile sensations by dynamically controlling lateral deformation patterns on the fingerpad in response to exploratory movements within its planar carrier's workspace. Extracting meaningful sensations from this mode of skin stimulation requires the specification of appropriate actuator activation patterns, a process that we term tactile rendering by analogy with graphics rendering. This section describes in details three laterotactile rendering methods that produce dotted out-

lines, vibrating patterns and virtual gratings. The tactile sensations produced by these rendering methods are modulated over the virtual surface using bitmapped grayscale images. This allows the creation of tactile patterns with standard image editing software. These renderings can also be combined to create more complex tactile graphics. Fig. 6.2 shows visual representations of squares rendered with all three methods.

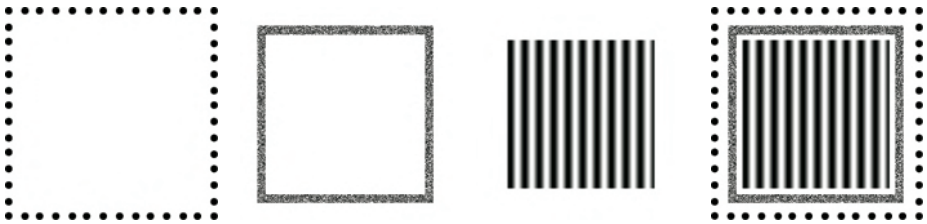

Fig. 6.2 Visual illustration of squares rendered with (a) dots, (b) vibration, (c) gratings, and (d) a combination of all three.

By convention, the following discussion specifies actuator deflections δ between 0 (right) and 1.0 (left). Deflecting actuators to the right when at rest provides a greater swing upon activation and increases the strength of some sensations. Although directional effects appear to be minimal, this resting position is also selected so that activation occurs against motion when moving the display from left to right. The deflection of unloaded actuators is used here as an approximation of the intended skin deformation patterns. Actual deformation patterns may differ due to the complex biomechanical properties of the skin. Fig. 6.3 illustrates the displacement of the tactile display over a virtual surface as well as the deflection of its actuators.

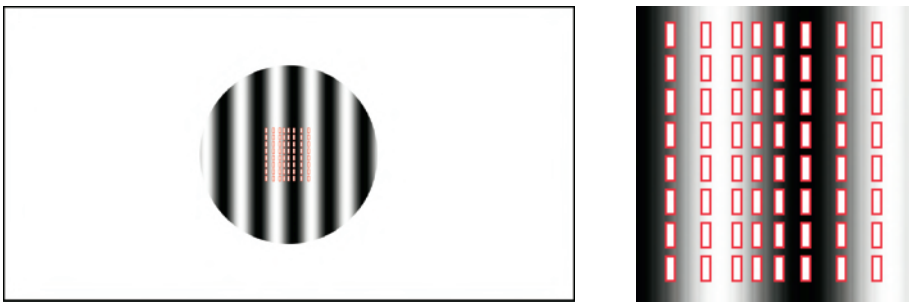

Fig. 6.3 (a) Virtual surface with a grated circle and (b) close-up on tactile display deflection pattern.

6.3.1 Dot Rendering

The sensation of brushing against a dot is produced by swinging actuators towards the left and then back to the right as they slide over a virtual dot. The deflection is expressed mathematically as follows:

$$\delta(r) = \begin{cases} 1.0 & \text{if } r \leq P, \\ \frac{1}{2} + \frac{1}{2}\cos\pi\frac{(r-P)}{(1-P)} & \text{if } P \leq r \leq 1.0, \\ 0.0 & \text{otherwise;} \end{cases} \tag{6.1}$$

where $r = \|p_{i,j} - p_{\text{center}}\|/\text{radius}$ is the relative distance from the center of the dot. As they move over the dot, actuators first follow a smooth sinusoid that takes them from their rest position on the right to their active position on the left. They then maintain this deflection over a plateau of radius P. A plateau of $P = 0.25$ was found to produce smooth transitions while giving each dot sufficient area to be easily perceptible from any direction. The location and amplitude of each dot is specified with blobs in a grayscale image. Dots can be positioned anywhere on the virtual surface provided that they do not overlap. Dot patterns are represented visually as shown in Fig. 6.2a.

This rendering method was inspired by earlier work on the display of Braille [160] and dot patterns [293] by lateral skin deformation. While these earlier attempts assumed that the dots were either exclusively or mostly explored by horizontal motion, the improved method presented here allows exploration from any direction, thereby improving the realism of the sensation and facilitating contour following. This improvement results from the use of a radial deflection pattern with a plateau at its center.

6.3.2 Vibration Rendering

This tactile rendering method produces a sensation of localized vibration within the virtual surface [293]. The vibratory sensation is produced by controlling the deflection of each actuator i, j as a temporal oscillation:

$$\delta(i,j,t) = \begin{cases} \frac{1}{2} + \frac{1}{2}\cos 2\pi f t & \text{if } (i \bmod 2) \neq (j \bmod 2), \\ \frac{1}{2} - \frac{1}{2}\cos 2\pi f t & \text{otherwise.} \end{cases} \tag{6.2}$$

The phase of vibration is inverted for adjacent actuators to maximize compression

and shearing deformation, and thereby increase the strength of the sensation. A vibration frequency of 50 Hz was similarly found to provide the strongest sensation. Higher frequencies could potentially increase contrast further but could not be used at present time due to limitations of the I/O hardware used to communicate with the STReSS^2.

Vibratory patterns are produced by modulating the amplitude of vibration of actuators as a function of their position within the virtual surface. The amplitude mapping is specified with a grayscale image mask. Vibrating patterns are represented visually using a white-noise texture (e.g. Fig. 6.2b).

6.3.3 Grating Rendering

This rendering method extends our earlier work on the display of vertical gratings to that of gratings of arbitrary orientation [293]. The grating rendering produces a sensation similar to that of brushing a finger against a corrugated surface. This sensation is obtained by propagating a sinusoidal wave across the tactile display at a specific angle. The deflection of each actuator is given by:

$$\delta(d) = \frac{1}{2} + \frac{1}{2}\cos\frac{2\pi d}{\lambda}, \tag{6.3}$$

where $d = y\cos\theta - x\sin\theta$ is the distance from the actuator position (x, y) to a reference line crossing the origin at angle θ. This produces a grating of spatial wavelength λ at an orientation of θ. Horizontal and vertical gratings produce natural sensations for a wide range of spatial frequencies. Diagonal orientations produce noisier sensations. The orientation of a grating can be judged either by attending to the subtle directional sensation on the fingertip or by finding the direction of movement with the strongest or weakest stimulus, corresponding to motion across or along ridges respectively. Again, the amplitude of the grating texture is modulated by an image mask. Grating patterns are represented visually as shown in Fig. 6.2c.

6.3.4 Composite Rendering

The three rendering methods described previously produce tactile patterns by deflecting the actuators only as they pass over specific regions of the virtual surface, otherwise leaving them at their resting position to the right. Provided that there is no overlap between their active regions, it is therefore possible to combine tactile layers rendered

with different methods by simply adding together their modulated actuator deflection functions. This allows complex tactile patterns to be created, as represented visually in Fig. 6.2d.

6.4 Experiments

This section describes five experiments that were conducted to gain a better understanding of the tactile display system's capabilities. The first experiment looked at the identification of simple geometrical shapes produced with either dots, vibration or gratings (Section 6.4.1). The second experiment investigated the difference in spatial frequency necessary to differentiate gratings (Section 6.4.2). The third and fourth experiments studied the identification of grating orientations, first with intervals of 30° and then of 45° (Sections 6.4.3 and 6.4.4). The fifth experiment looked at the identification of tactile icons composed of vibrating contours and grated interiors (Section 6.4.5).

Three groups of 10 sighted subjects (A, B and C) and one group of 6 visually impaired subjects (VI) participated in the experiments. Each subject took part in one or two experiments during a one-hour experimental session. Group A participated in the first experiment, group B in the second and third, and group C in the fourth and fifth. The fifth experiment was repeated with the visually impaired subjects of group VI. The subjects were selected solely based on availability and paid for their participation. They performed the experiment with the index of their preferred hand. Details about preferred hand, gender, and age distribution within the subject groups are shown in Table 6.1. Two of the subjects of group VI had previously participated in a study on the use of the STReSS^2 as a Braille display [160]. Two were blind from birth and the others had lost their sight between the ages of 3 and 20.

6.4.1 Shape

Description

The first experiment evaluated the perception of simple geometric shapes displayed on the tactile display. The experiment was designed to also evaluate the effect of rendering method and shape size on identification performance. The experiment consisted in the

group	size	age		gender		handedness	
		mean	*range*	*male*	*female*	*left*	*right*
A	10	22.4	19–29	2	8	1	9
B	10	21.8	19–26	4	6	1	9
C	10	24.1	18–52	3	7	2	8
VI	6	47.8	35–65	5	1	1	5

Table 6.1 Description of the four groups of subjects who participated in the experiments.

identification of six shapes rendered using the three methods described in the previous section at two different scales. Fig. 6.4 illustrates the six shapes as well as the six variations of the circle shape. The experiment was conducted with subject group A.

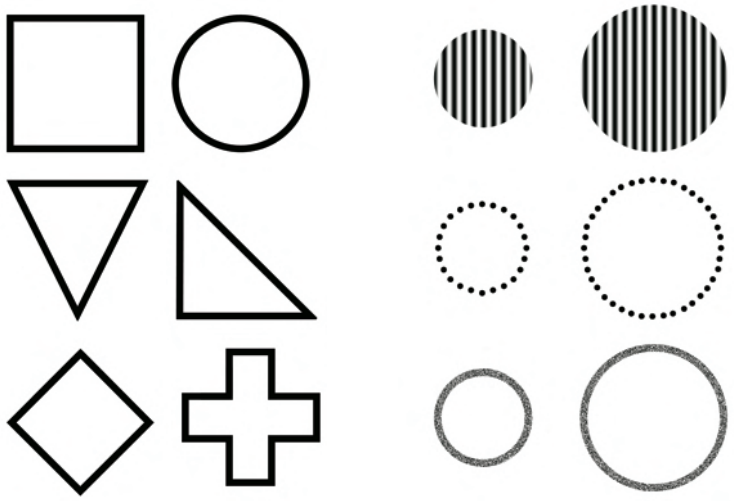

(a) (b)

Fig. 6.4 Experimental stimulus for shape identification experiment: (a) six shapes and (b) example of the six variations of a shape.

The shapes were selected so as to fill a 2 or 3 cm square. Vibrating shapes were produced with a 1.5-mm-thick outline that exceeds the spacing between actuators and therefore prevents aliasing effects. An approximation of the outline was similarly produced with dots of 1-mm radius. The grating was used to present filled shapes since it is intented as an areal texture and does not produce clear outlines. A spatial wavelength of 2 mm was selected to produce a well-defined boundary while still feeling natural. A vertical grating was used since it appears to give the strongest illusion.

Since the identification strategy differs depending on the rendering method, each method was tested separately in randomized order. Each experiment began with a short training session in which subjects familiarized themselves with the shapes. Subjects were then asked to identify 48 shapes (6 shapes $\times$ 2 sizes $\times$ 4 iterations) presented in random order with a one-minute break at half-time. The shapes were presented for a maximum of 20 s. Answers were entered by typing a key corresponding to idealized shape outlines shown on-screen.

Results

The performance of the subjects is shown for each rendering method in Fig. 6.5. Subject A1 performed significantly worse than all others and is therefore excluded from analysis. The remaining 9 subjects correctly identified 76.0% of the shapes. Identification was performed in 14.2 s on average, with 17.4% of the trials going over the time limit.

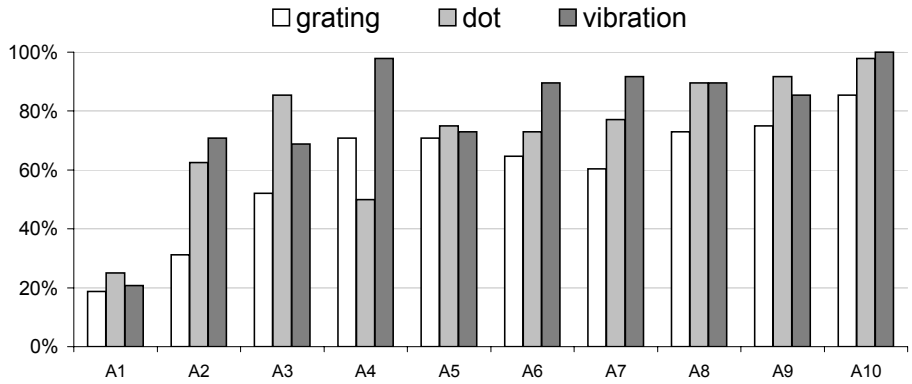

Fig. 6.5 Shape identification performance as a function of the rendering method. Subjects are sorted by overall performance.

Table 6.2 gives the performance for all conditions. A repeated measures two-way ANOVA[1] reveals no significant interaction between rendering method and scale on shape identification performance [F(2,16)=0.693, p=0.514]. The average performance was 85.2% for vibrating shapes, 78.0% for dotted shapes and 64.8% for grating-textured shapes. The difference in performance was significant between grating rendering and both dot rendering ($t=-2.489$, $p<0.05$) and vibration rendering ($t=-5.335$,

[1] A significant main effect was also found for both the rendering method [F(1,8)=28.47, p=0.001] and the scale of the shapes [F(1,8)=8.88, p=0.018].

p<0.05). The difference between dotted shapes and vibrating shapes was not significant (t=−1.167, p=0.277). Five subjects performed better with vibration, three with dots and one equally well with both. Seven of the nine subjects expressed a preference for the rendering method with which they performed best.

	small				large				all			
	G	D	V	all	G	D	V	all	G	D	V	all
◺	75	92	94	87	81	83	86	83	78	88	90	85
▽	86	64	86	79	83	89	78	83	85	76	82	81
○	58	97	86	81	47	89	89	75	53	93	88	78
□	44	78	69	64	86	83	94	88	65	81	82	76
◇	75	58	72	69	69	64	89	74	72	61	81	71
✚	19	64	81	55	53	75	97	75	36	69	89	65
all	60	76	82	72	70	81	89	80	65	78	85	76

Table 6.2 Shape identification performance (%) as a function of shape, scale and rendering method (G=grating, D=dot, V=vibration).

Performance was also affected by the scale of the shapes (t=−2.981, p<0.05). 79.8% of large shapes were identified correctly compared with 72.2% of small shapes. Overall, the best performance was obtained with large and small vibrating shapes (88.9% and 81.5%) followed by large dotted shapes (80.6%). Performance also varied with the shape displayed (see Table 6.3). Performance dropped from 85.2% for the right triangle to 64.8% for the plus sign. Asymetries are also visible, notably between plus and diamond, and diamond and circle.

		answered					
		◺	▽	○	□	◇	✚
presented	◺	**85.2**	2.8	2.3	2.3	5.1	2.3
	▽	2.3	**81.0**	0.9	1.9	8.3	5.6
	○	4.2	3.2	**77.8**	6.5	6.0	2.3
	□	6.0	3.7	7.4	**75.9**	5.6	1.4
	◇	2.3	5.6	17.1	1.9	**71.3**	1.9
	✚	3.7	7.9	2.3	6.5	14.8	**64.8**

Table 6.3 Distribution of answers (%) in shape identification experiment.

6.4.2 Grating Spatial Frequency

Description

The second experiment was conducted to determine the difference in spatial wavelength necessary to be able to differentiate and scale gratings. The experiment consisted in the identification of the vertical grating with highest spatial frequency among two gratings shown side-by-side. Fig. 6.6 illustrates the stimulus used. The experiment was conducted at the beginning of subject group B's experimental sessions.

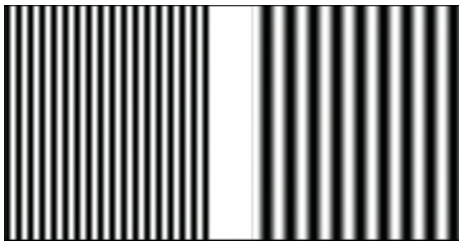

Fig. 6.6 Experimental stimulus for grating spatial frequency comparison experiment (shown with wavelengths of 3 mm and 6 mm).

The gratings were separated by a 1-cm-wide blank space so that the tactile display never touched both gratings at once. The spatial wavelength of the gratings was varied between 1.0 and 6.0 mm in 0.5 mm increments. Each experiment began with a short familiarization session in which various pairs of gratings were shown. Subjects were then asked to identify the grating with highest spatial frequency in 110 randomized trials (once per non-identical pair for 11 wavelengths). The sensation was presented for a maximum of 10 s. Answers were entered with the keyboard. Subjects wore sound blocking earphones. The number of trials decreased linearly from 20 for differences in wavelength of 0.5 mm down to 2 for differences of 5.0 mm ($n = 22 - 4\Delta$).

Results

Subject B9 performed far worse than all others (54.5% compared with 91.3±2.7%) and is therefore exluded from analysis. Four trials were also rejected because they resulted from accidental key presses (duration less than 0.5 s). The performance of the remaining 9 subjects is shown in Fig. 6.7 as a function of the difference in spatial wavelength. The success rate gradually increases from 74.4% at 0.5 mm to near perfection at and above 3.0 mm. The trial duration follows a similar pattern, gradually

decreasing from 6.5 s at 0.5 mm to 3.1 s at 5.0 mm. Only 5.4% of trials extended past the 10 s time limit.

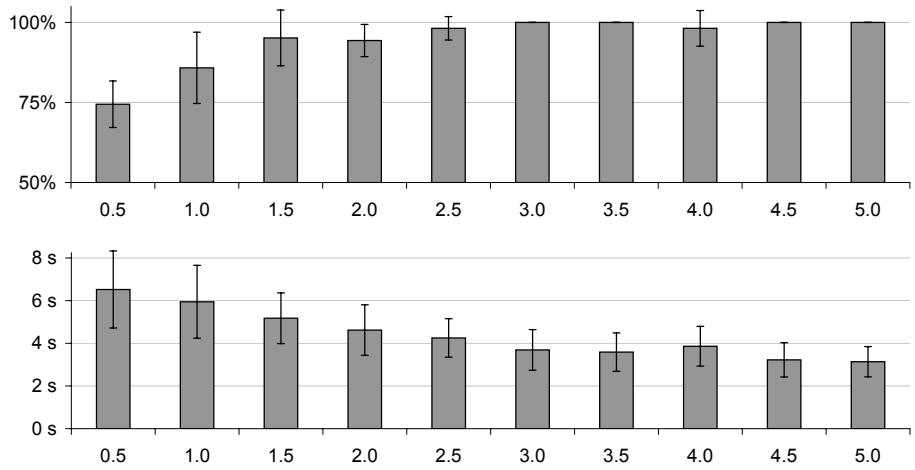

Fig. 6.7 Percentage of correct answers and average trial duration as a function of the difference in wavelength (mm) in the grating frequency comparison experiment. The standard deviation across subjects is shown as an error bar.

6.4.3 Grating Orientation (Fine)

Description

This experiment evaluated the subjects' ability to perceive the orientation of virtual gratings. The experiment was designed to also evaluate the effect of spatial frequency on orientation judgments. The experiment consisted in the identification of six orientations (0°, ±30° or ±60°, 90°) at three different spatial wavelengths (4 mm, 6 mm and 8 mm). Fig. 6.8 illustrates the grating orientations and spatial frequencies. This experiment was conducted in the second part of group B's experimental session.

Each experiment began with a short familiarization session during which subjects were exposed to the different grating orientations. Subjects were then asked to identify the orientation of 90 gratings (6 orientations × 3 spatial frequencies × 5 iterations) presented in randomized order with a 2-minute break at half-time. The gratings were presented for a maximum of 10 s. Subjects wore sound blocking earphones and were asked not to use diagonal motion to explore the virtual grating. This directive was given so that diagonal orientations would be identified by tactile motion on the fingertip

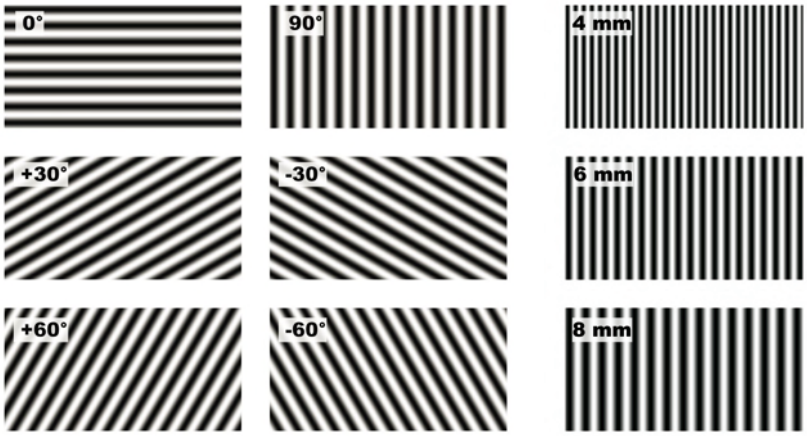

Fig. 6.8 (a) Grating orientations and (b) spatial wavelengths used during the fine orientation identification experiment.

rather than by finding the direction of motion with the weakest sensation. Answers were entered by typing a key corresponding to idealized grating representations shown on-screen.

Results

One trial was rejected because it resulted from an accidental key press. The performance of subjects at identifying orientation is shown in Fig. 6.9. Orientation was identified correctly 46.1% of the time. Trials lasted 8 s on average, with 25% extending past the 10 s time limit. Horizontal and vertical gratings were identified more easily (76.0% and 60.6%) than diagonal gratings (35.0%). Trial duration similarly dropped from 8.6 s for diagonal gratings to 6.7 s for horizontal and vertical gratings.

The distribution of answers for each orientation is shown in Fig. 6.10. The shape of the response distribution is similar for 30° and -30° orientations, showing a tendency to answer correctly or otherwise to select any other diagonal orientation. Similarly, subjects tended to select the correct sign for ±60° gratings but appeared unable to distinguish between 30° and 60°. ±60° gratings were also often confused with vertical gratings.

There was a statistically significant difference in performance between 4-mm and 6-mm gratings ($t=-3.279$, $p<0.05$), but not between 4-mm and 8-mm ($t=-1.111$,

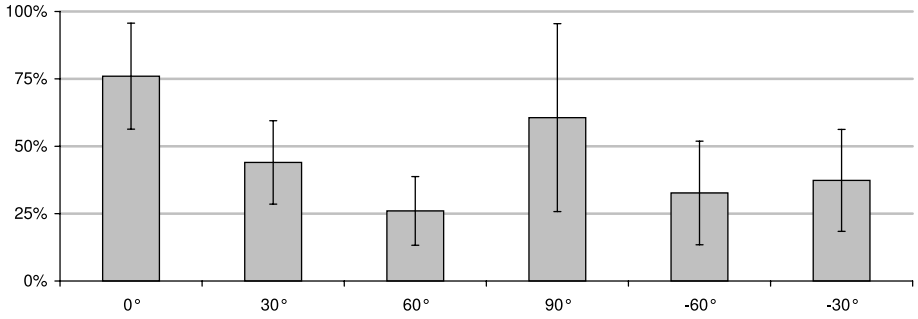

Fig. 6.9 Performance at identifying fine grating orientations. The standard deviation across subjects is shown as an error bar.

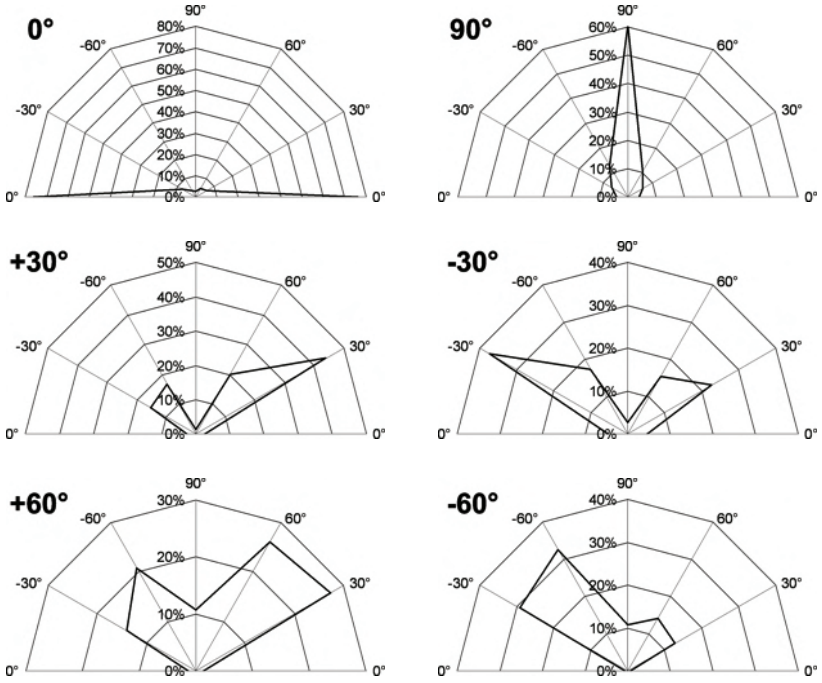

Fig. 6.10 Distribution of answers in the fine grating orientation identification experiment.

p=0.295) or 6-mm and 8-mm (t=−1.495, p=0.169). The orientation of 4-mm, 6-mm and 8-mm gratings was correctly identified 41.8%, 50.7% and 45.7% of the time respectively.

6.4.4 Grating Orientation (Coarse)

Description

This follow-up experiment repeated the previous experiment with an easier task in order to better understand where the perceptual limit lies when judging grating orientation. The number of orientations was reduced to four (0°, 90° and ±45°) and the spatial wavelength was set to the best value found in the previous experiment (6 mm). The maximum trial duration was extended to 15 s and subjects were allowed to move in diagonal. Strategies to accomplish the task were explained during the training session. Subjects were asked to identify the orientation of 40 gratings (4 orientations × 10 iterations) presented in randomized order. The experiment was conducted at the beginning of group C's experimental session.

Results

Subject C1 misunderstood the task and is excluded from analysis. The performance of the remaining subjects is shown in Fig. 6.11. 0° and 90° gratings were identified correctly 88% of the time, while +45° and -45° gratings were identified correctly 87% and 85% of the time. Trial duration was 8.8 s on average, with 14.2% of trials extending past the 15 s limit. The confusion matrix shows that vertical and horizontal gratings were rarely confused for one another (Table 6.4).

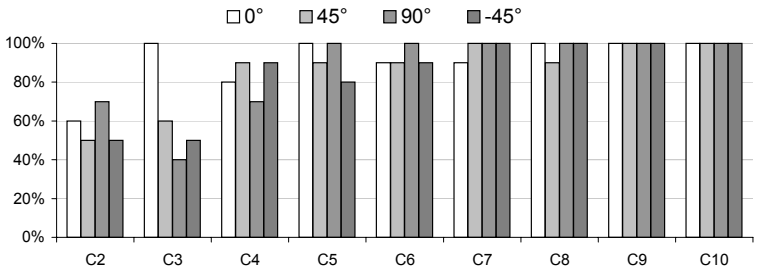

Fig. 6.11 Performance at identifying coarse grating orientations. Subjects are sorted by overall performance.

		answered			
		0°	45°	90°	-45°
presented	0°	**91.1**	6.7	1.1	1.1
	45°	1.1	**85.6**	10.0	3.3
	90°	0.0	6.7	**86.7**	6.7
	-45°	2.2	4.4	8.9	**84.4**

Table 6.4 Distribution of answers in coarse grating orientation identification experiment.

6.4.5 Tactile Icons

Description

The final experiment examined the perception of tactile icons composed of vibrating shapes filled with a grating texture. The experiment consisted of the identification of the shape (circle, square, inverted triangle or right triangle), grating orientation (vertical or horizontal) and grating frequency (high or low) of tactile icons. The tactile icons used are illustrated in Fig. 6.12. The experiment was conducted during the second part of group C's experimental session and repeated with the 6 visually-impaired subjects of group VI.

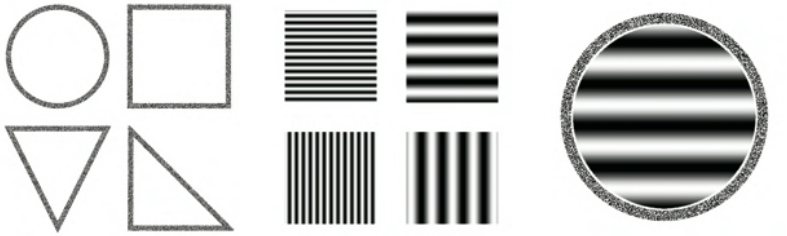

(a) (b) (c)

Fig. 6.12 Stimulus used in tactile icon identification experiment: (a) four shapes, (b) four textures and (c) example of icon.

The four shapes were selected based on their identifiability in the shape perception experiment. The vibration rendering method was selected because it yielded the best results in that experiment and because it provides greater contrast with gratings than dotted outlines. Shapes were drawn at the larger 3-cm scale that also produced the best results in the experiment. Larger shapes also increase the size of the textured area and facilitate texture identification. Vertical and horizontal texture orientations

were selected because they appear to be most easily identified, and rarely confused for one another. The spatial wavelengths were selected as far apart as possible without compromising orientation judgments. The values selected (2 mm and 6 mm) were sufficiently distinctive to be easily identified when maintaining a regular exploration speed.

The experiment began with a familiarization session lasting approximately 10 minutes during which subjects where shown the different icons and trained to judge their varying characteristics. The experiment consisted in the identification of 48 icons (4 shapes $\times$ 2 grating orientations $\times$ 2 grating frequencies $\times$ 3 iterations) presented in randomized order with a 2-minute break after each third of the trials. Icons were presented for a maximum of 40 s. Subjects identified the tactile patterns by making three selections on a modified numeric keypad. The available answers were shown to sighted subjects as symbolic illustrations on-screen. The visually impaired subjects were given a keypad with equivalent patterns made of thick solder wire glued to the keys. Their selections were confirmed by playing recorded speech after each key press. In both cases, subjects were allowed to modify their answers once entered if they felt that it was mistyped or if they revised their judgment. Subjects wore sound blocking earphones[2].

Results

Fig. 6.13 shows the percentage of correctly identified shapes, grating orientations, grating frequencies and icons (all three parameters combined). Fig. 6.14 shows the average trial duration for each subject.

There was no statistically significant difference between the performance of the sighted and visually impaired subjects. Sighted subjects correctly identified 88.5% of the shapes, 95.8% of the grating orientations and 88.8% of the grating frequencies, compared with 87.5%, 94.4% and 77.1% for the visually impaired. All three parameters were correctly identified 78.5% and 67.7% of the time for sighted and visually impaired participants respectively. The average trial duration was 24.5 s, with 11.7% of trials extending past the time limit for the sighted, and 23.2 s with 17.4% of timeouts for the visually impaired. The results, however, are heavily skewed by the low

[2]Subject VI4 did not wear sound-blocking earphones for a third of the experiment. Results are unlikely to have been affected since audio cues were barely audible and masked by ambient noise.

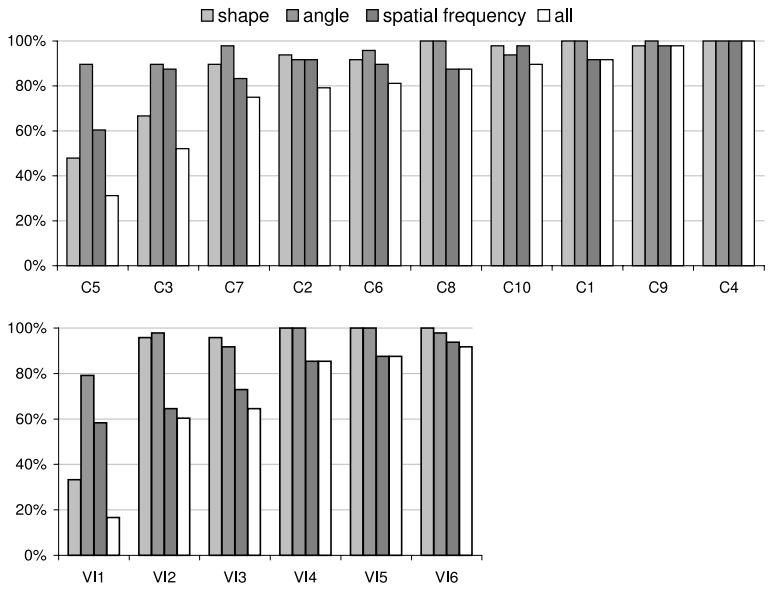

Fig. 6.13 Performance in tactile icon experiment for sighted subjects (group C) and visually-impaired subjects (group VI). Subjects are sorted by overall performance.

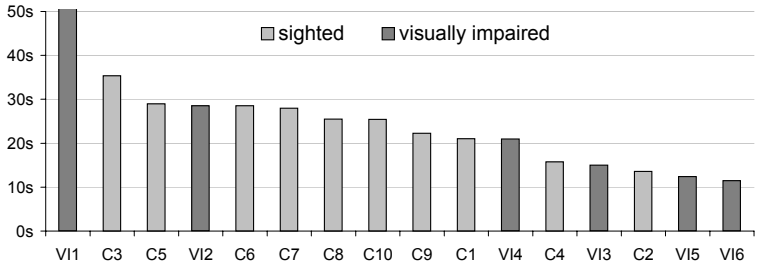

Fig. 6.14 Mean trial duration in tactile icon experiment. Subjects are sorted by performance.

performance of a single visually impaired subject (VI1).

6.5 Discussion

The first experiment showed that the tactile graphics system is capable of rendering simple geometric shapes of moderate size (2 or 3 cm) using all three rendering methods. Shapes rendered with dots or vibrations were more readily identified than those rendered with gratings, perhaps because the latter were filled. In agreement with many subjects' ambivalence when picking a favorite, there was no statistically significant dif-

ference in performance with dots or vibration. The larger of the two shape sizes was also easier to identify. Informal observations suggest that enlarging the shapes further could reduce performance by requiring more information to be integrated while following contours. Performance should similarly be expected to decrease at smaller scales as details become more difficult to discern. Performance could be further improved by tweaking various parameters such as the spatial frequency of the grating, the diameter of dots or the line thickness of vibrating contours. The salience of corners could also be increased using decorations, much like serifs in typography.

The second experiment showed that it is possible to scale vertical gratings with a difference in spatial wavelength as low as 0.5 mm. Simply discriminating gratings may be even easier. As shown in the final experiment though, identifying gratings by spatial frequency is a much harder task due to the difficulty of memorizing a reference for comparison. The dependence of the sensation on exploration velocity also increases the difficulty. Preliminary experiments also suggest that the task is more difficult for diagonal and, to a lesser extent, horizontal gratings. Similarly, small differences may be more difficult to detect when comparing two large wavelengths.

The third and fourth experiments showed that vertical and horizontal gratings can be identified. The third experiment showed that identifying diagonal orientations with a 30° resolution without diagonal movement is nearly impossible. Performance improved greatly with the reduction of the resolution to 45° and the use of diagonal movement. More experimentation will be necessary to determine if a finer resolution could be obtained when diagonal movement is allowed. Results also suggest that discrimination may be reduced at high spatial frequencies. This is reasonable considering that high frequency gratings feel less natural and that moving straight along their ridges is more difficult.

The fifth and final experiment showed that identifying the shape and texture of a set of 16 tactile icons is possible. This icon set could be expanded by using more shapes, by adding a diagonal grating orientation and by adding grating spatial frequencies. Training may become more important as the icon set grows, particularly for judging the spatial frequency of the texture. Dotted contours should also be investigated, although their low contrast with gratings would likely degrade performance.

In all cases, it is interesting to note that subjects were given less than 15 minutes of training. Many felt that they performed better with time, notably for shape and

icon identification. We can therefore expect performance to improve with practice. Many subjects, on the other hand, reported that their finger was getting numb over the duration of the experiments. Trial durations were also kept short to ensure that judgments were made intuitively rather than by persistence. Performance would likely have improved if more time was given.

This preliminary work on the display of tactile graphics by lateral skin deformation relied mostly on sighted subjects. Visual feedback may have played a part in some experiments by, for example, allowing the identification of shapes by visual observation of finger movements. Subjects were allowed to see the apparatus to facilitate monitoring of the orientation of the tactile display. As the results with visually impaired subjects show, this precaution was not essential. This issue will be resolved in future work by mounting the display on a carrier capable of measuring its orientation and by adjusting the rendering algorithms accordingly. The workspace of the display will also be increased to allow more practical applications.

Previous work also indicates that variations in performance can be expected between sighted, late blind and early blind participants due to their varying degrees of visual and tactile experience [93]. The similar performance of sighted and visually impaired subjects on the icon identification experiment suggests however that differences may be minimal with the simple tasks performed here. This may be due to the non-visual nature of the tasks or the novelty of the exploration strategies that had be learned by all subjects alike to use the device effectively. The findings of the rest of the study may therefore extend to the visually impaired population. Nevertheless, future work will focus on confirming these findings with visually impaired users.

These experiments provide an early assessment of the possibilities offered by the STReSS^2 for the rendering of virtual tactile graphics. Due to the large number of parameters involved, the experiments covered only a small fraction of the rendering possibilities. They nevertheless suggest that the device will be useful in a variety of applications of tactile graphics for visually impaired persons such as maps, graphs and diagrams. Shapes play an important part in tactile graphics by conveying both symbolic information (e.g. point symbols in a map) and more complex information (e.g. geometric concepts). Areal textures are also commonly used as a tactile color to highlight, label or otherwise mark part of a tactile graphics. The information gathered through these experiments provides a basis for using these drawing elements in tac-

tile graphics produced by laterotactile displays. A tactile map could, for example, be contructed with vibrating political boundaries and regions colored with easilly discriminable textures. Similarly, the tactile icons developed in the fifth experiment could be used as informative point symbols in a tactile map or diagram. The basic data obtained from these and other experiments will be used to design more complex tactile graphics appropriate for display by lateral skin deformation.

6.6 Conclusion

This article discussed three rendering methods capable of producing tactile graphics within a virtual surface by laterally deforming the skin. Five experiments were conducted to evaluate the system's ability to display basic elements for tactile graphics. The first experiment showed that simple shapes rendered with dots or vibration can be identified. The second showed that differences in spatial frequencies as low as 0.5 mm are sufficient to compare virtual gratings. The third and fourth experiments showed that determining the orientation of a virtual grating is possible within 45° if motion is not constrained. Finally, the fifth experiment showed that tactile icons composed of vibrating outlines filled with grating textures can be identified. The results obtained with visually impaired subjects on the final experiment suggest that the findings of the study are applicable to that user group. This work constitutes a first step toward the display of more complex tactile graphics in applications of relevance for visually impaired persons, such as tactile maps, diagrams and graphs.

Acknowledgements

The revision of the STReSS^2 used in this work was designed and implemented by Qi Wang and Vincent Hayward. The experiments were approved by the Research Ethics Boards of McGill University and of the Centre for Interdisciplinary Research in Rehabilitation of Greater Montreal (CRIR). Subjects gave their informed consent before participating. The authors would like to thank Jérôme Pasquero for his help with the statistical analysis of the results and for discussions about this work. They would also like to thank Andrew Gosline for his help with the experimental apparatus. This work was motivated in part by discussions on tactile graphics with Nicole Trudeau, Aude

Dufresne and Grégory Petit. Funding from Fonds québécois de la recherche sur la nature et les technologies (PR-114110) is gratefully acknowledged. The visually impaired subjects were recruited through the Institut Nazareth et Louis-Braille (INLB) and the Typhlophile website (`http://typhlophile.com`).

Supplementary Statistical Analysis

Shape

A three-way repeated measures ANOVA was conducted to evaluate the effect of the rendering method (grating, dot, or vibration), the size (2 or 3 cm), and the shape (square, circle, inverted triangle, right-angle triangle, lozange, and plus) on performance of the shape identification task.

A significant interaction was found between all three factors [$F(10,80)=2.364$, $p=0.017$], as well as between rendering method and shape [$F(10,80)=6.723$, $p<0.001$], and size and shape [$F(5,40)=4.420$, $p=0.003$], but not between rendering method and size [$F(2,16)=0.698$, $p=0.512$]. Significant main effects were found for the rendering method [$F(2,16)=7.955$, $p=0.004$], the size [$F(1,8)=8.884$, $p=0.018$], and the shape [$F(5,40)=4.862$, $p=0.001$].

Simple effect one-way repeated measures ANOVAs were conducted to evaluate the effect of the rendering method for each combination of size and shape. A significant effect could be found only for the circle and plus shapes of both sizes, and for 2-cm square shapes (see Table 6.5 for more details). Dependent sample t-tests indicated that in all five cases the difference between grating and both dot and vibration rendering was significant, but not between dot and vibration (see Table 6.6 for more details). The conclusions reached in Section 6.4.1 regarding the effect of the rendering method on shape identification are therefore valid only for the circle and plus shapes as well as 2-cm square shapes.

The effect of shape size was similarly investigated through paired t-tests. A significant effect of shape size could be found for both vibrating and grated square and plus shapes as well as dotted inverted triangle shapes, but not for other combinations (see Table 6.7 for more details). The conclusions reached in Section 6.4.1 regarding the effect of the size on shape identification are therefore valid only for these combinations of rendering methods and shapes.

	2 cm		3 cm	
	F(2,16)	p	F(2,16)	p
◇	1.000	0.390	3.045	0.076
□	**0.271**	**0.000**	0.698	0.512
◺	2.098	0.155	0.113	0.894
▽	2.197	0.143	0.842	0.449
○	**9.455**	**0.002**	**11.11**	**0.001**
✚	**26.76**	**0.000**	**8.258**	**0.003**

Table 6.5 Results of simple effect one-way repeated measures ANOVAs for the effect of the rendering method. Significant results are shown in bold.

		vibration vs grating		grating vs dot		vibration vs dot	
		t(8)	p	t(8)	p	t(8)	p
□	2 cm	**3.464**	**0.000**	**-5.657**	**0.000**	-1.155	0.200
○	2 cm	**2.626**	**0.000**	**-4.128**	**0.000**	-1.512	0.100
○	3 cm	**3.780**	**0.000**	**-4.082**	**0.000**	0.000	0.100
✚	2 cm	**8.315**	**0.000**	**-5.488**	**0.000**	1.633	0.100
✚	3 cm	**3.600**	**0.000**	**-1.835**	**0.000**	2.874	0.100

Table 6.6 Results of dependent sample t-tests for the effect of the rendering method. Significant results are shown in bold.

	vibration		grating		dot	
	t(8)	p	t(8)	p	t(8)	p
◇	2.000	0.081	0.426	0.681	0.512	0.622
□	**-2.449**	**0.040**	**4.472**	**0.002**	0.450	0.665
◺	0.894	0.397	0.686	0.512	1.155	0.282
▽	2.000	0.081	0.555	0.594	**3.464**	**0.009**
○	0.426	0.681	1.315	0.225	1.414	0.195
✚	**2.828**	**0.022**	**2.828**	**0.022**	0.710	0.498

Table 6.7 Results of paired t-tests for the effect of the shape size. Significant results are shown in bold.

Grating Orientation (Fine)

A two-way repeated measures ANOVA was conducted to evaluate the effect of grating orientation (0°, ±30°, ±60°, or 90°) and spatial wavelength (4, 6, or 8 mm) on performance at the identification task. A significant interaction was found between grating orientation and spatial wavelength [$F(10,90)=2.75$, $p=0.005$]. Significant main effects were found for grating orientation [$F(5,45)=11.64$, $p<0.001$] and spatial wavelength

[F(2,18)=3.92, p=0.4].

Simple effect one-way repeated measures ANOVAs were conducted to evaluate the effect of spatial wavelength for each grating orientation. No significant effect was found for -60° [F(2,18)=1.925, p=0.175], +60° [F(2,18)=1.976, p=0.168], 0° [F(2,18)= 0.336, p=0.719], and 90° [F(2,18)=0.088, p=0.916]. A significant effect was found for -30° [F(2,18)=7.042, p=0.006] and +30° [F(2,18)=5.062, p=0.018]. Dependent sample t-tests were conducted to further investigate the effect of spatial wavelength at the latter grating orientations. The difference between 4 and 6 mm was found to be significant for both -30° [t(9)=-3.000, p=0.015] and +30° [t(9)=-3.674, p=0.005]. The difference between 4 and 8 mm was found to be significant for -30° [t(9)=-3.597, p=0.006], but not for +30° [t(9)=-2.250, p=0.051]. The difference between 6 and 8 mm was found to be significant neither for -30° [t(9)=-0.391, p=0.705] nor +30° [t(9)=0.000, p=1.000].

A one-way repeated measures ANOVA indicated in Section 6.4.3 that a significant difference could be found between performance with 4-mm and 6-mm gratings, but not between 4-mm and 8-mm or 6-mm and 8-mm gratings. The statistical analysis presented here results in slightly different conclusions. A significant difference could be found between 4 mm and 6 mm only at $\pm 30°$, and an additional significant difference was found between 4 mm and 8 mm at -30°. No significant difference could be found for other combinations of grating orientations and spatial frequencies. The search for an optimal grating spatial frequency for orientation identification can therefore be considered inconclusive.

Grating Orientation (Coarse)

A one-way repeated measures ANOVA was conducted to determine the effect of grating orientation (0°, 90°, -45°, 45°) on performance at the identication task. Mauchly's test was significant, therefore sphericity was not assumed and the Greenhouse-Geisser correction was employed. The effect of grating orientation on performance was not significant [F(1.54,14)=0.67, p=0.52]. The descriptive statistics presented in Section 6.4.4 therefore remain correct but the minor differences in performance observed with respect to grating orientation are not statistically significant.

Tactile Icons

Independent-samples t-tests revealed no statistically significant differences between sighted and visually impaired subjects for trial durations [t(14)=0.224, p=0.826] or for the identification of shapes [t(14)=0.098, p=0.924], grating orientations [t(14)=0.451, p=0.659], grating spatial frequencies [t(14)=1.831, p=0.088], and icons [t(14)=0.870, p=0.399]. The statistical analysis performed in Section 6.4.5 therefore remains valid and no statistical difference was found between sighted and visually impaired subjects.

Chapter 7

The Tactograph: A Haptic Interface for Virtual Tactile Graphics

Preface to Chapter 7

This chapter describes a haptic interface designed specifically for the display of virtual tactile graphics that addresses many limitations of its Pantograph-based predecessor introduced in [289] and relied upon in Chapters 5 and 6. The term Tactograph is introduced to describe both the original and improved tactile graphics interfaces. The latter includes many improvements such as a larger virtual canvas and additional sensors for the measurement of the orientation of the tactile array and the pressure applied with the reading finger. The improved Tactograph is used in the next two chapters to experiment with the rendering of virtual tactile graphics by lateral skin deformation.

Contributions of Authors

This chapter was written by Vincent Lévesque and revised by Vincent Hayward. The work presented herein was similarly mainly performed by V. Lévesque under the supervision of V. Hayward. Andrew Gosline made significant contributions to the design and implementation of the improved Tactograph and provided expert advice on mechanical engineering and machining.

The Tactograph: A Haptic Interface for Virtual Tactile Graphics

Abstract

This chapter introduces the Tactograph, a haptic interface dedicated to the display of virtual tactile graphics by lateral skin deformation. The interface combines a STReSS^2 laterotactile display with 8×8 independent actuators and an instrumented planar carrier to allow the exploration of a virtual tactile graphics canvas 22×15 cm in size. The position and orientation of the tactile array are measured with a minimal resolution of 45.2 µm and $4.32'$ respectively. The tactile display is enclosed within an instrumented box that isolates the device and senses the pressure applied with the reading finger. The Tactograph was designed as a prototype for the evaluation of virtual tactile graphics applications.

7.1 Introduction

While voice synthesis and refreshable Braille displays have for years given visually impaired computer users access to digitized text, a similar technological breakthrough has yet to be made for online access to graphical content. Despite significant progress in the means of production, tactile graphics remain accessible almost exclusively offline on static media such as embossed paper, thermoformed plastic and collage of mixed materials [59]. Browsing online graphical content, panning and zooming within a large map and other complex tasks such as graphics editing, however, require realtime interaction with virtual or refreshable tactile graphics. Suitable haptic interfaces have received much attention from researchers and inventors but have yet to gain acceptance by the visually impaired community due to a variety of practical considerations. Virtual and refreshable tactile graphics have been displayed with force-feedback interfaces as well as tactile arrays that apply distributed stimuli to the skin. The latter can be divided in two classes: large arrays that approximate 3D surfaces and smaller movable arrays that dynamically alter the tactile sensations produced to create the impression of a larger virtual canvas.

This chapter introduces a virtual tactile graphics interface of the latter category. The Tactograph simulates the feeling of brushing against tactile graphics by altering the sensations produced by a laterotactile display as it is moved over a planar surface. The first revision of the Tactograph, shown in Figure 7.1, consisted of a STReSS^2 tactile display mounted on a Pantograph haptic device [289, 37]. The Pantograph was used as a passive, instrumented planar carrier and therefore did not provide haptic feedback through its motors. The resulting interface had a high spatial resolution of 13 µm and moved with very low friction. Its suitability for tactile graphics was limited, however, by the small size of its virtual canvas (11×6 cm) and the impossibility of measuring or restricting the rotation of the tactile display, hence preventing the orientation of the reading fingerpad from being taken into account by tactile rendering algorithms. The protective foam shell surrounding the display (not shown) also left some of the electronics exposed and therefore required a minimal effort on the part of the user to maintain a safe grip. This early revision of the Tactograph nevertheless demonstrated the feasibility of displaying tactile graphics by lateral skin deformation (Chapters 5 and 6, [211]).

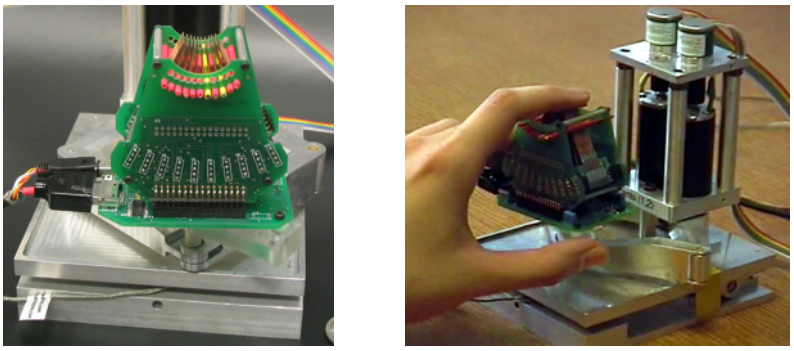

Fig. 7.1 Early revision of the Tactograph using the Pantograph haptic interface as a passive planar carrier.

The revision of the Tactograph introduced in this chapter, henceforth referred to simply as the Tactograph, addresses many of the limitations of its predecessor. The improved Tactograph, pictured in Figure 7.2, features a larger virtual canvas, precise measurement of both display position and orientation, sensing of the pressure applied with the reading finger, and an enclosure that protects and isolates the display. The interface was designed and optimized for a letter-sized virtual canvas (279.4 $\times$ 215.9 mm) equivalent to a sheet of microcapsule paper and later revised to a slightly smaller size (215.3 $\times$ 151.8 mm) for improved stability. The display position is measured with a nominal precision exceeding 45.2 µm through two high-resolution optical encoders mounted on a two-bar serial linkage. The tactile display is enclosed in an instrumented box and mounted on a circular carrier sliding within a rectangular tray.

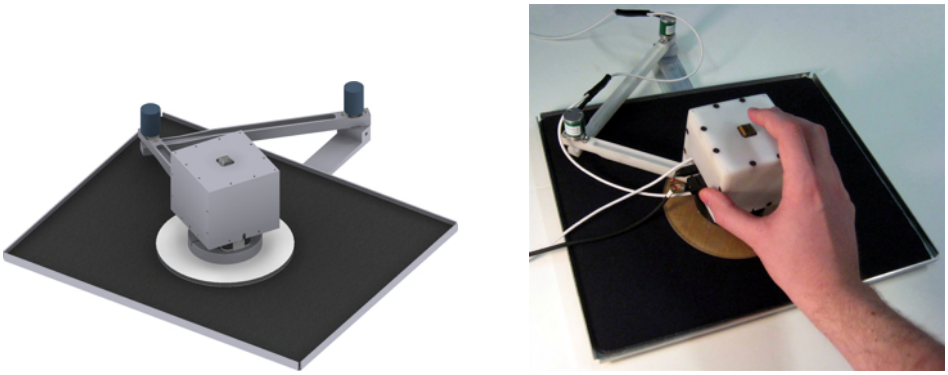

Fig. 7.2 The improved Tactograph tactile graphics interface.

The literature on conventional tactile graphics as well as electronic tactile graphics interfaces is first reviewed. The different components of the Tactograph are then

described, followed by a detailed analysis of the design and properties of the instrumented planar carrier. The Tactograph's driving software is finally discussed before concluding the chapter.

7.2 Tactile Graphics Interfaces

7.2.1 Conventional Tactile Graphics

Conventional tactile graphics can be produced with a variety of methods [59, 101, 275]. Tactile content can, for example, be creatively handcrafted using mixed materials such as glued objects, rubber bands or paper build-ups, resulting in displays that are rich but time consuming to produce and difficult to replicate. Lower quality but mass-producible tactile content can instead be created by thermoforming, a process by which the relief of a raised display is impressed by vacuum forming on a plastic sheet. A more common approach is to use microcapsule paper on which dark patterns are raised by heat, making it possible to inexpensively produce embossed graphics with a computer and conventional printer. Tactile graphics can alternatively be produced with specialized equipment such as 3D printers operating by material deposition [174] or embossers similar to Braille printers [288]. Although these developments have improved the accessibility of tactile graphics, the production process remains cumbersome and results in static content with far less flexibility than visual displays.

The usability of conventional tactile graphics has been improved by combining static media such as embossed paper with digitizing tablets such that location-specific speech or non-speech audio feedback can be produced [297, 13, 108, 212, 165, 181, 202]. This approach reduces clutter by eliminating the need for Braille labels and maintains the rich tactile experience of a large canvas, allowing, for example, an overview to be felt by two-handed exploration. The immediacy and flexibility of visual displays, however, can only be matched by producing virtual or refreshable tactile patterns with haptic interfaces such as force-feedback devices and tactile displays.

7.2.2 Force-Feedback Interfaces

The maturity and commercial availability of force-feedback interfaces has raised much interest for their use by visually impaired persons. Force-feedback interfaces such as

the Sensable PHANTOM, which consists of a pen or manipulandom attached to an actuated arm with three or six degrees of freedom, have, for example, been used to explore 3D scenes such as game environments or map-like models [255, 169, 103, 185, 186, 245, 170, 89], or simplified planar patterns such as relief surfaces similar to conventional tactile graphics [306, 305, 307, 176, 128, 224, 216, 240]. Lower-fidelity force-feedback or vibrotactile pointing devices such as pen, mice and joysticks have been used to similar effect by producing location-dependent haptic feedback on a plane [145, 255, 307, 305, 64, 82, 201]. Even though they typically limit interactions to a single point of contact, the dynamic nature of these interfaces offer many advantages over conventional static media, particularly when used in a multimodal context [307, 113].

7.2.3 Tactile Displays

Although less mature, tactile displays have the potential to improve the usability of virtual or refreshable graphics by allowing more natural distributed stimuli to be applied to the skin. The design of tactile displays is challenging as it requires packing a large number of actuators or skin stimulators within a small, densely innervated skin region such as the fingerpad. A wide variety of skin stimulation methods have been investigated, generally falling within the category of thermal [107, 126], electrical [118, 266], or mechanical stimulation [284, 280]. The latter is by far the most common and typically consists of pin arrays that either indent the skin [252, 187, 195] or vibrate against it [104, 31]. Actuation technologies also vary greatly and include miniature or remote motors [284, 208], piezoelectric ceramics [195, 139], shape memory alloys [280, 188, 283, 271, 171], microelectromechanical systems [304, 61], and magnetorheological or electrorheological materials [164, 129, 270, 67]. Readers are referred to [43, 44, 50, 30, 203] for detailed surveys of tactile display technologies, and to [287, 282] for their use as graphical displays.

Tactile displays intended for virtual or refreshable tactile graphics can be divided in two categories depending on the size of their stimulator array. Large arrays typically take the form of matrices of pins whose protrusion out of a plane is controlled to create raised tactile patterns that approximate 3D surfaces. Commercial tactile displays of this type include the Graphic Window Professional (Handy Tech Elektronic GmbH, Germany) and the Dot View Series DV-2 (KGS Corp., Japan), consisting re-

spectively of arrays of 24×16 and 32×48 pins. Based on refreshable Braille display technology, these arrays offer only a single elevation level and a relatively low pin density of 2.5 to 3.0 mm. These and similar arrays have nevertheless been successfully used for the display of tactile graphics such as mathematical equations and diagrams [4, 131, 58, 295, 249, 234]. More experimental tactile arrays have also been designed using alternative technologies, for example, allowing control over pin elevation and hence the creation of more complex relief patterns [123, 252, 251, 250]. Other stimulation methods such as vibration have also been investigated [23]. Large tactile arrays, provided that they offer a sufficient area, have the advantage of allowing natural exploration strategies such as the use of both hands to be employed. With few exceptions [229, 226], however, this flexibility comes with an increase in cost and power consumption since each pin must be individually actuated.

An alternative approach consists of dynamically altering the tactile sensations produced by a smaller array so as to create the impression of exploring large virtual tactile graphics, hence requiring fewer actuators. In order to be effective, this fingerpad-sized tactile array must be coupled with a pointing device such as a mouse or pen tablet so as to allow the active exploration of a virtual canvas. Although the tactile display and pointing device are often collocated, practical considerations occasionally results in the use of different hands for tactile feedback and positioning functions. The most famous tactile display of this type is the Optacon which consists of an array of 24×6 vibrating pins representing the visual patterns such as printed letters captured by a moving camera [31]. The VTPlayer (VirTouch, Israel) similarly presents tactile patterns through two 4×4 arrays of Braille pins mounted on a mouse. The device has notably been used to display maps [115], to provide directional cues to guide the exploration of a shape [193], and to passively provide guidance cues while tracing with a PHANTOM [215]. Braille cells have similarly been mounted on planar carriers [173, 221], used passively with pen tablets [309], and embedded in trackballs and pen [148]. Experimental pin arrays have similarly been embedded in mice [195, 104, 106] and pen [141]. Many other fingerpad-sized tactile arrays have been used to passively display small patterns but could potentially be coupled with pointing devices to display virtual graphics [280]. Although promising, tactile displays remain largely experimental and commercial devices such as the Optacon and VTPlayer have unfortunately been discontinued after meeting limited success.

7.2.4 Laterotactile Interfaces

The virtual tactile graphics interface introduced in this chapter belongs to the latter category of tactile displays. The improved Tactograph combines a laterotactile display called STReSS^2 with a planar carrier designed specifically for the display of virtual tactile graphics. The STReSS^2 is a third-generation 2D laterotactile array [289, 205, 92] and is part of a larger device family which includes 1D arrays such as the THMB, a miniature linear array embedded in a portable device [206]. Laterotactile displays have the particularity of deforming the skin laterally using arrays of miniature piezoelectric actuators that bend when activated, causing their tip to move sideways. They have been shown to elicit a range of useful tactile sensations in the context of Braille (Chapters 3 and 4), tactile graphics (Chapters 5 and 6, [211]) and mobile interaction [166, 206, 204] when combined with a linear or planar carrier.

This mode of tactile stimulation has received little attention from other research groups. Cholewiak and Sherrick nevertheless designed a similar display with an array of 64 widely-spaced piezoelectric benders intended for use on large body areas such as the thigh or palm [42]. The array operated by lateral skin deformation but was limited to the production of vibrations of controllable intensity at 250 Hz. Drewing et al. more recently designed a tactile display with a 2×2 array of laterally moving pins having a spacing a 3 mm [57]. The array supports large pin movements along two axes as well as the application of strong forces, making it ideal for basic studies of human touch. Its design, however, does not scale to denser arrays and is hence of limited use for more practical applications.

The use of lateral skin deformation may also provide advantages over more common approaches such as normal indentation. The fingerpad skin was, for example, found to be more sensitive to tangential than normal displacement, although less sensitive to forces [26]. The use of a flexible plastic sheet covered with pins was also shown to facilitate the tactile detection of surface undulations through the lateral movement of the pins [127]. A study of the contact-mechanics of tissue deformation resulting from the motion of an undulating surface against the skin finally suggests that lateral skin deformation may, under certain conditions, provide mechanical stimulation that is nearly indistinguishable from normal indentation from the perspective of the skin's mechanoreceptors [291].

7.3 Tactograph Components

The Tactograph consists of three main components: a laterotactile display that produces tactile sensations under computer control, an enclosure that isolates the display and measures the pressure applied with the reading finger, and a carrier that accurately measures the position and orientation of the display. Each component is discussed in turn. Detailed technical drawings can be found in Appendix A.

7.3.1 Tactile Display

The Tactograph relies on the STReSS^2 tactile display to produce controlled tactile sensations [289]. The STReSS^2 is part of a novel class of tactile displays, referred to as *laterotactile* displays, that stimulate the sense of touch through lateral deformation of the skin rather than more common methods such as indentation, vibration or electrical stimulation [282]. The latest revision of the STReSS^2 consists of an array of 8×8 independent piezoelectric actuators forming a dense array of 64 laterally-moving skin contactors within an area of 9×11 mm, approximately the size of a fingerpad. The tip of each actuator can be deflected towards the left or right by a maximum of approximately 0.1 mm when unloaded, and produce a blocked force in the order of 0.15 N. As illustrated in Figure 7.3, the electronics of the STReSS^2 serve a structural function and are therefore exposed, requiring a protective shell or enclosure which is described next.

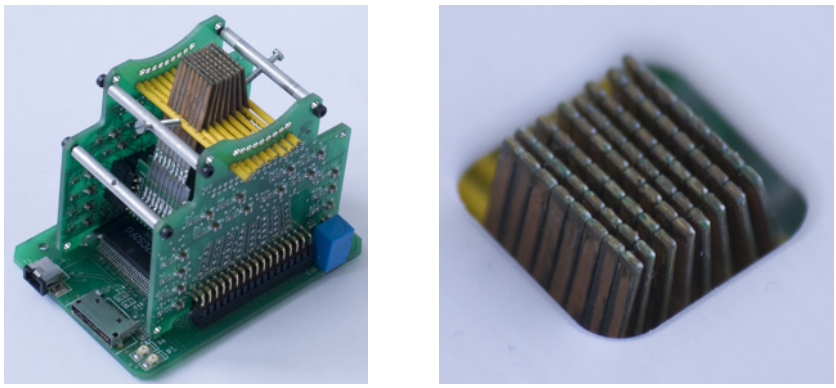

(a) (b)

Fig. 7.3 (a) The STReSS^2 tactile display and (b) its array of skin contactors protruding for the enclosure.

7.3.2 Tactile Display Enclosure

The tactile display is enclosed in a plastic box that protects the device and isolates the user's hand from its exposed electronics (Figure 7.4c). The tactile display is mounted on a bracket and suspended below three thin-beam load cells (LCL-816G, Omega Engineering, Inc., Connecticut) as illustrated in Figure 7.4a-b, thereby allowing measurement of the pressure applied by the reading finger independently of the force applied by resting the hand on the enclosure. The enclosure is fastened by set screws to a 4-mm rotating shaft on the planar carrier such that the axis of rotation is centered within the display's pin array. The insertion of a key in matching slots on the enclosure and carrier is used to set the display in a known orientation for zeroing.

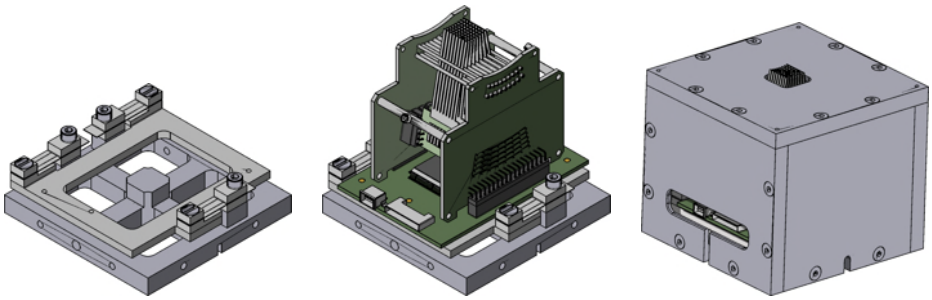

(a) (b) (c)

Fig. 7.4 (a) Force-sensing fixture, (b) mounting of the tactile display, and (c) tactile display enclosure.

7.3.3 Instrumented Planar Carrier

The instrumented planar carrier consists of a two-bar linkage supported by a disc sliding within a rectangular workspace (Figure 7.5). The base of the carrier is formed by an aluminium tray with folded tabs that delimit the boundaries of the workspace and thereby provide a reference frame for the virtual canvas and maintain the linkage in the appropriate posture. The size of the tray was selected such that the center of a 75-mm sliding disc moves within a letter-sized workspace (279.4 $\times$ 215.9 mm). A disc-shaped slider was selected so that a uniform distance to the borders is maintained as the posture of the linkage, and therefore the orientation of the slider, changes. The inner surface of the tray is covered with a large mouse pad to reduce friction against the sliding disc.

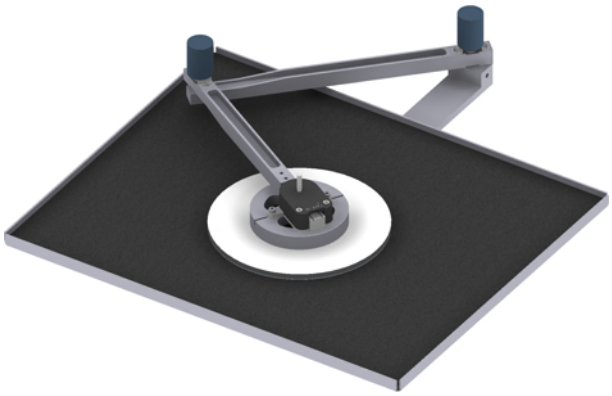

Fig. 7.5 Instrumented planar carrier consisting of a two-bar linkage supported by a sliding disc.

The slider was originally designed as a 75-mm-wide, pocketed plastic disc sliding on Teflon pads (Figure 7.6a). A 139.1-mm-wide Teflon-backed disc was later attached under the thinned slider to improve stability when the tall display enclosure is moved against the workspace borders (Figure 7.6b). Although feasible, enlarging the base tray to compensate for the reduction by 64.1 mm of the workspace dimensions would affect portability and was therefore not done. A 4-mm rotating steel shaft is held within two ball-bearings at the center of the slider and protrudes to allow mounting of the tactile display enclosure. The position of the shaft is measured with a 5000-CPR encoder (E5S-1250-157-HG, US Digital, Washington) mounted on top of the disc.

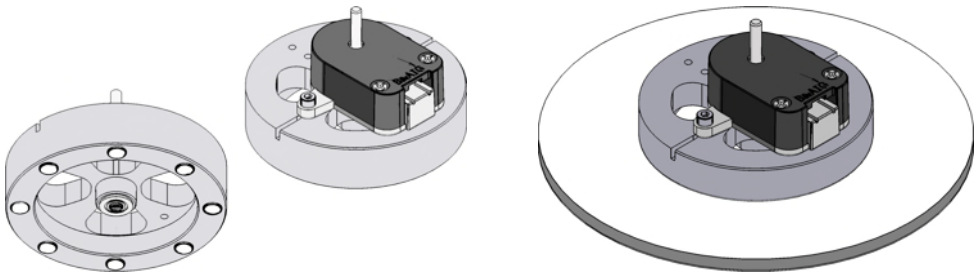

(a) (b)

Fig. 7.6 (a) Original slider and (b) revised slider with a Teflon-backed disc for improved stability.

The position of the carrier is measured through an instrumented two-bar serial linkage mounted on the base tray and attached to the slider. The linkage is made of two 12.7-mm-wide pocketed and tapered plastic bars and is supported by a metal fixture

attached under the tray (Figure 7.7a). The shaft-to-shaft length of the first and second links, 210 and 170 mm respectively, and the length of the fixture were selected to maximize resolution while respecting physical constraints imposed by the design (see Section 7.4.3 for more details). The joints of the linkage are formed of 3.175 mm steel shafts fastened by set screws on a side and rotating within tensioned ball bearings on the other (Figure 7.7b). The position of the shafts is measured by two high-resolution optical encoders (R120B, Gurley Precision Instruments, New York) with 65,536 CPR. These encoders and the display orientation encoder share power and ground signals within a single flexible cable loosely routed along the linkage.

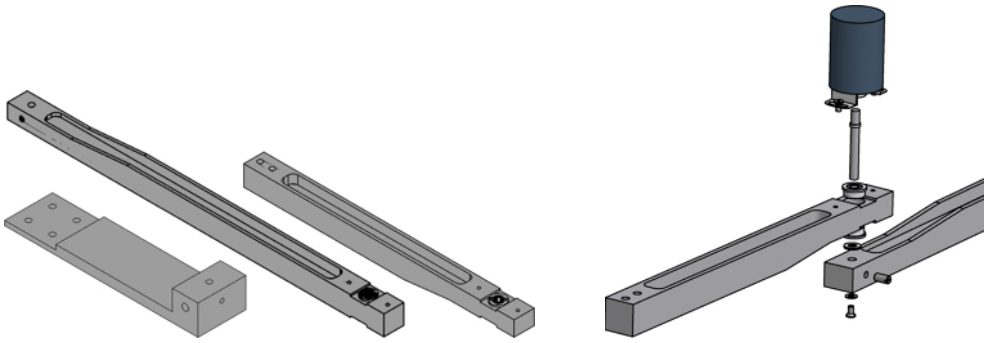

(a) (b)

Fig. 7.7 Components of (a) the carrier's linkage and (b) the joint between the rigid links.

7.4 Carrier Design and Analysis

The design of the carrier and its properties are summarized here and discussed in details in Appendix A. The kinematics of the carrier linkage are first given, followed by an analysis of the spatial resolution of the position measurement. The optimization of the link lengths and workspace location are then discussed before describing the properties of the design.

7.4.1 Kinematics

The Tactograph carrier can be represented as a serial linkage with two rigid links and two revolute joints as illustrated in Figure 7.8. The length of the first and second links

is given by a and b respectively. The position (x, y) of the end effector is measured indirectly through joint angles α and β. The ratio of link lengths $k = b/a$ and the distance to the end effector $r = \sqrt{x^2 + y^2}$ are used to simplify the analysis. The linkage is restricted to the illustrated posture and therefore obeys the condition $\beta > 0$. The kinematics of the Tactograph carrier are derived in Appendix A and summarized here.

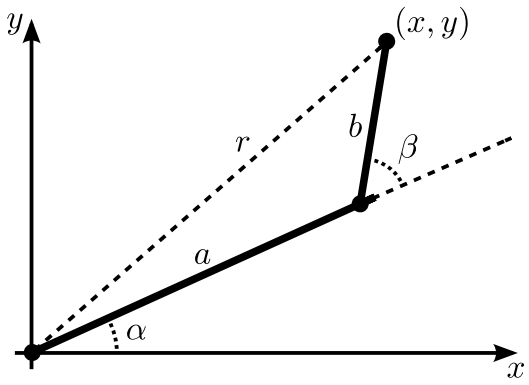

Fig. 7.8 Geometric model of the carrier as a two-bar serial linkage.

The forward kinematics provide the position of the end effector x, y given the joint angles α, β and are given by:

$$\begin{bmatrix} x \\ y \end{bmatrix} = \begin{bmatrix} \cos\alpha & \cos(\alpha+\beta) \\ \sin\alpha & \sin(\alpha+\beta) \end{bmatrix} \begin{bmatrix} a \\ b \end{bmatrix}. \tag{7.1}$$

The inverse kinematics, on the other hand, provide the joint angles given the end effector position and are given by:

$$\begin{bmatrix} \alpha \\ \beta \end{bmatrix} = \begin{bmatrix} \arctan\frac{y}{x} - \arccos\frac{a^2-b^2+r^2}{2ar} \\ \arccos\frac{r^2-a^2-b^2}{2ab} \end{bmatrix} \tag{7.2}$$

The Jacobian relates angular differences to spatial differences and is given by:

$$J = \begin{bmatrix} -a\sin\alpha - b\sin(\alpha+\beta) & -b\sin(\alpha+\beta) \\ a\cos\alpha + b\cos(\alpha+\beta) & b\cos(\alpha+\beta) \end{bmatrix} \tag{7.3}$$

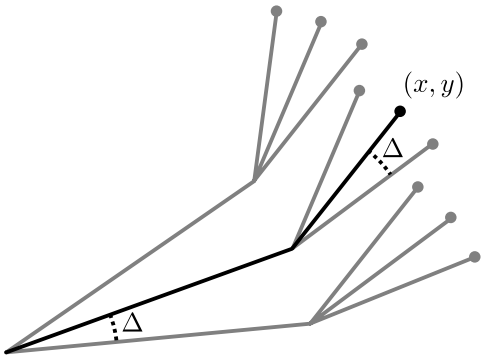

Fig. 7.9 Spatial offset introduced by a measurement error of a single count in one or both joint encoders.

7.4.2 Spatial Resolution

The spatial resolution of the Tactograph carrier is estimated by computing for each location on the reachable workspace the maximal position error introduced by a measurement error of a single count in one or both joint encoders. As illustrated in Figure 7.9, this entails determining the maximum of 8 possible spatial offsets resulting from different combinations of joint angle measurement errors. The maximum position error, derived in Appendix A, can be expressed as a function of the distance r from the origin:

$$e_{max}(r) = \Delta \begin{cases} \sqrt{2r^2 + a^2(2k^2 - 1)} & \text{if } r > a\sqrt{1-k^2} \text{ or } k > 1, \\ a & \text{otherwise.} \end{cases} \tag{7.4}$$

The angular error introduced by an encoder count is denoted by Δ and depends on the characteristics of the encoders, which are assumed identical. The resolution therefore decreases monotonically as the linkage is extended once a distance $r = a\sqrt{1-k^2}$ has been reached, or when $k > 1$. The resolution also decreases as the length of the rigid links increases.

7.4.3 Optimization

The length of the carrier's rigid links as well as the location of the rectangular workspace were selected so as to optimize the spatial resolution (see Appendix A for more details). The bounds of the annular workspace of the two-bar linkage were first expressed as a function of the link lengths such that a number of physical constraints imposed

by the Tactograph design were respected. The link lengths were then selected so as to fit a rectangular workspace of appropriate dimensions within the annular workspace while minimizing the length of the first link for a given link length ratio k. The link lengths were finally selected by observing the effect of variations in the ratio k on the minimum and maximum resolutions occurring at the points furthest and closest to the origin respectively, as illustrated in Figure 7.10a.

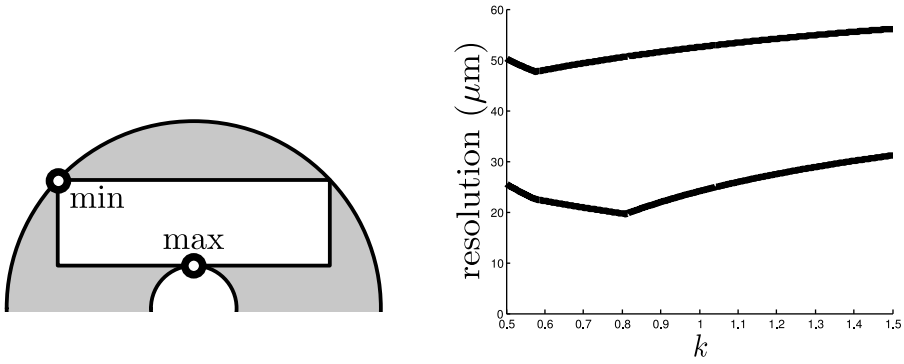

(a) (b)

Fig. 7.10 (a) Points of minimal and maximal resolution within the workspace, and (b) resolution range as a function of link length ratio k.

As illustrated in Figure 7.10b, the minimal resolution is optimal at 47.8 µm with $k = 0.57$ and $a = 234.23$ mm. The maximal resolution, on the other hand, is optimal at 19.6 µm with $k = 0.81$ and $a = 204.16$ mm. Given the small effect on resolution, the length of the links was optimized for the maximal resolution point such that the first link is shorter and encumbrance reduced. The link lengths were set to $a = 210$ mm and $b = 170$ mm ($k = 0.81$). The rectangular workspace is offset by 120 mm and therefore extends horizontally from -139.7 to 139.7 mm and vertically from 120.0 to 335.9 mm.

7.4.4 Characterization

The spatial resolution of the Tactograph ranges from 20.2 to 50.6 µm over the original letter-sized workspace and is illustrated in Figure 7.11. The reduction in workspace size due to the enlargement of the sliding disc, illustrated in grey, narrows the range to 23.6 to 45.2 µm. The orientation of the tactile display is measured with a resolution of $360°/5000\,\text{CPR} = 4.32'$.

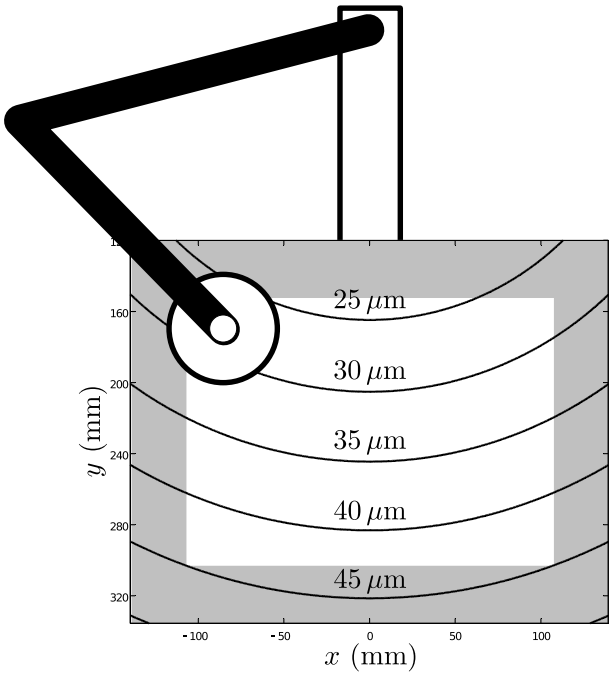

Fig. 7.11 Spatial resolution of the Tactograph carrier. The area inaccessible due to the enlargement of the slider is marked in grey.

7.5 Software Architecture and Control

The Tactograph interfaces with a personal computer running Linux and the Xenomai real-time framework (`http://www.xenomai.org`) through an industrial Input/Output (IO) expansion card. The actuator activation signals are generated with a resolution of 10 bits and the load sensors read with a resolution of 14 bits. The Tactograph is programmed through an object-oriented C++ library that provides a unified interface for different types of laterotactile displays and carriers. Low-level operations are handled by kernel modules through a set of predefined real-time synchronous messages, allowing transparent support for different IO cards. The activation signals of the tactile array are refreshed through a control loop running at 1 kHz according to tactile rendering algorithms dependent on sensor readings and described in the next two chapters. The low-level sequential refresh of the tactile display's sample-and-hold amplifiers is performed in software and causes a significant overhead which may be reduced in the future through the use of a dedicated microcontroller.

7.6 Conclusion

This chapter introduced the latest revision of the Tactograph, a haptic interface for the display of virtual tactile graphics by lateral skin deformation. The improved Tactograph provides a large virtual surface suitable for practical tactile graphics while maintaining the high spatial resolution necessary for laterotactile rendering. The tactile display is also enclosed in an instrumented box that isolates the device and allows measurement of the pressure applied with the reading finger. The rotation of the tactile display is moreover measured, allowing the orientation of the reading finger to be taken into account in tactile rendering algorithms.

Limitations of the current design will be addressed in future revisions. The tall sliding manipulandom was found to tilt dangerously when hitting the workspace borders, an issue that was resolved by enlarging the slider and consequently reducing the size of the virtual surface. The intended surface dimensions may be restored by enlarging the base tray, at the expense of portability, or redesigning the components for reduced height. Although beneficial for controlled motion, the friction between the Teflon disc and fabric base could also be reduced by lightening the manipulandom or improving the slipperiness of the contact. Finally, the sensing of the force applied by the finger has yet to be commissioned or taken advantage of to improve the realism of tactile renderings.

The Tactograph was mainly designed as a prototype suitable for tactile graphics experimentation in the laboratory. Although it serves this purpose well, wider use of the interface by visually impaired persons will require ergonomic improvements and a reduction in cost. The tactile display enclosure could, for example, be given a shape similar to that of pointing devices such as mice and trackballs, perhaps even providing buttons for interaction. A careful investigation of the required spatial resolution could also enable the use of more practical and cheaper position sensing mechanisms such as a mouse's optical sensor. A reduction in size of the tactile display could also enable reading of virtual graphics with multiple fingers or even both hands. Feedback obtained during numerous demonstrations and experiments suggests that a refined Tactograph could gain acceptance in the visually impaired community and be a valuable tool for graphical literacy beyond the laboratory.

Acknowledgments

The name *Tactograph* was coined by Pierre Ferland (Institut Nazareth et Louis-Braille). The STReSS^2 tactile display and the Pantograph-based Tactograph were designed and implemented by Qi Wang under the supervision of Vincent Hayward. Donald Pavlasek (Mechanical Workshop, ECE dept.) made significant contributions to the design and implementation of the revised Tactograph. This work was also influenced by discussions with Jérôme Pasquero, Nicole Trudeau, Aude Dufresne and Grégory Petit. The pictures shown in Figures 7.1 and 7.3 were taken by Qi Wang and Jérôme Pasquero respectively. Funding from Fonds québécois de la recherche sur la nature et les technologies (PR-114110) is gratefully acknowledged.

Chapter 8

Tactile Graphics Rendering by Lateral Skin Deformation

Preface to Chapter 8

This chapter presents a framework for the rendering of virtual tactile graphics by lateral skin deformation that extends the drawing primitives described in Chapter 6, introduces novel rendering algorithms, and re-frames the whole as a coherent set of tactile patterns. The concept of a grating texture is, for example, extended to include axial and radial gratings, and gaps optionally inserted between grating ridges for better definition. Major additions to the framework include a set of compositing operators allowing complex tactile patterns and textures to be created, as well as vector graphics drawing capabilities introduced through the concept of a tactile stroke. The framework was developed and validated using the improved Tactograph described in Chapter 7.

Contributions of Authors

This chapter was written by Vincent Lévesque and revised by Vincent Hayward. The work presented herein was similarly performed by V. Lévesque under the supervision of V. Hayward.

Tactile Graphics Rendering by Lateral Skin Deformation

Abstract

This chapter introduces a framework for the rendering of virtual tactile graphics by lateral skin deformation that offers basic vector graphics drawing capabilities suitable for the composition of complex graphics and the emulation of features such as raised lines, dot patterns and areal textures found in conventional tactile graphics. The framework takes the form of a coherent set of tactile patterns that includes textures, images, stroked shapes, dots and dotted shapes, as well as more complex composite patterns and textures. The framework is implemented as a flexible software library that allows the rapid development of experimental tactile graphics applications and the specification of tactile graphics content through a descriptive language. The effectiveness of the rendered patterns was informally evaluated by soliciting feedback from four visually-impaired volunteers.

8.1 Introduction

Haptic rendering most commonly consists of determining forces to be applied through a manipulandom according to interactions with a simulated model [238]. Tactile rendering similarly controls the activation of stimulator arrays to reproduce the sensation of touching a physical surface or to communicate information through abstract tactile patterns. A large pin array typically approximate a 3D surface by discretely reproducing a simple height map [248]. Smaller tactile arrays similarly dynamically approximate the local height of a surface as they are displaced [115] or modulate the intensity of a vibrotactile or electrotactile stimulus to provide equivalent information in an abstract form [163].

While it has much in common with earlier approaches, rendering by lateral skin deformation differs significantly due to the novelty of the stimulation mode and the paucity of information on the correlation between laterotactile stimulus and perceived tactile sensation. Laterotactile stimulation most notably allows tactile illusions, such as the presence of raised patterns, to be produced using skin deformation patterns that do not have an obvious physical interpretation. Previous work presented in Chapters 3 and 4 has, for example, demonstrated that raised features similar to Braille dots could be produced by propagating a wave of local stretch and compression across the fingerpad. Similar patterns have similarly been used in a mobile context to produce tactile markers in scrolled documents [166, 204, 206]. Patterns composed of vibrating or dotted contours and grating textures were also used to produce tactile graphics in Chapters 5 and 6.

The work presented in this chapter builds on the drawing primitives described in Chapter 6 to create a coherent framework for the tactile rendering of complex tactile graphics by lateral skin deformation. The framework provides basic vector graphics capabilities through a set of tactile patterns that includes textures, images, stroked and dotted shapes, as well as more complex composite textures and patterns, enabling conventional tactile graphics elements such as areal textures and raised lines to be emulated [59]. Previous work on conventional and refreshable tactile graphics as well as haptic rendering is first reviewed. Laterotactile rendering is then introduced before describing in details the framework's tactile patterns. The implementation of the framework is finally discussed and its effectiveness evaluated with four visually im-

paired volunteers.

8.2 Background

8.2.1 Conventional Tactile Graphics

Tactile graphics are commonly produced on static media such as embossed paper and thermoformed plastic [59, 235]. While their use spans a range similar to that of their visual counterparts, tactile graphics are most critical in education where scientific or technical topics often require access to diagrams, bar charts, mathematical or geometric illustrations, and geographical maps [59, 36, 99, 98, 6, 247]. Tactile graphics can also serve an important purpose in the development of visually impaired children [194], for example, by illustrating concepts that cannot easily be experienced first-hand such as the height of a building or shape of a wild animal. Specialized tactile maps are also used for orientation and mobility, providing visually impaired persons with the necessary information for autonomous travel [59]. Reading tactile graphics is nevertheless an acquired skill that many do not pursue beyond their formal education [94], likely due to the limited availability of content and effort required to acquire graphical information by touch.

The design of tactile graphics does not obey strict, unified rules and conventions, and must instead be adapted to the needs of individual readers and capabilities of the production method selected. Detailed guidelines for the design of effective tactile graphics have nevertheless been proposed by numerous practitioners [59, 34]. It is generally recommended, for example, to clearly separate tactile elements by leaving between them a blank space of 2.5 to 3.0 mm, similar to the distance between Braille dots [59, 34]. A clear contrast between tactile features is similarly critical [59]. More generally, graphical content must be stripped to its essential elements to reduce clutter and visual conventions such as perspective, although learnable, should be avoided [59]. Tactile maps are an interesting example built from point, line and areal symbols [59]. Point symbols are fingerpad-sized icons that symbolically represent cities or other points of interest. Line symbols delimit contours and indicate paths using strokes of varying tactile appearance. Areal symbols are bounded areas marked with identifiable textures in place of colors. A maximum of five distinct textures per canvas is recommended, and contrast is once more paramount. It is interesting to note that intuitive

tactile patterns are often sought for the representation of recurring elements such as water, mountains and cities. Readers are referred to [59, 34, 268, 278, 111] for more details on tactile graphics conventions.

The reading strategies employed to perform tasks such as obtaining an overview or evaluating distances often involve the use of both hands [59, 268, 114] and are hence currently supported only by large refreshable displays. Refreshable interfaces, discussed next, nevertheless present many advantages such as immediate access to digital content, interaction with dynamic graphics, and a reduction of clutter with audio tags.

8.2.2 Refreshable Tactile Graphics

Force-feedback interfaces have been used extensively to design applications for visually impaired persons. Interfaces such as the PHANTOM can be used to simulate physical interactions between a virtual probe and 3D environments [207, 89, 48, 170, 245, 276, 103, 169, 168]. This approach has, for example, been studied and applied by Sjöström for the design of haptic games and adapted interaction techniques [255], and by Moustakas et al. for the creation of detailed 3D maps [186]. An alternative approach consists of producing a close analog to physical tactile graphics in the form of 3D surfaces explored with either sophisticated interfaces or consumer-grade ones such as haptic mice. This approach has notably been used to produce maps [240, 201, 145, 82, 186], 3D data set visualizations [69], and electric circuits [216]. Speech or non-speech audio often augments the haptic presentation [201, 307, 128, 224]. The MultiVis project has, for example, extensively studied the multimodal display of graphics such as bar charts drawn as surface grooves [307]. Rassmus-Gröhn et al. have similarly developed a sophisticated system that allows tactile graphics to be drawn by visually impaired users as a positive or negative relief [128, 224]. A mixture of 3D environments and 2D surfaces with grooves and textures is often used in practice. This approach has, for example, been used for the design of educational material for the teaching of astronomy, with information such as planetary orbits and the Earth's surface being communicated through interactive models [237].

Tactile displays consisting of large pin arrays have also been used for the display of tactile graphics. Commercial tactile display modules based on Braille display technology have, for example, been used to create sophisticated applications for draw-

ing and the display of animations, complex patterns such as Chinese ideograms, and games [249, 131, 130, 295]. Similar displays have also been used to display mathematical graphics [4] and web pages [234]. Experimental displays with controllable elevation have similarly been used to display Chinese ideograms, familiar objects, maps and scientific illustrations [252, 123]. Braille displays and similar devices have also been used to produce stock quotes [58] and games [244]. Of note is a simple display with eight laterally moving pins that has been used to display mathematical curves [279]. Other displays have often been evaluated based on their ability to convey simple geometric patterns or letters [265, 23, 171, 250] and may have potential for the display of more complex tactile graphics.

Although many smaller tactile displays have been designed for the rendering of virtual tactile graphics, most have been evaluated mainly for the display of small tactile patterns. The VTPlayer has, for example, been used to display static and dynamic directional icons which were used as guidance cues for the exploration of shapes and electric circuits [215, 193]. Others displays have similarly been used to display simple geometric patterns [139, 143, 140, 14, 117, 116, 279] as well as bars or gratings [187, 120]. Although similarly used passively for numerous psychophysical or neurophysiological experiments [49, 71, 70, 72, 73, 199, 62, 136, 155, 95, 84, 258, 45], the Optacon has also been evaluated for the exploration of larger tactile patterns [31, 95, 135]. The VTPlayer has also been used for the display of virtual pattern either directly [115] or with a separate pointing device [287, 286]. Many other devices have been evaluated based on their performance for the display of virtual shapes, letters or textures [172, 173, 195, 309, 141]. Although few have been used to display complex virtual tactile graphics, many displays may have the potential to do so.

8.2.3 Haptic Rendering

The concept of haptic rendering refers to the specification of activation signals for a haptic interface in response to changes in measured inputs or in the state of a simulation. A rendering algorithm controls the interface's actuators or stimulators and hence the tactile or kinaesthetic stimulus applied to the user. Haptic rendering is similar to visual rendering where the color of each of a display's pixels is defined to obtain a desired effect.

Haptic rendering algorithms designed for force-feedback devices such as the PHAN-

TOM have received much attention [238]. Force-feedback rendering typically consists of simulating the interaction forces between a virtual tool representing the interface's manipulandom, and a virtual environment with 3D objects having physical properties such as shape, elasticity and texture. The challenge resides in efficiently simulating the physics of the interaction while taking into account the limitations of the interfaces, such as the resolution of the position sensors and maximum force output. Of particular concern is the stability of the interaction which, if compromised, can result in serious artefacts such as oscillations. Similar concepts apply to planar interfaces such as force-feedback mice with which textures and raised features can be simulated using the lateral component of interaction forces [184, 230]. In the context of tactile graphics, force-feedback interfaces are typically used to render 3D scenes [255, 186, 103], relief surfaces [307, 128, 224], or fixtures that guide the exploration of a pattern using attraction forces [69, 216].

Rendering algorithms designed for distributed tactile displays are comparatively much less mature, due in part to the variety of skin stimulation methods and actuators used. Large arrays of raised pins discretely approximate a 3D height map [189, 252, 250, 123] or a binary embossed pattern [171, 234, 4, 295, 249] and are hence the most straightforward to activate. Fingerpad-sized pin arrays can produce more complex spatio-temporal patterns [208] which are often used to approximate the local height map at the location of exploration [309, 195, 141]. Filtering can be used to smooth transitions as the virtual sensor moves over a discrete height map [141, 249]. The scope of the sensor and its rate of motion can also be amplified to create magnification effects [309, 195]. The simulation of friction by superposition of vibration has also been suggested but is not widely used [66].

The vibration amplitude of vibrotactile pin arrays can similarly be modulated to produced localized tactile sensations. Practical considerations often result in a fixed vibration frequency of approximately 230-250 Hz, at which the fingerpad skin is known to be very sensitive [106, 162]. Control over vibration amplitude is similarly often limited to a simple switch, as was the case with the Optacon [31]. Binary or multi-level vibrotactile patterns have nevertheless been used to render patterns such as letters [31] and textures [104, 105, 106]. Allerkamp et al. have recently suggested that more realistic patterns could be produced by superposition of modulated vibrations at 40 and 320 Hz, with each band targeting a different population of mechanoreceptors [7]. A

similar hypothesis has been made by Konyo and colleagues using a different actuation technology [133, 132, 134].

The targeted stimulation of mechanoreceptors has also been proposed with electrotactile arrays [119, 86]. A variety of other skin stimulation methods have been investigated [282] with tactile rendering approaches that generally do not substantially differ from the above.

8.3 Laterotactile Rendering

The Tactograph produces tactile sensations by deforming the fingerpad skin with a programmable array of laterally-moving contactors in response to exploratory movements and other system inputs. Virtual tactile patterns are created by producing controlled skin deformation patterns through the activation of the array's actuators, a process referred to as laterotactile rendering by analogy with graphics rendering. The specification of tactile rendering algorithms through actuator deflections is first discussed, followed by the special case of actuator vibration. Visualization techniques allowing tactile renderings to be illustrated and inspected are then introduced.

8.3.1 Deflection Rendering

The lateral displacement of the skin contactors results from the deflection of piezoelectric bending motors activated by computer-controlled voltages. The deflection of an actuator, and hence the lateral displacement of its skin-contacting tip, is approximately proportional to the activation voltage and is therefore used for the specification of laterotactile rendering algorithms. Although actual deflections may be reduced due to the stiffness and non-linear properties of the skin [290], the intended deflection has been found to describe the resulting strength of the stimulus to the fingerpad sufficiently accurately for practical applications.

Laterotactile rendering algorithms can be described as sets of deflection functions $\delta_{i,j}(\ldots)$ that depend on actuator index i, j as well as various inputs from the Tactograph. With the exception of vibration rendering, discussed next, the rendering algorithms described in this chapter depend exclusively on the position $\boldsymbol{P}$ and orientation θ of the tactile array on the virtual canvas. Some additional inputs, such as exploration velocity $\boldsymbol{v}$ and time t, are introduced in the next chapter in the context of dynamic

tactile graphics while others, such as the pressure applied with the reading finger, have yet to be used and are therefore not discussed. The proposed rendering algorithms are further restricted to a subclass of functions $\delta(\boldsymbol{p})$ such that the deflection of an actuator depends solely on its position $\boldsymbol{p}$ within the virtual canvas, obtained from the position and orientation of the array and the actuator location within it (Figure 8.1a). This approach was found to reduce the complexity of rendering algorithms while allowing a wide range of tactile effects to be produced.

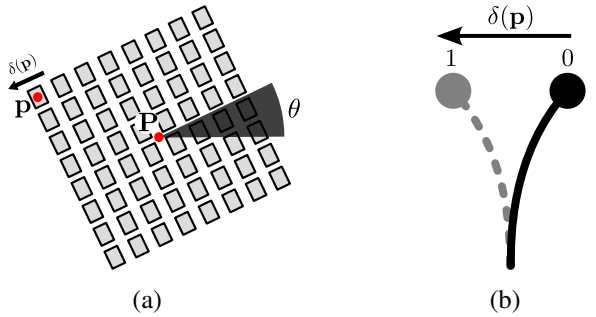

Fig. 8.1 (a) Tactile rendering inputs and (b) deflection range.

The deflection range is defined as $[0, 1]$ with the limits representing maximal activation towards the right and left of the fingerpad respectively (Figure 8.1b). Actuators hence rest on the right ($\delta = 0$), allowing the largest possible swing to be triggered upon activation. The directional effects introduced by this bias are generally minimal and compensated for by an overall increase in stimulus strength. This definition of the deflection range greatly facilitates compositing operations such as linear superposition and scaling.

8.3.2 Vibration Rendering

Vibration rendering is a special case of deflection rendering that produces a strong buzzing sensation through time-varying oscillations of the actuators. The phase of the sinusoidal oscillations is inverted for adjacent actuators to maximize compression and shearing, and thereby increase the vibration's strength. The corresponding deflection function is expressed as a function of time t and actuator index i, j:

$$\delta_{vib}(i,j,t) = \begin{cases} 0.5 + 0.5\sin 2\pi f t & \text{if parity}(i) \neq \text{parity}(j), \\ 0.5 - 0.5\sin 2\pi f t & \text{otherwise.} \end{cases} \tag{8.1}$$

The vibration frequency can reach up to 50 Hz while maintaining a smooth discretization at a refresh rate of 1 kHz, and may be further increased with improvements to the communication bandwidth of the Tactograph and hardware support for vibration. Vibration intensity increases with frequency and can alternatively be controlled by the deflection amplitude A, interpreted either as a scaling factor or as a ratio of vibration to deflection:

$$\delta^0_{vib}(i,j,t) = A\delta_{vib}(i,j,t) \tag{8.2}$$

$$\delta^1_{vib}(i,j,t) = (1-A) + A\delta_{vib}(i,j,t) \tag{8.3}$$

While both interpretations produce identical tactile sensations in isolation, the latter is often preferable when vibrations are multiplied against other deflection patterns. Note that the indirect dependence on time t and actuator index i, j of vibrating tactile patterns is implicit in the remainder of this document for clarity and readability.

8.3.3 Visualization

Visualization allows virtual tactile patterns to be represented visually and hence facilitates the inspection of rendering algorithm outputs and the communication of a canvas' content to sighted graphics producers. Three visualization techniques are illustrated in Figure 8.2 and discussed in turn.

The deflection map takes advantage of deflection rendering's sole dependence on actuator position to create an accurate visual representation of a tactile rendering. Actuator deflections at different locations are mapped to the opacity of a bitmap's pixels, thereby allowing the output of rendering algorithms to be visualized precisely. Vibration is taken into account by computing sequences of deflection maps for a given actuator at different points in time as illustrated in Figure 8.2a. The time-varying deflection of a vibration can alternatively be represented as random noise of the appropriate range as illustrated in Figure 8.2b, allowing vibrating patterns to be readily identified within a single semi-abstract deflection map. Symbolic or abstract illustrations of tactile pat-

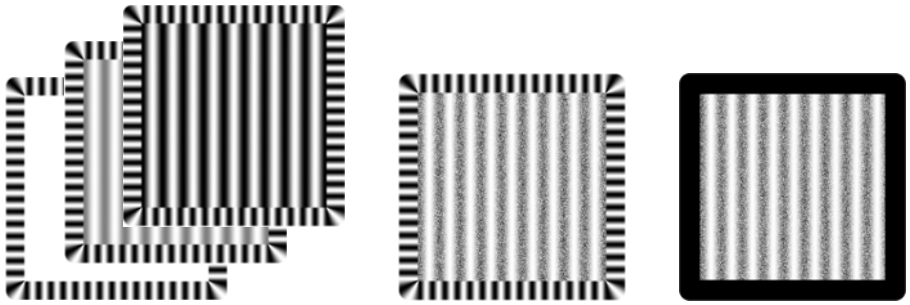

(a) (b) (c)

Fig. 8.2 Visualization of a tactile pattern as (a) a sequence of deflection maps, (b) a semi-abstract deflection map, and (c) an abstract illustration.

terns can finally be drawn efficiently with optimized vector graphics packages to allow realtime interaction with tactile graphics and more freedom in their visual representation, as shown in Figure 8.2c. Semi-abstract deflection maps with vibration as white noise are used extensively in this chapter and the next to illustrate and document tactile patterns and rendering algorithms. The deflection of a tactile array's actuators can also be simulated and visualized over a canvas' deflection map, as illustrated in Figure 8.3.

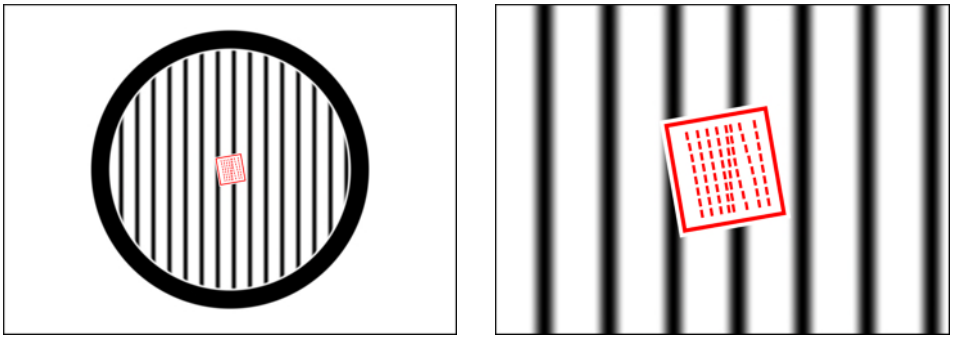

(a) (b)

Fig. 8.3 Simulation of actuator deflections superposed on the deflection map of a tactile pattern: (a) entire canvas and (b) close-up on tactile array.

8.4 Graphics Rendering Framework

The potential of lateral skin deformation for the rendering of virtual tactile graphics was investigated in Chapters 5 and 6 and further demonstrated in the context of educational illustrations [211]. The graphics rendering framework discussed here extends the drawing primitives introduced in this earlier work, proposes novel rendering algorithms, and reframes the whole as a coherent set of tactile patterns. The resulting framework offers basic vector graphics drawing capabilities suitable for the composition of complex tactile graphics and the emulation of tactile features such as raised lines, dot patterns and areal textures found in conventional tactile graphics [59]. Supported tactile patterns include textures, images, stroked shapes, dots and dotted shapes, as well as more complex patterns and textures obtained through compositing operations. Each pattern is discussed in turn.

8.4.1 Textures

Textures are unbounded tactile patterns that fill the entire virtual canvas with a regular arrangement of tactile features. Uniform, tiled and grating textures are first introduced before discussing texture scaling, inversion and vibration.

Uniform Textures

Uniform textures are independent of the actuator position and therefore result in either a fixed deflection or a uniform vibration over the entire virtual canvas as illustrated in Figure 8.4. Fixed deflections result in no perceptible tactile stimulus but can nevertheless serve a purpose for compositing. Vibrating textures, on the other hand, provide intense, easily identifiable tactile feedback.

Tiled Textures

Tiled textures are constructed by tiling small tactile patterns such as lines, circles and polygons to form regular patterns, as illustrated in Figure 8.5. This effect is obtained by wrapping around the position information used to render an arbitrary tactile pattern such that a window of programmable size is repeatedly drawn. Although identifiable with effort in isolation, the shape and details of the duplicated patterns are generally

(a) (b) (c)

Fig. 8.4 Uniform textures with (a) a fixed deflection at 50% intensity, and vibration at (b) 100% or (c) 30% intensity.

lost when tiled sufficiently densely for a unified texture to emerge. Carefully designed tiled textures may nevertheless leave a distinct impression through the interplay of tactile features and gaps.

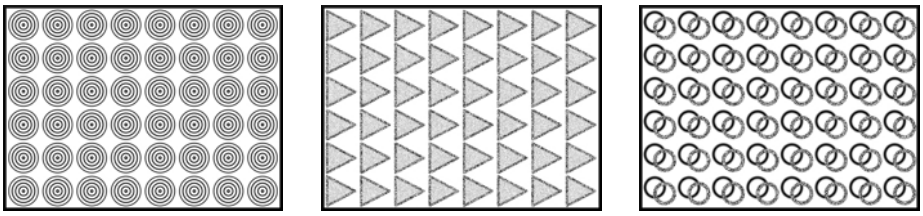

(a) (b) (c)

Fig. 8.5 Tiled textures with (a) discs, (b) triangles, and (c) composite circles.

Grating Textures

Grating textures imitate the sensation of brushing against corrugated surfaces by producing smooth swings in actuator deflections that are perceived as raised bumps or ridges. Three types of grating textures are obtained by varying the geometric interpretation of the distance x along a common grating waveform $g(x)$. Linear grating textures define x as the abscissa of a rotated Cartesian frame of reference, resulting in arbitrarily-oriented straight ripples as illustrated in Figure 8.6a. Radial grating textures, on the other hand, define x as the radial distance from a center point and create concentric rings as shown in Figure 8.6b. Axial grating textures finally define x as the angular distance around a center point, resulting in a spoke pattern as illustrated in

Figure 8.6c. Continuity is enforced by ensuring that a whole number of grating cycles fit within the pattern and high spatial frequencies eliminated by fading the pattern near its center.

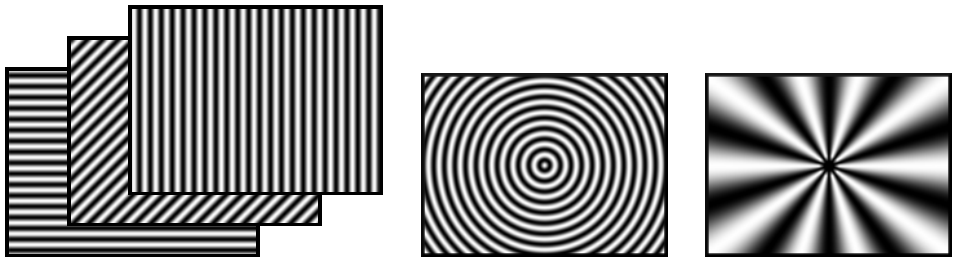

(a) (b) (c)

Fig. 8.6 (a) Linear, (b) radial and (c) axial grating textures.

Grating textures are rendered through a common grating waveform $g(x)$ which defines the periodic deflection pattern repeated along their length as illustrated in Figure 8.7. A grating cycle is composed of a sinusoidal swing that creates the sensation of a ridge followed by an optional gap that reinforces the salience of the tactile feature. Given ridge size λ_r, gap size λ_g, and cycle size $\lambda = \lambda_r + \lambda_g$, a grating waveform of amplitude k is expressed as:

$$g(x) = \begin{cases} \frac{k}{2} - \frac{k}{2}\cos(\frac{x \bmod \lambda}{\lambda_r} \cdot 2\pi) & \text{if } x \bmod \lambda < \lambda_r, \\ 0 & \text{otherwise.} \end{cases} \tag{8.4}$$

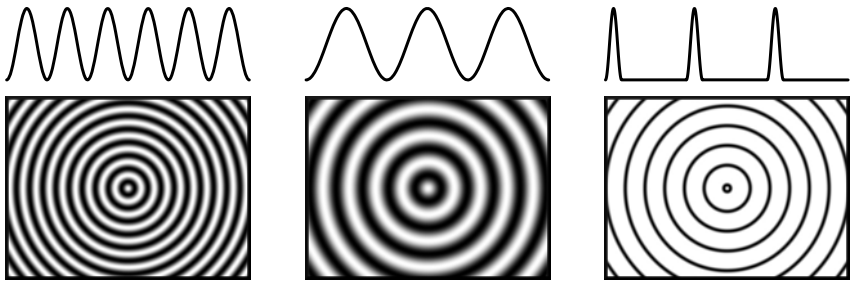

Fig. 8.7 Variations in the size of ridges and gaps in a radial grating texture.

A grating texture can finally be distorted to create a gradual increase or a peak in local spatial frequency or wavelength. These effects are introduced by rendering the

grating waveform $g(x)$ using a warped position $x'(x)$ with a derivative that follows the frequency scaling profiles illustrated in Figure 8.8 (see Appendix B for more details).

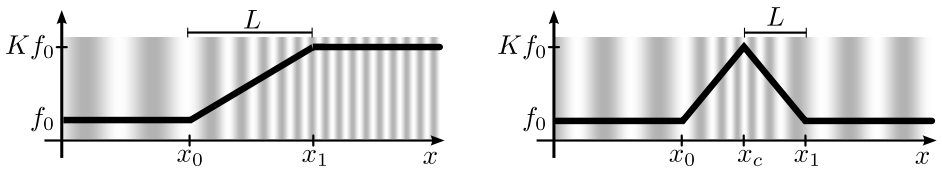

Fig. 8.8 (a) Gradual change and (b) peak in the frequency of a grating texture.

The spatial frequency is scaled gradually by a factor K between points x_0 and $x_1 = x_0 + L$ by applying the following warping function:

$$x'(x) = \begin{cases} x & \text{if } x \leq x_0, \\ x + (K-1)(x - x_0)^2/2L & \text{if } x_0 < x \leq x_1, \\ Kx - (K-1)(x_0 + L/2) & \text{otherwise.} \end{cases} \tag{8.5}$$

A peak is similarly obtained by gradually scaling the spatial frequency by a factor K from points $x_0 = x_c - L$ to x_c, and then back to normal at point $x_1 = x_c + L$ using the following warping function:

$$x'(x) = \begin{cases} x & \text{if } x \leq x_0, \\ x + (K-1)(x - x_0)^2/2L & \text{if } x_0 < x \leq x_c, \\ Kx + (K-1)(L^2 + 2Lx_c - (x - x_c)^2)/2L & \text{if } x_c < x \leq x_1, \\ x + (K-1)L & \text{otherwise.} \end{cases} \tag{8.6}$$

A gradual change in spatial frequency can create an impression of flow or indicate a direction within a linear or radial grating texture as illustrated in Figure 8.9a-d. A peak in special frequency can similarly be used to mark a location along a linear, radial or axial grating texture as illustrated in Figure 8.9e-h. In both cases, a strong or subtle contrast can be obtained by varying the scaling factor and the distance over which the transition occurs.

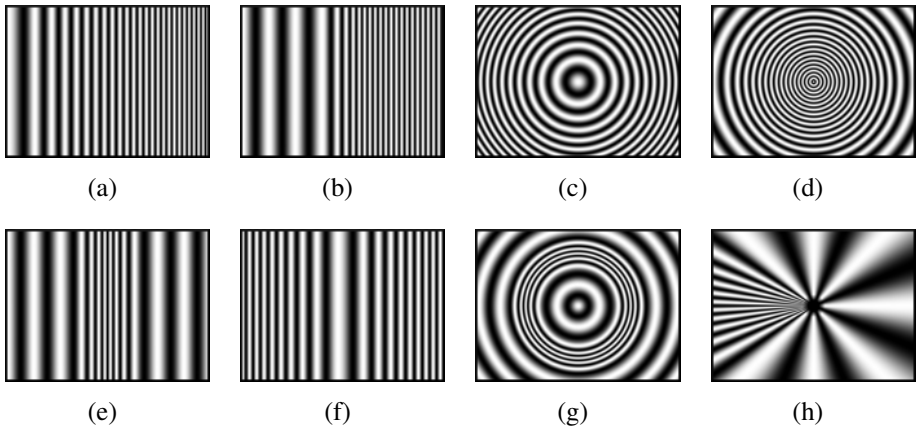

Fig. 8.9 Examples of grating distortions: (a-d) gradual change and (e-h) peak in spatial frequency for different types of grating textures.

Texture Modifiers

A texture's perceived intensity or amplitude can be modulated by scaling its deflection function and hence reducing its range of deflection (Figure 8.10a). A texture's deflection pattern can similarly be inverted, an operation sometimes useful for compositing (Figure 8.10b). A texture can finally be made to vibrate by multiplying its deflection pattern $\delta(\boldsymbol{p})$ with vibration $\delta^1_{vib}(i, j, t)$, resulting in vibrating patterns where the texture is active (Figure 8.10c). The inverse effect can also be obtained by inverting the texture pattern before and after applying the vibration (Figure 8.10d).

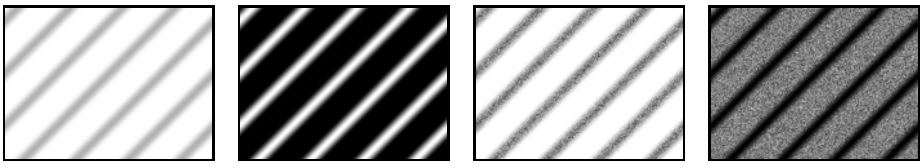

Fig. 8.10 Texture modifiers applied to a grating texture: (a) 30% amplitude modulation, (b) inversion, and vibration of (c) active and (d) inactive features.

8.4.2 Images

Images are tactile patterns that rely on a bitmap to produce an intensity map over a region of the virtual canvas. They are most useful as modulation masks applied against textures or other patterns as illustrated in Figure 8.11b, allowing virtual tactile graphics to be specified in part using conventional graphics editing software. Preliminary results suggest that images may also provide limited access to high-contrast photographs and illustrations such as the bicycle displayed with vibration in Figure 8.11c. Their use as deflection maps, illustrated in Figure 8.11a, has not been explored extensively but may prove useful to create deflection patterns with external tools or to precompute expensive tactile renderings.

(a) (b) (c)

Fig. 8.11 Simple image pattern used as a (a) deflection map or (b) texture mask, and (c) complex image pattern used as a vibration mask.

The physical extent of an image is controlled by altering its scale and position as illustrated in Figure 8.12. An image is defined through either the saturation (grayscale value) or opacity (alpha value) of a source bitmap. The bitmap can be obtained from image files in a variety of formats (e.g. GIF, BMP, JPG) but the Portable Network Graphics (PNG) format is recommended for its support of both lossless compression and transparency. The bitmap can similarly be obtained by seamlessly converting vector graphics written in the Scalable Vector Graphics (SVG) format to a raster image. A bitmap can finally be created programmatically through direct editing of an image buffer or through the intermediary of a 2D graphics library such as Cairo (`http://cairographics.org`). In all cases, a bitmap resolution of approximately 5 to 10 pixels per mm is recommended to allow smooth deflection transitions and avoid aliasing effects. Abrupt transitions should also be avoided by blurring sharp edges either at the source or through online filters.

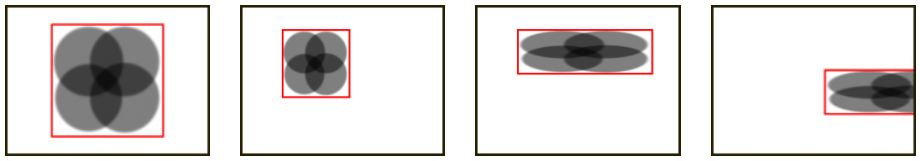

(a) (b) (c) (d)

Fig. 8.12 Variations in the position and scale of an image pattern.

8.4.3 Stroked Shapes

Stroked shapes are geometric patterns that reproduce the sensation of brushing against raised shape outlines. The rendering of a shape's stroke is first introduced before describing its use for the rendering of lines, circles and polygons. The reinforcement of a polygon's vertices with vibrating markers as well as the use of fill textures within closed shapes are finally discussed.

Stroke

The stroke is similar in concept to a brush stroke or raised line and defines the tactile appearance of a shape's outline. A stroke's rendering is composed of a transversal deflection profile that depends on the distance r across the shape's path as well as a longitudinal texture varying with the distance l along its length. Vibration can optionally be introduced in a stroke's rendering to increase its salience.

Transversal Profile. The transversal profile triggers the sensation of brushing across a raised line when moving across the stroke by causing a swing in actuator deflection similar to that used for the rendering of a grating texture's ridges. A stroke with amplitude k, width w and edge size ε is described by:

$$\rho(r) = \begin{cases} k & \text{if } |r| < w/2 - \varepsilon; \\ \frac{k}{2} + \frac{k}{2}\cos\left(\frac{r-w/2+\varepsilon}{\varepsilon}\pi\right) & \text{if } w/2 - \varepsilon \leq |r| < w/2; \\ 0 & \text{otherwise.} \end{cases} \tag{8.7}$$

The edge size determines the distance over which the sinusoidal activation and deactivation of actuators takes place and hence the sharpness of the stroke's edges. A long transition ($\varepsilon = w/2$) creates a smooth profile, as shown in Figure 8.13a, that is pleas-

ant for thin strokes but weakens with increases in thickness. Sharp stroke edges can be created by shortening the transition (e.g. $\varepsilon = 1\,\mathrm{mm}$) as illustrated in Figure 8.13b.

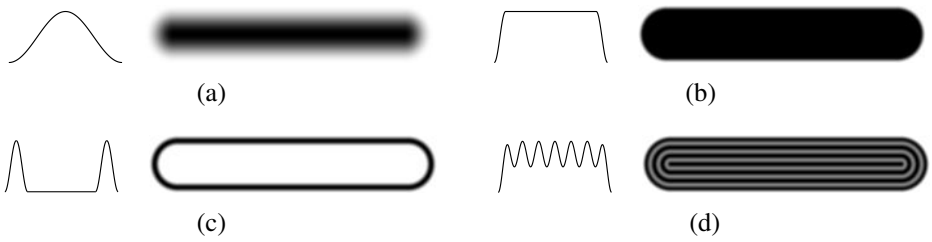

Fig. 8.13 Transversal stroke profile with (a) smooth, (b) sharp, or (c) outlined contour, and (d) superposed texture.

Sharp edges, however, can create the sensation of touching two distinct lines when separated by a certain distance. This effect can optionally be embraced and reinforced by rendering the stroke as an outline with maximal actuator swing at its edges as illustrated in Figure 8.13c and described by:

$$\rho_o(r) = \rho(r) \cdot (1 - \delta_o(r)) \tag{8.8}$$

where

$$\delta_o(r) = \begin{cases} 1 & \text{if } |r| < w/2 - 2\varepsilon; \\ \frac{1}{2} + \frac{1}{2}\sin\left(\frac{r - w/2 + 2\varepsilon}{\varepsilon}\pi\right) & \text{if } w/2 - 2\varepsilon \leq |r| < w/2 - \varepsilon; \\ 0 & \text{otherwise.} \end{cases} \tag{8.9}$$

A transversal texture in the form of a sinusoidal oscillation with n cycles and amplitude k_t can finally be superposed over a scaled-down deflection profile as illustrated in Figure 8.13d and described by:

$$\rho_t(r) = (1 - k_t) \cdot \rho(r) + k_t \cdot \left(\frac{k}{2} + \frac{k}{2}\cos(2\pi r n / w)\right) \tag{8.10}$$

Longitudinal Texture. The transversal profile conveys the sensation of passing over a raised line but provides only minimal feedback when following the length of a stroke. A longitudinal texture is therefore introduced to provide additional tactile feedback

while tracing a shape's contour. The resulting stroke deflection, described below, is produced by modulating the stroke profile $\rho(r)$ with an inverted grating waveform $g(l)$, first introduced in Section 8.4.1, varying along the length of the shape's path.

$$\delta(r, l) = \rho(r) \cdot (1 - g(l)) \tag{8.11}$$

The texture inversion ensures that the amplitude of the stroke is unaffected by that of the grating as illustrated in Figure 8.14. Although otherwise effective, a dense texture can interfere with the perception of the profile by introducing breaks in the edges (Figure 8.14a). The frequency of edge breaks can be reduced through the use of sparse gratings (Figure 8.14b). As an alternative, an outlined stroke with uniform edges (Figure 8.14c-d) can be produced by introducing the grating $g(l)$ into Equation 8.8 as follows:

$$\delta(r, l) = \rho(r) \cdot (1 - \delta_o(r) g(l)) \tag{8.12}$$

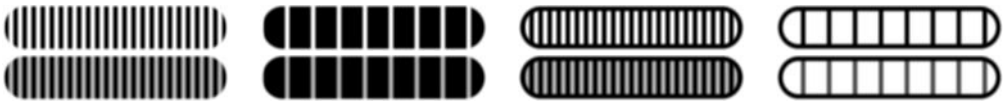

Fig. 8.14 Strokes with textures at 100% and 70% intensity: (a) dense and (b) sparse gratings, (c) dense and (d) sparse inverted gratings with outline.

The salience of the grating texture is dependent on its physical extent and hence affected by the presence of an outline and by the width and sharpness of the stroke profile.

Vibration. Vibration reinforces the intensity of a stroke and allows it to be felt even in the absence of exploratory movement. Vibration can be applied either to the active pattern of a stroke by vibrating its deflection pattern, or to the inactive pattern by vibrating only its grating texture. Both approaches are illustrated in Figure 8.15 and described by:

$$\delta_{hi}(r,l) = \delta(r,l) \cdot \delta^1_{vib}(i,j,t) \tag{8.13}$$

$$\delta_{lo}(r,l) = \rho(r) \cdot (1 - \delta^1_{vib}(i,j,t)g(l)) \tag{8.14}$$

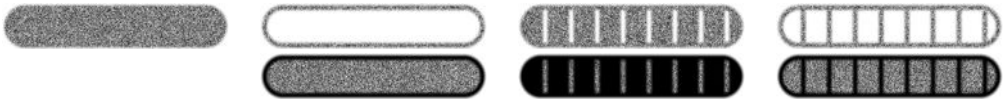

(a) (b) (c) (d)

Fig. 8.15 Vibration of active (top) and inactive (bottom) regions of strokes: (a) plain, (b) outlined and (c-d) textured strokes.

Shapes

Shapes are rendered by applying the stroke deflection profile according to the definition of a coordinate system that specifies both a transversal distance r from the shape contour and a longitudinal distance l along its length. The concept is described below for lines, circles and polygons but could easily be generalized and adapted to other common vector graphics primitives such as curves, arcs and open paths.

Line. The transversal distance r to a line with end points $\boldsymbol{p_0}$ and $\boldsymbol{p_1}$ is defined as the minimal distance to the segment and computed by projection of the actuator position $\boldsymbol{p}$ [32]. The closest point on the line segment is given by:

$$\boldsymbol{p_{min}} = \begin{cases} \boldsymbol{p_0} & \text{if } u < 0; \\ \boldsymbol{p_1} & \text{if } u > 1; \\ \boldsymbol{p_0} + u(\boldsymbol{p_1} - \boldsymbol{p_0}) & \text{otherwise.} \end{cases} \tag{8.15}$$

where $u = (\boldsymbol{p} - \boldsymbol{p_0}) \cdot (\boldsymbol{p_1} - \boldsymbol{p_0})$ is the relative distance at which the projection intersects along the line segment. The transversal distance is given by the distance to the closest point:

$$r = \| \boldsymbol{p} - \boldsymbol{p_{min}} \| \tag{8.16}$$

The longitudinal distance l, on the other hand, corresponds to the distance between $\boldsymbol{p_0}$ and the projection of $\boldsymbol{p}$ against the infinite line corresponding to the segment:

$$l = u \parallel \boldsymbol{p_1} - \boldsymbol{p_0} \parallel \tag{8.17}$$

The line's coordinate system is illustrated in Figure 8.16. The distance l is negative before $\boldsymbol{p_0}$ is reached and extends beyond the length of the line segment, resulting in rounded line caps through which textures extend gracefully.

(a) (b)

Fig. 8.16 (a) Definition of a stroked line's coordinate system and (b) rendering of transversal (top) and longitudinal textures (bottom).

Circle. The transversal and longitudinal distances r and l to a circle with radius R and center $\boldsymbol{p_c}$ are given by the minimal distance to the contour and arc length along its contour respectively:

$$r = | \parallel \boldsymbol{p} - \boldsymbol{p_c} \parallel - R| \tag{8.18}$$

$$l = R \cdot \angle \boldsymbol{p} - \boldsymbol{p_c} \tag{8.19}$$

The circle's coordinate system is illustrated in Figure 8.17. Continuity is ensured by fitting a whole number of texture cycles within the circle's circumference.

Polygon. The transversal distance r to a polygon is defined as the minimal distance to the polygon's contour (Figure 8.18a) and corresponds to the minimum transversal distance to its line segments. The definition of longitudinal distance l is more ambiguous due to complications at the vertices. The simplest approach consists of extending the longitudinal path to the midline of the joints as illustrated in Figure 8.18b. This definition, however, causes discontinuities in the rendering at the junction of the line segments which can be eliminated by rounding the longitudinal path as illustrated in

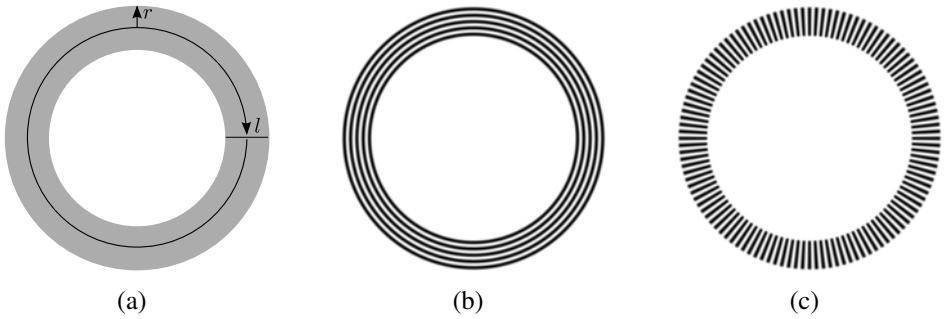

Fig. 8.17 (a) Definition of a stroked circle's coordinate system and rendering of (b) transversal and (c) longitudinal textures.

Figure 8.18c. Upon reaching the joint, the path follows an arc around the intersection point of the adjacent strokes' edges with the distance l increasing proportionally to the angular distance traversed. The wavelength of a longitudinal texture is therefore maintained in the middle of the stroke and distorted elsewhere while within joints. A further complication is encountered close to the arc's pivot point where the spatial frequency of textures increases without bounds. This singularity can be moved out of the stroke by defining the longitudinal path as if for a wider stroke, resulting in the early onset of the rounding near joints as illustrated in Figure 8.18d. Texture continuity is enforced at the first vertex by selecting grating parameters such that a whole number of cycles fits within the length of the selected longitudinal path.

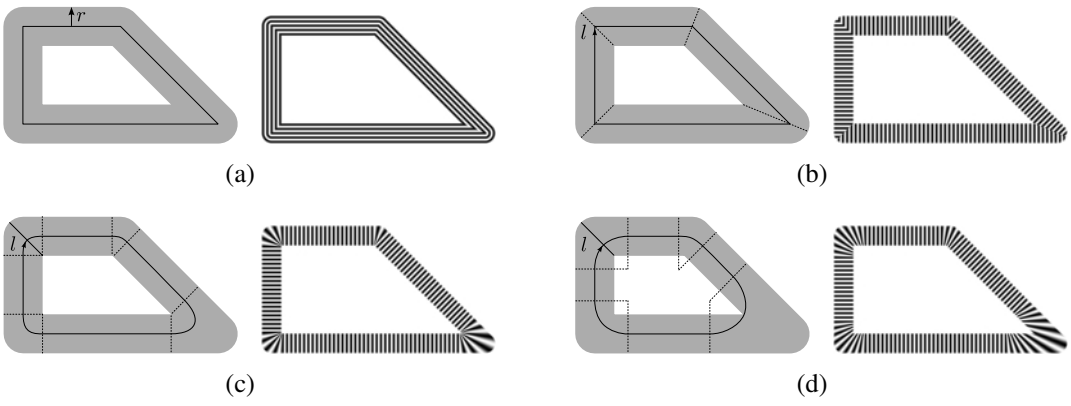

Fig. 8.18 Definition the coordinate system and corresponding textures for stroked polygons: (a) transversal distance and longitudinal distance with (b) straight path, (c) rounded path, or (d) rounded path with offset.

Vertex Markers

The vertices can be very important for the correct interpretation of a polygon's geometry and are sometimes reinforced in conventional tactile graphics [34]. Tactile markers can therefore be superposed over a polygon's vertices to improve their salience, facilitate their localization and hide discontinuities in their rendering. Vertex markers have a conic shape that extends from the point of intersection of the joint's edges and are rendered either as plain or vibrating patterns. Their angular coverage can either be fixed or set according to the properties of the joint as illustrated in Figure 8.19. In the latter case, the bounds of the marker can be orthogonal to the line segments, continuations of the stroke's edges, or delimited by the vertex's round arc.

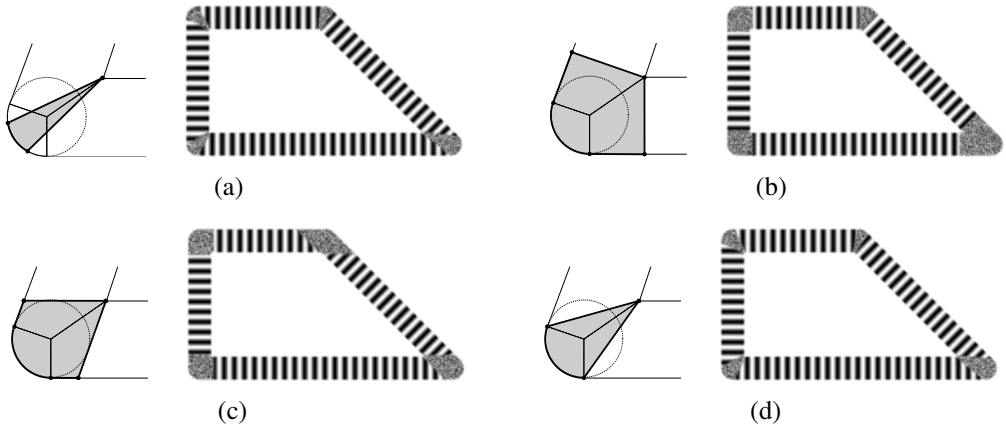

Fig. 8.19 Angular coverage of vibrating vertex markers: (a) fixed angle, (b) orthogonal to edges, (c) continuation of edges, and (d) extension to arc.

A marker is applied whenever the actuator position $\boldsymbol{p}$ is within the closest vertex's marker boundaries as illustrated in Figure 8.20a. More precisely, a marker is rendered if p falls within both the stroke ($r < w/2$) and the two half-planes defined by point $\boldsymbol{p}_a$ and normals $\boldsymbol{n}_{ab}$ and $\boldsymbol{n}_{ac}$ ($\boldsymbol{n}_{ab} \cdot \boldsymbol{v}_{ap} > 0$, $\boldsymbol{n}_{ac} \cdot \boldsymbol{v}_{ap} > 0$). A further check is performed to ensure that p falls within one of the vertex's connected edges, and hence avoid spilling to nearby line segments. The bounds of the markers are precomputed for efficiency and selected such that they extend a certain distance past the intersection point of the stroke's edges. This distance is used to linearly blend the marker pattern with the underlying stroke before application of the stroke's profile as illustrated in Figure 8.20b.

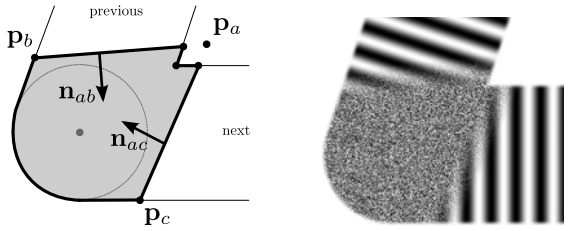

(a) (b)

Fig. 8.20 (a) Boundaries of a vertex marker and (b) blending with the stroke.

Fill Texture

Closed shapes such as circles and polygons can be filled with an arbitrary texture that begins at the inner edge of the stroke and fades in linearly over a small distance to avoid discontinuities (Figure 8.21a). A gap can optionally be inserted between the stroke and texture to increase contrast, as often done with conventional tactile graphics [115, 59, 34], or the stroke eliminated to leave only the texture (Figure 8.21b). The fill texture can alternatively be blended with the stroke pattern (Figure 8.21c), resulting in the elimination of gaps at the cost of a weakening of the inner stroke edge. This effect is obtained using the stroke profile $\rho(r)$:

$$\delta(r, l, \boldsymbol{p}) = \delta_{stroke}(r, l) + \delta_{tx}(\boldsymbol{p}) \cdot (1 - \rho(r)) \tag{8.20}$$

(a) (b) (c)

Fig. 8.21 Rendering of fill textures within stroked shapes (a) with gap and linear fade-in, (b) without stroke, and (c) with blending of stroke and texture.

8.4.4 Dots and Dotted Shapes

Dots are tactile patterns that simulate the sensation of brushing against small dimples similar to Braille dots. They are characterized by their position and radius, and rendered by radially applying a deflection profile nearly identical to that of a stroke as illustrated in Figure 8.22. A dot's edges can hence be smooth or sharp, and a radial texture superposed on its profile for increased salience. A dot can furthermore be vibrated to create a more intense stimulus and its amplitude reduced by scaling its deflection range.

Fig. 8.22 Dot rendering with (a) smooth or (b) sharp edges, and (c) texture.

While they can be used in isolation, dots are generally most useful in groups with shared properties. Sets of dots can notably be used to create dotted shapes analogous to stroked shapes as illustrated in Figure 8.23. The dots are disposed such that one is always present at the end points of a line and vertices of a polygon. The remaining dots are disposed at regular interval along the length of path segments such that a minimal separation between dots is respected both within the segments and across adjacent segments. Dotted shapes can also be filled with texture and polygon vertices marked with vibrating dots.

Fig. 8.23 Dotted (a) line, (b) circle, and (c) polygon.

8.4.5 Composite Patterns

Compositing allows complex tactile patterns to be formed from the combination of simpler patterns. Five compositing operators are first introduced before discussing their use with textures and more general tactile patterns.

Compositing Operators

The five compositing operators are illustrated in Figure 8.24. The intersection of multiple patterns can be obtained by multiplying their deflection functions with the masking operator (Figure 8.24a). Patterns can similarly be superposed using the addition operator either with saturation (Figure 8.24b) or with normalizing weights (Figure 8.24c). The local maximum of patterns can alternatively be rendered with the maximum operator (Figure 8.24d).

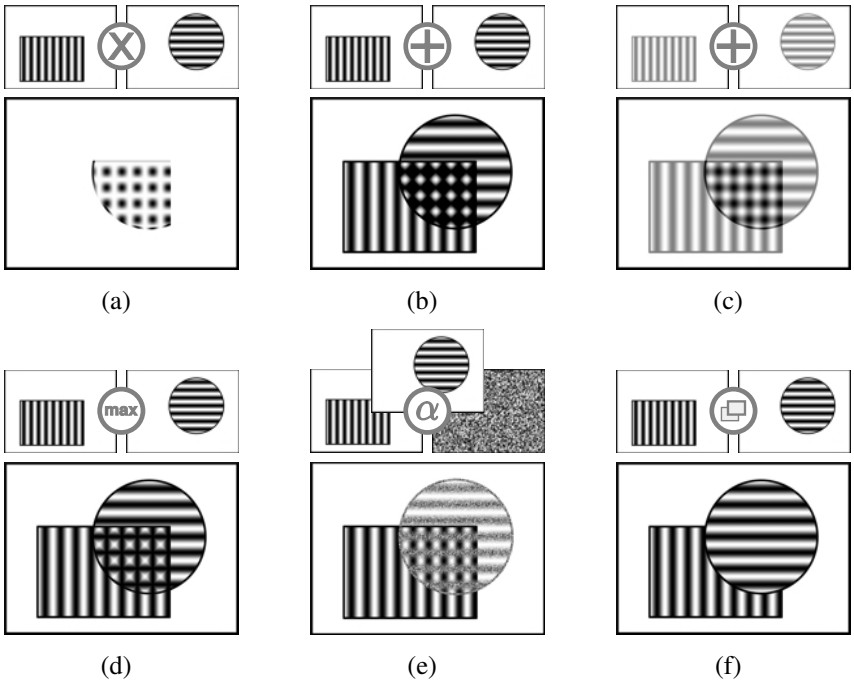

Fig. 8.24 Compositing operations: (a) masking, addition (b) with and (c) without saturation, (d) maximum, (e) alpha blending and (f) overwriting.

The alpha blending operator allows the rendering to smoothly alternate between two patterns using a weighted sum that depends on a third pattern, enabling, for exam-

ple, vibration to be blended into non-vibrating patterns as illustrated in Figure 8.24e. More precisely, deflection patterns $\delta_1(\boldsymbol{p})$ and $\delta_2(\boldsymbol{p})$ can be blended through an alpha mask $\alpha(\boldsymbol{p})$ such that:

$$\delta(\boldsymbol{p}) = (1 - \alpha(\boldsymbol{p})) \cdot \delta_1(\boldsymbol{p}) + \alpha(\boldsymbol{p}) \cdot \delta_2(\boldsymbol{p}) \tag{8.21}$$

The overwriting operator finally allows a pattern to cleanly overwrite underlying patterns (Figure 8.24f). More precisely, overwriting is performed by modulating the underlying pattern according to the top pattern's inherent opacity mask before adding its deflection pattern. Given patterns $\delta_1(\boldsymbol{p})$ and $\delta_2(\boldsymbol{p})$, and opacity mask $\gamma_2(\boldsymbol{p})$, the result is given by:

$$\delta(\boldsymbol{p}) = (1 - \gamma_2(\boldsymbol{p})) \cdot \delta_1(\boldsymbol{p}) + \delta_2(\boldsymbol{p}) \tag{8.22}$$

A pattern's opacity mask is a simplified rendering with smooth transitions and equal or superior deflection at all points. The opacity mask of a stroked shape consists of the stroke profile at maximal amplitude, without texture or vibration, and is completely filled in the presence of a fill texture (Figure 8.25a-c). The opacity mask of dotted shapes is identical (Figure 8.25d) while that of individual dots covers only their profile (Figure 8.25e). The opacity mask of an image is computed by saturating the bitmap and adding a linear gradient around its edges (Figure 8.25f). Textures are considered to have a uniform opacity mask and are therefore not used to overwrite.

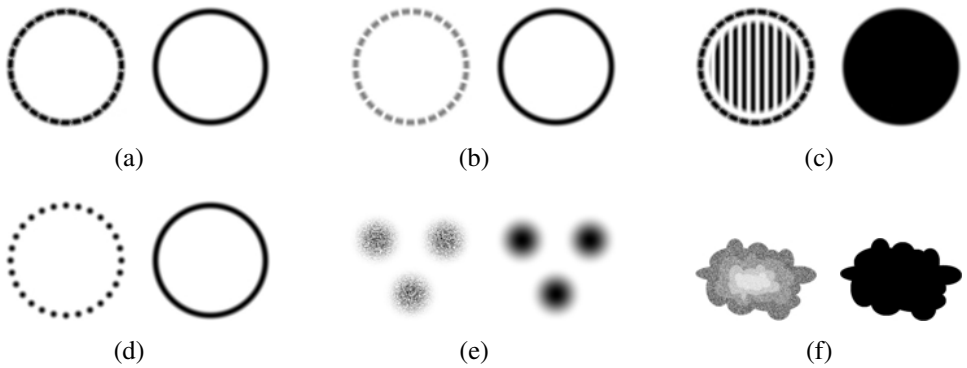

Fig. 8.25 Opacity mask of tactile patterns: stroked shape at (a) full and (b) half intensity, (c) filled stroked shape, (d) dotted shape, (e) dots, and (f) image.

Precautions should be taken when dealing with vibrating patterns within compositions. The masking operator results in the multiplication of the patterns' deflections, and hence of their vibrations. Masking of vibrating patterns can therefore create an interesting beat if the frequencies are far apart but otherwise results in sharpened oscillations that may be unpleasant and damaging to the actuators. The addition operator locally sums the patterns' vibrations and hence allows the use of different vibrations at different locations. Saturation should be avoided as it may cause partial suppression or accentuation of vibrations. The maximum operator should similarly be avoided as it causes incoherent interaction between vibrating patterns. The blending operation can be used without restriction provided that the alpha mask does not vibrate. No restrictions apply for the overwriting operator.

Composite Textures

Compositing can be used to create complex textures and is particularly useful with parallel or orthogonal linear grating textures as illustrated in Figure 8.26. A fine linear grating can be uniformly superposed over a coarse grating using the addition or blending operators, or selectively applied to the grooves or peaks of the latter using the masking or maximum operators (Figure 8.26a-f). Grids and dot patterns can similarly be created by using the masking and maximum operators with orthogonal gratings (Figure 8.26g-h).

Compositing operators can also be used with other textures such as radial gratings and arbitrarily-oriented linear gratings as illustrated in Figure 8.27. This can be used to create skewed grids patterns (Figure 8.27a), blend in vibration into a texture (Figure 8.27b), or create complex blended patterns (Figures 8.27c). The addition, masking and maximum operators can be used with an arbitrary number of sub-textures (Figure 8.27d). Compositing operations can furthermore be chained by using composite textures as subtextures.

Composite Patterns

Compositing operators can be used not only with textures, but also with generic tactile patterns such as stroked patterns and images. The masking operator is generally most useful to modulate the intensity of a texture according to an image (Figure 8.28a) or a

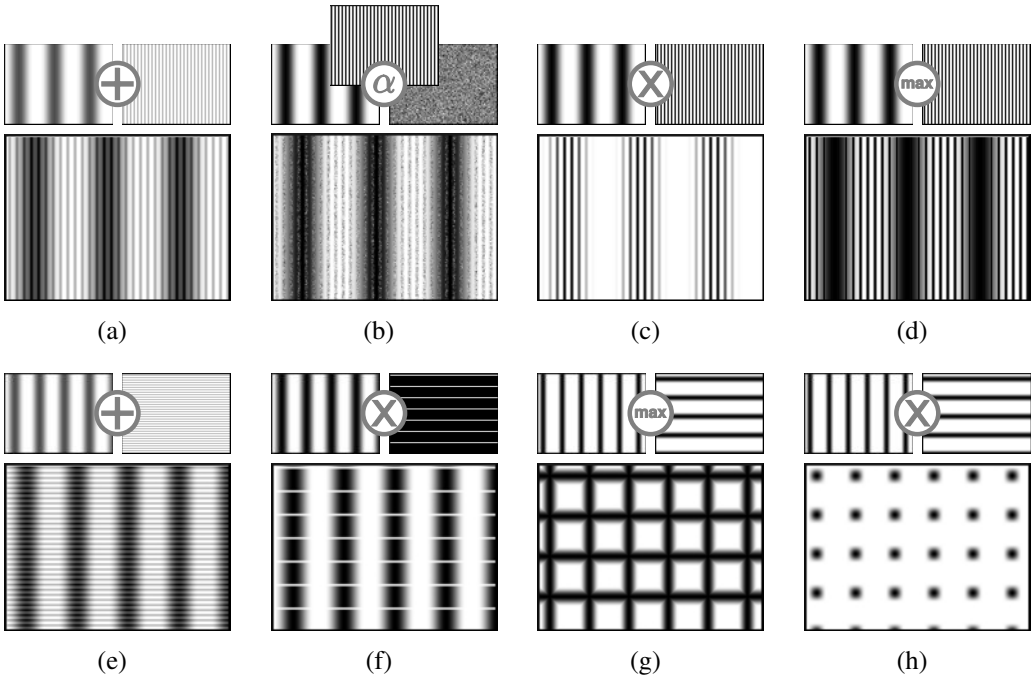

Fig. 8.26 Examples of textures composed of parallel or orthogonal gratings.

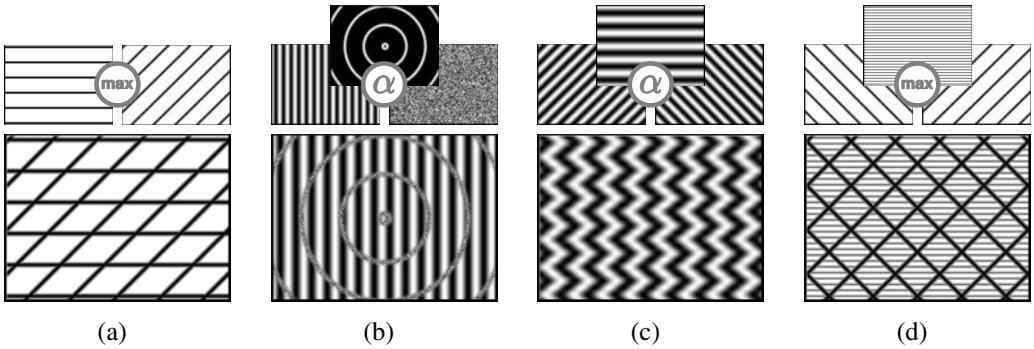

Fig. 8.27 Examples of textures composed of arbitrary subtextures.

more complex pattern (Figure 8.28b). Masking can also be used to clip a tactile pattern according to an opaque mask (Figure 8.28c). Masking of more complex patterns is also possible but does not always result in tactilely coherent compositions (Figure 8.28d).

The addition and maximum operators perform a union of the underlying patterns. Weighted addition reduces the intensity of the individual patterns but highlights their

overlap (Figure 8.28e-f). Unweighted addition, on the other hand, maintains the intensity of the patterns but causes saturation in overlapping regions (Figure 8.28g). A similar effect, without saturation artefacts, can be obtained with the maximum operator (Figure 8.28h). In all cases, the effect of interactions in overlapping regions depends on the simplicity and coherence of the patterns and is difficult to predict.

The blending and overwrite operators are used to mix different patterns together. The blending operator can be used to blend between a vibrating and non-vibrating version of a pattern (Figure 8.28i). It can also be used to blend in vibration according to a tactile pattern such as a grid texture (Figure 8.28j), and hence to create tactile guides [149, 59]. Overwrite operations similarly draw a pattern over all underlying patterns according to its opacity mask (Figure 8.28k) and can be chained to create layers (Figure 8.28l).

8.5 Framework Implementation

The tactile graphics framework described in the previous section was implemented as part of a software library and used within evaluation and demonstration software applications. The library is first described before discussing the evaluation of the computational cost of rendering algorithms and their optimization.

8.5.1 Software Implementation

The tactile rendering algorithms described in the previous section were implemented as part of a C++ library offering three interfaces for the creation, manipulation and display of virtual tactile graphics. The library provides realtime support for tactile rendering through the Xenomai extension (`http://www.xenomai.org`) to the Linux operating system.

At the lowest level, the library offers a flexible object-oriented Application Programming Interface (API) which can be used to quickly develop multi-threaded tactile graphics software for specific applications. The library's hierarchical structure closely follows the tactile graphics framework and includes classes for tactile patterns such as lines, circles and textures, as well as other tactile elements such as gratings and strokes. The library also includes a tactile rendering engine which periodically updates the state of the system, obtains a tactile frame from the active rendering object, and refreshes

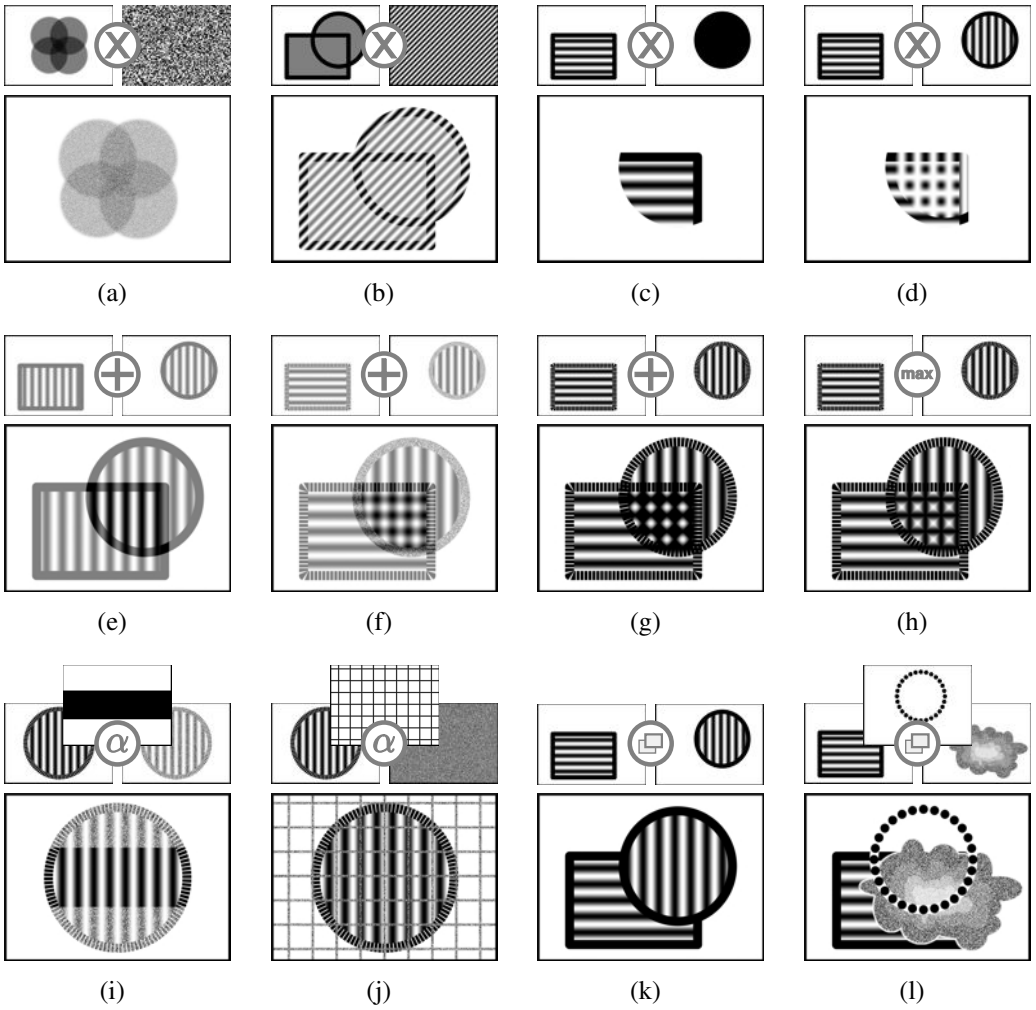

Fig. 8.28 Examples of composite patterns using the (a-d) masking, (e-g) addition, (h) maximum, (i-j) alpha blending, and (k-l) overwriting operators.

the tactile display's actuator deflections.

The library also defines graphical user interface widgets and visualization tools for most its classes using the gtkmm toolkit (`http://www.gtkmm.org`). Applications can therefore take advantage of this functionality to create fully-featured graphical user interfaces to interact with, modify and visualize virtual tactile graphics. Figure 8.29 shows the graphical user interface of a simple yet functional authoring tool built with the library that allows tactile graphics to be edited while displayed on the Tactograph. Similar software was developed for experimentation and demonstration purposes.

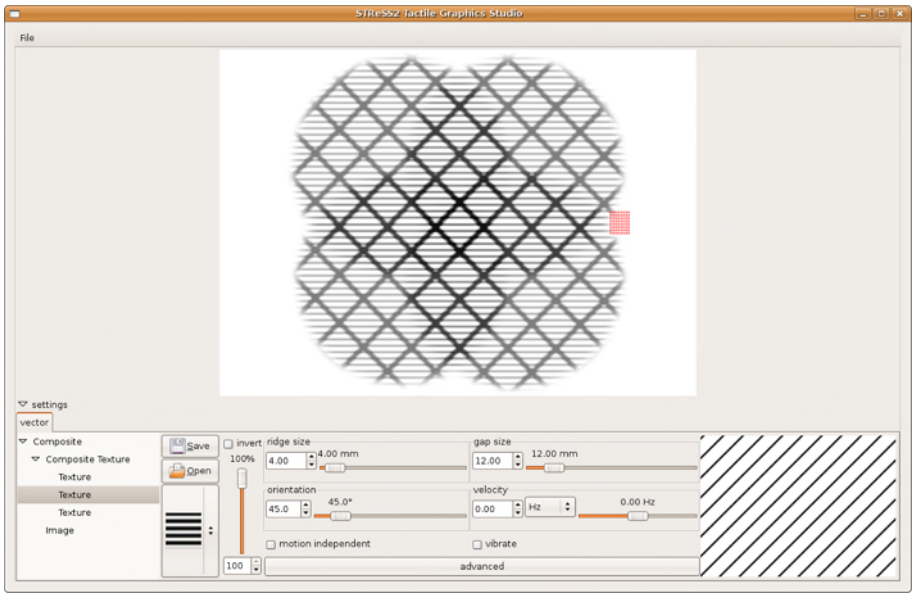

Fig. 8.29 Authoring application allowing online editing of tactile graphics.

Tactile graphics canvases, tactile patterns, and textures can finally be specified through text files written in a custom format based on the Extensible Markup Language (XML). Partial or complete tactile graphics can therefore be stored in external files and edited with text editors or specialized third-party software. A standalone application was, for example, written to semi-automatically adapt schoolbook illustrations and generate tactile graphics descriptions in the library's custom language [211]. A bank of predefined textures is similarly supplied with the library as a set of external files.

8.5.2 Computational Cost Measurement

The optimization of tactile rendering algorithms requires the ability to measure and compare the computational cost of different approaches. A profiling tool therefore allows measurement of the time taken to render the deflection of the entire array of actuators as a function of the tactile display's location on the virtual canvas. The tool relies on a simulation of the motion of the display over predefined exploration paths designed to provide maximum coverage of the virtual canvas or extensive coverage of a specific location as illustrated in Figure 8.30. Maximum coverage is obtained by

tracing the contour of the virtual canvas in an inward spiral of arbitrary density while spot coverage creates an oscillating path around a specific point of the canvas.

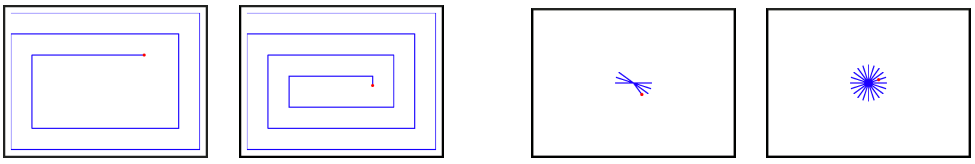

(a) (b)

Fig. 8.30 Simulated exploration paths for (a) wide and (b) local coverage.

The simulation data estimates the time required to render a complete frame at different positions along the exploration path and is visualized either as a histogram or map of the computational cost as illustrated in Figure 8.31. The example shown illustrates the higher cost of rendering a textured polygon compared to a plain circle, as well as the added cost of pattern overlap and vertex markers.

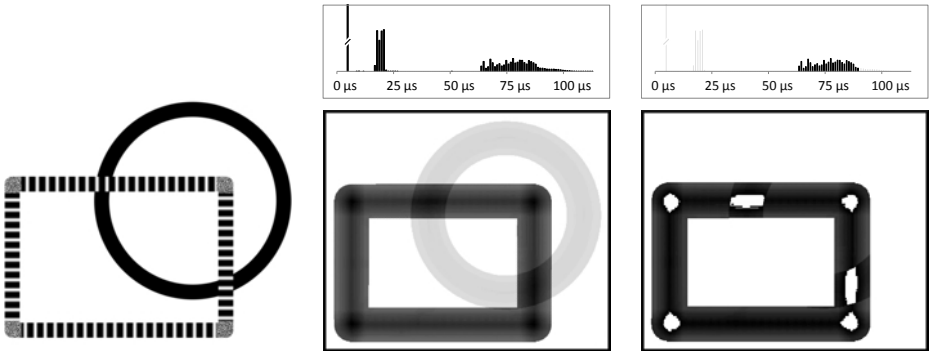

(a) (b) (c)

Fig. 8.31 Computational cost of rendering (a) a composite pattern illustrated with (b) a histogram and a spatial distribution plot. The histogram shows the frequency distribution of computational costs for the set of measurements. The spatial distribution illustrates the average computational cost at different locations over the virtual canvas. The spatial distribution of computational costs ranging from 62 to 90 µs is illustrated in (c). The histogram peak corresponding to blank areas has been truncated for clarity.

8.5.3 Rendering Optimization

Tactile rendering entails the refreshment of actuator deflections for the tactile display's entire array at a rate of approximately 1 kHz, leaving as little as 16 µs of computation time per actuator or even less when communications with the physical device and user interaction are considered. Computational efficiency of rendering algorithms is therefore an important concern. Rendering algorithms can, in many cases, be optimized by avoiding unnecessary computations such as the rendering of a tactile pattern that is to be fully overwritten by another. Significant gains can similarly be made by pruning tactile patterns beyond the range of the tactile display, defined as a disc covering all actuators. A tactile pattern can therefore be eliminated if known not to affect any actuator within that range, hence requiring a single check rather than one per actuator. A line, for example, can be pruned if the shortest distance to the center of the display is greater than the sum of the stroke radius and display footprint radius. As illustrated in Figure 8.32, pruning can reduce the cost of rendering 15 short lines by a factor of as much as 6 close to a line and 40 elsewhere.

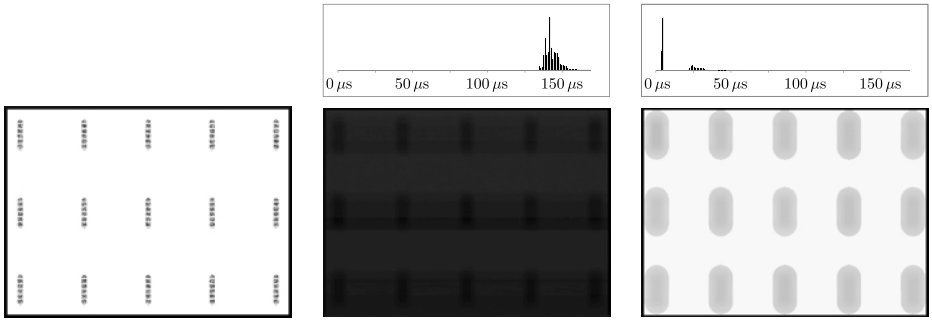

Fig. 8.32 Computational cost of rendering (a) a set of 15 lines (b) before and (c) after pruning of non-contacting patterns. The computational cost of rendering is nearly uniform over the virtual canvas prior to pruning, as illustrated in (b).

8.6 Validation and Discussion

The virtual tactile graphics framework was informally evaluated with the assistance of four visually-impaired volunteers, two of whom were tactile graphics experts. The

volunteers' comments were solicited on a wide range of tactile graphics features and tactile rendering parameters adjusted to their individual preferences. The following discussion presents a synthesis of the insight gained through these evaluation sessions as well as prior experimentations and numerous demonstrations including three at international conferences [158, 156, 293].

Vibrations result in less pleasant but much more intense sensations than smooth deflections and are therefore ideal to introduce contrast and highlight elements of a tactile drawing. While similar to a dense texture when brushed against, vibration also has the advantage of being perceptible even in the absence of motion. Much like sandpaper and other intense tactile patterns [102], however, vibration may cause tactile adaptation and a loss of sensation with prolonged exposure and should therefore be used sparingly. Vibration also tends to overpower nearby non-vibrating patterns, perhaps due to after-effects, for example, filling narrow gaps in a vibrating pattern. Although vibration intensity peaks at the 50 Hz upper limit, frequencies as low as 30 Hz may offer sufficient contrast and reduce tactile adaptation. Discrimination of vibration frequencies, however, appears to be relatively poor, requiring a difference in the order of 20 Hz for a clear distinction.

Linear grating textures produce a strong illusion of brushing against corrugated surfaces for spatial wavelengths approximately ranging from 2 to 15 mm. The ridges of coarser gratings are significantly weakened while those of finer ones are lost in a noisy and dense texture. Improved performance may be expected at orientation identification and wavelength scaling, two tasks investigated earlier in Chapter 6, with the addition of gaps between grating ridges and the introduction of display orientation as a rendering input. Gaps greatly improve the salience of the texture by allowing distinct lines with a clear separation to be felt while display orientation allows the tactile array to be aligned with gratings for optimal rendering. Axial and radial gratings also appear to be identifiable with minimal training but are more difficult to interpret. As expected, grating distortions are perceptible but most salient with abrupt wavelength changes. Tiled textures can finally create distinctive motifs but the details of the duplicated patterns are difficult to feel.

Images are most useful to create textured shapes and patterns using conventional graphics editing software (Chapters 5 and 6, [211]). Vibrating images also appear capable of conveying an overview of high-contrast pictures and diagrams, in a manner

similar to the Optacon [163], and may provide minimal access to otherwise inaccessible graphical content.

Although individual preferences vary, alteration of the sharpness, thickness and texture of a stroke results in distinctive tactile patterns that can be used to produce contrasting line types. Smooth strokes are noisy when thin and weak when thick, but otherwise pleasant for a range of approximately 2 to 10 mm. The edges of sharp or outlined strokes, on the other hand, remain strong but are felt as disjoint lines when the thickness exceeds approximately 5 mm. Transversal and longitudinal textures both add substance to the stroke with the latter providing better tracing feedback. A dense grating with a spatial wavelength of 2 mm is generally preferred and the breaks introduced in the edges do not appear to warrant correction with a sparse grating or a stroke outline. The geometry of the resulting stroked shapes can be traced and understood with relative ease. The rounding of the longitudinal path at polygon vertices appears to slightly weaken sharp corners while the discontinuities otherwise introduced have minimal effect. Vibrating markers are, on the other hand, effective at highlighting vertices but their exact shape is not perceptible and should therefore be selected to maximize area. Fill textures sometimes interfere with the contour of the shape, particularly in the absence of a gap or clear contrast between the stroke and texture. Dotted patterns, although found to convey the contour of a shape in Chapter 6, are generally less appreciated than stroked patterns due to their discontinuous nature but may nevertheless be useful in some contexts.

Composition can be a powerful tool for the creation of distinctive textures and complex patterns but must be applied with care to maintain coherence and avoid confusion. The superposition of coarse and fine gratings creates a range of interesting and easily-identifiable patterns even though the effect is occasionally subtle or distracting. More complex composite textures can create a distinctive effect but the details of the resulting patterns are often difficult to discern. Composition is more generally useful to combine non-overlapping patterns by addition, to apply texture by masking, and to introduce occlusion in a drawing by overwriting. Other uses of pattern composition may emerge with further experimentation and more sophisticated graphics become usable with training and better contextualization.

It is finally interesting to note that directional effects are limited despite significant differences in skin deformation patterns resulting from the actuators' deflection along

a single axis and their bias towards the right. Moving against a horizontal or vertical grating, for example, results in waves of compression and shearing respectively but is generally felt as at least superficially comparable. Similarly, the actuator swing triggered by a horizontal grating can either occur against or with the exploration motion yet is generally felt as nearly identical. Directional effects introduced by these rendering anisotropies are occasionally noticed but seem to be surprisingly weak in most cases and do not appear to significantly affect the functionality of the tactile rendering framework.

8.7 Conclusion

This chapter introduced a framework for the rendering of virtual tactile graphics by lateral skin deformation that offers basic vector graphics drawing capabilities suitable for the composition of complex graphics and the emulation of features such as raised lines, dot patterns and areal textures found in conventional tactile graphics. The framework extends the drawing primitives introduced in Chapters 5 and 6, proposes novel rendering algorithms, and re-frames the whole as a coherent set of tactile patterns that includes textures, images, stroked shapes, dots and dotted shapes, as well as more complex composite patterns and textures. The framework was implemented as a flexible software library allowing the rapid development of experimental tactile graphics applications. Insight into the effectiveness of the rendered patterns and user preferences was obtained by soliciting comments from four visually-impaired volunteers during informal evaluation sessions.

Although preliminary results are encouraging, further studies will be required to formally validate the rendering algorithms, determine optimal or preferred rendering parameters, and evaluate user performance at critical tasks. Despite promising early work on the topic [211], much also remains to be done to demonstrate the feasibility of producing practical tactile graphics such as mathematical diagrams and maps, and to develop a coherent tactile language that forges, for example, associations between water and gratings, or 3D patterns and a particular stroke type. At a lower level, the software implementation of the framework is a functional but experimental prototype and could be further optimized and refined, most notably by improving and formalizing the API and graphics description language. The framework finally covers only a

fraction of the possible rendering algorithms and could no doubt be further developed and expanded.

The development of the Tactograph and accompanying rendering framework are essential steps towards the creation of a practical virtual tactile graphics system. The adoption of the technology by the visually-impaired community, however, depends not only on the availability of usable hardware and software but also on that of adapted content. The establishment of drawing conventions and the development of authoring tools will therefore gain in importance as the technology matures. Basic support for content creation is at this point available through a functional but limited graphics editing application as well as an experimental tool for the semi-automated adaptation of graphical content [211]. Further developments could take advantage of one of virtual tactile graphics' greatest strengths by allowing visually impaired users to independently create and share their own drawings and hence be in charge of the content production process.

Acknowledgements

The rendering framework presented in this chapter was influenced by the work of Jérôme Pasquero and Qi Wang on tactile rendering as well as discussions with Gregory Petit, Aude Dufresne, Nicole Trudeau, Pierre Ferland and many others who experienced the virtual tactile graphics at different stages of development and shared their impressions. The author would like thank the volunteers who participated in the evaluation of the framework.

Chapter 9

Dynamic Tactile Graphics by Lateral Skin Deformation

Preface to Chapter 9

This chapter presents extensions to the virtual tactile graphics framework introduced in Chapter 8 that take advantage of the opportunities afforded by dynamic tactile rendering. Tactile flow is first introduced in the rendering of textures, stroked shapes and dotted shapes through the motion of tactile features. Reactive rendering is then investigated through the alteration of textures in response to changes in exploration behaviour. Interactive graphics are finally briefly explored in the form of alternative views of a canvas' content. The first two concepts were evaluated and validated using the improved Tactograph described in Chapter 7, while the third was evaluated with the Pantograph-based Tactograph in [211].

Contributions of Authors

This chapter was written by Vincent Lévesque and revised by Vincent Hayward. The work presented herein was similarly performed by V. Lévesque under the supervision of V. Hayward. Software support for interactive tactile graphics was implemented by V. Lévesque as part of a collaboration with Gregory Petit, Aude Dufresne and Nicole Trudeau of Université de Montréal. The interactive worldmap shown in Figure 9.12 was designed and evaluated by G. Petit, and the results published in [211]. The evaluation of the other dynamic tactile features was conducted by V. Lévesque.

Dynamic Tactile Graphics by Lateral Skin Deformation

Abstract

This chapter extends the framework presented in the previous chapter with support for dynamic and interactive tactile patterns that take advantage of the novel opportunities afforded by virtual tactile graphics. Tactile flow is first introduced in the rendering of textures, stroked shapes and dotted shapes through the motion of inherent or superposed tactile features. Reactive textures that alter their rendering in response to changes in the exploration behaviour, or more precisely the speed and direction of exploration, are then introduced. Interactive graphics allowing alternate views of a canvas to be displayed at the press of a button are finally discussed. Tactile flow and reactive textures were evaluated through informal experimentation sessions with four visually impaired volunteers while interactive graphics were investigated separately by Petit et al. [211].

9.1 Introduction

The potential of refreshable tactile graphics extends beyond the reproduction of features and conventions developed for commonly-used static media such as microcapsule paper or thermoformed plastic. The dynamic nature of refreshable tactile graphics presents a wealth of largely unexplored opportunities for innovation that could be exploited to compete in flexibility and expressivity with visual displays, and to address issues affecting the usability of conventional tactile graphics such as the need to reduce information density or split content across multiple drawings. Efforts to exploit the novel affordances of refreshable tactile graphics have included interactive and dynamic effects such as zooming, scrolling and directional cues displayed with force-feedback and tactile interfaces.

This chapter introduces innovative tactile rendering approaches that similarly exploit the potential of virtual tactile graphics produced by lateral skin deformation for the display of dynamic and interactive content. Tactile flow is first introduced in the rendering of textures, stroked shapes and dotted shapes through the motion of inherent or superposed tactile features, allowing directional cues to attract attention to elements of a drawing or to intuitively communicate information such as the direction of flow of a water stream. Reactive patterns that alter their rendering in response to the exploration behaviour are then introduced, enabling, for example, details to be reinforced at rest through vibration and directional information to be conveyed through anisotropic textures. Interaction with tactile graphics is then briefly explored in the form of a keypress-activated swap between alternate views of a canvas, allowing complementary content to be spread across uncluttered drawings. The visualization and optimization of dynamic rendering algorithms are finally discussed before concluding with an evaluation of the extended framework through informal experimentation sessions conducted with four visually impaired volunteers.

9.2 Background

The refreshable display of tactile graphics is often considered a direct alternative to conventional physical media such as embossed paper. The resulting refreshable graphics present many advantages since they do not deteriorate with use, can be transferred and stored electronically, and are immediately accessible without a cumbersome print-

ing process [286]. The experience offered by refreshable graphics is however generally inferior to that of conventional media due to technical limitations such as the low actuator density of practical pin arrays. The adoption of refreshable tactile graphics interfaces may therefore require these limitations to be compensated for by fully exploiting the largely untapped opportunities afforded by the dynamic nature of the novel media.

The dynamic properties of refreshable tactile graphics have been explored most extensively with force-feedback interfaces due to their maturity and commercial availability. A close analog to physical tactile graphics is typically produced as a relief pattern on a virtual surface explored with a probe attached to an articulated arm such as the Sensable PHANTOM [224, 307, 240]. The forces generated by the manipulandom can however produce other physical effects such as springs and magnets that have notably been used to attract a probe to raised lines [216, 69], to guide it towards a collaborator or teacher's pointing device [267, 128, 224, 177], or to direct it towards previously annotated locations in a canvas [128, 224, 285]. Short impulses have similarly been used as directional cues at intersections of an electrical circuit and as markers denoting individual components [216].

Interaction with virtual tactile graphics has also been explored. Alternate views of a map have, for example, been used to support different tasks such as obtaining an overview or detailed information [103]. The use of a haptic zoom has been investigated as a means to provide details without introducing clutter [168, 245]. The use of interchangeable virtual tools, such as a magnet or cross, has also been proposed to simplify the performance of certain tasks such as searching in 3D environments [255]. Dynamic models have similarly been used to create haptic games such as Sjöström's *Submarines* in which animations such as water waves convey a tile's state [255]. Perhaps most importantly, virtual graphics can be created and edited by visually impaired users [255, 128, 224, 176]. Rassmus-Gröhn, Magnusson, and Eftring, for example, designed a drawing application that allows objects to be moved, copied, erased and converted to idealized shapes such as straight lines and circles [224]. McGookin and Brewster similarly created an application in which bar charts can be edited by direct manipulation [176]. These applications are extremely valuable since conventional computer-based production methods are inaccessible for lack of haptic feedback, and accessible methods such as heat pen are limited and do not allow erasing.

Similar concepts have been explored with tactile displays. Animated patterns passively displayed on the VITAL, a small vibrotactile array, were, for example, shown to convey emotions such as surprise and anger [22] and to be spontaneously associated with categories such as *motor* and *liquid* [179]. The motion of tactile patterns was also shown to convey four directions [23]. Static, blinking and animated tactile icons were similarly produced on the VTPlayer's 4×4 array of Braille pins to communicate eight directions as well as additional information through pattern size and blinking rate [215]. These icons were used to guide the exploration of a maze and provide additional cues while tracing an electrical circuit with a force-feedback device. The usability of a zoomable interface for tactile graphics was extensively studied with the Tactos, a device that combines two immobile Braille cells with a graphical tablet [309]. A game involving a moving ball has also been implemented using an experimental display with six movable Braille cells [172].

Dynamic rendering has also been investigated on large tactile arrays despite the slow refresh rate of some technologies. Position sensing, essential for interaction, has been accomplished using a variety of methods including individual pin switches [183], force/torque sensors [249], ultrasonic pen [131] and instrumented arms [130, 295]. Shimada et al., for example, designed an interactive interface using a 32×48 array of Braille pins mounted on a force/torque sensor that allows drawing by applying pressure, scrolling by pushing in a direction, and zooming in an out [249]. Similar interfaces were also used to display animations such as moving sine waves and games such as ping-pong, whack-a-mole and tic-tac-toe [130, 131, 295]. A similar but slower array with 120×60 Braille pins was used to interactively display webpages, interestingly allowing components of scalable vector graphics (SVG) to be displayed incrementally [234]. The large pin spacing of a 16×16 array was similarly compensated for by displaying alternate views of tactile patterns [123]. Interactive features such as zooming are also inherently supported by the Graphic Window Professional (Handy Tech Elektronik GmbH, Germany), a tactile array of 24×16 Braille pins [123]. Refreshable Braille displays and similar arrays have finally been used to create animated games [244] and to zoom in on graphics [58].

This chapter presents tactile rendering approaches that similarly attempt to exploit the possibilities offered by dynamic tactile graphics produced by lateral skin deformation. Tactile flow, reactive textures and interactive graphics are discussed in turn.

9.3 Motion and Tactile Flow

The motion of features within virtual tactile graphics creates an impression of tactile flow which can be used to guide the exploration and attract attention to important elements or to provide supplemental information such as the direction of flow of a water stream on a map. The introduction of motion effects in the rendering of textures as well as stroked and dotted shapes is discussed in turn.

9.3.1 Textures

An impression of tactile flow can be produced with an arbitrary texture such as a tiled or composite texture by translating the entire pattern as illustrated in Figure 9.1. A translation with velocity $\boldsymbol{v}$ is then introduced in a texture $\delta(\boldsymbol{p})$ through an offset $\boldsymbol{v}t$:

$$\delta_v(\boldsymbol{p}, t) = \delta(\boldsymbol{p} - \boldsymbol{v}t) \tag{9.1}$$

The time t is reset at periodic intervals to prevent a loss of numerical precision as the positional offset $\boldsymbol{v}t$ grows, introducing occasional rendering discontinuities unless the texture's periodicity is known.

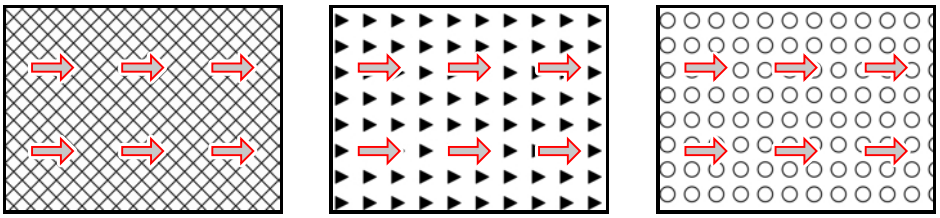

(a) (b) (c)

Fig. 9.1 Translation of (a) composite gratings and (b-c) tiled textures.

Tactile flow can alternatively be introduced in a grating texture through the displacement of the grating ridges. A motion with velocity v is hence produced with an offset vt to the rendering position x along the grating waveform $g(x)$. A loss of numerical precision is avoided by taking advantage of the periodicity introduced by the grating wavelength λ:

$$g_v(x, t) = g\left(x + v \cdot (t \bmod \lambda/v)\right) \tag{9.2}$$

As illustrated in Figure 9.2, ridge motion can be used to create forward or backward flow within a linear grating, inward or outward flow within a radial grating, and rotational flow within an axial grating. The salience of the flow, and particularly its direction, depends on the velocity of the motion and grating properties such as the presence of gaps.

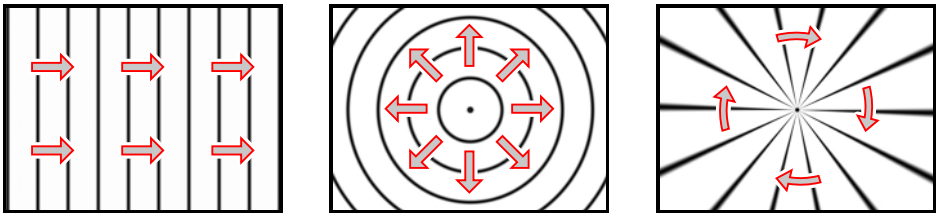

(a) (b) (c)

Fig. 9.2 Motion within (a) linear, (b) radial and (c) axial grating textures.

While it succeeds at producing an impression of tactile flow, the motion of a texture affects its ability to present a stable tactile pattern. Tactile flow is hence best introduced in a texture through the composition of a secondary moving texture. A motion cue can, for example, be superposed on a fixed texture by weighted addition as illustrated in Figure 9.3a, resulting in a reduction in intensity of both patterns. It can alternatively be applied by masking such that the underlying texture is suppressed where active as illustrated in Figure 9.3b. A similar but weaker motion cue can be applied more uniformly by blending of a mid-range deflection as illustrated in Figure 9.3c. Vibration can finally be blended in such that both patterns are uniformly applied at full intensity as illustrated in Figure 9.3d.

It should finally be noted that the motion of a texture can adversely interact with the exploratory motion of the user, resulting, for example, in an increase or decrease in perceived spatial frequency of a moving grating. These effects can optionally be avoided by rendering moving patterns as though the tactile array position $\boldsymbol{P}$ was fixed at an artificial location on the tactile canvas, resulting in a tactile flow through the fingerpad that is independent of exploratory motion.

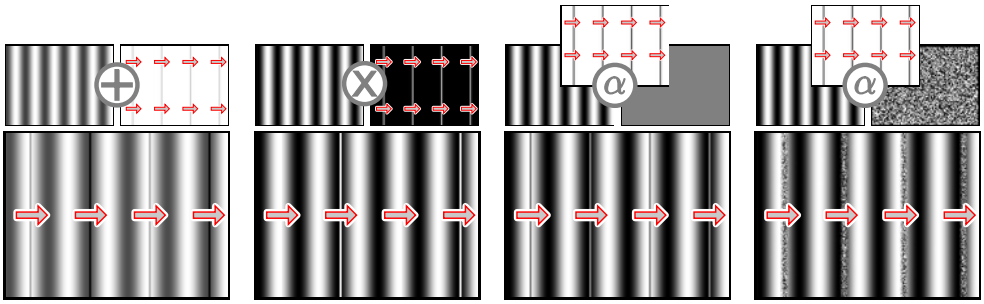

Fig. 9.3 Compositing of motion cues by (a) addition at 30% intensity, (b) masking, and blending with (c) a mid-range deflection or (d) vibration.

9.3.2 Stroked Shapes

Tactile flow can be introduced in a stroked shape by displacing the longitudinal texture rendered along its length in a manner analogous to the motion of a grating texture's ridges. Motion cues can hence be applied to lines, circles and polygons through a variety of stroke textures including dense, sparse and vibrating gratings as illustrated in Figure 9.4. The rendering artefacts introduced by a polygon's discontinuous longitudinal path are slightly more problematic in the presence of motion and can be corrected once more by rounding, as illustrated in Figure 9.4c, or by suppression with vertex markers. The salience of the motion depends not only on the velocity and grating properties but also on the width and sharpness of the stroke's cross-section.

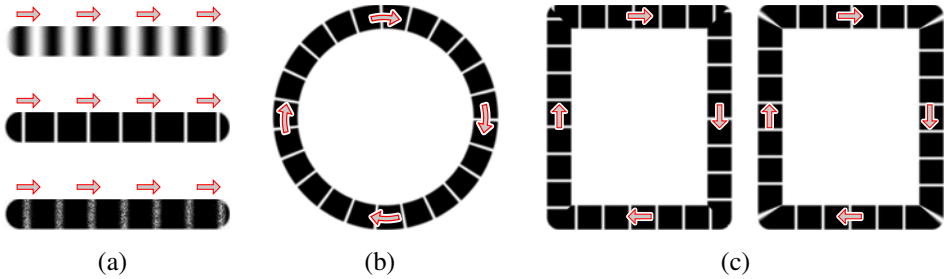

Fig. 9.4 Texture motion along stroked (a) lines, (b) circles, and (c) polygons.

Once again, the motion of a stroke's longitudinal texture affects its ability to provide feedback as a shape is traced and is hence best used within a composition of dy-

namic and static tactile patterns. Motion cues can be applied to the textured strokes of lines, circles and polygons using the same compositing operations proposed for areal textures such as weighted addition, masking and blending, as illustrated in Figure 9.5.

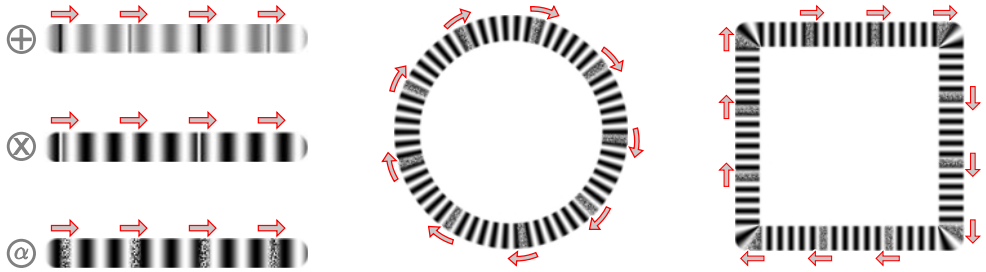

(a) (b) (c)

Fig. 9.5 Motion compositing in stroked (a) lines, (b) circles and (c) polygons.

The salience of the resulting motion cues depends once again on their width and hence requires thick strokes for a clear tactile flow to be felt. Thin strokes can alternatively be enabled by producing oversized motion cues that extend past the stroke as illustrated in Figure 9.6, affecting fill textures if present. As shown in Figure 9.6b, oversized motion cues applied through masking have limited value since an underlying pattern is required.

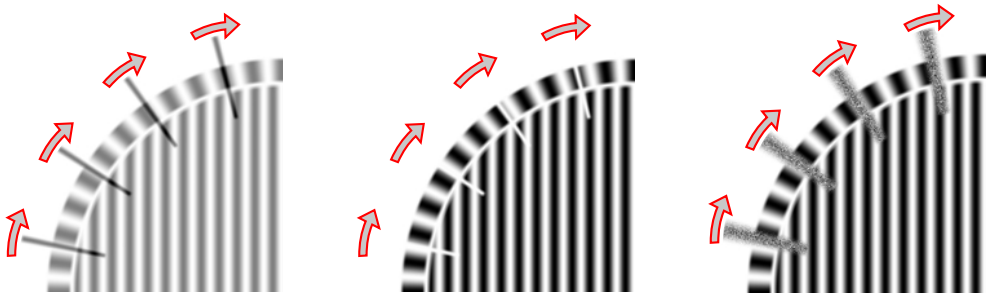

(a) (b) (c)

Fig. 9.6 Compositing of oversized motion cues on stroked circles by (a) addition, (b) masking and (c) vibration blending.

Normal-sized motion cues are rendered by first compositing the dynamic and static stroke textures before blending with the areal fill texture according to the stroke profile, as illustrated in Figure 9.7a-b. Oversized motion cues, on the other hand, are

rendered as though for a wider stroke and applied to the fully-rendered stroked shape as illustrated in Figure 9.7c.

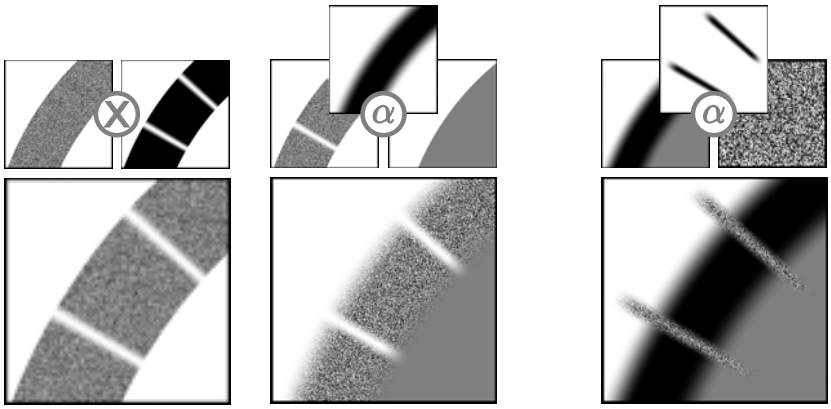

Fig. 9.7 Composition of (a-b) normal and (c) oversized motion cues.

9.3.3 Dotted Shapes

Tactile flow can be introduced in the rendering of dotted shapes either by displacement of the dots or superposition of a moving texture as applied to stroked shapes. The former case, illustrated in Figure 9.8a, results in the translation of the dots along the length of the shape contour with dots fading in and out at the extremities of lines and polygon segments, and polygon vertices remaining immobile. Normal or oversized motion cues can alternatively be applied to the dotted pattern using the composition operations introduced in the context of stroked shapes, as illustrated in Figure 9.8b.

9.4 Reactive Tactile Patterns

The rendering of a reactive tactile pattern varies according to the reading behaviour of the user, or more precisely the velocity $\boldsymbol{v}$ with which the canvas is explored. Although generalizable to other patterns, reactive rendering is demonstrated with the adaptive blending of areal textures in response to changes in the speed v and direction θ of exploration. A reactive texture is hence rendered by composition of underlying textures according to a blending function $\alpha(\boldsymbol{v}, t)$ such that:

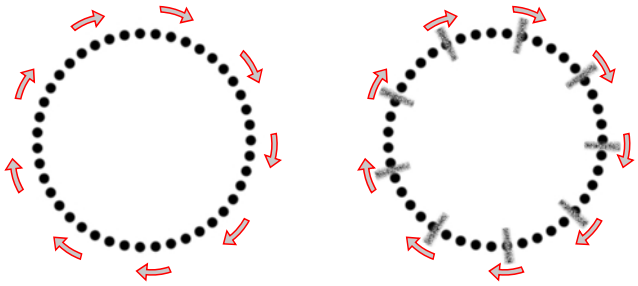

(a) (b)

Fig. 9.8 Tactile flow within a dotted shape by (a) dot motion and (b) superposition of motion cues.

$$\delta(\boldsymbol{p}, \boldsymbol{v}, t) = \alpha(\boldsymbol{v}, t) \cdot \delta_1(\boldsymbol{p}) + (1 - \alpha(\boldsymbol{v}, t)) \cdot \delta_2(\boldsymbol{p}) \tag{9.3}$$

Velocity estimation is first discussed before introducing reactive textures based on either the speed or velocity of exploration.

9.4.1 Velocity Estimation

While slight delays and inaccuracies may not be perceptible, a smooth and continuous estimation of the exploration velocity is critical to produce fluid changes in the rendering of a reactive tactile pattern. The instantaneous velocity is hence obtained by differentiation of the position $\boldsymbol{p}[T]$, obtained at regular interval of Δt, over intervals of N samples:

$$\boldsymbol{V}[T] = \frac{\boldsymbol{p}[T] - \boldsymbol{p}[T - N]}{N\Delta t} \tag{9.4}$$

The resulting velocities are further filtered by taking their average within a moving window of M past values:

$$\boldsymbol{v}[T] = \frac{1}{M} \sum_{i=0}^{M-1} \boldsymbol{V}[T - i] \tag{9.5}$$

Differentiation and averaging windows with $N = 10$ and $M = 50$ were found to be acceptable for a 1 kHz update rate, despite the introduction of a 50 ms delay.

9.4.2 Speed-Based Textures

A reactive texture can fluidly alternate between two representations as a function of the speed with which the canvas is explored. As illustrated in Figure 9.9, this effect can, for example, be used to introduce vibration into a pattern as exploration halts and therefore compensate for the loss of tactile feedback when immobile on a static texture. It could also be used to reduce the density or complexity of a canvas as speed increases, hence enabling a coherent overview or detailed view to be felt depending on the exploration behaviour.

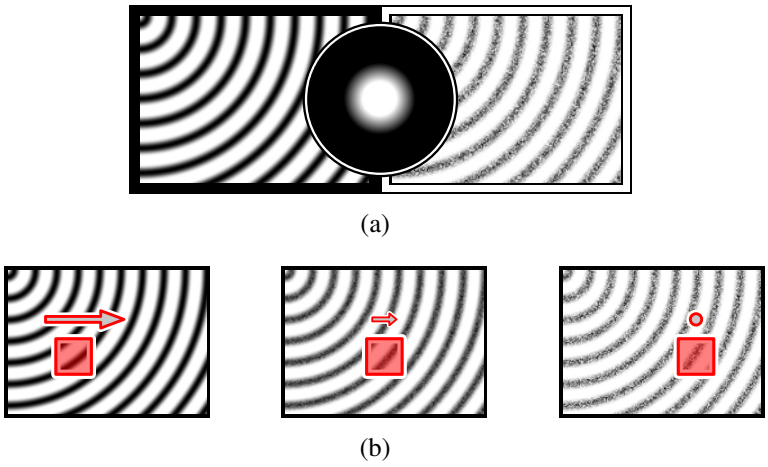

Fig. 9.9 Speed-based reactive texture illustrated as (a) a texture pair and velocity plot of the blending function, and (b) a sequence of tactile renderings. The black and white framed textures respectively represent the rendering of the reactive texture at high and low exploration speeds as illustrated in the polar plot of the blending function.

These effects are obtained by composition with a blending function that triggers a linear transition as the speed drops from v_1 to v_0:

$$\alpha(v) = \begin{cases} 1 & \text{if } v < v_0; \\ \frac{v - v_0}{v_1 - v_0} & \text{if } v_0 \leq v < v_1; \\ 0 & \text{otherwise.} \end{cases} \tag{9.6}$$

The onset of the transition can optionally be delayed to prevent the activation of low-speed effects as exploration reverses course or briefly slows down. The transition is hence delayed until the speed has remained below the upper threshold v_1 for a period

of τ, and then introduced gradually over the same period:

$$\alpha(v,t) = \alpha(v) \cdot \begin{cases} 0 & \text{if } t - t_0 < \tau; \\ (t - t_0 - \tau)/\tau & \text{if } \tau \leq t - t_0 < 2\tau; \\ 1 & \text{otherwise.} \end{cases} \tag{9.7}$$

9.4.3 Velocity-Based Textures

A reactive texture can also alternate between two representations as a function of both the speed and direction of the exploration velocity, and hence create a variety of directional patterns. As illustrated in Figure 9.10, this effect can, for example, be used to introduce vibration into a pattern as exploration veers off a preferred direction and hence warn users of a deviation.

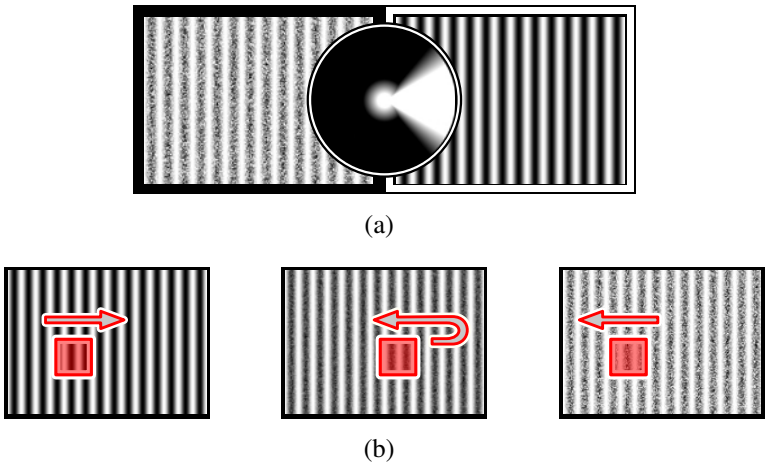

Fig. 9.10 Velocity-based reactive texture illustrated as (a) a texture pair and velocity plot of the blending function, and (b) a sequence of tactile renderings.

A grating texture can similarly alternate to a uniform vibration as exploration deviates from a preferred axis as shown in Figure 9.11a, or fade away as in Figure 9.11b. Velocity-based rendering can also be used to alternate between a fine and coarse texture as a function of the direction of exploration as illustrated in Figure 9.11c, or produce orthogonal gratings while exploring horizontally or vertically as illustrated in Figure 9.11d.

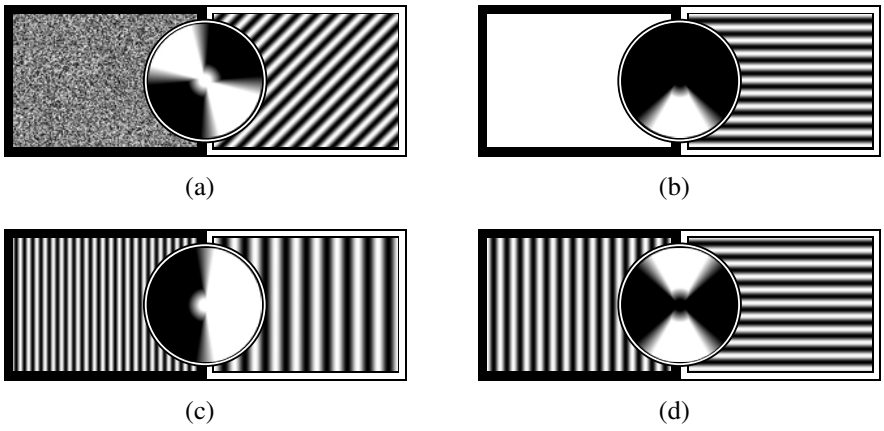

Fig. 9.11 Examples of velocity-based reactive textures.

These effects are obtained with a blending function that triggers a linear transition as the deviation $\Delta\theta$ from the preferred direction or axis increases from σ_0 to σ_1:

$$\alpha(\theta) = \begin{cases} 1 & \text{if } \Delta\theta < \sigma_0; \\ (\Delta\theta - \sigma_0)/(\sigma_1 - \sigma_0) & \text{if } \sigma_0 \leq \Delta\theta < \sigma_1; \\ 0 & \text{otherwise.} \end{cases} \tag{9.8}$$

The direction of the exploration velocity, however, tends to be noisy and generally meaningless when nearly immobile, hence requiring alterations to the blending function at low speeds. The speed-based blending function $\alpha(v)$ introduced in the previous section is hence applied to force the blending function low or high at low speeds:

$$\alpha_{hi}(v, \theta) = \max(\alpha(\theta), \alpha(v)) \tag{9.9}$$

$$\alpha_{lo}(v, \theta) = \min(\alpha(\theta), 1 - \alpha(v)) \tag{9.10}$$

The low-speed behaviour can alternatively be biased towards the current state and toggle only when the velocity triggers a transition so as to avoid artefacts while slowing down temporarily or changing course.

9.5 Interactive Graphics

Limitations in tactile acuity often require a reduction in the density of information when converting visual graphics to a tactile form. Complex graphics such as maps are hence commonly adapted as sets of tactile graphics with each drawing focused on conveying a specific subset of the original content [59]. The refreshable display of tactile graphics presents further opportunities to flexibly alter the level of information displayed through interactive controls. Layers of information could hence be selectively activated, or complex content explored without interruption or clutter by scrolling and zooming within a large canvas. The potential of interactive tactile graphics was explored through a keypress-actived toggle between arbitrary tactile canvases, and demonstrated in [211] with an audio-tactile worldmap highlighting either continents or target regions as illustrated in Figure 9.12 .

(a) (b)

Fig. 9.12 Interactive display of a worldmap with (a) textured continents and (b) textured regions (adapted from [211]).

9.6 Visualization and Optimization

The visualization tools introduced in Section 8.3.3 can be adapted for use with dynamic tactile patterns and hence allow visual communication of their content and inspection of their rendering. Although implemented only for reactive textures at this time, symbolic patterns such as arrows can, for example, be overlaid on illustrations to convey dynamic content. Time-varying patterns such as moving textures or strokes

can alternatively be visualized as a sequence of deflection maps in the same way as vibrating patterns. A deflection map of a reactive texture can similarly be obtained for a given velocity provided that the rendering does not depend on the past exploration behaviour. A more accurate visualization can otherwise be obtained offline by producing deflection maps along a simulated exploration path, resulting in a animated sequence of renderings similar to those shown in Figures 9.9b and 9.10b. The tactile canvases of swappable interactive graphics can be visualized individually.

The computational cost measurement tools introduced in Section 8.5.2 can similarly be adapted by taking into consideration the potential impact of velocity variations. A sinusoidal disturbance as well as speed variations and reversals are hence introduced along the simulated path providing wide spatial coverage such that a quadrant of the velocity range is explored thoroughly in each direction, as illustrated in Figure 9.13a. The simulated path providing local spatial coverage, illustrated in Figure 9.13b, already covers a wide range of velocities and requires no modification. The computational cost information gathered by simulation can be plotted either with respect to the position on the canvas or the velocity of exploration, illustrated in Figure 9.14.

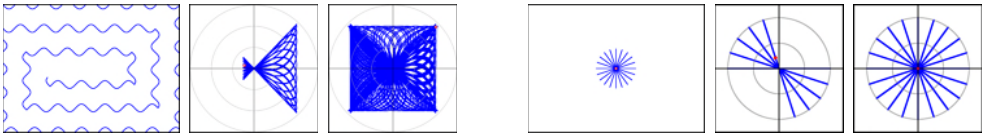

(a) (b)

Fig. 9.13 Simulated exploration paths for (a) wide and (b) local spatial coverage, and corresponding velocity coverage at two points along the paths.

9.7 Validation and Discussion

The dynamic tactile graphics were informally evaluated along with the static tactile graphics, as discussed in Section 8.6. The comments of the four visually-impaired volunteers were once again solicited on a range of dynamic tactile graphics features and rendering parameters adjusted to their individual preferences. The following discussion presents a synthesis of the insight gained through these sessions as well as prior experimentations and numerous demonstrations.

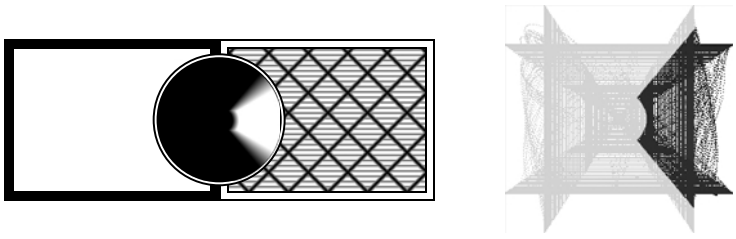

(a) (b)

Fig. 9.14 Distribution of the computational cost of (a) a directional texture with respect to (b) the velocity of exploration.

Although the translation of arbitrary textures composed of simple, sparse patterns is generally perceptible, tactile flow is most effectively rendered through the ridge motion of linear gratings. The salience of the tactile flow, and more particularly its direction, is however greatly affected by the properties of the grating and its speed of displacement. Motion is generally most easily felt with thin, sparse gratings (e.g. 2 mm ridges and 15 mm gaps) creating distinct, well-separated moving features on the fingerpad. The intensity of the motion cue can also be slightly increased with the use of wider vibrating ridges. The optimal speed of motion is typically between 1 and 5 Hz but varies with individual preferences and grating properties.

The salience of superposed motion cues depends on the composition method and properties of the underlying texture. The reduction in intensity resulting from a weighted sum significantly weakens both patterns and may at best provide a subtle motion cue. The motion cue is similarly weakened by blending with a mid-range deflection. Suppression with masking ridges creates a much stronger tactile flow with discontinuities that may or may not be perceptible depending on the properties of the underlying texture. The blending of moving vibrating ridges within a fixed texture preserves both patterns' integrity and generally results in the most salient superposed motion cue.

In all cases, active exploration introduces artefacts as the reading finger moves against or with a moving texture and generally prevents the perception of the motion's direction. These artefacts, such as an increase in perceived grating frequency, can be eliminated with display-centric motion rendering but the direction of motion remains identifiable mainly when immobile.

Tactile flow within stroked shapes is similar to that within linear grating textures

but slightly weaker due to the limited width of the stroke. Motion cues are hence perceptible with sharp-edged, wide strokes (e.g. 10 mm) but otherwise very subtle. As expected, oversized superposed motion cues greatly improve the salience of the tactile flow for thinner strokes. Superposed motion cues are similarly effective with dotted shapes but dot motion prevents contour following and is subtle even with large, widely-spaced dots.

Speed-based reactive textures with a delayed onset of approximately 500 ms result in smooth, artefact-free transitions and may well be useful to allow the focused exploration of a drawing's details. Velocity-based reactive textures are similarly effective at conveying directional information when configured such that low-speed modulation either favours a non-disruptive rendering, such as a non-vibrating pattern, or toggles between both states to avoid unnecessary transitions.

The interactive display of an audio-tactile map highlighting either the continents or specific regions was evaluated in [211] and much appreciated by the participants. The possibilities offered by such interactive use of virtual tactile graphics have also raised much interest with tactile graphics practitioners.

9.8 Conclusion

This chapter introduced extensions to the framework presented in Chapter 8 that take advantage of the novel opportunities for dynamic and interactive content afforded by virtual tactile graphics. Tactile flow was first produced within textures, stroked shapes, and dotted shapes through the motion of tactile features either inherent to the patterns or superposed with compositing operations. Salient motion cues were found to result from the displacement of sparse gratings within textures and strokes, or their composition with fixed patterns through masking or vibration blending. Reactive textures altering their tactile rendering in responses to the exploration behaviour where then introduced, allowing, for example, a pattern to vibrate when slowly traced or a texture to change depending on the direction in which it is felt. Interactive graphics allowing the content of a canvas to alternate between two representations at the press of a button were finally briefly discussed. Swappable graphics were investigated in [211] while tactile flow and reactive textures were evaluated through informal experimentation sessions with four visually impaired volunteers.

Although preliminary results are encouraging, further studies will be necessary to formally validate the novel rendering algorithms, determine the optimal or preferred rendering parameters, and evaluate human performance at critical tasks such as motion detection. Much work also remains to demonstrate the applications of dynamic and interactive rendering concepts in the context of practical tactile graphics such as maps and mathematical diagrams. Tactile flow could supplement a drawing with directional information, for example, indicating the direction of flow of a river or road on a map, or subtly guide the reader's attention towards important drawing elements. Reactive patterns could similarly convey directional information or adapt their content to the speed of exploration, for example, vibrating when immobile or reducing complexity when explored rapidly. Interactive graphics could with minor improvements enable complex content to be distributed onto multiple canvases, allowing, for example, geographic and political elements of a map to be shown separately.

The dynamic and interactive graphics concepts introduced in this chapter represent a first attempt to exploit the novel possibilities offered by refreshable tactile graphics produced by lateral skin deformation. Motion and animation could be extended to arbitrary patterns, perhaps allowing games or other dynamic applications to be developed. Reactive rendering could similarly be generalized and take into account other inputs such as the pressure applied with the reading finger. Rendering parameters such as the amplitude of a pattern could alternatively be directly modulated by the exploration velocity or other other inputs. Interactive controls could be further developed, allowing, for example, zooming and panning within a large, complex tactile canvas. These dynamic rendering concepts, and others yet to be discovered, may help overcome the limitations of conventional tactile graphics and enable virtual tactile graphics to reach their full potential.

Chapter 10

Conclusion

Thesis Summary

This thesis has presented contributions to the development of knowledge on lateral skin deformation and its applications for the accessibility of textual and graphical information for visually impaired persons. Tactile rendering by lateral skin deformation was first explored and evaluated in the context of virtual Braille, demonstrating that reading lines of Braille dots and complete 6-dot Braille is demanding but generally possible and suggesting future steps towards making the approach a practical alternative to conventional refreshable Braille displays. Tactile rendering was then further developed and refined in the context of virtual tactile graphics, resulting in the design of a dedicated haptic interface and a sophisticated rendering framework providing flexible support for traditional tactile graphics as well as more experimental tactile patterns that take advantage of the possibilities for interactive, dynamic content afforded by the novel approach. This work has not only demonstrated the potential of laterotactile stimulation for the display of virtual Braille and tactile graphics, but also provided a preliminary investigation of the ways in which this novel skin stimulation method can be used to produce meaningful tactile sensations under computer control.

Braille

Despite the growing popularity of voice synthesis for the accessibility of textual information, Braille remains a preferred or secondary medium for many visually impaired persons for the level of control over reading that it affords and granular view that it pro-

vides, allowing, for example, a word's spelling to be inspected. Computerized Braille, however, requires effective but expensive refreshable Braille displays that generally provide only a single line of Braille cells at a time due to size and cost constraints. The investigation of the feasibility of producing Braille by lateral skin deformation presented in this thesis was therefore motivated by the potential of this technology to enable a virtual page of Braille of arbitrary size to be displayed affordably with a small array of tactile stimulators. The long term vision of a practical laterotactile Braille display is best conveyed through the following usage scenario.

> **Scenario 1.** *Louise is a journalist for a leading newspaper. She is writing from a press conference and trying to meet the next edition's deadline. Until recently she used voice synthesis to revise her articles but she missed the freedom of reading at her own pace and worried about overlooking typographical errors. She had appreciated her refreshable Braille display but the more expensive aid wasn't covered by her insurance and she couldn't afford to replace it when it broke down. She is now ignoring her noisy surroundings as she edits her article with her laterotactile Braille display, quickly going through full pages of text with the mouse-like reader attached to her portable computer. Losing her concentration at the end of a long day, she turns a knob and increases the Braille's contrast. She still uses voice synthesis but likes having the option of reading Braille, especially in demanding situations like this one.*

This scenario illustrates many potential advantages of laterotactile Braille displays over conventional refreshable Braille displays and voice synthesis, including the ability to adjust the tactile appearance of Braille patterns to suit one's preferences or aptitudes. Although this vision has yet to be fully realized, important steps towards its concretization have nevertheless been presented in this thesis.

The display of a line of Braille dots was first demonstrated in Chapter 3 through the design and evaluation of tactile rendering patterns consisting of travelling waves of skin compression produced with a simplified laterotactile display formed of a linear array of large piezoelectric actuators. This approach was then extended in Chapter 4 to the display of a line of 6-dot Braille cells by distributing virtual dots along the rows of actuators of a general-purpose 2D laterotactile display called STReSS^2. In both

cases, the laterotactile display was mounted on a linear slider and activation patterns were produced in response to exploratory movements to create the illusion of brushing against stationary objects. Formal evaluations demonstrated that reading Braille produced by lateral skin deformation is generally possible but demanding and slow. Results obtained with textured dot representations, however, suggest that performance could be improved by abandoning realism in favour of contrast in the rendering of Braille patterns. A specialized laterotactile Braille display with more forceful actuators could alternatively be devised to increase the perceived height or intensity of the virtual Braille dots. These preliminary results and observations lead to believe that displaying Braille by lateral skin deformation would be feasible and practical given further efforts to refine the tactile rendering algorithms and display interfaces.

Tactile Graphics

While laterotactile Braille could improve upon them, refreshable Braille displays and voice synthesis are widely used and fulfill basic needs for digital access to textual information by visually impaired persons. Access to graphical information is comparatively much poorer due in large part to the limited availability and functionality of refreshable tactile graphics interfaces. Despite much experimental work on the topic, the refreshable display of tactile graphics remains an open research problem with few interfaces available commercially and none having gained widespread acceptance for a variety of practical reasons. Tactile graphics therefore remain available almost exclusively on physical media such as embossed paper and are hence much less flexible and immediately accessible than their visual counterparts. The investigation of virtual tactile graphics by lateral skin deformation presented in this thesis was therefore motivated by the potential of this technology to adequately address the unmet needs of the visually impaired community for computerized access to graphical content. The long term vision for laterotactile graphics is best conveyed through the following usage scenarios.

> **Scenario 2.** *Robert is planning a visit to a travel agent in a part of town that he is unfamiliar with. He uses a popular online mapping system to trace a route from his house to the travel agent. As he explores the map with the Tactograph, he notices the pulsating icons representing his origin*

and destination on the map. He traces the selected route with his index finger, exploring along the way to feel buildings and other landmarks. A smooth wave travels through the recommended path, naturally directing his finger towards the destination. As he traverses the path, a synthetic voice provides directions and street names. When he reaches the travel agent's location, Robert increases the zoom level of the map and explores the details of the building's surroundings. He notices the pleasant texture of a nearby park and makes a note to visit it after the meeting. Robert now feels ready to make the trip and is looking forward to planning his routes for his vacation in Madrid.

Scenario 3. *Alice is a manager in a large corporation. She is reviewing an electronic document detailing the sales projections of her department that was sent by a colleague. She uses the Tactograph to explore the layout of the document and to direct her screen reader to different portions of the text. She notices that the logo of the company is incorrectly positioned and quickly moves it with a few clicks. Reaching a chart of past sales for a particular product, she explores the curve and quickly grasps the trend hidden in the data. As she selects different portions of the curve, the sales figures are read out-loud, confirming her impressions. She quickly annotates the diagram, circling an important part of the curve and typing a comment for her colleagues. Later that day she will use the Tactograph again to prepare her slides for a presentation to the corporation's upper management. The Tactograph has improved her independence and allows her to communicate with her sighted colleagues using their visual language.*

Scenario 4. *Peter is writing a report for his 6th-grade mathematics class. Earlier today, he learned about the different types of triangles and felt their shape with the Tactograph. When his teacher asked him to draw an equilateral triangle, Peter quickly drew three lines and felt them to make sure that they had the same length. He is now reading about geometry in an online encyclopaedia, feeling the structure of the page with the Tactograph and skipping to the section on quadrilaterals. As he reads the text, he touches the rectangles, squares and other polygons that are shown*

on the web page. He is looking forward to finishing his assignment so that he can play his favourite game on the Tactograph. When Peter was younger, he enjoyed listening to stories and feeling the animated pictures that accompanied them on the Tactograph. He would laugh at the tickling sensation of blowing wind and remove his scared finger as he felt the buzz of angry monsters. Now that he's older, Peter prefers to play role-playing games with his friends.

These scenarios highlight the strengths of virtual tactile graphics and their potential to restore equal access to information for visually impaired persons despite the increasingly pervasive use of graphics in computer interfaces and digital documents. Dynamic rendering is notably foreseen to be the most important novelty introduced by virtual tactile graphics, allowing many traditional limitations to be overcome with the use of interactive or active content and complex applications such as computer games to be made accessible. Perhaps most importantly, the dynamic properties of laterotactile graphics could enable graphical content to be efficiently created or modified by the visually impaired users themselves, hence greatly increasing their independence and the amount of content available to them. Although much work remains, significant progress towards the realization of this long term vision has been made.

This thesis has documented the gradual development and refinement of a flexible framework for the rendering of virtual tactile graphics by lateral skin deformation. Described in detail in Chapter 8, the framework emulates tactile features found in conventional tactile graphics through a coherent set of tactile patterns that includes gratings and other areal textures, raster image patterns, stroked or dotted shapes, as well as more complex composite patterns. The framework was informally evaluated with the assistance of four visually impaired volunteers, allowing much insight to be gained about the strengths of laterotactile graphics as well as preferred or optimal rendering parameters. An earlier version of the framework was more formally evaluated in Chapter 6, investigating the effect of rendering parameters on shape identification, grating orientation identification and grating pitch scaling, and ultimately demonstrating that the shape and texture of simple tactile icons can be identified. The framework was first introduced in a simplified form in Chapter 5 through a haptic memory game in which cards were matched tactily rather than visually.

Further experimental developments exploring the novel possibilities offered by dynamic tactile graphics were presented in Chapter 9. Tactile flow was first introduced in the rendering of textures, stroked shapes and dotted shapes through the motion of inherent or superposed tactile features. The framework was then further extended with reactive textures that alter their rendering in response to changes in the exploration behaviour, for example, vibrating when exploration deviates from a preferred course. Interactive graphics were then briefly discussed in the form of alternative views of a tactile canvas. These developments were validated with four visually impaired volunteers as part of the main evaluation sessions.

These investigations of virtual tactile graphics were conducted with the Tactograph, a haptic interface that initially consisted of a STReSS^2 tactile display mounted on a Pantograph force-feedback device used as a passive planar carrier. An improved Tactograph designed specifically for the display of tactile graphics was presented in Chapter 7, introducing many improvements including a larger canvas and measurement of the tactile array's orientation and pressure applied with the reading finger.

These preliminary developments have demonstrated the potential of lateral skin deformation for the rendering of virtual tactile graphics and hold great promise for the improvement of the accessibility of graphical information for visually impaired persons.

Laterotactile Rendering

The virtual display of Braille and tactile graphics for visually impaired persons has proved to be a rich context for the empirical development of laterotactile rendering algorithms and, more broadly, has allowed a better understanding of the relation between lateral skin deformation and tactile perception to emerge. While a fundamental investigation of the mechanisms through which lateral skin deformation functions is beyond the scope of this thesis, the rendering algorithms developed provide much insight for practical use of the laterotactile display technology and may inform further studies aimed at the psychology or physiology of touch.

The synchronization of travelling skin deformation patterns with the displacement of a laterotactile display was shown to create the illusion of brushing against stationary virtual objects such as Braille dots or grating textures. A variety of such artificial tactile sensations were shown to be synthesizable by activating actuators as a function

of their position on the virtual canvas alone. Directional effects were shown to be surprisingly limited despite the fundamentally-different skin deformation patterns applied depending on the exploration direction. Lateral skin deformation was moreover shown to allow the production of either ecologically-plausible sensations through the smooth deflection of actuators or intense localized sensations by vibrations or abrupt deflections. The judicious use of these very distinct types of tactile sensations was a recurring issue in the practical use of laterotactile rendering, as exemplified by the idiosyncratic preferences of Braille readers for either smooth or textured Braille dots.

These findings as well as the framework developed for tactile graphics may prove useful for the extension of tactile rendering by lateral skin deformation to other domains such as the display of 3D environments with a combination of tactile and kinaesthetic feedback.

Future Directions

This thesis represents a significant step forward in the realization of the long term vision of virtual Braille and tactile graphics by lateral skin deformation as practical alternatives to more established technologies for the accessibility of textual and graphical content by visually impaired persons. Much work nevertheless remains to fully realize the potential of laterotactile rendering in these and other domains.

Braille

The rendering of virtual Braille by lateral skin deformation has reached a crossroad. The results obtained with the rendering of 6-dot Braille are sufficiently promising to support further studies but nevertheless indicate that reading is too difficult as currently implemented to compete with well-entrenched technologies such as refreshable Braille displays and voice synthesis. The work presented in this thesis suggests that laterotactile Braille could remain viable if either rendered for contrast rather than realism — hence leveraging knowledge of the Braille code with better defined tactile patterns — or produced on a specialized display with fewer and stronger skin stimulators. The former approach may allow Braille and tactile graphics to be presented with the same tactile interface, while the latter may provide more satisfying tactile sensations for experienced Braille readers. The success of laterotactile Braille will in both cases be

contingent on a better exploitation of the technology's differentiating strengths such as portability and the ability to display a full page of Braille, and potentially graphics, without added cost or encumbrance.

Tactile Graphics

The rendering of virtual tactile graphics by lateral skin deformation has been explored extensively in this thesis and its potential for the accessibility of graphical content by visually impaired persons demonstrated through both formal and informal evaluations. This promising work nevertheless remains preliminary and represents only an initial survey of the possibilities offered by lateral skin deformation in the context of tactile graphics. While early features of the rendering framework have been formally evaluated in Chapter 6, validation of later additions has been limited to informal evaluation sessions with visually impaired volunteers. Further investigation will be required to formally determine preferred or optimal rendering parameters and evaluate the usability of the novel features. Despite promising early efforts on the topic, much work also remains to demonstrate the practicality of laterotactile graphics in real-world usage scenarios such as maps and mathematical diagrams. Tactile graphics conventions adapted to this novel medium will moreover need to be developed to facilitate the communication of information.

The use of dynamic tactile rendering and interactive content has only been explored superficially in this thesis but presents a wealth of untapped opportunities. Dynamic rendering holds the potential to revolutionize tactile graphics by allowing interaction and hence content editing, selective information presentation, zooming and panning, and other operations taken for granted by sighted computer users but often inaccessible to the visually impaired. Dynamic rendering could moreover allow active content to present supporting information in an intuitive manner. These novel features are not available on conventional static media and have hence received little attention yet. Much more work will be necessary to fully develop their potential but the impact on accessibility could be significant.

This thesis has also introduced the improved Tactograph as a haptic interface dedicated to the display of virtual tactile graphics. Although suitable for its purpose, the interface could be much improved. The ergonomics of the device could be redesigned to facilitate gliding, reduce the height of the manipulandom, and make its handling

more comfortable. The arm-based instrumented carrier could also be replaced with a mouse-like input device for better portability and reduced encumbrance. The use of multiple reading fingers would also be a significant improvement but would require a major re-engineering of the interface.

The success of laterotactile rendering for the display of tactile graphics is finally largely contingent on the availability of adapted content. This will require further work on the automated or semi-automated conversion of visual content, as well as the development of robust and flexible graphics authoring tools. Perhaps its most significant strength, the immediacy of interaction with laterotactile graphics could allow content to be created, modified and shared by the visually impaired users themselves, freeing them from the usual dependence on content publishers.

Laterotactile Rendering

This thesis has documented the development and refinement of tactile rendering algorithms using lateral skin deformation in the context of Braille and tactile graphics. These developments, however, represent only a fraction of the potential offered by laterotactile rendering and could be expanded with further efforts and experimentation. The empirical findings from such experimentation will hopefully allow the development of a better understanding of the relation between lateral skin deformation and tactile perception, which will in turn influence further refinement of tactile rendering algorithms. The work presented in this thesis could hence have an impact not only on accessibility and other related applications such as virtual reality, but also inform the design of experiments aimed at gaining a better understanding of the physiological, psychological and neurological basis for this novel method for computerized skin stimulation.

Appendices

Appendix A

Design and Optimization of the Tactograph

This Appendix discusses in more details the design and properties of the Tactograph introduced in Chapter 7. The forward, inverse and differential kinematics of the linkage are first derived. A closed-form expression of the resolution of the position measurement over the carrier's workspace is then obtained. The properties of the reachable workspace and their relation to the length of the rigid links are then discussed. The optimal link lengths are finally selected based on the specifications of the Tactograph and the effect on the resolution of the position measurement discussed. The appendix closes with technical drawings describing in details the design of the carrier and tactile display enclosure of the Tactograph.

Kinematics

The Tactograph carrier can be represented as a serial linkage with two rigid links and two revolute joints as illustrated in Figure A.1. The length of the first and second links is given by a and b respectively. The planar linkage has two degrees of freedom (2 DOF). The position (x, y) of the end effector is measured indirectly through joint angles α and β. The ratio of link lengths $k = b/a$ and the distance to the end effector $r = \sqrt{x^2 + y^2}$ are used to simplify the analysis. The linkage is restricted to the illustrated posture and therefore obeys the condition $\beta > 0$. The forward, inverse and differential kinematics of the system are derived in turn [243].

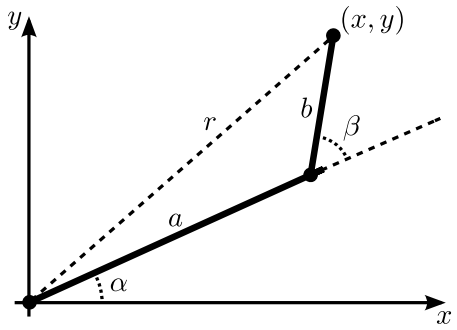

Fig. A.1 Geometric model of the carrier as a two-bar serial linkage.

Forward Kinematics

The forward kinematics are computed by taking the sum of the two vectors corresponding to the orientation and length of the rigid links. Given the joint angles, the position of the end effector can therefore be expressed as:

$$\begin{bmatrix} x \\ y \end{bmatrix} = \begin{bmatrix} \cos\alpha & \cos(\alpha+\beta) \\ \sin\alpha & \sin(\alpha+\beta) \end{bmatrix} \begin{bmatrix} a \\ b \end{bmatrix} \tag{A.1}$$

or alternatively as:

$$\begin{bmatrix} x \\ y \end{bmatrix} = a \begin{bmatrix} \cos\alpha & k\cos(\alpha+\beta) \\ \sin\alpha & k\sin(\alpha+\beta) \end{bmatrix}. \tag{A.2}$$

.

Inverse Kinematics

The inverse kinematics are obtained using the law of cosines and the geometric models illustrated in Figure A.2. Joint angle α is computed as follows:

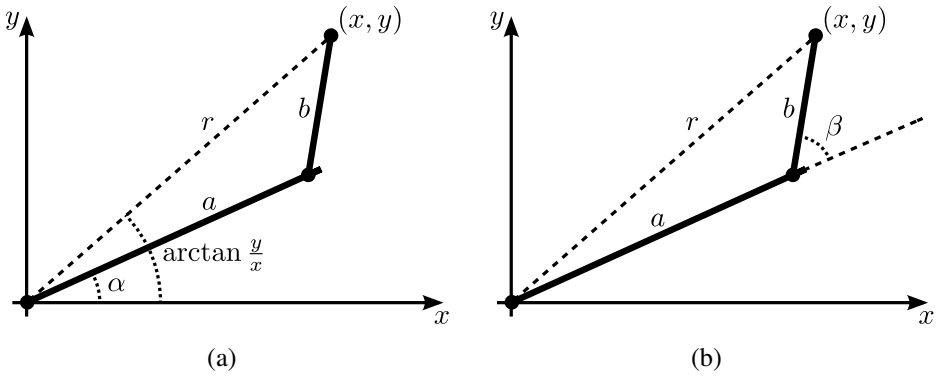

Fig. A.2 Inverse kinematics computations for joint angles (a) α and (b) β.

$$\cos(\arctan\frac{y}{x}-\alpha)=\frac{b^2-a^2-r^2}{-2ar} \tag{A.3}$$

$$\cos(\arctan\frac{y}{x}-\alpha)=\frac{a^2-b^2+r^2}{2ar} \tag{A.4}$$

$$\arctan\frac{y}{x}-\alpha=\pm\arccos\frac{a^2-b^2+r^2}{2ar} \tag{A.5}$$

$$-\alpha=-\arctan\frac{y}{x}\pm\arccos\frac{a^2-b^2+r^2}{2ar} \tag{A.6}$$

$$\alpha=\arctan\frac{y}{x}\pm\arccos\frac{a^2-b^2+r^2}{2ar} \tag{A.7}$$

The smaller value corresponds to the intended posture of the linkage and the joint angle can therefore be expressed as:

$$\alpha=\arctan\frac{y}{x}-\arccos\frac{a^2-b^2+r^2}{2ar} \tag{A.8}$$

Joint angle β is similarly computed as follows:

$$\cos(\pi - \beta) = \frac{r^2 - a^2 - b^2}{-2ab} \tag{A.9}$$

$$\cos(\beta - \pi) = \frac{r^2 - a^2 - b^2}{-2ab} \tag{A.10}$$

$$-\cos\beta = \frac{r^2 - a^2 - b^2}{-2ab} \tag{A.11}$$

$$\cos\beta = \frac{r^2 - a^2 - b^2}{2ab} \tag{A.12}$$

$$\beta = \pm \arccos \frac{r^2 - a^2 - b^2}{2ab} \tag{A.13}$$

Again the required posture dictates that $\beta > 0$ and hence:

$$\beta = \arccos \frac{r^2 - a^2 - b^2}{2ab} \tag{A.14}$$

The inverse kinematics are therefore given by:

$$\begin{bmatrix} \alpha \\ \beta \end{bmatrix} = \begin{bmatrix} \arctan \frac{y}{x} - \arccos \frac{a^2 - b^2 + r^2}{2ar} \\ \arccos \frac{r^2 - a^2 - b^2}{2ab} \end{bmatrix} \tag{A.15}$$

or alternatively by:

$$\begin{bmatrix} \alpha \\ \beta \end{bmatrix} = \begin{bmatrix} \arctan \frac{y}{x} - \arccos \frac{a^2(1-k^2) + r^2}{2ar} \\ \arccos \frac{r^2 - a^2(1+k^2)}{2ka^2} \end{bmatrix} \tag{A.16}$$

Differential Kinematics

The Jacobian is computed by taking the partial derivatives of the forward kinematics:

$$J = \begin{bmatrix} \frac{\partial x}{\partial \alpha} & \frac{\partial x}{\partial \beta} \\ \frac{\partial y}{\partial \alpha} & \frac{\partial y}{\partial \beta} \end{bmatrix} \tag{A.17}$$

$$= \begin{bmatrix} -a\sin\alpha - b\sin(\alpha+\beta) & -b\sin(\alpha+\beta) \\ a\cos\alpha + b\cos(\alpha+\beta) & b\cos(\alpha+\beta) \end{bmatrix} \tag{A.18}$$

or alternatively:

$$J = a \begin{bmatrix} -\sin\alpha - k\sin(\alpha+\beta) & -k\sin(\alpha+\beta) \\ \cos\alpha + k\cos(\alpha+\beta) & k\cos(\alpha+\beta) \end{bmatrix} \tag{A.19}$$

Spatial Resolution

The spatial resolution of the Tactograph carrier is estimated by computing for each location on the reachable workspace the maximal position error introduced by a single-count measurement error in one or both joint encoders. As illustrated in Figure A.3, this entails determining the maximum of 8 possible spatial offsets resulting from different combinations of joint angle measurement errors.

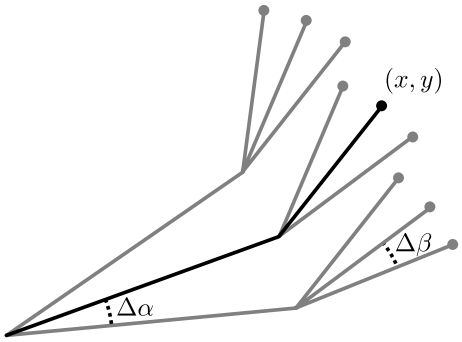

Fig. A.3 Spatial offset introduced by a measurement error of a single count in one or both joint encoders.

The symmetry of the workspace first implies that the resolution is independent of the orientation, and therefore of joint angle α. The angle is set to 0 and the Jacobian simplified to the following expression:

$$J_0 = a \begin{bmatrix} -\sin 0 - k\sin\beta & -k\sin\beta \\ \cos 0 + k\cos\beta & k\cos\beta \end{bmatrix} \tag{A.20}$$

$$= a \begin{bmatrix} -k\sin\beta & -k\sin\beta \\ 1 + k\cos\beta & k\cos\beta \end{bmatrix} \tag{A.21}$$

Given joint angle errors $\Delta\alpha$ and $\Delta\beta$, the position error can then be decomposed into its Cartesian components:

$$\begin{bmatrix} \Delta x \\ \Delta y \end{bmatrix} = J_0 \begin{bmatrix} \Delta\alpha \\ \Delta\beta \end{bmatrix} \tag{A.22}$$

$$= a \begin{bmatrix} -k\sin\beta & -k\sin\beta \\ 1+k\cos\beta & k\cos\beta \end{bmatrix} \begin{bmatrix} \Delta\alpha \\ \Delta\beta \end{bmatrix} \tag{A.23}$$

$$= a \begin{bmatrix} -k(\Delta\alpha+\Delta\beta)\sin\beta \\ (1+k\cos\beta)\Delta\alpha + k\Delta\beta\cos\beta \end{bmatrix} \tag{A.24}$$

$$= a \begin{bmatrix} -k(\Delta\alpha+\Delta\beta)\sin\beta \\ \Delta\alpha + k(\Delta\alpha+\Delta\beta)\cos\beta \end{bmatrix} \tag{A.25}$$

The position error is then computed as $e(a,k,\beta) = \sqrt{\Delta x^2 + \Delta y^2}$. Using the notation $s_\beta = \sin\beta$ and $c_\beta = \cos\beta$ for compactness, the square of the error can be expressed as:

$$e^2(\beta) = (\Delta x)^2 + (\Delta y)^2 \tag{A.26}$$

$$= a^2\left[k^2(\Delta\alpha+\Delta\beta)^2{s_\beta}^2 + (\Delta\alpha + k(\Delta\alpha+\Delta\beta)c_\beta)^2\right] \tag{A.27}$$

$$= a^2\left[k^2(\Delta\alpha+\Delta\beta)^2{s_\beta}^2 + \Delta\alpha^2 + 2k\Delta\alpha(\Delta\alpha+\Delta\beta)c_\beta + k^2(\Delta\alpha+\Delta\beta)^2{c_\beta}^2\right] \tag{A.28}$$

$$= a^2\left[k^2(\Delta\alpha+\Delta\beta)^2({s_\beta}^2+{c_\beta}^2) + \Delta\alpha^2 + 2k\Delta\alpha(\Delta\alpha+\Delta\beta)c_\beta\right] \tag{A.29}$$

$$= a^2\left[k^2(\Delta\alpha+\Delta\beta)^2 + \Delta\alpha^2 + 2k\Delta\alpha(\Delta\alpha+\Delta\beta)c_\beta\right] \tag{A.30}$$

Assuming that identical encoders with a resolution Δ are used, the error term can be simplified by considering all possible combinations of $\Delta\alpha \in [-\Delta, 0, +\Delta]$ and $\Delta\beta \in [-\Delta, 0, +\Delta]$. The square of the error can then be expressed as:

$$e^2(\beta) = a^2\Delta^2 \begin{cases} k^2 & \text{if } \Delta\alpha = 0 \text{ and } \Delta\beta = \pm\Delta, \\ k^2 + 2k\cos\beta + 1 & \text{if } \Delta\alpha = \pm\Delta \text{ and } \Delta\beta = 0, \\ 4k^2 + 4k\cos\beta + 1 & \text{if } \Delta\alpha = \Delta\beta = \pm\Delta, \\ 1 & \text{if } \Delta\alpha = -\Delta\beta = \pm\Delta \end{cases} \tag{A.31}$$

An upper bound can therefore be found by determining the worst-case position error for different values of k and β:

$$e^2(\beta) \leq a^2\Delta^2 \max_{i\in 1\ldots 4} f_i(\beta) \tag{A.32}$$

where

$$f_1(\beta) = k^2 \tag{A.33}$$
$$f_2(\beta) = k^2 + 2k\cos\beta + 1 \tag{A.34}$$
$$f_3(\beta) = 4k^2 + 4k\cos\beta + 1 \tag{A.35}$$
$$f_4(\beta) = 1 \tag{A.36}$$

It will first be shown that f_1 cannot be greater than both f_3 and f_4 and is therefore never maximal. f_1 is greater than f_4 if and only if:

$$f_1(\beta) > f_4(\beta) \tag{A.37}$$
$$k^2 > 1 \tag{A.38}$$
$$k > 1 \tag{A.39}$$

It is however greater than f_3 if and only if:

$$f_1(\beta) > f_3(\beta) \tag{A.40}$$
$$k^2 > 4k^2 + 4k\cos\beta + 1 \tag{A.41}$$
$$(-3k^2 - 1)/4k > \cos\beta \tag{A.42}$$

The left-hand side is monotonically decreasing and therefore has its maximum at the lower limit $k = 0$, which results in a value of -1. This in turn implies that $\cos\beta < -1$ which is impossible by definition. It can similarly be shown that f_2 is never greater than both f_3 and f_4:

$$f_2(\beta) > f_3(\beta) \tag{A.43}$$
$$k^2 + 2k\cos\beta + 1 > 4k^2 + 4k\cos\beta + 1 \tag{A.44}$$
$$\cos\beta < -3k/2 \tag{A.45}$$

$$f_2(\beta) > f_4(\beta) \tag{A.46}$$
$$k^2 + 2k\cos\beta + 1 > 1 \tag{A.47}$$
$$\cos\beta > -k/2 \tag{A.48}$$

These two inequalities are contradictory since $-3k/2 < -k/2$. The maximum error is therefore found by comparing f_3 and f_4:

$$f_3(\beta) > f_4(\beta) \tag{A.49}$$
$$4k^2 + 4k\cos\beta + 1 > 1 \tag{A.50}$$
$$\cos\beta > -k \tag{A.51}$$

This inequality is always true if $k > 1$. It is otherwise true within the range $\beta \in [0, \pi]$ when $\beta < \arccos -k$. The upper bound on the position error can therefore be expressed as:

$$e_{max}(\beta) = a\Delta \begin{cases} \sqrt{4k^2 + 4k\cos\beta + 1} & \text{if } \beta > \arccos -k \text{ or } k > 1, \\ 1 & \text{otherwise.} \end{cases} \tag{A.52}$$

Alternatively, the position error can be expressed in terms of the distance r between the end effector and the origin. Using the inverse kinematics of the linkage, condition A.51 can be rewritten as:

$$\cos\beta > -k \tag{A.53}$$

$$\frac{r^2 - a^2(1+k^2)}{2ka^2} > -k \tag{A.54}$$

$$r^2 - a^2(1+k^2) > -2k^2a^2 \tag{A.55}$$

$$r^2 > -k^2a^2 + a^2 \tag{A.56}$$

$$r^2 > a^2(1-k^2) \tag{A.57}$$

$$r > a\sqrt{1-k^2} \tag{A.58}$$

The first term of the position error can similarly be rewritten as:

$$a\Delta\sqrt{4k^2 + 4k\cos\beta + 1} = a\Delta\sqrt{4k^2 + 4k\frac{r^2 - a^2(1+k^2)}{2ka^2} + 1} \tag{A.59}$$

$$= a\Delta\sqrt{4k^2 + \frac{2r^2}{a^2} - 2 - 2k^2 + 1} \tag{A.60}$$

$$= a\Delta\sqrt{2k^2 + \frac{2r^2}{a^2} - 1} \tag{A.61}$$

$$= \Delta\sqrt{2r^2 + a^2(2k^2 - 1)} \tag{A.62}$$

The maximum position error, or resolution, can therefore be written either in terms of joint angle β:

$$e_{max}(\beta) = a\Delta \begin{cases} \sqrt{4k^2 + 4k\cos\beta + 1} & \text{if } \beta > \arccos -k \text{ or } k > 1, \\ 1 & \text{otherwise;} \end{cases} \tag{A.63}$$

or equivalently in terms of the radial distance r:

$$e_{max}(r) = \Delta \begin{cases} \sqrt{2r^2 + a^2(2k^2 - 1)} & \text{if } r > a\sqrt{1-k^2} \text{ or } k > 1, \\ a & \text{otherwise.} \end{cases} \tag{A.64}$$

Inspection of Equations A.63 and A.64 shows that the resolution increases mono-

tonically from a minimum of $a\Delta\sqrt{4k^2+4k+1}$ as the linkage bends from its fully extended position. The maximal resolution of $a\Delta$ is reached when $\beta = \arccos(-k)$, or equivalently $r > a\sqrt{1-k^2}$, and maintained as the linkage is further bent. The resolution moreover decreases as the length of the links is increased.

Reachable Workspace

A two-link planar linkage has a reachable workspace in the shape of an annulus. The bounds of the circular workspace are first derived while taking into account constraints imposed by the design of the Tactograph. A rectangular workspace is then fitted within the circular workspace, allowing optimal link lengths to be determined for any ratio k.

Annular Workspace

The reachable workspace of a two-link planar linkage has an annulus shape with bounds determined by the position of the end effector when completely folded or extended. The physical design of the Tactograph imposes three further constraints:

1. A distance R_{min} must be maintained between the end effector and the first joint to prevent contact between the tactile display enclosure and the linkage fixture.

2. The range of motion of the second joint must be restricted to prevent contact between the rigid links.

3. A clearance of D must be maintained between the center of the slider and the first link.

The upper and lower bounds of the annulus-shaped workspace are determined by these three constraints. The first constraint imposes a lower bound on the distance r:

$$r > R_{min} \tag{A.65}$$

The second constraint imposes bounds on r corresponding to the extreme positions of the arm (Figure A.4a). Given joint angle β and referring to Figure A.4b, the distance r can be expressed as:

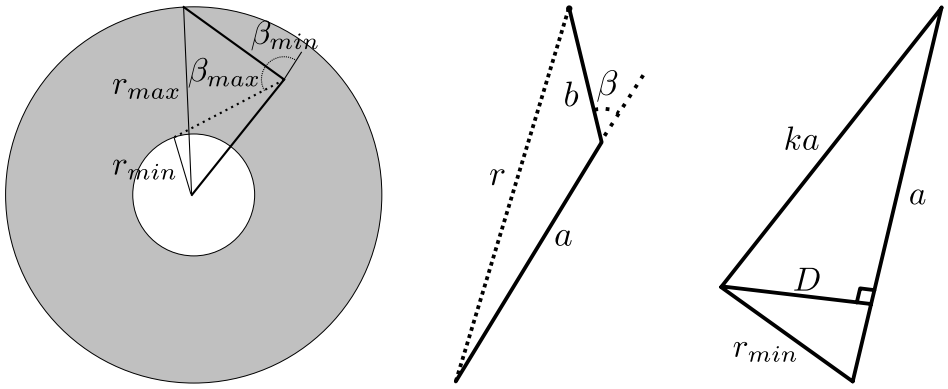

Fig. A.4 (a) Workspace resulting from a restriction in the range of β, (b) computation of distance r as a function of β, and (c) computation of the lower bound of r necessary to maintain a clearance D between the first link and end effector.

$$r = \sqrt{a^2 + b^2 - 2ab\cos(\pi - \beta)} \tag{A.66}$$
$$= \sqrt{a^2 + b^2 + 2ab\cos\beta} \tag{A.67}$$
$$= a\sqrt{k^2 + 2k\cos\beta + 1} \tag{A.68}$$

The workspace is therefore restricted to the range:

$$a\sqrt{k^2 + 2k\cos\beta_{max} + 1} < r < a\sqrt{k^2 + 2k\cos\beta_{min} + 1} \tag{A.69}$$

The third constraint finally imposes a further lower limit on the distance r. Referring to Figure A.4c, the minimal distance r required to maintain a clearance of D between the center of the slider and the first link can be expressed as:

$$r > \sqrt{D^2 - (a - \sqrt{k^2a^2 - D^2})^2} \tag{A.70}$$

Taking all three constraints into consideration, the reachable workspace can be expressed as:

$$r_{min} < r < r_{max} \tag{A.71}$$

where

$$r_{min} = max \begin{cases} a\sqrt{k^2 + 2k\cos\beta_{max} + 1} \\ R_{min} \\ \sqrt{D^2 - (a - \sqrt{k^2a^2 - D^2})^2} \end{cases} \tag{A.72}$$

$$r_{max} = a\sqrt{k^2 + 2k\cos\beta_{min} + 1} \tag{A.73}$$

Rectangular Workspace

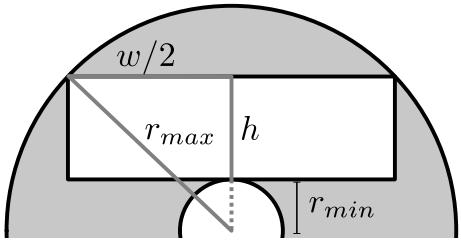

Fig. A.5 Geometric properties of the largest rectangular workspace fitting within an annular workspace.

The design of Tactograph requires a rectangular workspace to be fitted within the annular workspace of the serial linkage. Equation A.64 indicates that the resolution decreases with the distance from the origin as well as the length of the links. For optimal resolution, the rectangular workspace should therefore be placed as close as possible to the first joint and occupy as much of the annular workspace as possible so as to minimize the length of the links. The relation between the dimensions $w \times h$ of the largest rectangular workspace and the bounds of the annular workspace r_{min} and r_{max} is illustrated in Figure A.5 and expressed mathematically as:

$$r_{max}^2 = (w/2)^2 + (h + r_{min})^2 \tag{A.74}$$

This equation can be used in combination with Equation A.71 to numerically search for the minimal length of the first link a necessary to respect all constraints for a given set of link ratio k and workspace dimensions. The offset r_{min}, and hence

the location of the rectangular workspace, can then be computed.

Linkage Optimization

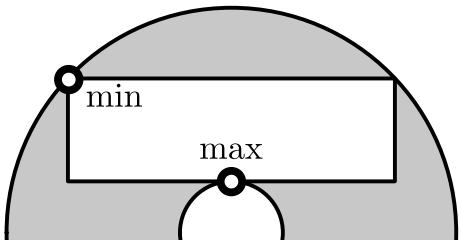

(a)

Fig. A.6 Points of minimal and maximal resolution within the rectangular workspace.

Since the resolution decreases with the distance from the origin, the design of the linkage can be optimized for spatial resolution by considering the effect of parameter variations on only the points closest and furthest away from the first joint within the rectangular workspace. This corresponds to the two extreme points illustrated in Figure A.6.

As previously noted, the minimal length a and workspace offset r_{min} necessary to respect the constraints of the Tactograph design can be computed for a given link length ratio k. The resolution, or maximum position error, at the two points of interest can therefore be plotted against different value of k to find optimal link lengths.

This optimization process is performed using the following specifications of the Tactograph:

1. The workspace is rectangular and letter-sized: $w = 279.4\,\text{mm}$, $h = 215.9\,\text{mm}$.

2. The range of motion of joint angle β is restricted to 140°: $\beta_{min} = 20°$, $\beta_{max} = 160°$.

3. The tactile display enclosure and the first encoder have a radius of 66.5 mm and 14.1 mm respectively. The minimal distance between the end effector and the first joint is therefore set to 120 mm to prevent any risk of contact: $R_{min} = 120\,\text{mm}$.

4. The base of the end effector has a radius of 37.5 mm and the first link a width of 12.7 mm. The minimal clearance is therefore set to 50 mm: $D = 50\,\text{mm}$.

5. The high-resolution encoders have 65,536 counts per revolution: $\Delta = 19.8''$.

Figure A.7a shows the effect of variations of the link length ratio k on the minimal and maximal resolution over the workspace. The minimal resolution is optimal at 47.8 µm with $k = 0.57$ and $a = 234.23\,\text{mm}$. The maximal resolution, on the other hand, is optimal at 19.6 µm with $k = 0.81$ and $a = 204.16\,\text{mm}$. Figure A.7b illustrates the effect of scaling both link lengths by a factor g and confirms that the shortest link lengths are optimal.

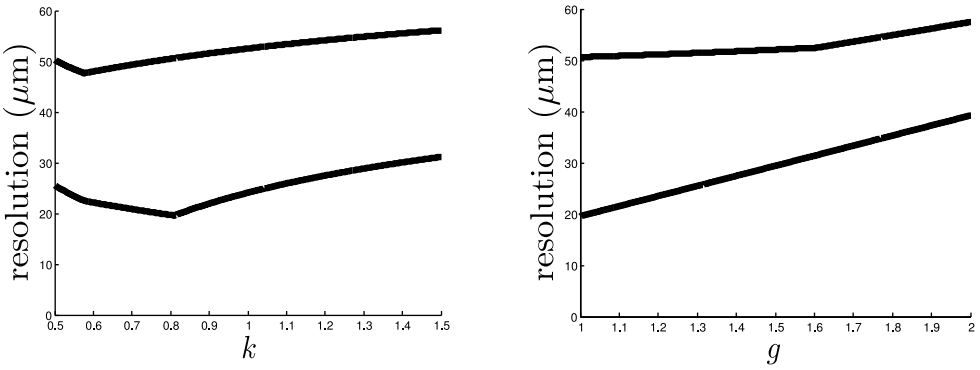

Fig. A.7 Minimum and maximum resolution within the workspace as a function of (a) link length ratio k and (b) link length scaling factor g.

Given the small effect on resolution, the length of the links is optimized for the maximal resolution point such that the first link is shorter and encumbrance reduced. The link lengths are set to $a = 210\,\text{mm}$ and $b = 170\,\text{mm}$ ($k = 0.81$), resulting in a resolution ranging from 20.2 to 50.6 µm over the workspace as illustrated in Figure A.8. The rectangular workspace is offset by 120 mm and therefore extends horizontally from -139.7 to 139.7 mm and vertically from 120.0 to 335.9 mm.

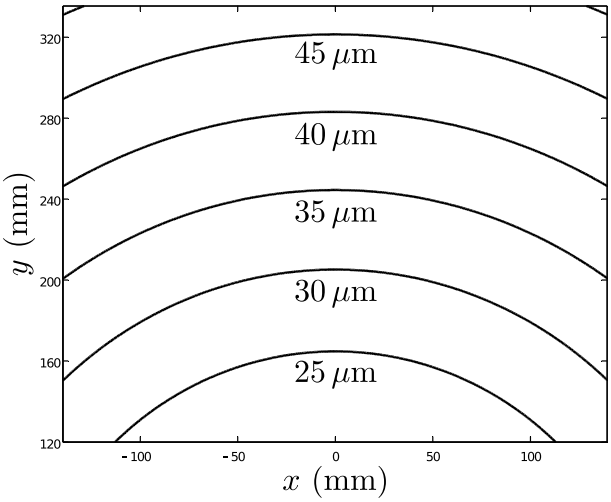

Fig. A.8 Resolution of the Tactograph carrier over its rectangular workspace.

Technical Drawings

The following technical drawings describe in details the design and specifications of the different components of the Tactograph carrier and enclosure.

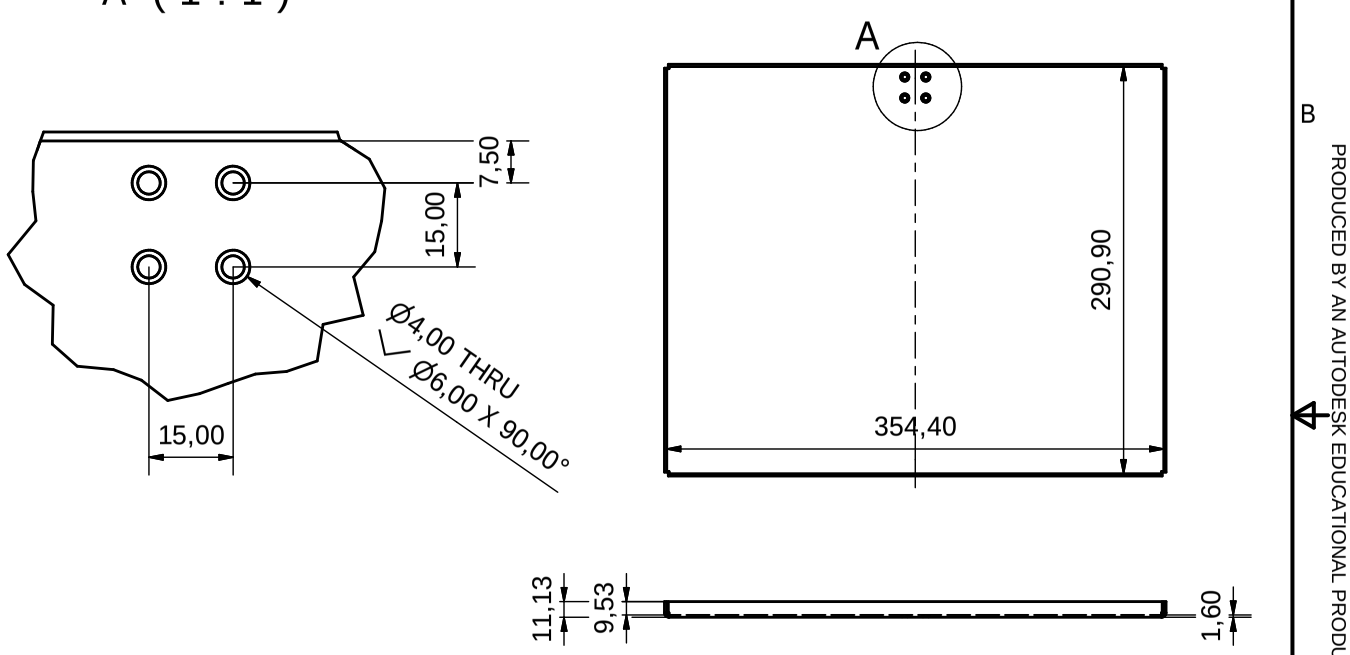

Designed by	Checked by	Approved by	Date		Date	
V. Levesque					21/01/2008	

Haptics Lab, McGill University	Base Tray		
		Edition	Sheet
		1	1 / 1

Material: aluminum (1.6 mm thickness)

PRODUCED BY AN AUTODESK EDUCATIONAL PRODUCT

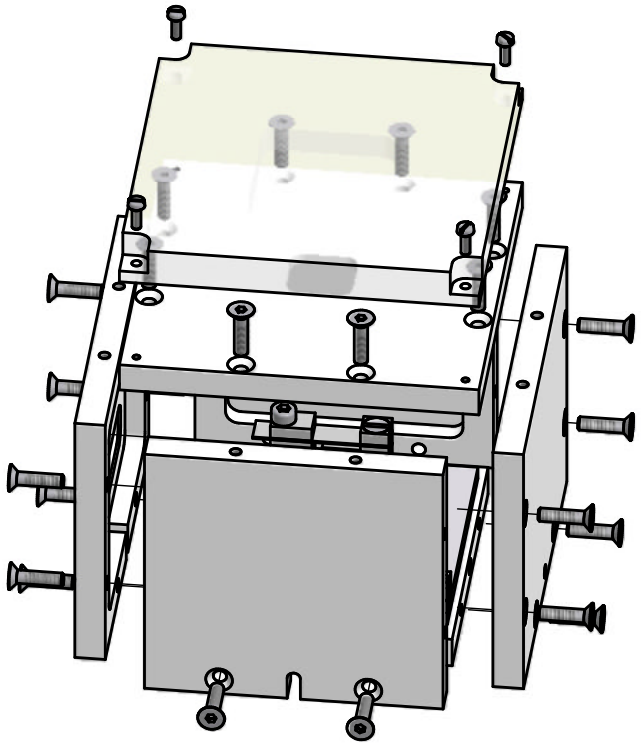

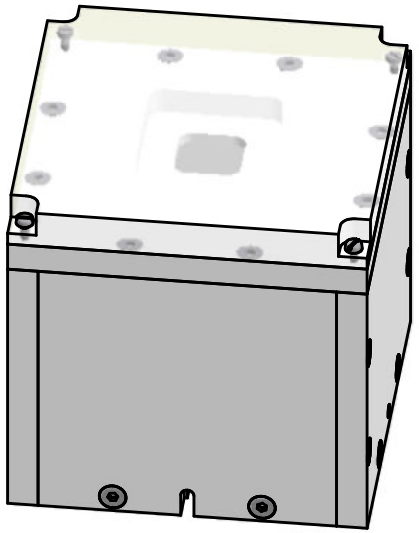

Designed by	Checked by	Approved by	Date		Date	
V. Levesque					21/01/2008	

Haptics Lab, McGill University	Enclosure		
		Edition 1	Sheet 1 / 1

PRODUCED BY AN AUTODESK EDUCATIONAL PRODUCT

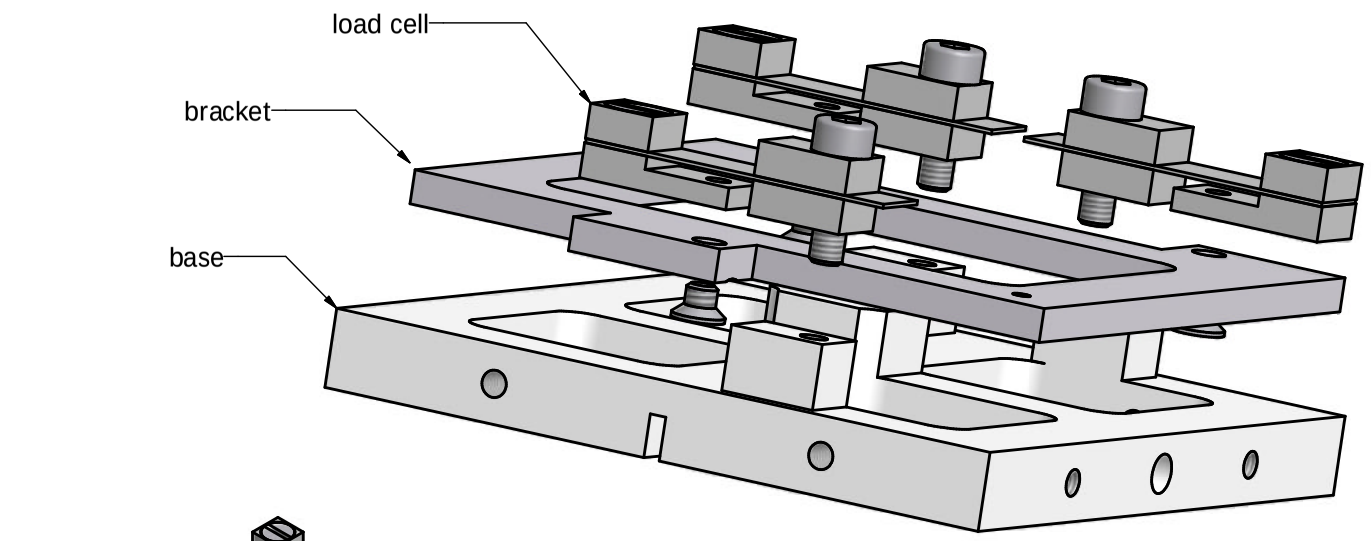

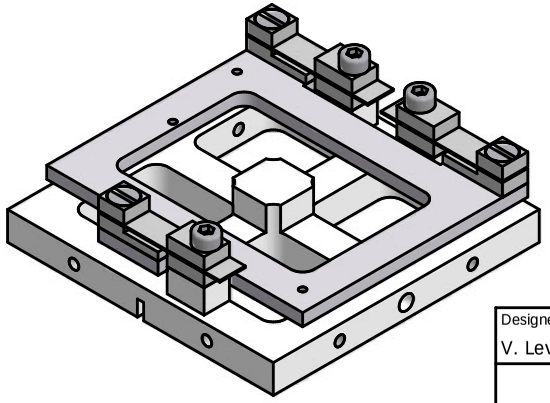

Designed by	Checked by	Approved by	Date		Date	
V. Levesque					21/01/2008	

Haptics Lab, McGill University	Load Sensor		
		Edition 1	Sheet 1 / 1

PRODUCED BY AN AUTODESK EDUCATIONAL PRODUCT

Zeroing Slots (2)

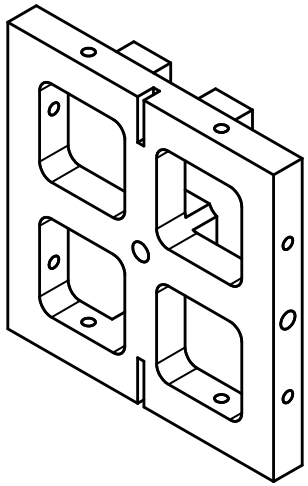

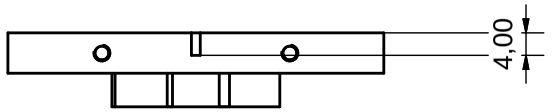

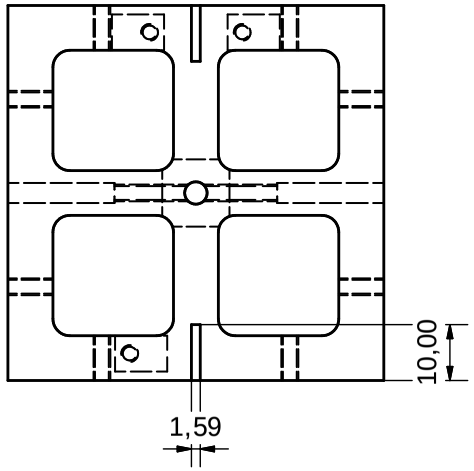

Designed by	Checked by	Approved by	Date		Date	
V. Levesque					05/02/2008	

Haptics Lab, McGill University	Enclosure Base		
		Edition 1	Sheet 3 / 3

PRODUCED BY AN AUTODESK EDUCATIONAL PRODUCT

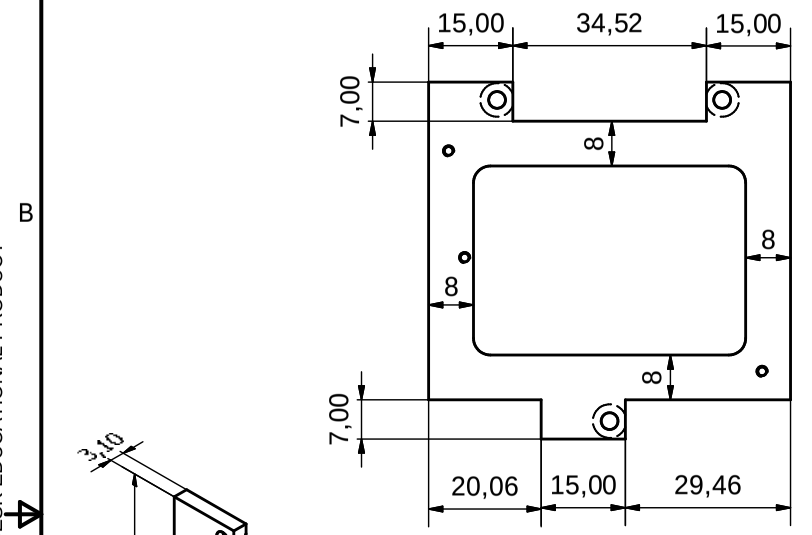

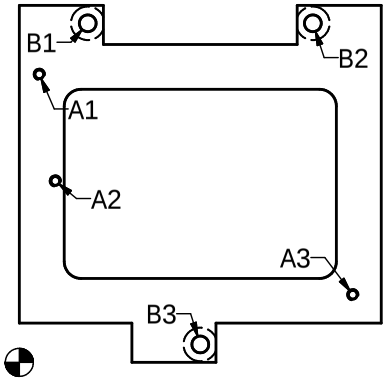

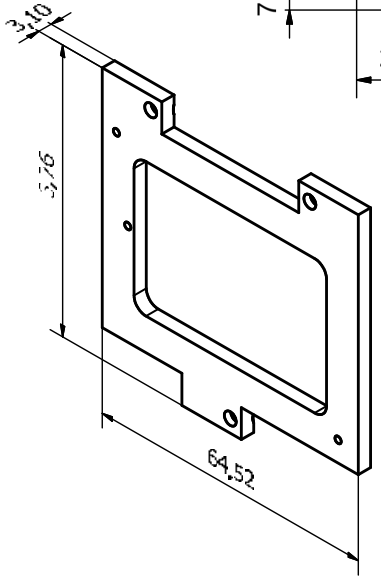

Material: aluminum

Hole Table			
HOLE	XDIM	YDIM	DESCRIPTION
A1	3,56	51,45	M2x0.4 - 6H
A2	6,42	32,40	M2x0.4 - 6H
A3	59,44	12,08	M2x0.4 - 6H
B1	12,20	60,56	Ø3,00 THRU ⌵ Ø6,00 X 90,00°
B2	52,32	60,56	Ø3,00 THRU ⌵ Ø6,00 X 90,00°
B3	32,26	3,20	Ø3,00 THRU ⌵ Ø6,00 X 90,00°

Designed by	Checked by	Approved by	Date	Date
V. Levesque				05/02/2008

Haptics Lab, McGill University

Enclosure Bracket

Edition 1

Sheet 1 / 1

PRODUCED BY AN AUTODESK EDUCATIONAL PRODUCT

FRONT

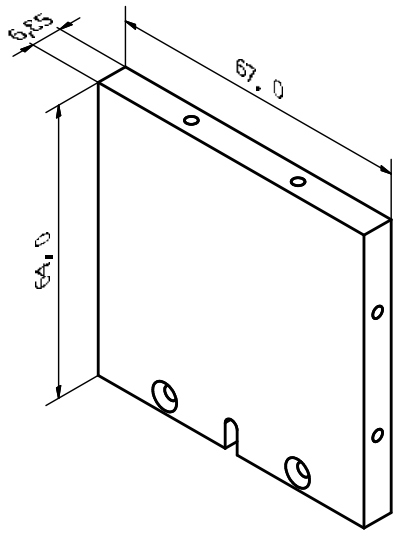

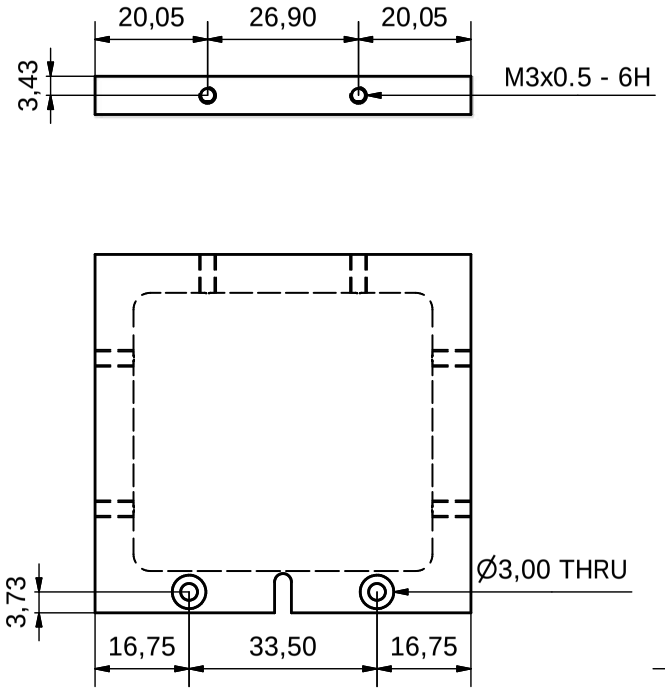

Designed by	Checked by	Approved by	Date		Date	
V. Levesque					21/01/2008	

Haptics Lab, McGill University	Enclosure Side (back/front)		
		Edition 1	Sheet 1 / 2

BACK

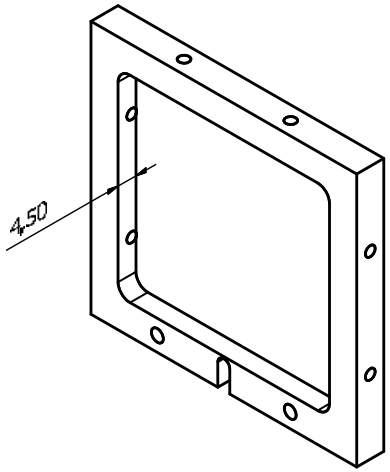

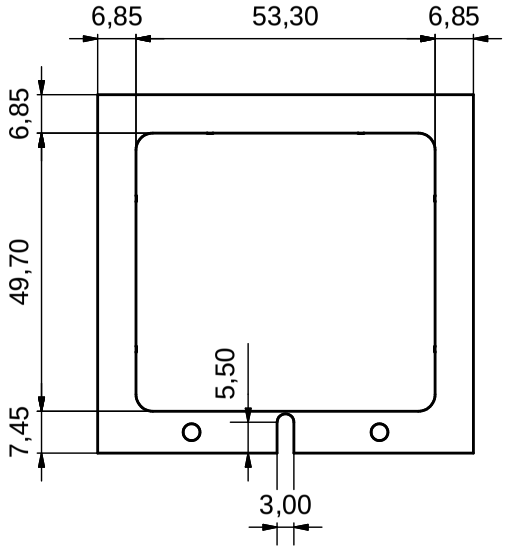

Designed by	Checked by	Approved by	Date		Date	
V. Levesque					21/01/2008	

Material: delrin

Haptics Lab, McGill University

Enclosure Side (back/front)

Edition	Sheet
1	2 / 2

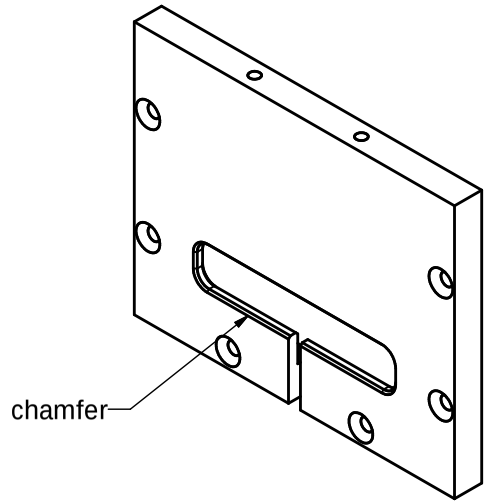

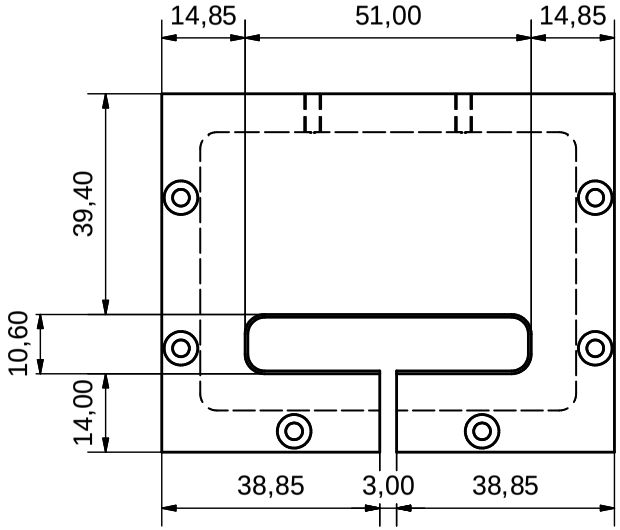

Designed by	Checked by	Approved by	Date		Date	
V. Levesque					21/01/2008	

Haptics Lab, McGill University	Enclosure Side (left)		
		Edition 1	Sheet 1 / 1

Material: delrin

FRONT

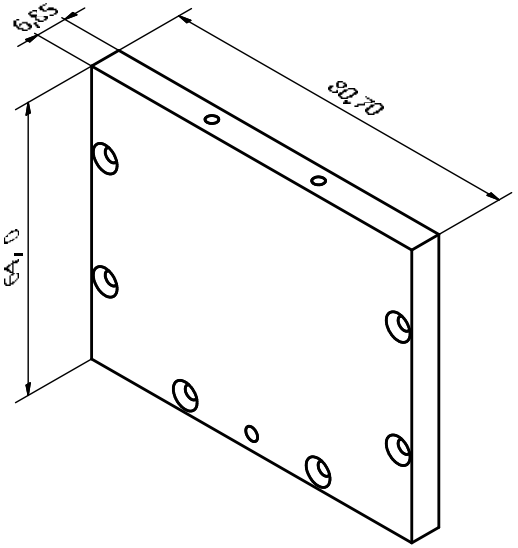

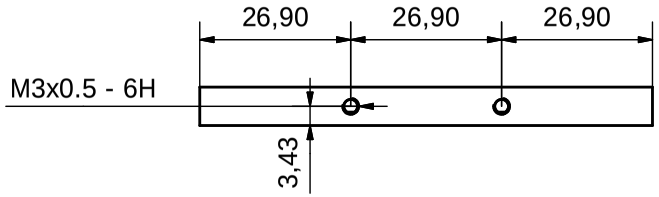

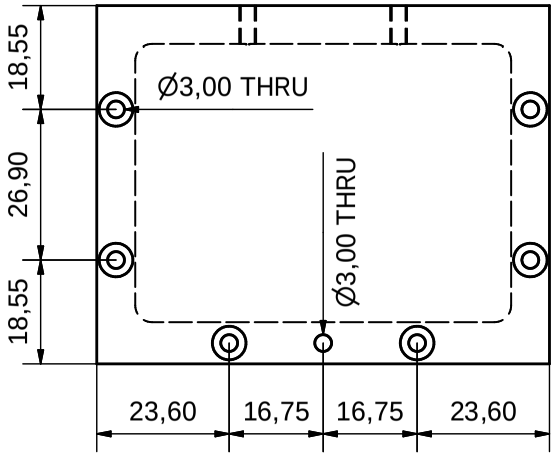

Designed by	Checked by	Approved by	Date		Date	
V. Levesque					21/01/2008	

Material: delrin

Haptics Lab, McGill University

Enclosure Side (right)

Edition	Sheet
1	1 / 2

PRODUCED BY AN AUTODESK EDUCATIONAL PRODUCT

BACK

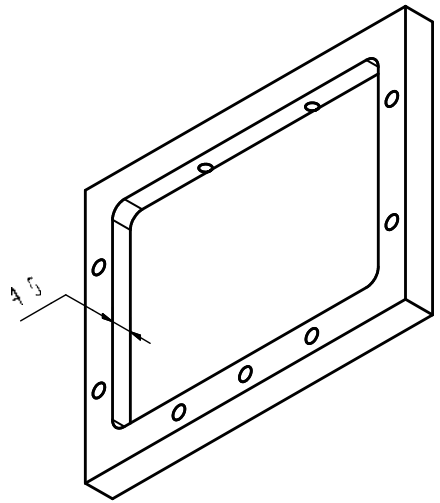

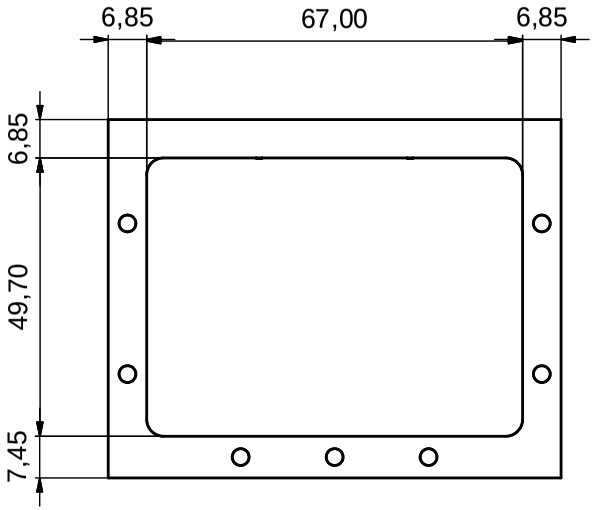

Designed by	Checked by	Approved by	Date		Date	
V. Levesque					21/01/2008	

Haptics Lab, McGill University	Enclosure Side (right)		
		Edition 1	Sheet 2 / 2

FRONT

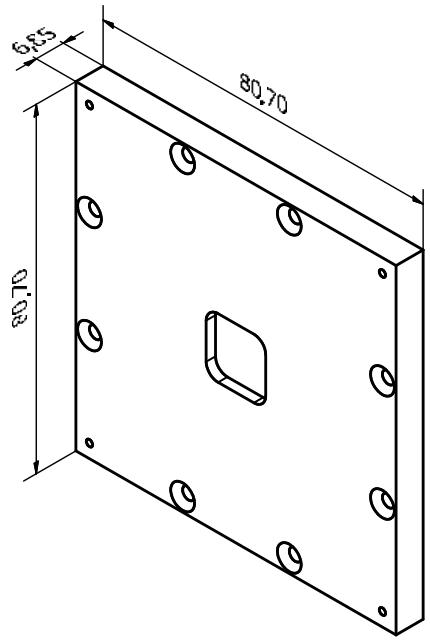

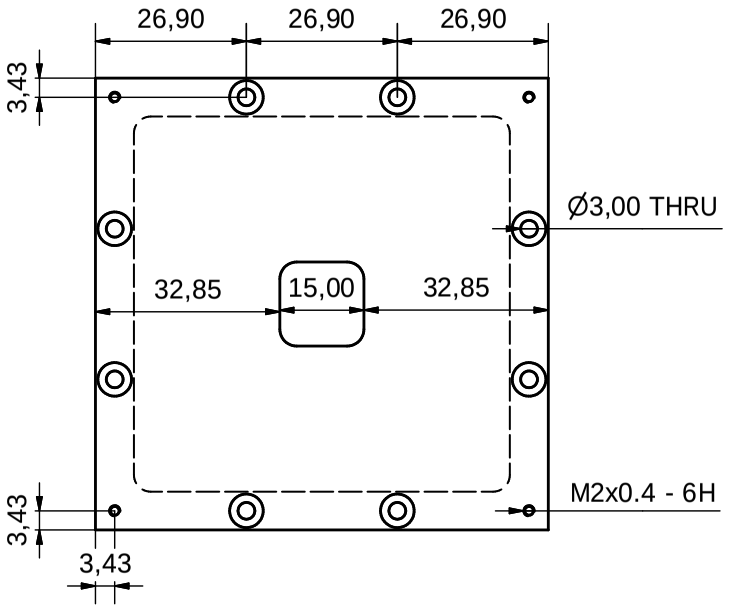

Designed by	Checked by	Approved by	Date		Date	
V. Levesque					21/01/2008	

Material: delrin

Haptics Lab, McGill University

Enclosure Top

Edition 1

Sheet 1 / 2

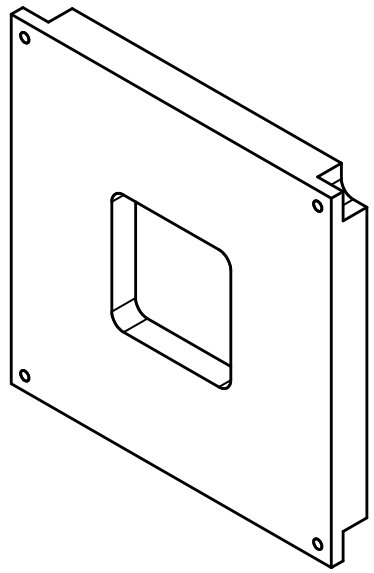

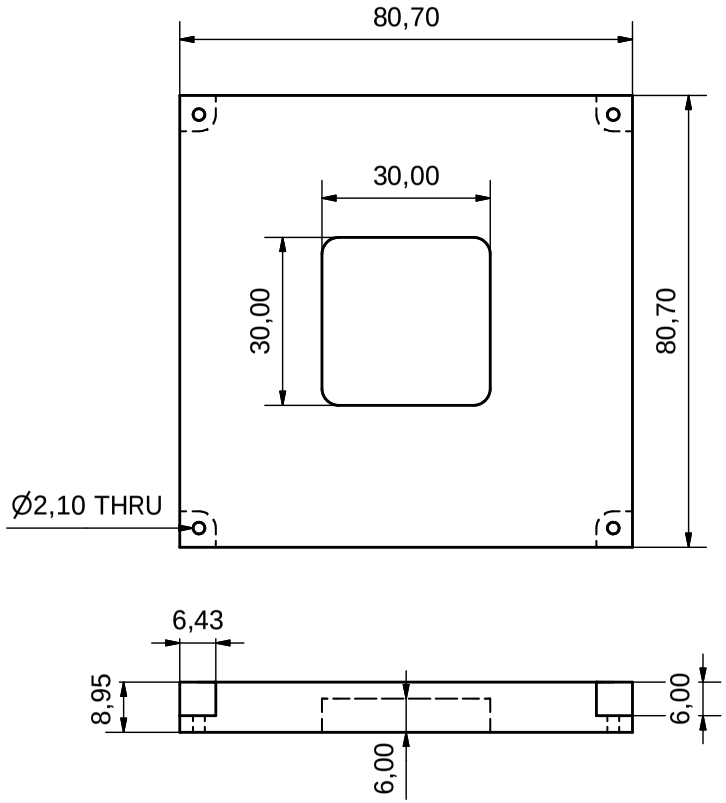

Material: plexiglass

Designed by	Checked by	Approved by	Date		Date	
V. Levesque					21/01/2008	

Haptics Lab, McGill University	Enclosure Cover		
		Edition 1	Sheet 1 / 1

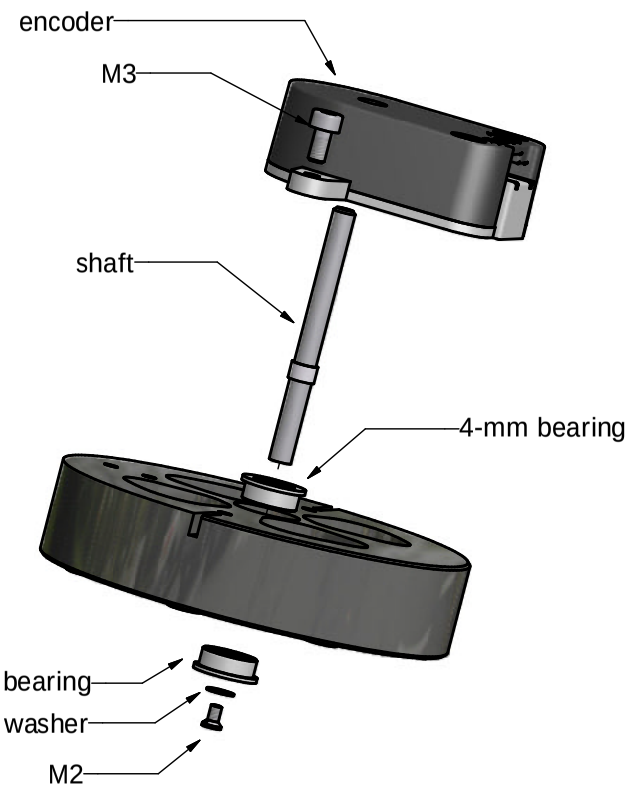

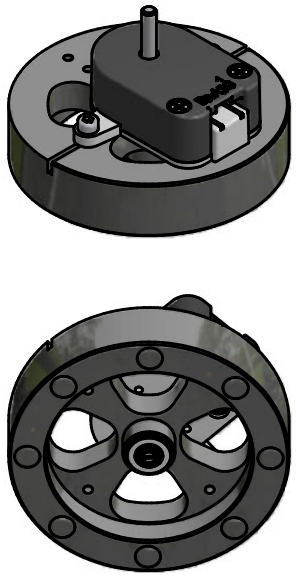

Designed by	Checked by	Approved by	Date		Date	
V. Levesque					21/01/2008	

Haptics Lab, McGill University	Original Slider		
		Edition 1	Sheet 1 / 1

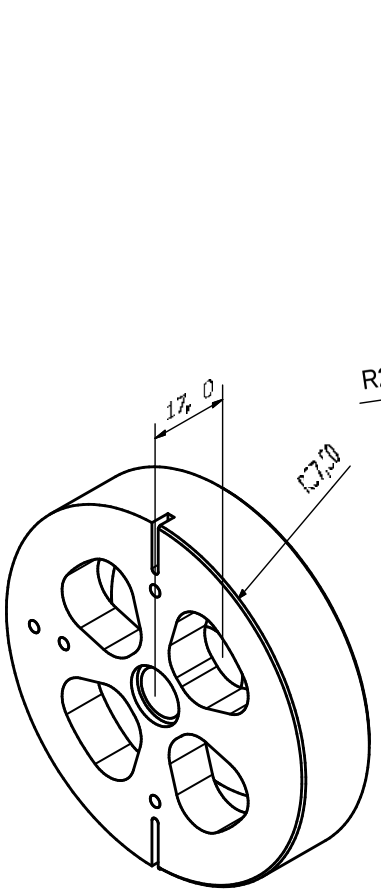

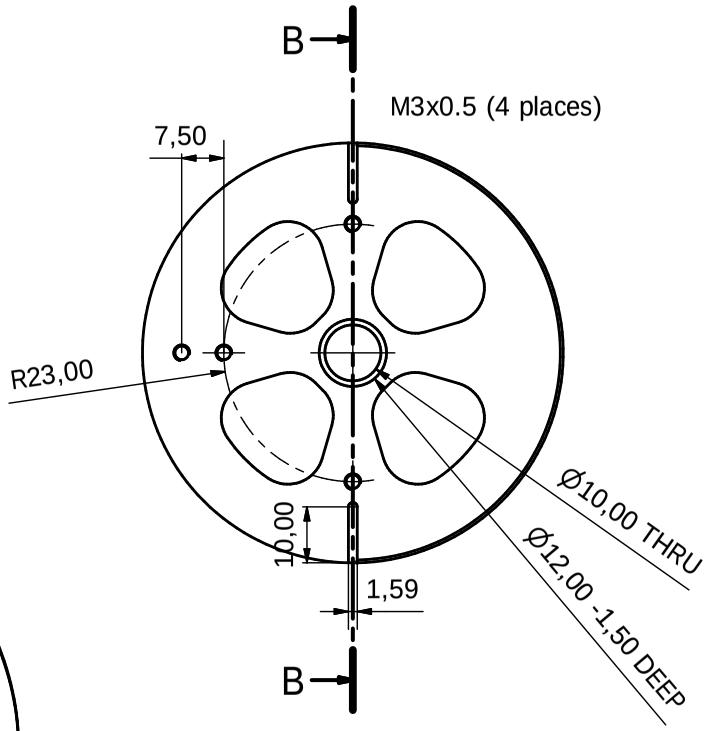

B-B (1 : 1)

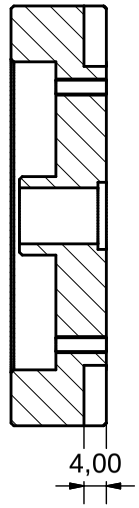

Designed by	Checked by	Approved by	Date		Date	
V. Levesque					05/02/2008	

Haptics Lab, McGill University	Original Sliding Disc		
		Edition 1	Sheet 1 / 2

Material: delrin

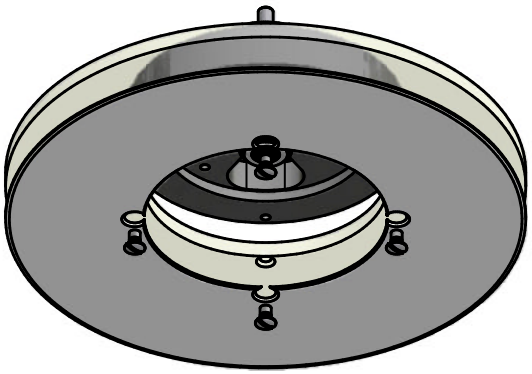

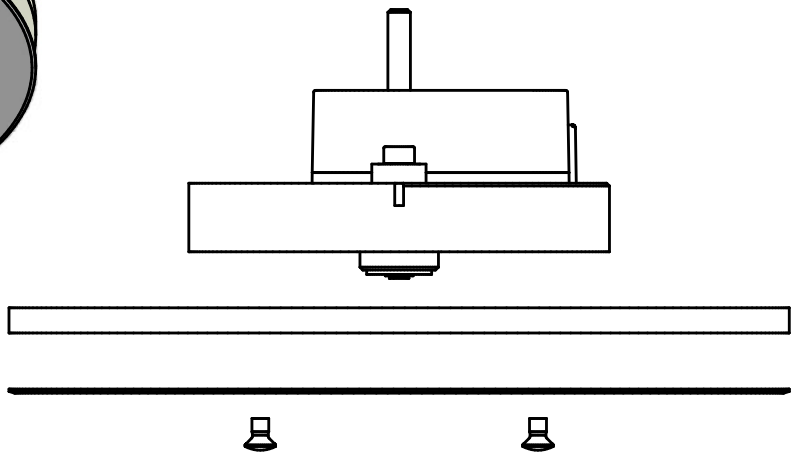

Designed by	Checked by	Approved by	Date		Date	
V. Levesque					21/01/2008	

Haptics Lab, McGill University	Revised Slider		
		Edition 2	Sheet 1 / 1

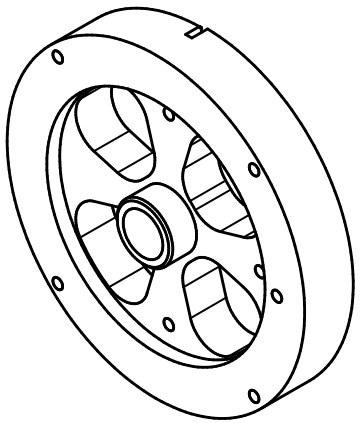

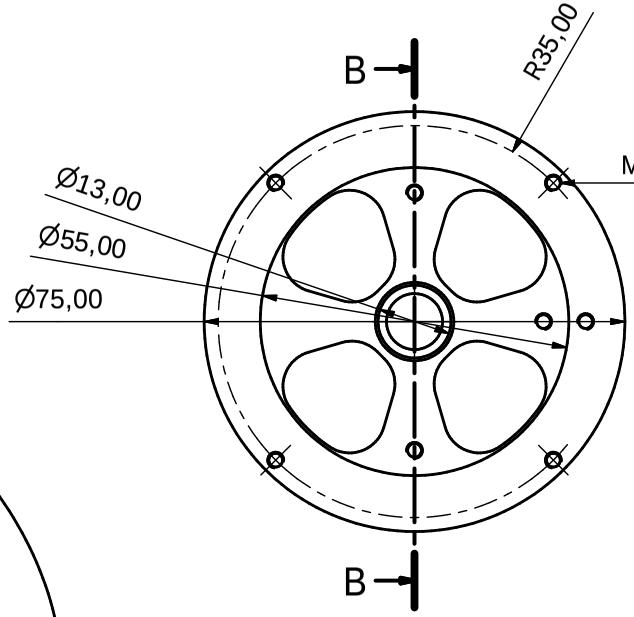

B-B (1 : 1)

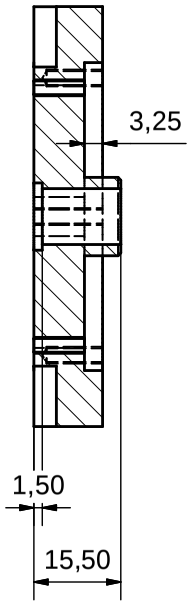

Designed by	Checked by	Approved by	Date		Date	
V. Levesque					27/01/2008	

Haptics Lab, McGill University	Revised Sliding Disc		
		Edition 2	Sheet 2 / 2

PRODUCED BY AN AUTODESK EDUCATIONAL PRODUCT

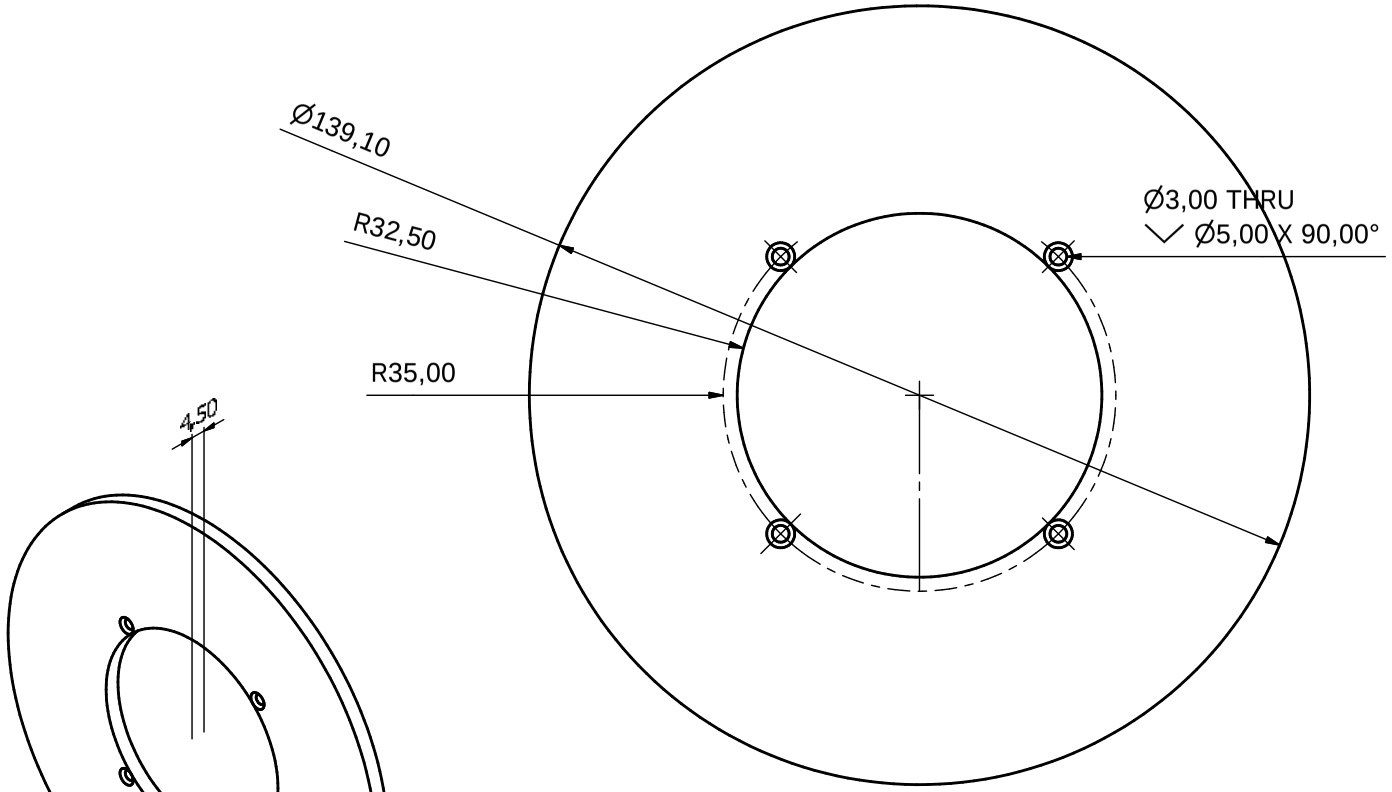

Designed by	Checked by	Approved by	Date		Date	
V. Levesque					21/01/2008	
Haptics Lab, McGill University		Acrylic Disc				
					Edition 2	Sheet 1 / 1

Material: acrylic (plexiglass)

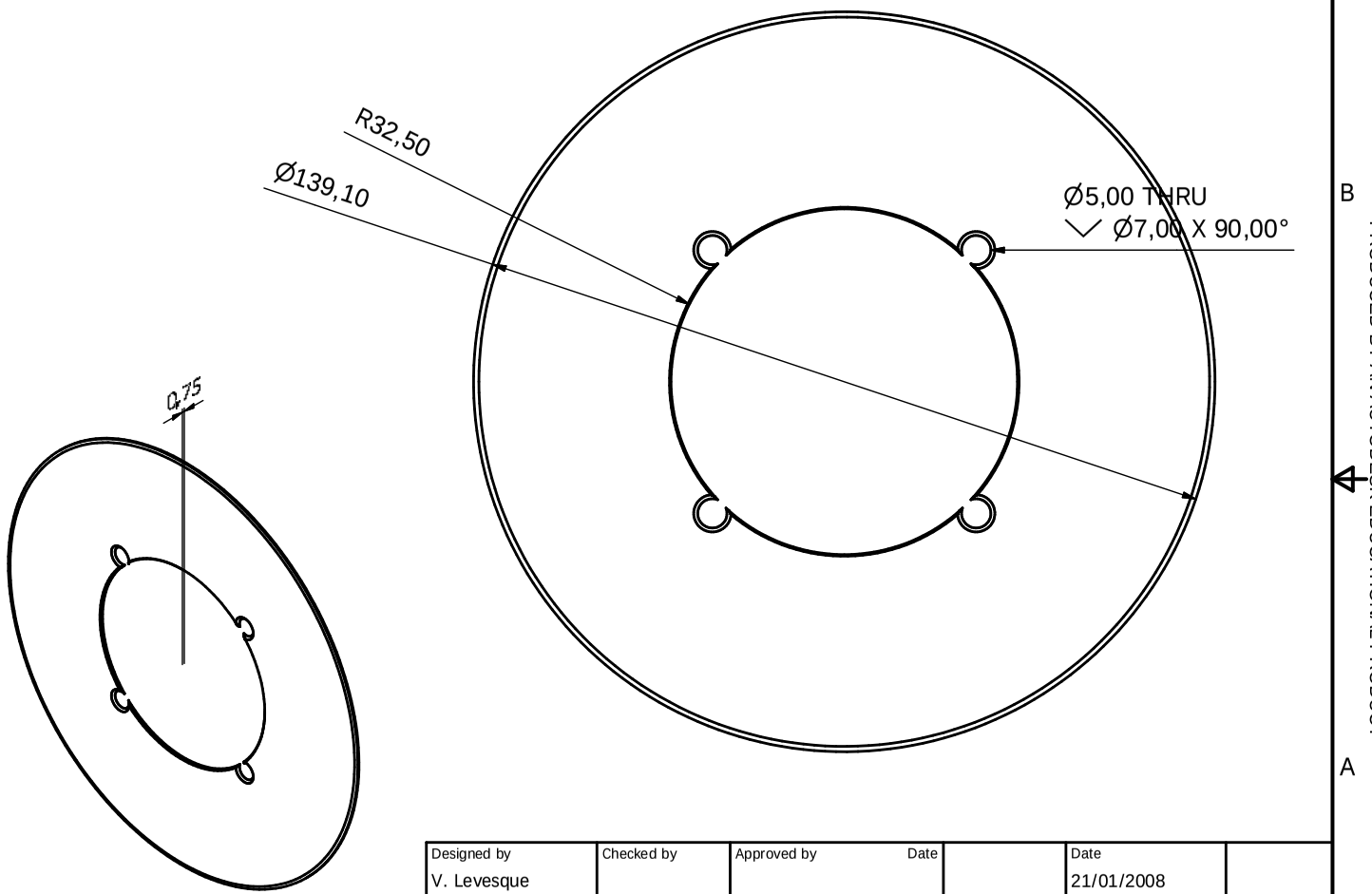

Designed by	Checked by	Approved by	Date		Date	
V. Levesque					21/01/2008	

Material: bondable teflon

Haptics Lab, McGill University

Teflon Disc

Edition 2

Sheet 1 / 1

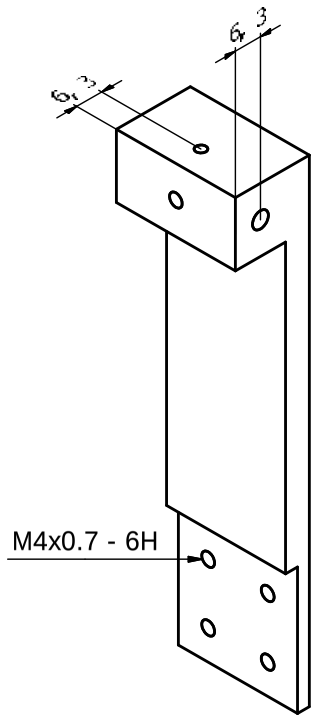

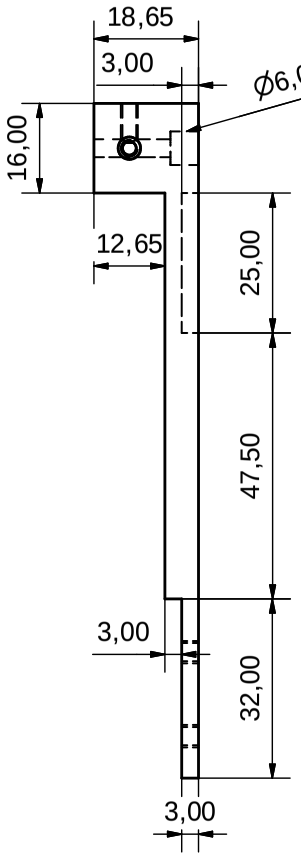

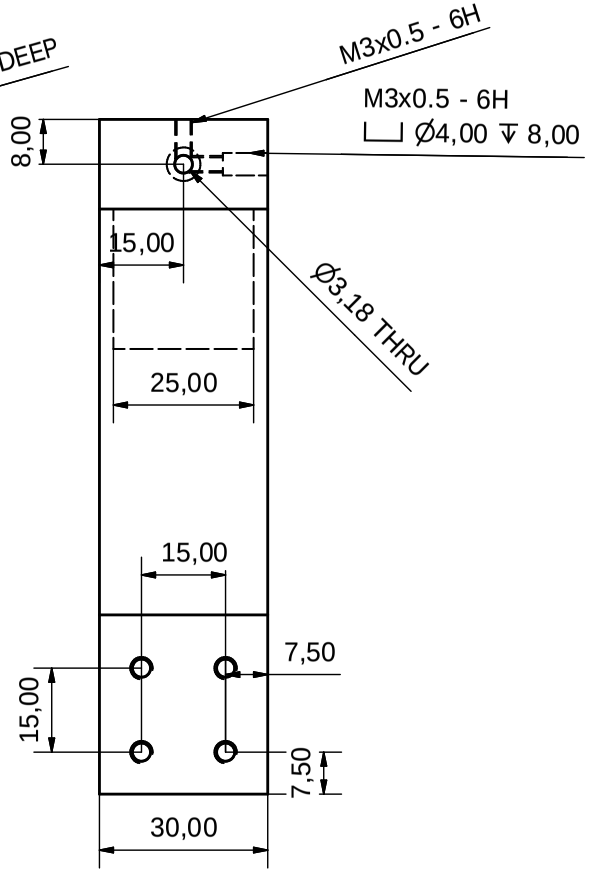

Designed by	Checked by	Approved by	Date		Date	
V. Levesque					21/01/2008	

Haptics Lab, McGill University	Fixture		
		Edition	Sheet
		1	1 / 1

Material: aluminum

PRODUCED BY AN AUTODESK EDUCATIONAL PRODUCT

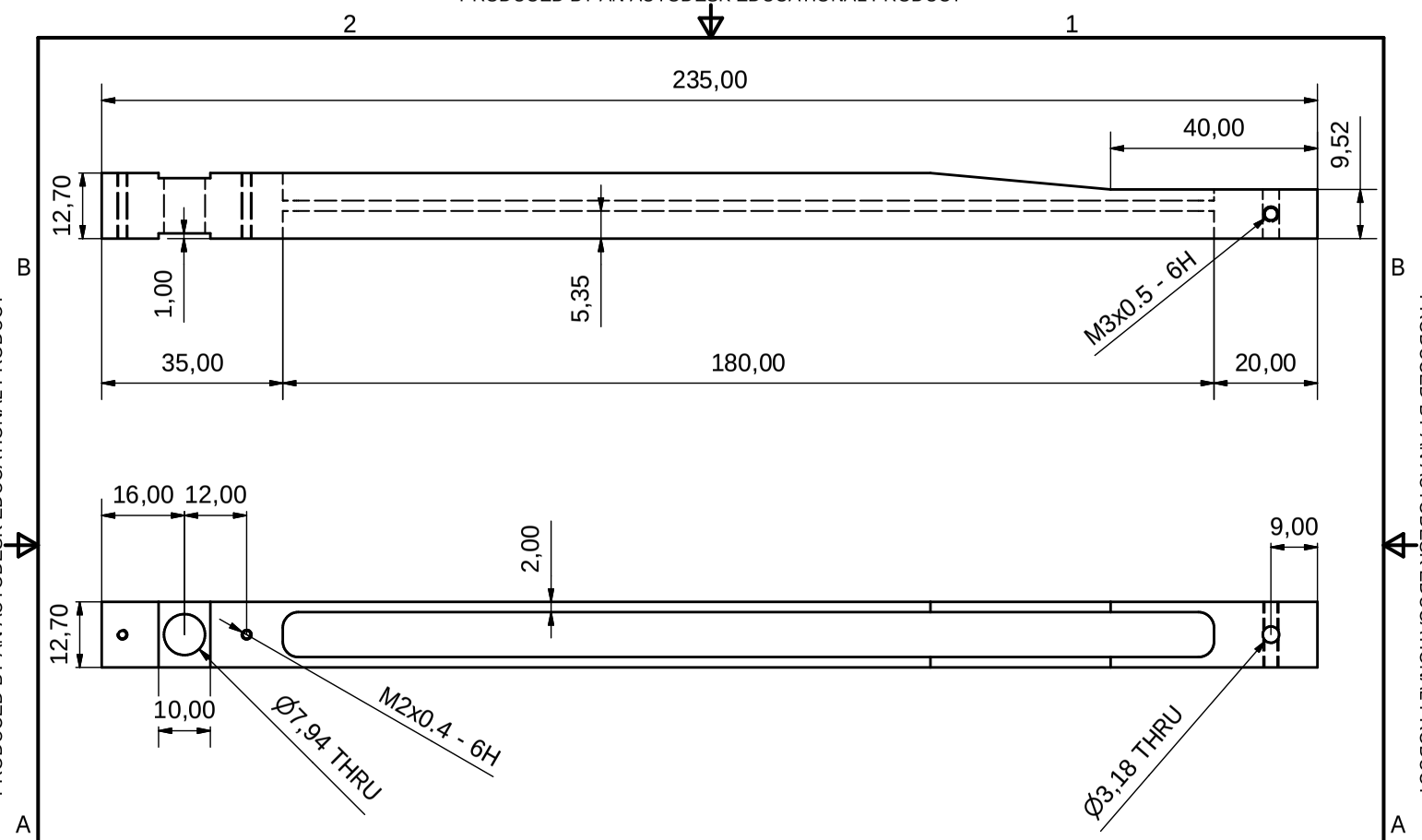

Designed by	Checked by	Approved by	Date		Date	
V. Levesque					21/01/2008	

Material: delrin

Haptics Lab, McGill University

First Link

Edition 1

Sheet 1 / 1

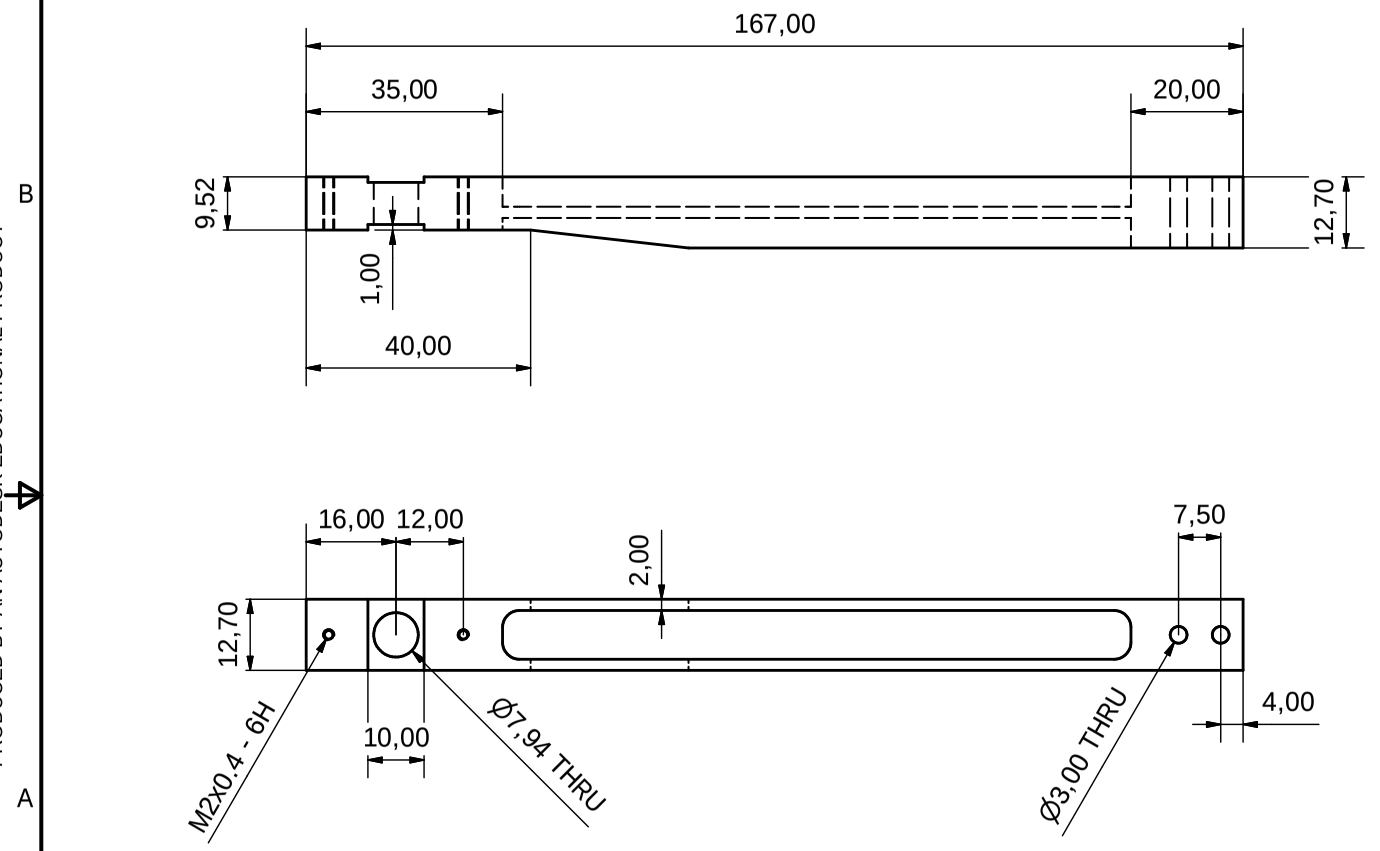

Designed by	Checked by	Approved by	Date		Date	
V. Levesque					04/02/2008	

Material: delrin

Haptics Lab, McGill University

Second Link

Edition 1

Sheet 1 / 1

PRODUCED BY AN AUTODESK EDUCATIONAL PRODUCT

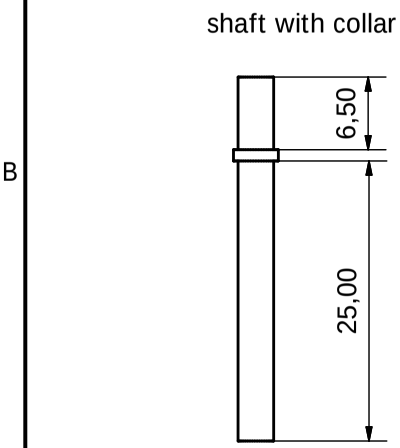

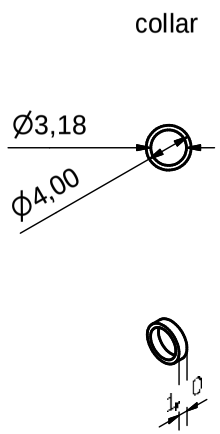

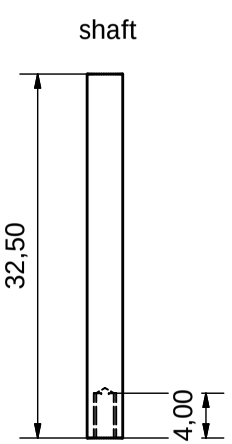

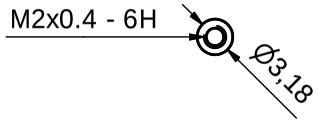

Material:
steel (shaft)
aluminum (collar)

Designed by	Checked by	Approved by	Date		Date	
V. Levesque					21/01/2008	

Haptics Lab, McGill University	First Shaft		
		Edition 1	Sheet 1 / 1

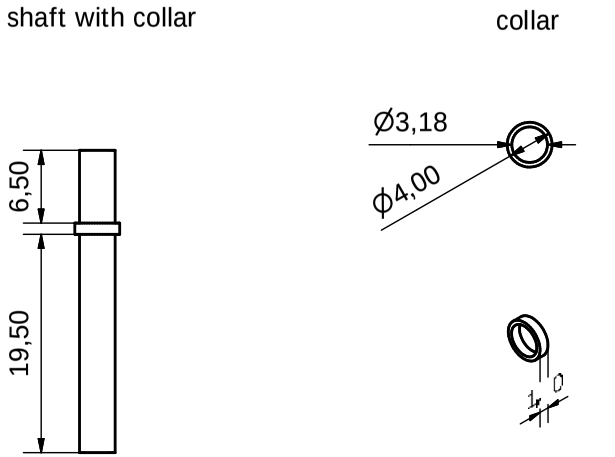

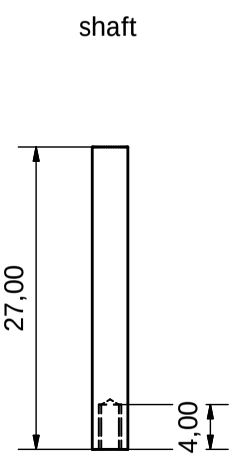

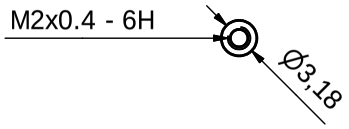

Designed by	Checked by	Approved by	Date		Date	
V. Levesque					21/01/2008	

Material:
steel (shaft)
aluminum (collar)

Haptics Lab, McGill University

Second Shaft

Edition	Sheet
1	1 / 1

PRODUCED BY AN AUTODESK EDUCATIONAL PRODUCT

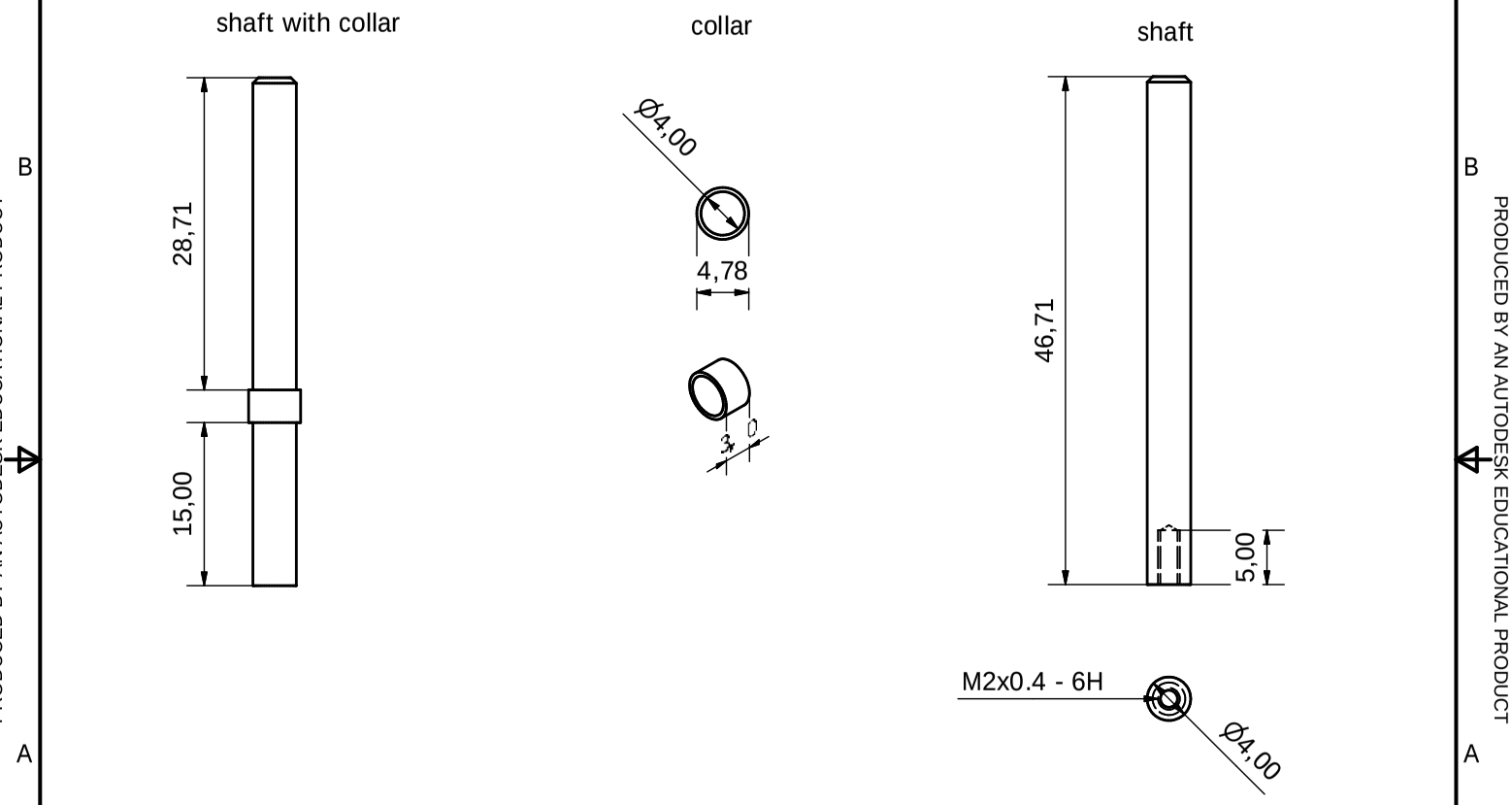

Designed by	Checked by	Approved by	Date		Date	
V. Levesque					21/01/2008	

Material:
steel (shaft)
aluminum (collar)

Haptics Lab, McGill University

Third Shaft

Edition 1

Sheet 1 / 1

PRODUCED BY AN AUTODESK EDUCATIONAL PRODUCT

Appendix B

Wavelength Distortion in Grating Textures

This appendix provides additional details about the distortion of a grating texture's spatial wavelength, which was first introduced in Section 8.4.1. The wavelength of a grating is distorted by redefining the position x along the grating waveform $g(x)$ such that the spatial frequency is scaled by a factor $k(x)$. More precisely, distortions are introduced through a position transform $x'(x)$ resulting in a scaling of distances such that $\delta x' = k(x)\delta x$. The position transform is therefore given by:

$$x'(x) = \int k(x)\, dx \tag{B.1}$$

Wavelength distortions are used to create either a gradual change or a peak in a grating's frequency, as described below.

Gradual Change

A gradual scaling of a grating's spatial frequency is obtained by linearly increasing (or decreasing) the scaling factor $k(x)$ from 1 at point x_0 to K at point $x_1 = x_0 + L$ as illustrated in Figure B.1:

$$k(x) = \begin{cases} 1 & \text{if } x \leq x_0, \\ 1 + \frac{K-1}{L}(x - x_0) & \text{if } x_0 < x \leq x_1, \\ K & \text{otherwise.} \end{cases} \tag{B.2}$$

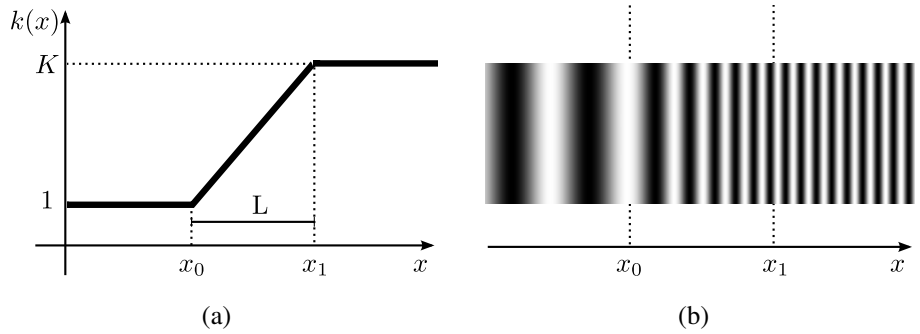

Fig. B.1 (a) Plot of the scaling factor $k(x)$ resulting in (b) a linear increase in grating frequency.

The position transform is then obtained by piecewise integration:

$$x'(x) = \int k(x)dx \tag{B.3}$$

$$= \begin{cases} x + k_0 & \text{if } x \leq x_0, \\ x + \frac{K-1}{L}(x^2/2 - x_0 x) + k_1 & \text{if } x_0 < x \leq x_1, \\ Kx + k_2 & \text{otherwise.} \end{cases} \tag{B.4}$$

$$= \begin{cases} x + k_0 & \text{if } x \leq x_0, \\ x + \frac{K-1}{2L}(x - 2x_0)x + k_1 & \text{if } x_0 < x \leq x_1, \\ Kx + k_2 & \text{otherwise.} \end{cases} \tag{B.5}$$

Constant k_0 is set to 0 such that the position is unmodified prior to reaching x_0:

$$x'(x) = \begin{cases} x & \text{if } x \leq x_0, \\ x + \frac{K-1}{2L}(x - 2x_0)x + k_1 & \text{if } x_0 < x \leq x_1, \\ Kx + k_2 & \text{otherwise.} \end{cases} \tag{B.6}$$

Constant k_1 is set such that $x'(x)$ is continuous at $x = x_0$:

$$x_0 = x_0 + \frac{K-1}{2L}(x_0 - 2x_0)x_0 + k_1 \tag{B.7}$$

$$k_1 = \frac{K-1}{2L}x_0^2 \tag{B.8}$$

Equation B.6 can then be simplified:

$$x + \frac{K-1}{2L}(x - 2x_0)x + k_1 = x + \frac{K-1}{2L}(x - 2x_0)x + \frac{K-1}{2L}x_0^2 \tag{B.9}$$

$$= x + \frac{K-1}{2L}(x^2 - 2x_0x + x_0^2) \tag{B.10}$$

$$= x + \frac{K-1}{2L}(x - x_0)^2 \tag{B.11}$$

Hence,

$$x'(x) = \begin{cases} x & \text{if } x \leq x_0, \\ x + \frac{K-1}{2L}(x - x_0)^2 & \text{if } x_0 < x \leq x_1, \\ Kx + k_2 & \text{otherwise.} \end{cases} \tag{B.12}$$

Constant k_2 is finally set such that $x'(x)$ is continuous at $x = x_1$:

$$x_1 + \frac{K-1}{2L}(x_1 - x_0)^2 = Kx_1 + k_2 \tag{B.13}$$

$$x_1 + \frac{K-1}{2L}L^2 = Kx_1 + k_2 \tag{B.14}$$

$$x_1 + \frac{K-1}{2}L = Kx_1 + k_2 \tag{B.15}$$

$$k_2 = -(K-1)x_1 + \frac{K-1}{2}L \tag{B.16}$$

$$= -(K-1)(x_0 + L) + \frac{K-1}{2}L \tag{B.17}$$

$$= -(K-1)(x_0 + L/2) \tag{B.18}$$

The position transform $x'(x)$ can therefore be rewritten as:

$$x'(x) = \begin{cases} x & \text{if } x \leq x_0, \\ x + (K-1)(x - x_0)^2/2L & \text{if } x_0 < x \leq x_1, \\ Kx - (K-1)(x_0 + L/2) & \text{otherwise.} \end{cases} \tag{B.19}$$

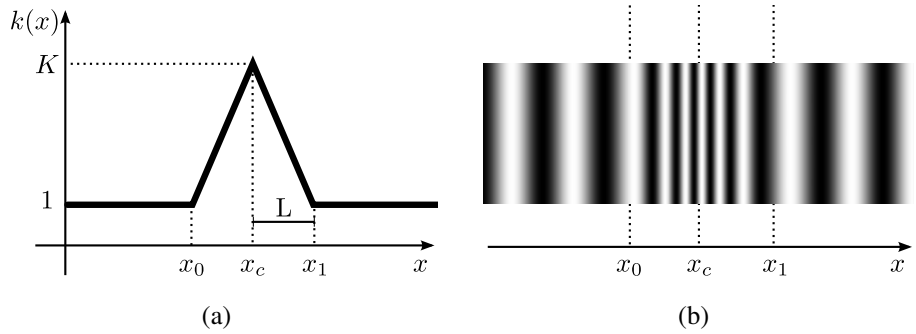

Fig. B.2 (a) Plot ot the scaling factor $k(x)$ resulting in (b) a peak in grating frequency.

Peak

A peak in a grating's spatial frequency or wavelength is obtained by linearly increasing (or decreasing) the scaling factor $k(x)$ from a peak of K at x_c to 1 at outer points $x_0 = x_c - L$ and $x_1 = x_c + L$ as illustrated in Figure B.2:

$$k(x) = \begin{cases} 1 & \text{if } x \leq x_0, \\ 1 + m(x - x_0) & \text{if } x_0 < x \leq x_c, \\ K - m(x - x_c) & \text{if } x_c < x \leq x_1, \\ 1 & \text{otherwise.} \end{cases} \tag{B.20}$$

where $m = \frac{K-1}{L}$ is the slope of the transition. The position transform is then obtained, once again, by piecewise integration:

$$x'(x) = \int k(x)dx = \begin{cases} x + k_0 & \text{if } x \leq x_0, \\ x + m(\frac{x^2}{2} - xx_0) + k_1 & \text{if } x_0 < x \leq x_c, \\ Kx - m(\frac{x^2}{2} - xx_c) + k_2 & \text{if } x_c < x \leq x_1, \\ x + k_3 & \text{otherwise.} \end{cases} \tag{B.21}$$

Constant k_0 is set to 0 so that the position is unmodified prior to reaching x_0. Constant k_1 is set such that $x'(x)$ is continuous at $x = x_0$:

$$x_0 = x_0 + m(\frac{x_0^2}{2} - x_0^2) + k_1 \tag{B.22}$$

$$k_1 = \frac{mx_0^2}{2} \tag{B.23}$$

This allows the following simplification to be made:

$$x + m(\frac{x^2}{2} - xx_0) + k_1 = x + m(\frac{x^2}{2} - xx_0) + \frac{mx_0^2}{2} \tag{B.24}$$

$$= x + \frac{m}{2}(x^2 - 2xx_0 + x_0^2) \tag{B.25}$$

$$= x + \frac{m}{2}(x - x_0)^2 \tag{B.26}$$

Constant k_2 is similarly set such that $x'(x)$ is continuous at $x = x_1$:

$$x_c + \frac{m}{2}(x_c - x_0)^2 = Kx_c - m(\frac{x_c^2}{2} - x_c x_c) + k_2 \tag{B.27}$$

$$\frac{m}{2}(x_c - x_0)^2 = (K-1)x_c + m\frac{x_c^2}{2} + k_2 \tag{B.28}$$

$$\frac{m}{2}L^2 = (K-1)x_c + \frac{m}{2}(x_c^2) + k_2 \tag{B.29}$$

$$k_2 = \frac{m}{2}L^2 - (K-1)x_c - \frac{m}{2}(x_c^2) \tag{B.30}$$

$$k_2 = \frac{m}{2}(L^2 - x_c^2) - (K-1)x_c \tag{B.31}$$

This once again allows the following simplification to be made:

$$Kx - m(\frac{x^2}{2} - xx_c) + k_2 = Kx - m(\frac{x^2}{2} - xx_c) + \frac{m}{2}(L^2 - x_c^2) - (K-1)x_c \tag{B.32}$$

$$= Kx - \frac{m}{2}(x^2 - 2xx_c - L^2 + x_c^2) - (K-1)x_c \tag{B.33}$$

$$= Kx - \frac{m}{2}((x - x_c)^2 - L^2) - (K-1)x_c \tag{B.34}$$

Constant k_3 is finally set such that $x'(x)$ is continuous at $x = x_1$:

$$Kx_1 - \frac{m}{2}((x_1 - x_c)^2 - L^2) - (K-1)x_c = x_1 + k_3 \tag{B.35}$$

$$Kx_1 - \frac{m}{2}(L^2 - L^2) - (K-1)x_c = x_1 + k_3 \tag{B.36}$$

$$Kx_1 - (K-1)x_c - x_1 = k_3 \tag{B.37}$$

$$k_3 = (K-1)(x_1 - x_c) \tag{B.38}$$

$$k_3 = (K-1)L \tag{B.39}$$

The position transform $x'(x)$ can therefore be rewritten as:

$$x'(x) = \begin{cases} x & \text{if } x \leq x_0, \\ x + \frac{m(x-x_0)^2}{2} & \text{if } x_0 < x \leq x_c, \\ kx - \frac{m}{2}((x - x_c)^2 - L^2) - (K-1)x_c & \text{if } x_c < x \leq x_1, \\ x + (k-1)L & \text{otherwise.} \end{cases} \tag{B.40}$$

Substituting $m = (K-1)/L$, we finally obtain:

$$\int k(x)dx = \begin{cases} x & \text{if } x \leq x_0, \\ x + \frac{(K-1)(x-x_0)^2}{2L} & \text{if } x_0 < x \leq x_c, \\ kx - \frac{K-1}{2L}((x - x_c)^2 - L^2) - (K-1)x_c & \text{if } x_c < x \leq x_1, \\ x + (k-1)L & \text{otherwise.} \end{cases} \tag{B.41}$$

$$= \begin{cases} x & \text{if } x \leq x_0, \\ x + \frac{(K-1)(x-x_0)^2}{2L} & \text{if } x_0 < x \leq x_c, \\ kx + \frac{K-1}{2L}(L^2 + 2Lx_c - (x - x_c)^2) & \text{if } x_c < x \leq x_1, \\ x + (k-1)L & \text{otherwise.} \end{cases} \tag{B.42}$$

Appendix C

Ethics Certificates

MCGILL UNIVERSITY
FACULTY OF EDUCATION

Received
AUG 12 2003
McGill University
Faculty of Education
Associate Dean (Academic Programs, Graduate Studies and Research)

CERTIFICATE OF ETHICAL ACCEPTABILITY FOR FUNDED AND NON FUNDED RESEARCH INVOLVING HUMANS

The Faculty of Education Ethics Review Committee consists of 6 members appointed by the Faculty of Education Nominating Committee, an appointed member from the community and the Associate Dean (Academic Programs, Graduate Studies and Research) who is the Chair of this Ethics Review Board.

The undersigned considered the application for certification of the ethical acceptability of the project entitled:
FOUNDATION OF HAPTIC INTERFACES FOR VIRTUAL ENVIRONMENTS AND COMMUNICATIONS
Project acronym: HI-VEC (NCE IRIS)
Concerning the topic of Haptic perception in humans as applied to the design of human-machine interfaces

as proposed by:

Applicant's Name Jerome Pasquero
Applicant's Signature/Date Jerome Pasquero
Degree / Program / Course PhD Eng. – Electrical

Supervisor's Name Dr. Vincent Hayward
Supervisor's Signature
Granting Agency NCE-IRIS/NSERC
Grant Title (s)

The application is considered to be:
A Full Review _____
An Expedited Review _____
A Renewal for an Approved Project X
A Departmental Level Review _____
Signature of Chair / Designate

The review committee considers the research procedures and practices as explained by the applicant in this application, to be acceptable on ethical grounds.

1. Prof. René Turcotte
Department of Kinesiology and Physical Education
Signature / date

2. Prof. Ron Morris
Department of Integrated Studies in Education
Signature / date

3. Prof. Ron Stringer
Department of Educational and Counselling Psychology
Signature / date

4. Prof. Kevin McDonough
Department of Integrated Studies in Education
Signature / date

5. Prof. Brian Alters
Department of Integrated Studies in Education
Signature / date

6. Prof. Ada Sinacore
Department of Educational and Counselling Psychology
Signature / date

7. Member of the Community
Signature / date

Mary H. Maguire Ph. D.
Chair of the Faculty of Education Ethics Review Committee
Associate Dean (Academic Programs, Graduate Studies and Research)
Faculty of Education, Room 230
Tels: (514) 398-7039/398-2183 Fax: (514) 398-1527
Signature / date august 11, 2003

Office Use Only
REB #: 333 - 0799 APPROVAL PERIOD: Aug. 11, 2003 to Aug. 11, 2004
(Updated January 2003)

MCGILL UNIVERSITY
FACULTY OF EDUCATION

CERTIFICATE OF ETHICAL ACCEPTABILITY FOR FUNDED AND NON FUNDED RESEARCH INVOLVING HUMANS

The Faculty of Education Ethics Review Board consists of 6 faculty members appointed by the Faculty of Education, an appointed member from the community, and the Chair of the Ethics Review Board.

The undersigned considered the application for certification of the ethical acceptability of the project entitled:
Foundation of Haptic Interfaces for Virtual Environments and Communications
Project acronym: HI-VEC (NCE IRIS)
Concerning the topic of Haptic perception in humans as applied to the design of human-machine interfaces

Applicant's Name Jerome Pasquero — Supervisor's Name Vincent Hayward

Applicant's Signature/Date Jerome Pasquero 2004-11-02 — Supervisor's Signature

Degree / Program / Course Ph.D. electrical engineering — Granting Agency NCE-IRIS/NSERC

Grant Title (s)

The application is considered to be:
A Full Review _____ — An Expedited Review _____

A Renewal for an Approved Project X — A Departmental Level Review _____
Signature of Chair / Designate

The review committee considers the research procedures and practices as explained by the applicant in this application, to be acceptable on ethical grounds.

1. Prof. René Turcotte
   Department of Kinesiology and Physical Education
   _____ Signature / date

2. Prof. Ron Morris
   Department of Integrated Studies in Education
   _____ Signature / date

3. Prof. Ron Stringer
   Department of Educational and Counselling Psychology
   _____ Signature / date

4. Prof. Joan Russell
   Department of Integrated Studies in Education
   _____ Signature / date

5. Prof. Doreen Starke-Meyerring
   Department of Integrated Studies in Education
   _____ Signature / date

6. Prof. Ada Sinacore
   Department of Educational and Counselling Psychology
   _____ Signature / date

7. Member of the Community
   _____ Signature / date

Office of the Associate Dean (Research & Graduate Students)
Faculty of Education, Room 230
Tel: (514) 398-7039 Fax: (514) 398-1527

Signature / date Chair of the Ethics Review Board — May 5, 2004

Office Use Only

REB #: 333-0799 — APPROVAL PERIOD: May 5/04 to May 5/05

(Updated September 2003)

Comité d'éthique de la recherche des établissements du CRIR

CRIR

Certificat d'éthique

Par la présente, le comité d'éthique de la recherche des établissements du CRIR (CÉR) atteste qu'il a évalué, lors de sa réunion du 22 juin 2006, le projet de recherche **CRIR-212-0406** intitulé:

« Integrated Braille Display Based on Laterotactile Stimulation».

Présenté par: **Jerome Pasquero, Vincent Lévesque, Vincent Hayward**

Le présent projet répond aux exigences éthiques de notre CÉR. Le Comité autorise donc sa mise en œuvre sur la foi des documents suivants :

- Formulaire A daté du 31 mai 2006 ;
- Attestation de bourse de doctorat en recherche du Fonds de recherche sur la nature et les technologies (datée du 31 mai 2006) ;
- Document intitulé « Application for Ethics Approval for Human Subject Research » de McGill (Board-1) ;
- Document intitulé « Study Budget » ;
- Formulaire d'évaluation de la convenance institutionnelle de l'Institut Nazareth et Louis-Braille, daté du 23 mai 2006, confirmant l'acceptation du projet sur le plan de la convenance institutionnelle ;
- Protocole de recherche intitulé « Integrated Braille Display Based on Laterotactile Stimulation » ;
- Formulaire de consentement (version du 1er août 2006, telle qu'approuvée et datée par le CÉR) ;
- Questionnaire (on personnal information) ;
- Curriculum vitae de Jerome Pasquero ;
- Courriel réponse de Jerome Pasquero daté du 1er août 2006.

Ce projet se déroulera dans les sites du CRIR suivants : **Institut Nazareth et Louis-Braille.**

Ce certificat est valable pour un an. En acceptant le présent certificat d'éthique, le chercheur s'engage à :

1. Informer le CÉR de tout changement qui pourrait être apporté à la présente recherche ou aux documents qui en découlent (Formulaire M) ;
2. Fournir annuellement au CÉR un rapport d'étape l'informant de l'avancement des travaux de recherche (formulaire R) ;

3. Demander le renouvellement annuel de son certificat d'éthique ;
4. Aviser le CÉR de la clôture (abandon ou interruption prématurée) du projet de recherche ;
5. Tenir et conserver, selon la procédure prévue dans la *Politique portant sur la conservation d'une liste des sujets de recherche*, incluse dans le cadre réglementaire des établissements du CRIR, une liste des personnes qui ont accepté de prendre part à la présente étude ;
6. Envoyer au CÉR une copie de son rapport de fin de projet / publication.

Me Michel T. Giroux
Président du CÉR

Date d'émission
1er août 2006

Composition du comité d'éthique de la recherche des établissements du CRIR

Mme Isabelle Bilodeau/Mme Saïda El Haïli (membre substitut)	Une personne possédant une vaste connaissance du domaine psychosocial en réadaptation
Dr. Céline Lamarre/ Mme Imen Khelia (substitut)	Une personne possédant une vaste connaissance du domaine biomédical en réadaptation
M. Jean-Marie D'Amour/M. Stéphane McDuff (membre substitut)	Clinicienne détenant une vaste connaissance des déficits sensoriel visuels ou auditifs
Mme Monique Désilets/Mme Marie-Josée Drolet (membre substitut)	Clinicienne détenant une vaste connaissance des déficits moteurs ou neurologiques
Mme Marie-Ève Bouthillier/Mme Delphine Roigt (membre substitut)	Une personne spécialisée en éthique
Me Michel T. Giroux/Me Nathalie Lecoq (membre substitut)	Une personne spécialisée en droit
M. André Vincent/Mme Monique Provost (membre substitut)	Une personne non affiliée à l'établissement et provenant de la clientèle des personnes adultes et aptes
Mme Nadine Landry/Mme Diane Gaumond (substitut)	Une personne non affiliée à l'établissement et provenant de la clientèle des personnes mineures ou inaptes
Mme Elizabeth Markakis/M. Michel Sinotte (membre substitut)	Une personne siégeant à titre de représentante du public
Mme Frédérique Courtois	Représentante de l'UQAM
Mme Patricia McKinley	Représentante de l'Université McGill
Me Anik Nolet	Secrétaire du CÉR et membre non-votant

Comité d'éthique de la recherche
des établissements du CRIR

CRIR

Certificat d'éthique

Par la présente, le comité d'éthique de la recherche des établissements du CRIR (CÉR) atteste qu'il a évalué, par voie accélérée, le projet de recherche **CRIR-306-0607** intitulé:

« Informatisation du graphisme tactile à l'usage des personnes aveugles ou handicapées visuelles ».

Présenté par: **Vincent Lévesque, Vincent Hayward, Jerome Pasquero, Aude Dufresne, Gregory Petit, Nicole Trudeau**

Le présent projet répond aux exigences éthiques de notre CÉR. Le Comité autorise donc sa mise en œuvre sur la foi des documents suivants :

- Formulaire A daté du 12 juin 2007 ;
- Preuve d'octroi de fonds du FQRNT ;
- Document intitulé « Budget » ;
- Formulaire de l'Institut Nazareth et Louis-Braille mentionnant l'acceptation du projet sur le plan de la convenance institutionnelle (daté du 20 juin 2007) ;
- Protocole de recherche intitulé « Informatisation du graphisme tactile à l'usage des personnes aveugles ou handicapées visuelles » (version du 22 juin 2007, telle que datée et approuvée par le CÉR) ;
- Formulaire de consentement (version du 22 juin 2007, telle que datée et approuvée par le CÉR) ;
- Lettre ou annonce de recrutement (version du 22 juin 2007, telle que datée et approuvée par le CÉR) ;
- Document intitulé « Information supplémentaire » (version du 22 juin 2007, telle que datée et approuvée par le CÉR) ;
- Questionnaire (version du 22 juin 2007, telle que datée et approuvée par le CÉR) ;
- Certificat d'éthique de l'Université McGill ;
- Curriculum Vitae de Vincent Lévesque, Nicole Trudeau, Grégory Petit, Jerome Pasquero, Aude Dufresne ;
- Article intitulé « Refeshable Tactile Graphics by Lateral Skin Deformation ».

Ce projet se déroulera dans le site du CRIR suivant : **Institut Nazareth et Louis-Braille.**

Ce certificat est valable pour un an. En acceptant le présent certificat d'éthique, le chercheur s'engage à :

1. Informer le CÉR de tout changement qui pourrait être apporté à la présente recherche ou aux documents qui en découlent (Formulaire M) ;
2. Fournir annuellement au CÉR un rapport d'étape l'informant de l'avancement des travaux de recherche (formulaire R) ;
3. Demander le renouvellement annuel de son certificat d'éthique ;
4. Aviser le CÉR de la clôture (abandon ou interruption prématurée) du projet de recherche ;
5. Tenir et conserver, selon la procédure prévue dans la *Politique portant sur la conservation d'une liste des sujets de recherche*, incluse dans le cadre réglementaire des établissements du CRIR, une liste des personnes qui ont accepté de prendre part à la présente étude ;
6. Envoyer au CÉR une copie de son rapport de fin de projet / publication.

Me Michel T. Giroux
Président du CÉR

Date d'émission
22 juin 2007

Comité d'éthique de la recherche
des établissements du CRIR

CRIR

Certificat d'éthique
(Renouvellement)

Pour fins de renouvellement, le Comité d'éthique de la recherche des établissements du CRIR, selon la procédure d'évaluation accélérée en vigueur, a examiné le projet de recherche **CRIR-306-0607** intitulé :

« Informatisation du graphisme tactile à l'usage des personnes aveugles ou handicapées visuelles ».

Présenté par: **Vincent Lévesque, Vincent Hayward, Jérôme Pasquero, Aude Dufresne, Gregory Petit, Nicole Trudeau.**

Le présent projet répond aux exigences éthiques de notre CÉR. Ce projet se déroule dans le site du CRIR suivant : **Institut Nazareth et Louis-Braille.**

Ce certificat est valable pour un an. En acceptant le présent certificat d'éthique, le chercheur s'engage à :

1. Informer, dès que possible, le CÉR de tout changement qui pourrait être apporté à la présente recherche ou aux documents qui en découlent (Formulaire M) ;
2. Notifier, dès que possible, le CÉR de tout incident ou accident lié à la procédure du projet ;
3. Notifier, dès que possible, le CÉR de tout nouveau renseignement susceptible d'affecter l'intégrité ou l'éthicité du projet de recherche, ou encore, d'influer sur la décision d'un sujet de recherche quant à sa participation au projet ;
4. Notifier, dès que possible, le CÉR de toute suspension ou annulation d'autorisation relative au projet qu'aura formulée un organisme de subvention ou de réglementation ;
5. Notifier, dès que possible, le CÉR de tout problème constaté par un tiers au cours d'une activité de surveillance ou de vérification, interne ou externe, qui est susceptible de remettre en question l'intégrité ou l'éthicité du projet ainsi que la décision du CÉR ;
6. Notifier, dès que possible, le CÉR de l'interruption prématurée, temporaire ou définitive du projet. Cette modification doit être accompagnée d'un rapport faisant état des motifs à la base de cette interruption et des répercussions sur celles-ci sur les sujets de recherche ;
7. Fournir annuellement au CÉR un rapport d'étape l'informant de l'avancement des travaux de recherche (formulaire R) ;
8. Demander le renouvellement annuel de son certificat d'éthique ;
9. Tenir et conserver, selon la procédure prévue dans la *Politique portant sur la conservation d'une liste des sujets de recherche*, incluse dans le cadre réglementaire des établissements du CRIR, une liste des personnes qui ont accepté de prendre part à la présente étude ;
10. Envoyer au CÉR une copie de son rapport de fin de projet / publication.

Me Michel T. Giroux
Président du CÉR

Date d'émission
22 juin 2008

McGill

Research Ethics Board Office
McGill University
845 Sherbrooke Street West
James Administration Bldg., rm 419
Montreal, QC H3A 2T5

Tel: (514) 398-6831
Fax: (514) 398-4644
Ethics website: www.mcgill.ca/research/compliance/human/

Research Ethics Board I
Certificate of Ethical Acceptability of Research Involving Humans

REB File #: 193-0306

Project Title: On the integration of force feedback and distributed lateral skin deformation

Principal Investigator: Vincent Levesque **Department:** Electrical&Computer Engineering
Co-Investigators: J. Pasquero,Q. Wang

Status: Ph.D. students **Supervisor:** Prof. V. Hayward

Granting Agency and Title (if applicable): études des deformations de la peau du doigt humain et de la perception tactile; NSERC discovery-V. Hayward

This project was reviewed on 5 April 2006 by

Expedited Review ✓
Full Review ____

George Wenzel

George Wenzel, Ph.D.
Chair, REB I

Approval Period: May 19, 2006 to May 18, 2007

This project was reviewed and approved in accordance with the requirements of the McGill University Policy on the Ethical Conduct of Research Involving Human Subjects and with the Tri-Council Policy Statement: Ethical Conduct For Research Involving Humans

---

*All research involving human subjects requires review on an annual basis. A Request for Renewal form should be submitted at least one month before the above expiry date.
*If a project has been completed or terminated and ethics approval is no longer required, a Final Report form must be submitted.
*Should any modification or other unanticipated development occur before the next required review, the REB must be informed and any modification can't be initiated until approval is received.

cc: Prof. V. Hayward

McGill University

ETHICS REVIEW
RENEWAL REQUEST/FINAL REPORT

Continuing review of human subjects research requires, at a minimum, the submission of an annual status report to the REB. This form must be completed to request renewal of ethics approval. If a renewal is not received before the expiry date, the project is considered no longer approved and no further research activity may be conducted. When a project has been completed, this form can also be used as a Final Report, which is required to properly close a file. To avoid expired approvals and, in the case of funded projects, the freezing of funds, this form should be returned 3-4 weeks before the current approval expires.

REB File #: 193-0306
Project Title: ON THE INTEGRATION OF FORCE FEEDBACK AND DISTRIBUTED HAPTICS SKIN DEFORMATION
Principal Investigator: VINCENT LEVESQUE VLEVES@CIM.MCGILL.CA
Department/Phone/Email: CENTER FOR INTELLIGENT MACHINES 8206
Faculty Supervisor (for student PI): VINCENT HAYWARD

1. Were there any significant changes made to this research project that have any ethical implications? ___Yes _X_No
   If yes, describe these changes and append any relevant documents that have been revised.

2. Are there any ethical concerns that arose during the course of this research? ___ Yes _X_ No. If yes, please describe.

3. Have any subjects experienced any adverse events in connection with this research project? ___ Yes _X_ No
   If yes, please describe.

4. _X_ This is a request for renewal of ethics approval.

5. ____ This project is no longer active and ethics approval is no longer required.

6. List all current funding sources for this project and the corresponding project titles **if not exactly the same** as the project title above. Indicate the Principal Investigator of the award if not yourself.
   NSERC, Discovery Grant (Vincent Hayward)
   FQRNT, Information du graphisme tactile à l'usage des personnes aveugles ou handicappées visuelles (PR-114110, Vincent Hayward)

Principal Investigator Signature: Vincent Levesque Date: April 17, 2007

Faculty Supervisor Signature: Date: APRIL 6 2007
(for student PI)

For Administrative Use	**REB:** ___AGR ___EDU ✓REB-I ___REB-II
____ The closing report of this terminated project has been reviewed and accepted	
✓ The continuing review for this project has been reviewed and approved	
✓ Expedited Review ___ Full Review	
Signature of REB Chair or designate: L McNeil Date: April 19, 2007	
Approval Period: May 19, 2007 to May 18, 2008	

Submit to Lynda McNeil, Research Ethics Officer, James Administration Bldg., rm 419, fax: 398-4644 tel:398-6831

(version October 2002)

McGill University

ETHICS REVIEW
RENEWAL REQUEST/FINAL REPORT

Continuing review of human subject research requires, at a minimum, the submission of an annual status report to the REB. This form must be completed to request renewal of ethics approval. If a renewal is not received before the expiry date, the project is considered no longer approved and no further research activity may be conducted. When a project has been completed, this form can also be used as a Final Report, which is required to properly close a file. To avoid expired approvals and, in the case of funded projects, the freezing of funds, this form should be returned 3-4 weeks before the current approval expires.

REB File #: 193-0306
Project Title: On the integration of force feedback and distributed lateral skin deformation
Principal Investigator: Vincent Levesque
Department/Phone/Email: ECSE / 8206 / vleves@cim.mcgill.ca
Faculty Supervisor (for student PI): Vincent Hayward

1. Were there any significant changes made to this research project that have any ethical implications? ___Yes __x_No
   If yes, describe these changes and append any relevant documents that have been revised.

2. Are there any ethical concerns that arose during the course of this research? ___ Yes _x_ No. If yes, please describe.

3. Have any subjects experienced any adverse events in connection with this research project? ___ Yes _x_ No
   If yes, please describe.

4. __x_ This is a request for renewal of ethics approval.

5. ____ This project is no longer active and ethics approval is no longer required.

6. List all current funding sources for this project and the corresponding project titles **if not exactly the same** as the project title above. Indicate the Principal Investigator of the award if not yourself.

NSERC, Discovery Grant (Vincent Hayward)

Principal Investigator Signature: Vincent Levesque Date: April 20 2009

Faculty Supervisor Signature: _____ Date: April 17 2009
(for student PI)

For Administrative Use **REB:** ✓REB-I ___REB-II ____REB-III

____ The closing report of this terminated project has been reviewed and accepted

✓___ The continuing review for this project has been reviewed and approved

✓___ Expedited Review ____ Full Review

Signature of REB Chair or designate: L McNeil Date: May 8, 2009

Approval Period: May 19, 2009 to May 18, 2010

****NOTE NEW MAILING ADDRESS****
Submit to Lynda McNeil, Research Ethics Officer, 1555 Peel Street, 11th floor, fax: 398-4644 tel:398-6831

(version 12/07)

References

[1] M. Abrams. Sight unseen. *The Braille Monitor*, 45(9), 2002.

[2] S. D. Ahn, S. Y. Kang, C. A. Kim, J. Y. Oh, I. K. You, G. H. Kim, K. H. Baek, and K. S. Suh. Braille display device using electrorheological fluid and manufacturing. U.S. Patent Application No. 11/999,471.

[3] S. Aitken and T. G. R. Bower. The use of the Sonicguide in infancy. *Journal of Visual Impairment & Blindness*, 76:91, 1982.

[4] P. Albert. Math class: An application for dynamic tactile graphics. In *Computers Helping People with Special Needs*, volume 4061 of *Lecture Notes in Computer Science*, pages 1118–1121, 2006.

[5] F. K. Aldrich and L. Sheppard. Graphicacy: The fourth 'r'? *Primary Science Review*, 64:8–11, 2000.

[6] F. K. Aldrich and L. Sheppard. Tactile graphics in school education: perspectives from pupils. *British Journal of Visual Impairment*, 19(2):69–73, 2001.

[7] D. Allerkamp, G. Böttcher, F.-E. Wolter, A. C. Brady, J. Qu, and I. R. Summers. A vibrotactile approach to tactile rendering. *The Visual Computer*, 23(2):97–108, 2007.

[8] G. Ambrose-Zaken. Knowledge of and preferences for long cane components: A qualitative and quantitative study. *Journal of Visual Impairment & Blindness*, 99(10):633–646, 2005.

[9] A. Amedi, A. Floel, S. Knecht, E. Zohary, and L. G. Cohen. Transcranial magnetic stimulation of the occipital pole interferes with verbal processing in blind subjects. *Nature Neuroscience*, 7(11):1266–1270, 2004.

[10] American Diabetes Association. Diabetes and retinopathy (eye complications). Retrieved May 19, 2009 from the World Wide Web: `http://www.diabetes.org/diabetes-statistics/eye-complications.jsp`.

[11] American Foundation for the Blind. Statistical snapshots. Retrieved May 19, 2008 from the World Wide Web: `http://www.afb.org/Section.asp?SectionID=15`.

[12] B. Ando. Electronic sensory systems for the visually impaired. *IEEE Instrumentation & Measurement Magazine*, 6(2):62–67, 2003.

[13] A. Arditi, E. Holmes, P. Reedijk, and R. Whitehouse. Interactive tactile maps, visual disability, and accessibility of building interiors. *Visual Impairment Research*, 1(1):11–21, 1999.

[14] P. Bach–y–Rita, K. A. Kaczmarek, M. Tyler, and J. Garcia-Lara. Form perception with a 49-point electrotactile stimulus array on the tongue: a technical note. *Journal of Rehabilitation Research and Development*, 35(4):427–430, 1998.

[15] P. Bach–y–Rita, M. Tyler, and K. Kaczmarek. Seeing with the brain. *International journal of human-computer-interaction*, 15(2):285–295, 2003.

[16] D. Baldwin. Inventing the future of wayfinding technology. Retrieved December 6, 2005 from the World Wide Web: `http://www.wayfinding.net/iibnNECJVIB.htm`.

[17] D. Baldwin. Tips for inventors and researchers. Retrieved December 6, 2005 from the World Wide Web: `http://www.wayfinding.net/Tips.html`.

[18] D. Baldwin. Wayfinding technology: A road map to the future. *Journal of Visual Impairment & Blindness*, 97(10):612–620, 2003.

[19] D. Bavelier and H. Neville. Cross-modal plasticity: where and how? *Nature Reviews Neuroscience*, 3(6):443–452, 2002.

[20] Y. Bellik and D. Burger. Multimodal interfaces: New solutions to the problem of computer accessibility for the blind. In *Proc. ACM Conference on Human Factors in Computing Systems (CHI '94)*, pages 24–28, 1994.

[21] M. Benali-Khoudja, M. Hafez, J. Alexandre, and A. Kheddar. Tactile interfaces. a state of the art survey. In *Proc. International Symposium on Robotics (ISR 2004)*, pages 721–726, 2004.

[22] M. Benali-Khoudja, M. Hafez, A. Sautour, and S. Jumpertz. Towards a new tactile language to communicate emotions. In *Proc. IEEE International Conference on Mechatronics and Automation*, volume 1, pages 286–291, 2005.

[23] M. Benali-Khoudja, C. Orange, F. Maingreaud, M. Hafez, A. Kheddar, and E. Pissaloux. Shape and direction perception using VITAL: A VIbro-TActiLe interface. In *Proc. Touch and Haptics Workshop (IROS 2004)*, 2004.

[24] P. Bertelson, P. Mousty, and G. D'Alimonte. A study of braille reading: 2. patterns of hand activity in one-handed and two-handed reading. *Quarterly Journal of Experimental Psychology*, 37A(2):235–56, 1985.

[25] D. K. Biegelsen, W. B. Jackson, L.-E. Swartz, A. A. Berlin, and P. C. Cheung. Pneumatic actuator with elastomeric membrane and low-power electrostatic flap valve arrangement. U.S. Patent No. 6,807,892, 2004.

[26] J. Biggs and M. A. Srinivasan. Tangential versus normal displacements of skin: Relative effectiveness for producing tactile sensations. In *Proc. 10th Symposium on Haptic Interfaces for Virtual Environments and Teleoperator Systems*, 2002.

[27] M. Blades, S. Ungar, and C. Spencer. Map use by adults with visual impairments. *Professional Geographer*, 51(4):539–553, 1999.

[28] B. Blasch, R. Long, and N. Griffin-Shirley. Results of a national survey of electronic travel aid use. *Journal of Visual Impairment & Blindness*, 83:449–453, 1989.

[29] D. Blazie. Refreshable braille now and in the years ahead. *Braille Monitor*, 43(1), 2000.

[30] J. Bliss. A provisional bibliography on tactile displays. *IEEE Transactions on Man-Machine Systems*, 11(1):101–108, 1970.

[31] J. Bliss, M. Katcher, C. Rogers, and R. Shepard. Optical-to-tactile image conversion for the blind. *IEEE Transactions on Man-Machine Systems*, 11(1):58–65, 1970.

[32] P. Bourke. Minimum distance between a point and a line. Retrieved May 19, 2009 from the World Wide Web: `http://local.wasp.uwa.edu.au/~pbourke/geometry/pointline`.

[33] J. Brabyn. A review of mobility aids and means of assessment. In *Electronic Spatial Sensing for the Blind, Proc. of the NATO Advanced Research Workshop on Visual Spatial Prostheses for the Blind*, pages 13–27, 1985.

[34] M. Bris. Recommandations pour la transcription de documents. Cours Dessin en Relief, CNEFEI Suresne, 2003.

[35] R. Browne. Toward a mobility aid for the blind. In *Proc. Image and Vision Computing 2003 (IVCNZ 2003)*, 2003.

[36] J. D. Brule. A workstation for tactile graphics. *Journal of Microcomputer Applications*, 15(1):21–30, 1992.

[37] G. Campion, Q. Wang, and V. Hayward. The Pantograph Mk-II: a haptic instrument. In *Proc. International Conference on Intelligent Robots and Systems (IROS 2005)*, pages 193–198, 2005.

[38] S. Cardin, D. Thalmann, and F. Vexo. Wearable obstacle detection system for visually impaired people. In *Proc. HAPTEX'05*, 2005.

[39] S. Chandrashekar, T. Stockman, D. Fels, and R. Benedyk. Using think aloud protocol with blind users:: a case for inclusive usability evaluation methods. In *Proc. 8th ACM Conference on Computers and Accessibility (ASSETS '06)*, pages 251–252, 2006.

[40] H.-C. Cho, B.-S. Kim, J.-J. Park, and J.-B. Song. Development of a braille display using piezoelectric linear motors. In *Proc. International Joint Conference SICE-ICASE*, pages 1917–1921, 2006.

[41] H. Choi, S. Lee, K. Jung, J. Koo, S. Lee, H. Choi, J. Jeon, and J. Nam. Tactile display as a Braille display for the visually disabled. In *Proc. IEEE/RSJ International Conference on Intelligent Robots and Systems (IROS 2004)*, 2004.

[42] R. W. Cholewiak and C. E. Sherrick. A computer-controlled matrix system for presentation to the skin of complex spatiotemporal patterns. *Behavior Research Methods & Instrumentation*, 13(5):667–673, 1981.

[43] V. Chouvardas, A. Miliou, and M. Hatalis. Tactile displays: a short overview and recent developments. In *Proc. 5th International Conference on Technology and Automation (ICTA'05)*, 2005.

[44] V. G. Chouvardas, A. N. Milion, and M. K. Hatalis. Tactile display applications: a state of the art survey. In *Proc. 2nd Balkan Conference in Informatics*, 2005.

[45] M. A. Clements, L. D. Braida, and N. I. Durlach. Tactile communication of speech: II. comparison of two spectral displays in a vowel discrimination task. *Journal of the Acoustical Society of America*, 72(4):1131–1135, 1982.

[46] M. Cohen. An innovative approach to a refreshable braille display. Technical report, Duke University Department of Electrical and Computer Engineering, 2003.

[47] C. Collins. On mobility aids for the blind. In *Electronic Spatial Sensing for the Blind, Proc. of the NATO Advanced Research Workshop on Visual Spatial Prostheses for the Blind*, 1985.

[48] C. Colwell, H. Petrie, D. Kornbrot, A. Hardwick, and S. Furner. Haptic virtual reality for blind computer users. In *Proc. 3rd ACM Conference on Assistive Technologies (ASSETS '98)*, 1998.

[49] J. Craig. Identification of scanned and static tactile patterns. Perception and Psychophysics 64(1), pp 107-120, 2002.

[50] J. Craig and C. Sherrick. Dynamic tactile displays. in Tactual Perception: A Sourcebook, W. Schiff and E. Foulke Eds., Cambridge University Press, 1982.

[51] G. Dalrymple. An electromechanical numeric braille display. *AFB Research Bulletin*, 29:149, 1975.

[52] P. Davidson, S. Appelle, and R. Haber. Haptic scanning of braille cells by low- and high-proficiency blind readers. *Research in Developmental Disabilities*, 13(2):99–111, 1992.

[53] L. di Stefano, C. Melchiorri, and G. Vassura. Haptic interfaces as aids for visually impaired persons. In *Proc. 8th IEEE International Workshop on Robot and Human Interaction (RO-MAN '99)*, 1999.

[54] W. Dobelle. Artificial vision for the blind by connecting a television camera to the visual cortex. *ASAIO Journal*, 46:3–9, 2000.

[55] C. L. V. Doren. A model of spatiotemporal tactile sensitivity linking psychophysics to tissue mechanics. *Journal of the Acoustical Society of America*, 85(5):2065–2080, 1989.

[56] A. Downie. A consumers view of electronic navigational technology. Retrieved November 28, 2005 from the World Wide Web: `http://www.wayfinding.net/consumerview.htm`.

[57] K. Drewing, M. Fritschi, R. Zopf, M. O. Ernst, and M. Buss. First evaluation of a novel tactile display exerting shear force via lateral displacement. *ACM Transactions on Applied Perception*, 2(2):118–131, 2005.

[58] T. Ebina, S. Igi, T. Miyake, and H. Takahashi. Graph access system for the visually impaired. In *Proc. of the Third Asian Pacific Computer and Human Interaction*, 1998.

[59] P. K. Edman. *Tactile Graphics*. AFB Press, New York, 1992.

[60] K. Edwards, E. Mynatt, and K. Stockton. Access to graphical interfaces for blind users. *Interactions*, 2(1), 1995.

[61] E. T. Enikov and K. V. Lazarov. Micro-mechanical switch array for meso-scale actuation. *Sensors and Actuators A: Physical*, 121(1):282–293, 2005.

[62] W. Epstein, B. Hughes, S. L. Schneider, and P. Bach–y–Rita. Perceptual learning of spatiotemporal events: evidence from an unfamiliar modality. *Journal of Experimental Psychology: Human Perception and Performance*, 15(1):28–44, 1989.

[63] S. Ertan, C. Lee, A. Willets, H. Tan, and A. Pentland. A wearable haptic navigation guidance system. In *Proc. Second International Symposium on Wearable Computers*, pages 164–165, 1998.

[64] T. G. Evreinova, G. Evreinov, R. Raisamo, and L. K. Vesterinen. Non-visual interaction with graphs assisted with directional-predictive sounds and vibrations: a comparative study. *Universal Access in the Information Society*, 7:93–102, 2008.

[65] E. Foulke. *The Psychology of Touch*, chapter Braille, pages 219–233. Lawrence Erlbaum Associates, 1991.

[66] J. Fricke. Substituting friction by weak vibration on a tactile pin array. In *IEE Colloquium on Developments in Tactile Displays (Digest No. 1997/012)*, pages 3/1–3/3, 1997.

[67] J. Fricke and H. Baehring. Design of a tactile graphic I/O tablet and its integration into a personal computer system for blind users. *Journal of Microcomputer Applications*, 16(3):259–269, 1993.

[68] J. Fricke and H. Baehring. Displaying laterally moving tactile information. In *Proc. 4th international conference on Computers for handicapped persons*, pages 461–468, 1994.

[69] J. Fritz and K. Barner. Design of a haptic data visualization system for people with visual impairments. *IEEE Transactions on Rehabilitation Engineering*, 7(3), 1999.

[70] E. P. Gardner and C. I. Palmer. Simulation of motion on the skin. I. receptive fields and temporal frequency coding by cutaneous mechanoreceptors of optacon pulses delivered to the hand. *Journal of Neurophysiology*, 62(6):1410–1436, 1989.

[71] E. P. Gardner and C. I. Palmer. Simulation of motion on the skin. II. cutaneous mechanoreceptor coding of the width and texture of bar patterns displaced across the optacon. *Journal of Neurophysiology*, 62(6):1437–1460, 1989.

[72] E. P. Gardner and C. I. Palmer. Simulation of motion on the skin. III. mechanisms used by rapidly adapting cutaneous mechanoreceptors in the primate hand for spatiotemporal resolution and two-point discrimination. *Journal of Neurophysiology*, 63(4):841–859, 1990.

[73] E. P. Gardner, C. I. Palmer, H. A. Hamalainen, and S. Warren. Simulation of motion on the skin. V. effect of stimulus temporal frequency on the representation of moving bar patterns in primary somatosensory cortex of monkeys. *Journal of Neurophysiology*, 67(1):37–63, 1992.

[74] E. Gentaz and M. Badan. *Touching for Knowing*, chapter Anatomical and functional organization of cutaneous and haptic perceptions: The contribution of neuropsychology and cerebral functional imagery, pages 33–47. John Benjamins Publishing Company, 2003.

[75] E. Gerber. Surfing by ear: Usability concerns of computer users who are blind or visually impaired. *AccessWorld*, 3(1), 2002.

[76] S. J. Gilbert and V. Walsh. Vision: The versatile 'visual' cortex. *Current Biology*, 14:R1056–R1057, 2004.

[77] J. Gill. Technological developments for blind people: The next ten years. *The British Journal of Healthcare Computing & Information Management*, 20(9), 2003.

[78] B. Gillespie and S. O'Modhrain. The Moose: A haptic user interface for blind persons with application to the digital sound studio. Stanford University Department of Music Technical Report STAN-M-95, 1995.

[79] L. H. Goldish and H. E. Taylor. The Optacon: A valuable device for blind persons. *New Outlook for the Blind*, 68:49–56, 1974.

[80] D. Goldreich and I. M. Kanics. Tactile acuity is enhanced in blindness. *The Journal of Neuroscience*, 23(8):3439–3445, 2003.

[81] E. B. Goldstein. *Sensation & Perception*, chapter The Cutaneous Senses, pages 405–437. Brooks/Cole Publishing Company, 5th edition, 1999.

[82] R. G. Golledge, M. Rice, and R. D. Jacobson. A commentary on the use of touch for accessing on-screen spatial representations: The process of experiencing haptic maps and graphics. *The Professional Geographer*, 57(3):339–349, 2005.

[83] D. Grant. Two new commercial haptic rotary controllers. In *Proc. EuroHaptics 2004*, pages 451–455, 2004.

[84] B. G. Green, J. C. Craig, A. M. Wilson, D. B. Pisoni, and R. P. Rhodes. Vibrotactile identification of vowels. *Journal of the Acoustical Society of America*, 73(5):1766–1778, 1983.

[85] A. P. Grunwald. A braille-reading machine. *Science, New Series*, 154(3745):144–146, 1966.

[86] T. M. H. Kajimoto, N. Kawakami and S. Tachi. Tactile feeling display using functional electrical stimulation. In *Proc. Ninth International Conference on Artificial reality and Telexistence (ICAT'99)*, 1999.

[87] Y. Haga, W. Makishi, K. Iwami, K. Totsu, K. Nakamura, and M. Esashi. Dynamic Braille display using SMA coil actuator and magnetic latch. *Sensors and Actuators A: Physical*, 119(2):316–322, 2005.

[88] T. Hampel, R. Keil-Slawik, B. G. Claassen, F. Plohmann, and C. Reimann. Pragmatic solutions for better integration of the visually impaired in virtual communities. In *Proc. International ACM SIGGROUP Conference on Supporting Group Work*, pages 258–266, 1999.

[89] A. Hardwick, S. Furner, and J. Rush. Tactile display of virtual reality from the world wide web-a potential access method for blind people. *Displays*, 18(3):153–161, 1998.

[90] S. Harper. Standardising electronic travel aid interaction for visually impaired people. Master's thesis, Univ. Manchester Inst. Science and Technology (UMIST), 1998.

[91] Y. Hatwell and F. Martinez-Sarocchi. *Touching for Knowing*, chapter The tactile reading of maps and drawings, and the access of blind people to works of art, pages 255–273. John Benjamins Publishing Company, 2003.

[92] V. Hayward and M. Cruz-Hernandez. Tactile display device using distributed lateral skin stretch. In *Proc. 9th Symposium on Haptic Interfaces for Virtual Environments and Teleoperator Systems*, volume DSC-69-2, pages 1309–1314. ASME IMECE2000, Orlando, Florida, 2000.

[93] M. Heller. Picture and pattern perception in the sighted and the blind: the advantage of the late blind. *Perception*, 18:379–389, 1989.

[94] M. A. Heller. Society, science, and values. *Perception*, 29(7):757–760, 2000.

[95] M. A. Heller, G. J. Rogers, and C. L. Perry. Tactile pattern recognition with the optacon: superior performance with active touch and the left hand. *Neuropsychologia*, 28(9):1003–1006, 1990.

[96] N. Henze, W. Heuten, and S. Boll. Non-intrusive somatosensory navigation support for blind pedestrians. In *Proc. EuroHaptics 2006*, pages 459–464, 2006.

[97] J. Hill and J. Black. The miniguide: A new electronic travel device. *Journal of Visual Impairment & Blindness*, 97(10):655–656, 2003.

[98] R. Hinton and D. Ayres. The development of tactile diagrams for blind biology students. *Journal of Visual Impairment & Blindness*, 81:24, 1987.

[99] R. Hinton and D. Hinton. Tactile diagrams for the able undergraduate chemistry student. *Journal of Visual Impairment & Blindness*, 93(7):429–, 1999.

[100] M. Hollins. *Understanding Blindness: An Integrative Approach*. Lawrence Erlbaum Associates, 1989.

[101] B. Horsfall. Tactile maps: New materials and improved designs. *Journal of Visual Impairment & Blindness*, 91(1):61, 1997.

[102] R. Horsfall and D. Vanston. Tactual maps: discriminability of textures and shapes. *Journal of Visual Impairment & Blindness*, 75:363–367, 1981.

[103] R. Iglesias, S. Casado, T. Gutierrez, J. Barbero, C. Avizzano, S. Marcheschi, and M. Bergamasco. Computer graphics access for blind people through a haptic and audio virtual environment. In *Proc. 3rd IEEE International Workshop on Haptic, Audio and Visual Environments and Their Applications (HAVE 2004)*, pages 13–18, 2004.

[104] Y. Ikei, K. Wakamatsu, and S. Fukuda. Vibratory tactile display of image-based textures. *IEEE Computer Graphics and Applications*, 17(6):53–61, 1997.

[105] Y. Ikei, K. Wakamatsu, and S. Fukuda. Image data transformation for tactile texture display. In *Proc. IEEE Virtual Reality Annual International Symposium*, pages 51–58, 1998.

[106] Y. Ikei, M. Yamada, and S. Fukuda. A new design of haptic texture display - Texture Display2 - and its preliminary evaluation. In *Proc. IEEE Virtual Reality*, 2001.

[107] S. Ino, S. Shimizu, T. Odagawa, M. Sato, M. Takahashi, T. Izumi, and T. Ifukube. A tactile display for presenting quality of materials by changing the temperature of skin surface. In *Proc. 2nd IEEE International Workshop on Robot and Human Communication*, pages 220–224, 1993.

[108] R. Jacobson. Navigating maps with little or no sight: A novel audio-tactile approach. In *Proc. Content Visualization and Intermedia Representations*, 1998.

[109] C. Jacquet, Y. Bellik, and Y. Bourda. Electronic locomotion aids for the blind: Towards more assistive systems. In *Intelligent Paradigms for Assistive and Preventive Healthcare*, volume 19 of *Studies in Computational Intelligence*, chapter 5, pages 133–163. Springer Berlin / Heidelberg, 2006.

[110] G. A. James. *in Tactual Perception: A Sourcebook*, chapter Mobility maps. Cambridge University Press, 1982.

[111] G. A. James and J. M. Gill. A pilot study on the discriminability of tactile areal and line symbols for the blind. *AFB Research Bulletin*, 29:23–31, 1975.

[112] G. Jansson. Can a haptic force feedback display provide visually impaired people with useful information about texture roughness and 3D form of virtual objects? In *Proc. 2nd European Conference on Disability, Virtual Reality and Associated Technologies*, 1998.

[113] G. Jansson. Basic issues concerning visually impaired people's use of haptic displays. In P. Sharkey, A. Cesarani, L. Pugnatti, and A. Rizzo, editors, *Proc. 3rd International Conference on Disability, Virtual Reality and Associated Technologies*, pages 33–38, 2000.

[114] G. Jansson. Two recommendations for tactile/haptic displays: One for all kinds of presentations and one for the development of haptic displays. In *Proc. Guidelines On Tactile and Haptic Interactions (GOTHI'05)*, 2005.

[115] G. Jansson, I. Juhasz, and A. Cammilton. Reading virtual maps with a haptic mouse: Effects of some modifications of the tactile and audio-tactile information. *British Journal of Visual Impairment*, 24(2):60–66, 2006.

[116] K. Kaczmarek and S. Haase. Pattern identification and perceived stimulus quality as a function of stimulation waveform on a fingertip-scanned electrotactile display. *IEEE Transactions on Neural Systems and Rehabilitation Engineering*, 11(1):9–16, 2003.

[117] K. A. Kaczmarek, M. E. Tyler, and P. Bach–y–Rita. Pattern identification on a fingertip-scanned electrotactile display. In *Proc. 19th Annual International Conference of the IEEE Engineering in Medicine and Biology Society*, pages 1694–1697, 1997.

[118] H. Kajimoto, M. Inami, N. Kawakami, and S. Tachi. SmartTouch - augmentation of skin sensation with electrocutaneous display. In *Proc. 11th Symposium on Haptic Interfaces for Virtual Environments and Teleoperator Systems*, pages 40–46, 2003.

[119] H. Kajimoto, N. Kawakami, S. Tachi, and M. Inami. SmartTouch: electric skin to touch the untouchable. *IEEE Computer Graphics and Applications*, 24(1):36–43, 2004.

[120] P. Kammermeier, M. Buss, and G. Schmidt. Dynamic display of distributed tactile shape information by a prototypical actuator array. In *Proc. IEEE/RSJ International Conference on Intelligent Robots and Systems (IROS 2000)*, volume 2, pages 1119–1124, 2000.

[121] M. Karam and D. I. Fels. Designing a model human cochlea: issues and challenges in crossmodal audio-haptic displays. In *Proc. Ambi-Sys workshop on Haptic user interfaces in ambient media systems (HAS '08)*, pages 1–9, 2008.

[122] Y. Kato, T. Sekitani, M. Takamiya, M. Doi, K. Asaka, T. Sakurai, and T. Someya. Sheet-type braille displays by integrating organic field-effect transistors and polymeric actuators. *IEEE Transactions on Electron Devices*, 54(2):202–209, 2007.

[123] Y. Kawai and F. Tomita. A support system for the visually impaired to recognize three-dimensional objects. *Technology & Disability*, 12(1):13, 2000.

[124] L. Kay. Sonic glasses for the blind. *AFB Research Bulletin*, 25:25, 1973.

[125] J. Kennedy, P. Gabias, and M. Heller. Space, haptics and the blind. *Geoforum*, 23(2):175–189, 1992.

[126] M. B.-K. Khoudja, M. Hafez, J.-M. Alexandre, A. Kheddar, and V. Moreau. VITAL: A VIbroTActiLe interface with thermal feedback. In *Proc. IEEE International Conference on Robotics and Automation (ICRA 2004)*, 2004.

[127] R. Kikuuwe, A. Sano, H. Mochiyama, N. Takesue, and H. Fujimoto. Enhancing haptic detection of surface undulation. *ACM Transactions on Applied Perception*, 2(1):46–67, 2005.

[128] H. E. Kirsten Rassmus-Gröhn, Charlotte Magnusson. User evaluations of a virtual haptic-audio line drawing prototype. In *Proc. Workshop on Haptic and Audio Interaction Design*, 2006.

[129] D. Klein, H. Freimuth, G. Monkman, S. Egersdorfer, A. Meier, H. Bose, M. Baumann, H. Ermert, and O. Bruhns. Electrorheological tactel elements. *Mechatronics*, 15(7):883–897, 2005.

[130] M. Kobayashi and T. Watanabe. A tactile display system equipped with a pointing device - MIMIZU. In *Computers Helping People with Special Needs (LNCS 2398)*, volume 2398, pages 527–, 2002.

[131] M. Kobayashi and T. Watanabe. Communication system for the blind using tactile displays and ultrasonic pens - MIMIZU. In *Computers Helping People with Special Needs (LNCS 3118)*, pages 731–738, 2004.

[132] M. Konyo and S. Tadokoro. Wearable tactile display in response to human active touch. In *Proc. Touch and Haptics Workshop (IROS 2004)*, 2004.

[133] M. Konyo, S. Tadokoro, and T. Takamori. Artificial tactile feel display using soft gel actuators. In *Proc. IEEE International Conference on Robotics and Automation (ICRA 2000)*, 2000.

[134] M. Konyo, S. Tadokoro, A. Yoshida, and N. Saiwaki. A tactile synthesis method using multiple frequency vibrations for representing virtual touch. In *Proc. IEEE/RSJ International Conference on Intelligent Robots and Systems (IROS 2005)*, pages 3965–3971, 2005.

[135] C. E. Kops and E. P. Gardner. Discrimination of simulated texture patterns on the human hand. *Journal of Neurophysiology*, 76(2):1145–1165, 1996.

[136] Z. Kuc. A bidirectional vibrotactile communication system: tactual display design and attainable data rates. In *Proc. VLSI and Computer Peripherals (CompEuro '89)*, pages 2/101–2/103, 1989.

[137] M. Kurze. TDraw: A computer-based tactile drawing tool for blind people. In *Proc. 2nd ACM Conference on Assistive Technologies (ASSETS '96)*, pages 131–138, 1996.

[138] H.-J. Kwon, S. W. Lee, and S. S. Lee. Braille dot display module with a PDMS membrane driven by a thermopneumatic actuator. *Sensors and Actuators A: Physical*, In Press, 2008.

[139] K.-U. Kyung, M. Ahn, D.-S. Kwon, and M. Srinivasan. A compact broadband tactile display and its effectiveness in the display of tactile form. In *Proc. 1st*

Joint EuroHaptics Conference and Symposium on Haptic Interfaces for Virtual Environment and Teleoperator Systems (World Haptics Conference '05), pages 600–601, 2005.

[140] K.-U. Kyung, S.-C. Kim, and D.-S. Kwon. Texture display mouse: Vibrotactile pattern and roughness display. *IEEE/ASME Transactions on Mechatronics*, 12(3):356–360, 2007.

[141] K.-U. Kyung and J.-Y. Lee. Ubi-pen: A haptic interface with texture and vibrotactile display. *IEEE Computer Graphics and Applications*, 29(1):56–64, 2009.

[142] K.-U. Kyung, J.-Y. Lee, and J. Park. Haptic stylus and empirical studies on braille, button, and texture display. *Journal of Biomedicine and Biotechnology*, 2008.

[143] K.-U. Kyung, G.-H. Yang, and D.-S. Kwon. A novel interactive computer interface: Enabling tangible interaction using a tactile feedback mouse. *Journal of Korean Institute of Next Generation PC*, 1(2):7–16, 2005.

[144] R. E. Ladner, M. Y. Ivory, R. Rao, S. Burgstahler, D. Comden, S. Hahn, M. Renzelmann, S. Krisnandi, M. Ramasamy, B. Slabosky, A. Martin, A. Lacenski, S. Olsen, and D. Groce. Automating tactile graphics translation. In *Proc.7th ACM Conference on Computers and Accessibility (ASSETS '05)*, pages 150–157, 2005.

[145] O. Lahav and D. Mioduser. Multisensory virtual environment for supporting blind persons' acquisition of spatial cognitive mapping - a case study. In *Proc. ED-MEDIA 2001 Conference*, 2001.

[146] S. Landau, M. Russell, K. Gourgey, J. N. Erin, and J. Cowan. Use of the Talking Tactile Tablet in mathematics testing. *Journal of Visual Impairment & Blindness*, 97(2):85, 2003.

[147] H. Lauer. The reading machine that hasn't been built yet. *AccessWorld*, 4(2), 2003.

[148] E. Lecolinet and G. Mouret. TACTIBALL, TACTIPEN, TACTITAB, ou comment toucher du doigt les données de son ordinateur. In *Proc. 17e conférence francophone sur l'Interaction Homme-Machine (IHM'05)*, 2005.

[149] S. Lederman and J. Campbell. Tangible line graphs: An evaluation and some systematic strategies for exploration. *Journal of Visual Impairment & Blindness*, 77:108, 1983.

[150] J. S. Lee and S. Lucyszyn. A micromachined refreshable braille cell. *Journal of Microelectromechanical Systems*, 14:673–682, 2005.

[151] G. E. Legge, C. M. Madison, and S. J. Mansfield. Measuring braille reading speed with the mnread test. *Visual Impairment Research*, 1(3):131–145, 1999.

[152] C. Lenay, O. Gapenne, S. Hanneton, C. Marque, and C. Genouelle. *Touching for Knowing*, chapter Sensory substitution: Limits and perspectives, pages 275–292. John Benjamins Publishing Company, 2003.

[153] C. Lenay, S.Canu, and P.Villon. Technology and perception: the contribution of sensory substitution systems. In *2nd International Conference on Cognitive Technology (CT '97)*, pages 44–53, 1997.

[154] R. Leonard. Statistics on vision impairment: A resource manual. Arlene R. Gordon Research Institute of Lighthouse International, 5th edition, 2002.

[155] E. A. Lerner and J. C. Craig. The prevalence of tactile motion aftereffects. *Somatosensory & motor research*, 19(1):24–29, 2002.

[156] V. Lévesque, A. H. C. Gosline, and V. Hayward. Refreshable tactile graphics with the STReSS^2 laterotactile display. Technical Demonstration, 16th Symposium on Haptic Interfaces for Virtual Environments and Teleoperator Systems, March 13-14, Reno, Nevada, 2008.

[157] V. Lévesque and V. Hayward. Experimental evidence of lateral skin strain during tactile exploration. In *Proc. Eurohaptics 2003*, pages 261–275, 2003.

[158] V. Lévesque and V. Hayward. Refreshable tactile graphics with the STReSS^2 laterotactile display. Technical Demonstration, EuroHaptics 2008, June 11-13, 2008, Madrid, Spain, 2008.

[159] V. Lévesque and V. Hayward. Tactile graphics rendering using three laterotactile drawing primitives. In *Proc. 16th Symposium on Haptic Interfaces For Virtual Environment And Teleoperator Systems*, pages 429–436, 2008.

[160] V. Lévesque, J. Pasquero, and V. Hayward. Braille display by lateral skin deformation with the STReSS^2 tactile transducer. In *Proc. 2nd Joint EuroHaptics Conference and Symposium on Haptic Interfaces for Virtual Environment and Teleoperator Systems (World Haptics Conference '07)*, pages 115–120, 2007.

[161] V. Lévesque, J. Pasquero, V. Hayward, and M. Legault. Display of virtual braille dots by lateral skin deformation: Feasibility study. *ACM Transactions on Applied Perception*, 2(2):132–149, 2005.

[162] J. Linvill. Development progress on a microelectronic tactile facsimile reading aid for the blind. *IEEE Transactions on Audio and Electroacoustics*, 17(4):271–274, 1969.

[163] J. G. Linvill and J. C. Bliss. A direct translation reading aid for the blind. *Proceedings of the IEEE*, 54(1):40–51, 1966.

[164] Y. Liu, R. Davidson, P. Taylor, J. Ngu, and J. Zarraga. Single cell magnetorheological fluid based tactile display. *Displays*, 26(1):29–35, 2005.

[165] J. Lotzsch. Computer-aided access to tactile graphics for the blind. In *Computers for Handicapped Persons (LNCS 860)*, pages 575–581, 1994.

[166] J. Luk, J. Pasquero, S. Little, K. MacLean, V. Lévesque, and V. Hayward. A role for haptics in mobile interaction: initial design using a handheld tactile display prototype. In *Proc. ACM Conference on Human Factors in Computing Systems (CHI '06)*, pages 171–180, 2006.

[167] D. A. L. Maberley, H. Hollands, J. Chuo, G. Tam, J. Konkal, M. Roesch, A. Veselinovic, M. Witzigmann, and K. Bassett. The prevalence of low vision and blindness in Canada. *Eye*, 20(3):341–346, 2006.

[168] C. Magnuson and K. Rassmus-Gröhn. Non-visual zoom and scrolling operations in a virtual haptic environment. In *Proc. EuroHaptics 2003*, 2003.

[169] C. Magnusson, K. Rassmus-Gr"ohn, C. Sj"ostr"om, and H. Danielsson. Navigation and recognition in complex haptic virtual environments - reports from an extensive study with blind users. In *Proc. EuroHaptics 2002*, 2002.

[170] C. Magnusson, S. C. C. Tan, and W. Yu. Haptic access to 3D objects on the web. In *Proc. EuroHaptics 2006*, pages 593–596, 2006.

[171] T. Matsunaga, K. Totsu, M. Esashi, and Y. Haga. Tactile display for 2-D and 3-D shape expression using SMA micro actuators. In *Proc. 3rd IEEE/EMBS Special Topic Conference on Microtechnology in Medicine and Biology*, pages 88–91, 2005.

[172] T. Maucher, K. Meier, and J. Schemmel. An interactive tactile graphics display. Proc. Sixth International Symposium on Signal Processing and its Applications (ISSPA 2001), 2001.

[173] T. Maucher, J. Schemmel, and K. Meier. The Heidelberg tactile vision substitution system. In *Proc. 7th International Conference on Computer Helping People with Special Needs (ICCHP 2000)*, 2000.

[174] D. McCallum, K. Ahmed, S. Jehoel, S. Dinar, and D. Sheldon. The design and manufacture of tactile maps using an inkjet process. *Journal of Engineering Design*, 16(6):525–544, 2005.

[175] D. McCallum and S. Ungar. An introduction to the use of inkjet for tactile diagram production. *British Journal of Visual Impairment*, 21(2):73–77, 2003.

[176] D. McGookin and S. Brewster. Graph Builder: Constructing non-visual visualizations. In *Proc. BCS HCI 2006*, 2006.

[177] D. McGookin and S. Brewster. An initial investigation into non-visual computer supported collaboration. In *CHI '07 Extended Abstracts on Human Factors in Computing Systems*, pages 2573–2578, 2007.

[178] D. McGookin, S. Brewster, and W. Jiang. Investigating touchscreen accessibility for people with visual impairments. In *Proc. 5th Nordic conference on Human-computer interaction (NordiCHI '08)*, pages 298–307, 2008.

[179] C. Megard, S. Roselier, and J.-M. Burkhardt. Verbal associations to tactile patterns: a step towards textured legends in multimodal maps. In *CHI '08 Extended Abstracts on Human Factors in Computing Systems*, pages 3579–3584, 2008.

[180] L. B. Merabet, L. Battelli, S. Obretenova, S. Maguire, P. Meijer, and A. Pascual-Leone. Functional recruitment of visual cortex for sound encoded object identification in the blind. *NeuroReport*, 20(2):132–138, 2009.

[181] J. A. Miele, S. Landau, and D. Gilden. Talking TMAP: Automated generation of audio-tactile maps using Smith-Kettlewell's TMAP software. *British Journal of Visual Impairment*, 24(2):93–100, 2006.

[182] S. Millar. *Reading by Touch*. Routledge, 1997.

[183] H. Minagawa, N. Ohnishi, and N. Sugie. Tactile-audio user interface for blind persons. In *Computers for Handicapped Persons (LNCS 860)*, pages 569–574, 1994.

[184] M. Minsky. *Computational haptics : the Sandpaper system for synthesizing texture for a force-feedback display*. PhD thesis, MIT, 1995.

[185] D. Morris and N. Joshi. Alternative "vision": a haptic and auditory assistive device. In *CHI '03 Extended Abstracts on Human Factors in Computing Systems*, pages 966–967, 2003.

[186] K. Moustakas, G. Nikolakis, K. Kostopoulos, D. Tzovaras, and M. Strintzis. Haptic rendering of visual data for the visually impaired. *IEEE Multimedia*, 14(1):62–72, 2007.

[187] G. Moy, C. Wagner, and R. Fearing. A compliant tactile display for teletaction. In *Proc. IEEE International Conference on Robotics and Automation (ICRA 2000)*, 2000.

[188] M. Nakatani, H. Kajimoto, D. Sekiguchi, N. Kawakami, and S. Tachi. 3D form display with Shape Memory Alloy. In *Proc. 13th International Conference on Artificial reality and Telexistence (ICAT 2003)*, pages 179–184, 2003.

[189] M. Nakatani, H. Kajimoto, K. Vlack, D. Sekiguchi, N. Kawakami, and S. Tachi. Control method for a 3D shape display with coil-type Shape Memory Alloy. In *Proc. IEEE International Conference on Robotics and Automation (ICRA 2005)*, pages 1344–1349, 2005.

[190] P. Nater. Tactile graphics with the aid of a conventional braille printer. *Journal of Microcomputer Applications*, 16(3):307–314, 1993.

[191] National Research Council. *Electronic Travel Aids: New Directions for Research*. National Academy Press, 1986.

[192] T. Nobels, G. Desmet, J. Van den Keybus, and R. Belmans. Development of a portable braille display using a fast prototyping platform for power electronics. In *International Conference on Power Electronics, Machines and Drives (PEMD)*, 2006.

[193] N. Noble and B. Martin. Shape discovering using tactile guidance. In *Proc. EuroHaptics 2006*, pages 561–564, 2006.

[194] J. Norman. If I remember rightly - tactile illustrations enable greater access to books. *British Journal of Visual Impairment*, 22(2):71–73, 2004.

[195] M. Ohka, H. Koga, T. Sugiura, and Y. Misuya. Surface texture presentation using a tactile display featuring an array of piezoelectric bimorph actuators. In *Proc. Seventh International Pacific Conference On Manufacturing and Management*, 2002.

[196] S. O'Modhrain. Touch and Go - Designing haptic feedback for a hand-held mobile device. *BT Technology Journal*, 22(4):139–145, 2004.

[197] S. O'Modhrain and B. Gillespie. The Moose: A haptic user interface for blind persons. In *Proceedings of the Third WWW6 Conference*, 1997.

[198] R. Ondricek, F. Meehan, and J. Love. A new braille medium. *AFB Research Bulletin*, 25:69, 1973.

[199] C. I. Palmer and E. P. Gardner. Simulation of motion on the skin. IV. responses of pacinian corpuscle afferents innervating the primate hand to stripe patterns on the optacon. *Journal of Neurophysiology*, 64(1):236–247, 1990.

[200] M. Paré, C. Behets, and O. Cornu. Paucity of presumptive ruffini corpuscles in the index finger pad of humans. *Journal of Comparative Neurology*, 456:260–266, 2003.

[201] P. Parente and G. Bishop. BATS: The Blind Audio Tactile Mapping System. In *Proc. ACM Southeast Regional Conference*, 2003.

[202] D. Parkes. Nomad: An audio-tactile tool for the acquisition, use and management of spatially distributed information by visually impaired people. In *Proc. Second International Symposium on Maps and Graphics for Visually Handicapped People*, 1988.

[203] J. Pasquero. Survey on communication through touch. Technical Report TR-CIM 06.04, McGill University, 2006.

[204] J. Pasquero. *Tactile Display for Mobile Interaction*. PhD thesis, McGill University, 2008.

[205] J. Pasquero and V. Hayward. STReSS: A practical tactile display system with one millimeter spatial resolution and 700 Hz refresh rate. In *Proc. Eurohaptics 2003*, pages 94–110, 2003.

[206] J. Pasquero, J. Luk, V. Lévesque, Q. Wang, V. Hayward, and K. E. MacLean. Haptically enabled handheld information display with distributed tactile transducer. *IEEE Transactions on Multimedia*, 9(4):746–753, 2007.

[207] S. Patomäki, R. Raisamo, J. Salo, V. Pasto, and A. Hippula. Experiences on haptic interfaces for visually impaired young children. In *Proc. 6th international conference on Multimodal interfaces (ICMI '04)*, pages 281–288, 2004.

[208] D. Pawluk, C. van Buskirk, J. Killebrew, S. Hsiao, and K. Johnson. Control and pattern specification for a high density tactile display. In *Haptics Symposium 1998*, 1998.

[209] W. Penrod, M. D. Corbett, and B. Blasch. A master trainer class for professionals in teaching the UltraCane electronic travel device. *Journal of Visual Impairment & Blindness*, 99(11):711–716, 2005.

[210] R. C. Petersen. Tactile display system. U.S. Patent No. 6,734,785, 2004.

[211] G. Petit, A. Dufresne, V. Lévesque, V. Hayward, and N. Trudeau. Refreshable tactile graphics applied to schoolbook illustrations for students with visual impairment. In *Proc. 10th ACM Conference on Computers and Accessibility (ASSETS '08)*, pages 89–96, 2008.

[212] H. Petrie, V. Johnson, P. McNally, S. Morley, A.-M. O'Neill, and D. Majoe. Inexpensive tactile interaction for blind computer users: two application domains. In *Proc. IEE Colloquium on Developments in tactile displays*, 1997.

[213] J. Phillips and K. O. Johnson. Tactile spatial resolution. III. a continuum mechanics model of skin predicting mechanoreceptor responses to bars, edges, and gratings. *Journal of Neurophysiology*, 46(6):1204–1225, 1981.

[214] J. R. Phillips and K. O. Johnson. Neural mechanisms of scanned and stationary touch. *Journal of the Acoustical Society of America*, 77(1):220–224, 1985.

[215] T. Pietrzak, A. Crossan, S. Brewster, B. Martin, and I. Pecci. Creating usable pin array tactons for non-visual information. *IEEE Transactions on Haptics*, In Press, 2009.

[216] T. Pietrzak, N. Noble, I. Pecci, and B. Martin. Evaluation d'un logiciel d'exploration de circuits électriques pour déficients visuels. In *Proc. Rencontres Jeunes Chercheurs en Interaction Homme-Machine (RJH-IHM 2006)*, 2006.

[217] I. Poupyrev and S. Maruyama. Tactile interfaces for small touch screens. In *Proc. 16th ACM Symposium on User Interface Software and Technology (UIST '03)*, pages 217–220, 2003.

[218] A. Puertas, P. Purés, A. M. Echenique, and Graffigna. Braille line using electrical stimulation. *Journal of Physics: Conference Series*, 90(1), 2007.

[219] R. Raisamo. Haptic interaction becomes mainstream. In *Proc. 20th International Conference of the Association Francophone d'Interaction Homme-Machine (IHM '08)*, pages 25–26, 2008.

[220] R. Raisamo, A. Hippula, S. Patomaki, E. Tuominen, V. Pasto, and M. Hasu. Testing usability of multimodal applications with visually impaired children. *IEEE MultiMedia*, 13(3):70–76, 2006.

[221] C. Ramstein. Combining haptic and Braille technologies: Design issues and pilot study. In *Proc. 2nd ACM Conference on Assistive Technologies (ASSETS '96)*, pages 37–44, 1996.

[222] C. Ramstein, O. Martial, A. Dufresne, M. Carignan, P. Chassé, and P. Mabilleau. Touching and hearing GUI's: design issues for the PC-Access system. In *Proc. 2nd ACM Conference on Assistive Technologies (ASSETS '96)*, pages 2–9, 1996.

[223] J. Rantala, R. Raisamo, J. Lylykangas, V. Surakka, J. Raisamo, K. Salminen, T. Pakkanen, and A. Hippula. Methods for presenting braille characters on a mobile device with a touchscreen and tactile feedback. *IEEE Transactions on Haptics*, 2(1):28–39, 2009.

[224] K. Rassmus-Gröhn, C. Magnusson, and H. Eftring. AHEAD - audio-haptic drawing editor and explorer for education. In *Proc. IEEE International Workshop on Haptic, Audio and Visual Environments and Games (HAVE 2007)*, pages 62–66, 2007.

[225] S. Resnikoff, D. Pascolini, D. Etya'ale, I. Kocur, R. Pararajasegaram, G. P. Pokharel, and S. P. Mariotti. Global data on visual impairment in the year 2002. *Bulletin of the World Health Organization*, 82(11):844–851, 2004.

[226] J. Roberts. NIST refreshable tactile graphic display: A new low-cost technology. In *Proc. CSUN Technology & Persons with Disabilities Conference*, 2004.

[227] J. Roberts, O. Slattery, and D. Kardos. Rotating-wheel braille display for continuous refreshable braille. In *Digest of Technical Papers, Society for Information Display International Symposium , Vol. XXXI*, pages 1130–1133, 2000.

[228] J. Roberts, O. Slattery, D. Kardos, and B. Swope. New technology enables many-fold reduction in the cost of refreshable braille displays. In *Proc. 4th ACM Conference on Assistive Technologies (ASSETS '00)*, pages 42–49, 2000.

[229] J. W. Roberts, O. T. Slattery, B. Swope, D. W. Kardos, V. Min, M. Sutton, E. C. Mulkens, G. Rodgers, N. Guttenberg, and T. Comstock. Extended refreshable tactile graphic array for scanned tactile display. U.S. Patent No. 7,009,595, 2006.

[230] G. Robles-De-La-Torre and V. Hayward. Force can overcome object geometry in the perception of shape through active touch. *Nature*, 412:445–448, 2001.

[231] U. R. Roentgen, G. J. Gelderblom, M. Soede, and L. P. de Witte. Inventory of electronic mobility aids for persons with visual impairments: A literature review. *Journal of Visual Impairment & Blindness*, 102(11):702 – 724, 2008.

[232] D. Ross. Implementing assistive technology on wearable computers. *IEEE Intelligent Systems*, 16(3), 2001.

[233] D. Ross and B. Blasch. Wearable interfaces for orientation and wayfinding. In *Proc. 4th ACM Conference on Assistive Technologies (ASSETS '00)*, pages 193–200, 2000.

[234] M. Rotard, C. Taras, and T. Ertl. Tactile web browsing for blind people. *Multimedia Tools and Applications*, 37(1):53–69, 2008.

[235] J. Rowell and S. Ungar. The world of touch: an international survey of tactile maps. part 1: production. *British Journal of Visual Impairment*, 21(3):98–104, 2003.

[236] R. Ryles. The impact of braille reading skills on employment, income, education, and reading habits. *Journal of Visual Impairment & Blindness*, 90(3):219–, 1996.

[237] R. Saarinen, J. Järvi, R. Raisamo, E. Tuominen, M. Kangassalo, K. Peltola, and J. Salo. Supporting visually impaired children with software agents in a multimodal learning environment. *Virtual Reality*, 9(2):108–117, 2006.

[238] K. Salisbury, F. Conti, and F. Barbagli. Haptic rendering: introductory concepts. *Computer Graphics and Applications, IEEE*, 24(2):24–32, 2004.

[239] W. Schiff and E. Foulke, editors. *Tactual Perception: A Sourcebook*, chapter Reading Braille, pages 168–208. Cambridge Univ Press, 1982.

[240] J. Schneider and T. Strothotte. Constructive exploration of spatial information by blind users. In *Proc. 4th ACM Conference on Assistive Technologies (ASSETS '00)*, pages 188–192, 2000.

[241] F. Schroeder. Perceptions of braille usage by legally blind adults. *Journal of Visual Impairment & Blindness*, 90(3):210, 1996.

[242] J. H. Schwartz and T. M. Jessel, editors. *Principles of Neural Science*, chapter The Bodily Senses, pages 430–450. McGraw-Hill, 2000.

[243] L. Sciavicco and B. Siciliano. *Modelling and Control of Robot Manipulators, 2nd Edition*. Springer-Verlag, 2000.

[244] A. Sepchat, N. Monmarché, M. Slimane, and D. Archambault. Semi automatic generator of tactile video games for visually impaired children. In *Computers Helping People with Special Needs (LCNS 4061)*, pages 372–379, 2006.

[245] J. Sevilla. *Touch and Blindness: Psychology and Neuroscience*, chapter Tactile Virtual Reality: A New Method Applied to Haptic Exploration, page 95. Lawrence Erlbaum Associates, 2005.

[246] H. Shen, K.-Y. Chan, J. Coughlan, and J. Brabyn. A mobile phone system to find crosswalks for visually impaired pedestrians. *Technology and Disability*, 20(3), 2008.

[247] L. Sheppard and F. K. Aldrich. Tactile graphics in school education: perspectives from teachers. *British Journal of Visual Impairment*, 19(3):93–97, 2001.

[248] S. Shimada, M. Shinohara, Y. Shimizu, and M. Shimojo. An approach for direct manipulation by tactile modality for blind computer users: Development of the second trial production. In *Computers Helping People with Special Needs (LNCS 4061)*, pages 1039–1046, 2006.

[249] S. Shimada, S. Yamamoto, Y. Uchida, M. Shinohara, Y. Shimizu, and M. Shimojo. New design for a dynamic tactile graphic system for blind computer users. In *Proc. SICE Annual Conference*, pages 1474–1477, 2008.

[250] Y. Shimizu. Tactile display terminal for visually handicapped. *Displays*, 7(3):116–120, 1986.

[251] Y. Shimizu, M. Shinohara, and H. Nagaoka. Recognition of tactile patterns in a graphic display: Evaluation of presenting modes. *Journal of Visual Impairment & Blindness*, 94(7):456–, 2000.

[252] M. Shinohara, Y. Shimizu, and A. Mochizuki. Three-dimensional tactile display for the blind. *IEEE Transactions on Rehabilitation Engineering*, 6(3), 1998.

[253] S. Shoval, I. Ulrich, and J. Borenstein. NavBelt and the GuideCane. *IEEE Robotics and Automation Magazine*, 10(1):9–20, 2003.

[254] C. Simon and J. A. Huertas. How blind readers perceive and gather information written in braille. *Journal of Visual Impairment & Blindness*, 92(5):322, 1998.

[255] C. Sjöström. Designing haptic computer interfaces for blind people. In *Proc. Sixth International Symposium on Signal Processing and its Applications*, 2001.

[256] C. Sjöström, H. Danielsson, C. Magnusson, and K. Rassmus-Gröhn. Phantom-based haptic line graphics for blind persons. *Visual Impairment Research*, 5(1):13–32, 2003.

[257] S. S. Snibbe, K. E. MacLean, R. Shaw, J. Roderick, W. L. Verplank, and M. Scheeff. Haptic techniques for media control. In *Proc. 14th ACM Symposium on User Interface Software and Technology (UIST '01)*, pages 199–208, 2001.

[258] J. C. Snyder, M. A. Clements, C. M. Reed, N. I. Durlach, and L. D. Braida. Tactile communication of speech. I. comparison of tadoma and a frequency-amplitude spectral display in a consonant discrimination task. *Journal of the Acoustical Society of America*, 71:1249–1254, 1982.

[259] N. Sriskanthan and K. R. Subramanian. Braille display terminal for personal computers. *IEEE Transactions on Consumer Electronics*, 36(2):121–128, 1990.

[260] D. K. Stein. The Optacon: Past, Present, and Future. *The Braille Monitor*, 41(5), 1998.

[261] O. Stephens. Braille - implications for living. *Journal of Visual Impairment & Blindness*, 83:288, 1989.

[262] A. A. Stevens and K. Weaver. Auditory Perceptual Consolidation in Early-Onset Blindness. *Neuropsychologia*, 43(13):1901–1910, 2005.

[263] B. Stöger and K. Miesenberger. The conventional braille display - state of the art and future perspectives. In *Computers Helping People with Special Needs (LNCS 860)*, pages 447–454, 1994.

[264] S. Tachi, K. Tanie, K. Komoriya, and M. Abe. Electrocutaneous communication in a guide dog robot (MELDOG). *IEEE Transactions on Biomedical Engineering*, 32:461–469, 1985.

[265] H. Tang and D. Beebe. A microfabricated electrostatic haptic display for persons with visual impairments. *IEEE Transactions on Rehabilitation Engineering*, 6(3), 1998.

[266] H. Tang and D. Beebe. Design and microfabrication of a flexible oral electrotactile display. *Journal of Microelectromechanical Systems*, 12(1):29–36, 2003.

[267] E. Tanhua-Piiroinen, V. Pasto, R. Raisamo, and E.-L. Sallnäs. Supporting collaboration between visually impaired and sighted children in a multimodal learning environment. In *Proc. 3rd International Workshop on Haptic and Audio Interaction Design*, pages 11–20, 2008.

[268] A. F. Tatham. The design of tactile maps: Theoretical and practical considerations. In *Proc. 15th International Cartographic Conference*, volume 1, pages 157–166, 1991.

[269] H. R. Taylor. The economics of vision loss. *Visual Impairment Research*, 7(2/3):53–58, 2005.

[270] P. Taylor, A. Hosseini-Sianaki, C. Varley, and D. Pollet. Advances in an electrorheological fluid based tactile array. In *Proc. IEE Colloquium on Developments in Tactile Displays (Digest No. 1997/012)*, pages 5/1–5/5, 1997.

[271] P. Taylor, A. Moser, and A. Creed. The design and control of a tactile display based on shape memory alloys. In *Proc. IEE Colloquium on Developments in Tactile Displays (Digest No. 1997/012)*, pages 1/1–1/4, 1997.

[272] The Eye Diseases Prevalence Research Group. Causes and prevalence of visual impairment among adults in the united states. *Archives of Ophthalmology*, 122(4):477–485, 2004.

[273] C. Thinus-Blanc and F. Gaunet. Representation of space in blind persons: Vision as a spatial sense? *Psychological Bulletin*, 121(1), 1997.

[274] O. Tretiakoff and A. Tretiakoff. Electromechanical transducer for relief display panel. U.S. Patent No. 4,044,350, 1977.

[275] Turner and Sherman. The construction of tactile maps. *American Cartographer*, 13:199, 1986.

[276] D. Tzovaras, G. Nikolakis, G. Fergadis, S. Malasiotis, and M. Stavrakis. Design and implementation of haptic virtual environments for the training of the visually impaired. *IEEE Transactions on Neural Systems and Rehabilitation Engineering*, 12(2):266–278, 2004.

[277] C. L. Van Doren, D. G. Pelli, and R. T. Verillo. A device for measuring tactile spatiotemporal sensitivity. *Journal of the Acoustical Society of America*, 81(6):1906–1916, 1987.

[278] R. Vasconcellos. Representing the geographical space for handicapped students: a case study on map use. In *Proc. International Cartographic Conference*, 1993.

[279] R. Velazquez and E. E. Pissaloux. Tactile displays in human-machine interaction: Four case studies. *International Journal of Virtual Reality*, 7(2):51–58, 2008.

[280] R. Velazquez, E. E. Pissaloux, and M. Wiertlewski. A compact tactile display for the blind with shape memory alloys. In *Proc. IEEE International Conference on Robotics and Automation (ICRA 2006)*, pages 3905–3910, 2006.

[281] R. Velazquez, E. Preza, and H. Hernandez. Making eBooks accessible to blind braille readers. In *Proc. IEEE International Workshop on Haptic Audio visual Environments and Games (HAVE 2008)*, pages 25–29, 2008.

[282] F. Vidal-Verdú and M. Hafez. Graphical tactile displays for visually-impaired people. *IEEE Transactions on Neural Systems and Rehabilitation Engineering*, 15(1):119–130, 2007.

[283] R. Vitushinsky, F. Khelfaoui, S. Schmitz, and B. Winzek. Metallic thin film composites with shape memory alloys for microswitches and tactile graphical displays. *International Journal of Applied Electromagnetics and Mechanics*, 23:113–118, 2006.

[284] C. Wagner, S. Lederman, and R. Howe. A tactile shape display using RC servomotors. Proc. 10th Symposium on Haptic Interfaces for Virtual Environments and Teleoperator Systems, 2002.

[285] S. Wall and S. Brewster. Providing external memory aids in haptic visualisations for blind users. *International Journal of Disability and Human Development*, 4(4):331–338, 2005.

[286] S. Wall and S. Brewster. Feeling what you hear: tactile feedback for navigation of audio graphs. In *Proc. ACM Conference on Human Factors in Computing Systems (CHI '06)*, pages 1123–1132, 2006.

[287] S. A. Wall and S. Brewster. Sensory substitution using tactile pin arrays: Human factors, technology and applications. *Signal Processing*, 86(12):3674 – 3695, 2006.

[288] P. Walsh and J. A. Gardner. TIGER, a new age of tactile text and graphics. In *Proc. CSUN Technology & Persons with Disabilities Conference*, 2001.

[289] Q. Wang and V. Hayward. Compact, portable, modular, high-performance, distributed tactile display device based on lateral skin deformation. In *Proc. 14th Symposium on Haptic Interfaces for Virtual Environments and Teleoperator Systems*, pages 67–72, 2006.

[290] Q. Wang and V. Hayward. In vivo biomechanics of the fingerpad skin under local tangential traction. *Journal of Biomechanics*, 40(4):851–860, 2007.

[291] Q. Wang and V. Hayward. Tactile synthesis and perceptual inverse problems seen from the viewpoint of contact mechanics. *ACM Transactions on Applied Perception*, 5(2):1–19, 2008.

[292] Q. Wang, V. Hayward, and A. M. Smith. A new technique for the controlled stimulation of the skin. In *Proc. Canadian Medical and Biological Engineering Society Conference*, 2004.

[293] Q. Wang, V. Levesque, J. Pasquero, and V. Hayward. A haptic memory game using the STReSS^2 tactile display. In *CHI '06 Extended Abstracts on Human Factors in Computing Systems*, pages 271–274, 2006.

[294] D. H. Warren. *Handbook of Perception, Vol. X (Perceptual Ecology)*, chapter Perception by the Blind. Academic Press, 1978.

[295] T. Watanabe, M. Kobayashi, S. Ono, and K. Yokoyama. Practical use of interactive tactile graphic display system at a school for the blind. In *Proc. Fourth International Conference on Multimedia and Information and Communication Technologies in Education (m-ICTE 2006)*, pages 1111–1115, 2006.

[296] T. Way and K. Barner. Automatic visual to tactile translation. II. Evaluation of the TACTile image creation system. *IEEE Transactions on Rehabilitation Engineering*, 5(1):95–105, 1997.

[297] L. R. Wells and S. Landau. Merging of tactile sensory input and audio data by means of the Talking Tactile Tablet. In *Proc. EuroHaptics 2003*, 2003.

[298] L. Whitmarsh. The benefits of guide dog ownership. *Visual Impairment Research*, 7(1):27–42, 2005.

[299] World Wide Web Consortium. Web content accessibility guidelines 1.0. etrieved May 19, 2008 from the World Wide Web: `http://www.w3.org/TR/WCAG10/`, 1999.

[300] X. Wu, H. Zhu, S.-H. Kim, and M. G. Allen. A portable pneumatically-actuated refreshable braille cell. In *Proc. International Solid-State Sensors, Actuators and Microsystems Conference*, pages 1409–1412, 2007.

[301] P. Yang. Electroactive polymer actuator braille cell and braille display. U.S. Patent No. 6,881,063, 2005.

[302] F.-H. Yeh and S.-H. Liang. Mechanism design of the flapper actuator in chinese braille display. *Sensors and Actuators A: Physical*, 135(2):680 – 689, 2007.

[303] L. Yobas, D. M. Durand, G. G. Skebe, F. J. Lisy, and M. A. Huff. A novel integrable microvalve for refreshable braille display system. *Journal of Microelectromechanical Systems*, 12(3):252–263, 2003.

[304] L. Yobas, M. A. Huff, F. J. Lisy, and D. M. Durand. A novel bulk-micromachined electrostatic microvalve with a curved-compliant structure applicable for a pneumatic tactile display. *Journal of Microelectromechanical Systems*, 10(2), 2001.

[305] W. Yu and S. Brewster. Comparing two haptic interfaces for multimodal graph rendering. In *Proc. 10th Symposium on Haptic Interfaces for Virtual Environments and Teleoperator Systems*, pages 3–9, 2002.

[306] W. Yu and S. Brewster. Multimodal virtual reality versus printed medium in visualization for blind people. In *Proc. 5th ACM Conference on Assistive Technologies (ASSETS '02)*, 2002.

[307] W. Yu and S. Brewster. Evaluation of multimodal graphs for blind people. *Journal of Universal Access in the Information Society*, 2(2), 2003.

[308] M. Zajicek and C. Powell. Enabling visually impaired people to use the internet. In *Proc. IEE Colloquium 'computers helping people in the service of mankind'*, 1997.

[309] M. Ziat, O. Gapenne, J. Stewart, and C. Lenay. Haptic recognition of shapes at different scales: A comparison of two methods of interaction. *Interacting with Computers*, 19(1):121–132, 2007.

[310] G. Zimmermann, G. Vanderheiden, M. Gandy, S. Laskowski, M. Ma, S. Trewin, and M. Walker. Universal remote console standard - toward natural user interaction in ambient intelligence. In *Proc. ACM Conference on Human Factors in Computing Systems (CHI '04)*, pages 1608–1609, 2004.

[311] M. P. Zwiers, A. J. V. Opstal, and J. R. M. Cruysberg. A spatial hearing deficit in early-blind humans. *Journal of Neuroscience*, 21(RC142):1–5, 2001.